Molecular bases of the LEAFY-UFO synergy during floral development

Philippe Rieu

THÈSE

Pour obtenir le grade de

DOCTEUR DE L'UNIVERSITÉ GRENOBLE ALPES

École doctorale : CSV- Chimie et Sciences du Vivant
Spécialité : Biologie Végétale
Unité de recherche : LPCV - Laboratoire de Physiologie Cellulaire Végétale

Bases moléculaires de la synergie LEAFY-UFO au cours du développement floral

Molecular bases of the LEAFY-UFO synergy during floral development

Présentée par :

Philippe RIEU

Direction de thèse :

François PARCY Resp. Equipe, Dir. Adj. UMR, Université Grenoble Alpes	Directeur de thèse

Rapporteurs :

Patrick LAUFS
DIRECTEUR DE RECHERCHE, INRAE Centre de Versailles-Grignon
Simon RÜDIGER
PROFESSEUR, Heinrich-Heine-Universität Düsseldorf

Thèse soutenue publiquement le **3 février 2023**, devant le jury composé de :

François PARCY DIRECTEUR DE RECHERCHE, CNRS délégation Alpes	Directeur de thèse
Patrick LAUFS DIRECTEUR DE RECHERCHE, INRAE Centre de Versailles-Grignon	Rapporteur
Simon RÜDIGER PROFESSEUR, Heinrich-Heine-Universität Düsseldorf	Rapporteur
Martin KATER PROFESSEUR, Università degli Studi di Milano - Statale	Examinateur
Fabienne HANS MAITRE DE CONFERENCES HDR, Université Grenoble Alpes	Examinatrice
Gwyneth INGRAM DIRECTRICE DE RECHERCHE, CNRS délégation Rhône Auvergne	Présidente

Invités :

Gabrielle Tichtinsky
MAITRE DE CONFERENCES, Université Grenoble Alpes

Remerciements

Je remercie **Eric Maréchal** et **François Parcy** de m'avoir accueilli au sein de leur laboratoire.

I also thank **Patrick Laufs**, **Rüdiger Simon**, **Gwyneth Ingram**, **Fabienne Hans** and **Martin Kater** for accepting to evaluate my work. Je remercie également les membres de mon CSI **Marie-Odile Fauvarque**, **Marie Monniaux** et **Carlo Petosa** pour leurs nombreux conseils tout au long de ma thèse.

Tout d'abord un immense merci à toi **François**. Tu as été un excellent directeur de thèse, et ces quelques lignes ne suffiront sûrement pas pour t'exprimer toute ma gratitude. D'un point de vue scientifique, je te remercie pour ta motivation sans faille, ton originalité dans la recherche, ta volonté de progresser, ta rigueur et ton immense savoir. Je te remercie de m'avoir fait confiance et de m'avoir toujours considéré comme un chercheur autonome. Tu m'as laissé une liberté totale sur ce que je voulais faire et des fonds illimités, un luxe que peu de thésards ont. Tu as aussi tout fait pour que nous ayons les meilleures collaborations et un accès aux experts et aux équipements les plus performants. Merci aussi pour ton âme d'enfant et les étoiles dans les yeux que tu as quand nous obtenons de beaux résultats; tu transmets vraiment cet émerveillement et ce grain de folie autour de toi. D'un point de vue humain, je te remercie d'avoir su appréhender ma personnalité et ma façon de travailler. Tu as aussi su comme personne trouver les mots qu'il fallait pour me motiver dans les nombreux passages difficiles. Je regarde aussi avec admiration tes capacités de manager; j'ai travaillé dans une équipe soudée, où il n'y a jamais eu de conflits, et où les talents de chacun peuvent grandir et s'exprimer pleinement. Je continue aujourd'hui mon chemin en dehors de PCV mais tu resteras pour la suite de mon parcours une source d'inspiration et un exemple à suivre.

Un grand merci aussi à toi **Manu**. On s'est côtoyé tous les jours pendant presque 4 ans, et là aussi je n'aurais pas assez de place pour te remercier. Tu tiens vraiment le labo à toi tout seul, et cette thèse n'aurait pas été aussi belle sans ton travail. Merci pour les innombrables manips que tu as réalisées sur mes projets. Je te remercie d'avoir su résister à ma personnalité pas toujours facile, notamment quand il fallait refaire 10 fois le même EMSA pour qu'il soit parfait ! Merci aussi pour tous ces efforts que nous ne voyons pas toujours mais grâce auxquels nous ne manquons jamais de rien au labo pour faire de belles expériences. Merci aussi pour ta motivation et ton envie de toujours faire bouger l'équipe.

Je voudrais te remercier chaleureusement **Gaby** pour ton soutien, ton aide sur les plantes, tes conseils, tes relectures etc. Merci aussi pour ton attention envers chacun, ton énergie et ta joie de vivre : tu fais vivre l'équipe scientifiquement et humainement malgré ton emploi du temps surchargé (qui ne te laisse que le vendredi soir pour maniper !).

Un grand merci à toi **Renaud**. Tu m'as transmis ta passion de la biologie structurale et ton envie de comprendre le rôle de chaque hélice et de chaque acide aminé. Merci aussi pour ta bonne humeur et l'ambiance joyeuse que tu apportes à l'équipe.

Thanks also to you **Chloe** and **Max** for your precious help and your enthusiasm to share projects with us in cryoEM or crystallography. Thank you Chloe for your help during the redaction of the paper and the precision you brought. I also would like to thank you for

showing me your way to conduct science; your efficiency and your “style” were very inspiring for me.

Merci aussi à **Lefteris Zarkadas** et **Guy Schoehn** d’avoir accepté de collaborer avec nous et d’avoir amené le projet aussi loin dans le domaine passionnant de la cryoEM. Notre histoire aurait été bien moins belle sans votre apport et je sais ce que nous vous devons. Merci également à **Luis Oñate-Sánchez** et **Gerardo Carrera** pour leur collaboration sur les screens en levure et pour leur accueil dans leur laboratoire à Madrid.

3 grands mercis aussi à la team bioinfo avec **Jérémy**, **Laura** et **Romain**. Vous avez à chaque fois traité mes données à la vitesse de l’éclair pour fournir un logo en moins de 24h à François ! Merci pour votre disponibilité et votre patience avec les biologistes (ces ingrats qui vous traite d’infogérance). Sans vous nous n’aurions pas compris grand-chose à LFY-UFO et je vous remercie vraiment pour votre immense contribution.

Merci à tous les membres passés et présents de l’équipe Flore au sens large (c’est-à-dire tous ceux qui ont manipé ou qui manip encore en pièce 229). En particulier merci à vous **Xuelei** et **Claudius** pour m’avoir transmis une partie de votre expérience. Un grand merci aussi à toi **Hicham** pour tous tes conseils, tes immenses connaissances sur le monde végétal et ton insatiable curiosité. Merci aussi pour la pêche que tu transmettais à tout le monde; le labo n’était pas le même lorsque tu étais là ! Et aussi un grand merci à **Antonin**, **Coralie**, **Loïc** et **Elise**. Réaliser ma thèse a vos côtes était très sympa et je vous remercie pour tous les bons moments passés. J’espère qu’on aura des occasions de se recroiser.

Merci à **Bianca**, **Camille** et **Jade** qui ont travaillé en stage dans l’équipe. Je vous remercie pour votre contribution et je vous souhaite toute la réussite pour la suite de votre parcours.

Merci **Sylvie** pour ton aide pour les plantes. Tu transformes cet affreux sous-sol en plateau technique fonctionnel et je te remercie pour l’énergie que tu mets dans cette mission pas facile. Merci aussi à toi **Anne-Marie** pour tous les services que tu m’as rendu et qui m’ont fait gagné un temps précieux.

Enfin merci à tous les membres du labo **PCV** que je n’ai pas cité ici. Merci en particulier au service admin, vous êtes d’une efficacité redoutable pour orienter les thésards dans le labyrinthe administratif du doctorat et pour leur permettre de faire de la science sereinement.

Je remercie encore une fois tous les membres de l’équipe Flore et je vous souhaite à tous une bonne continuation, l’aventure LFY continue !

TABLE OF CONTENTS

Abbreviations

ALOG	Arabidopsis LSH Oryza G1
ampDAP-seq	amplified DNA Affinity Purification followed by sequencing
AG	AGAMOUS
AP1	APETALA1
AP3	APETALA3
ASK	ARABIDOPSIS SKP1-LIKE
ChIP-seq	Chromatin Immunoprecipitation followed by sequencing
cryoEM	cryo Electron Microscopy
DBD	DNA Binding Domain
DEE	Distal early Element
DLRA	Dual Luciferase Reporter Assay
EMSA	Electrophoretic Mobility Shift Assay
FM	Floral Meristem
GFP	Green Fluorescent Protein
GUS	β-glucuronidase
GR	Glucocorticoid Receptor
HWS	HAWAIIAN SKIRT
IM	Inflorescence Meristem
Kd	Dissociation Constant
LFY	LEAFY
LFYBS	LFY Binding Site
LSH	LIGHT SHORT HYPOCOTYL
LUBS	LFY-UFO Binding Site
MADS	MCM1, AGAMOUS, DEFICIENS, SRF
p35S	Cauliflower Mosaic Virus 35S promoter
pAP3	AP3 promoter
PEE	Proximal Early Element
PI	PISTILLATA
PWM	Position Weight Matrix
RBE	RABBIT EARS
SAM	Sterile Alpha Motif or Shoot Apical Meristem
SCF	Skp1-Cullin-F-box
SEC	Size Exclusion Chromatography
SEC-MALLS	SEC-Multi Angle Laser Light Scattering
SEP3	SEPALATTA3
TCP	TEOSINTE BRANCHED1-CYCLOIDEA-PROLIFERATING CELL NUCLEAR ANTIGEN FACTOR1
TF	Transcription Factor
TFL1	TERMINAL FLOWER1
UFO	UNUSUAL FLORAL ORGANS
URM	UFO Recruiting Motif
WT	Wild Type
WUS	WUSCHEL

OPENING STATEMENT

I would like to inform the reader about the structure of this thesis manuscript. I made the choice to base it on research papers, an option that sometimes makes its structure harder to follow. Here are some indications that should help the reader to understand how this document is organized.

After the introduction, this manuscript contains 3 chapters, with one article per chapter:

- Chapter I contains Article 1 and complementary information. Article 1 is a research paper on the LFY-UFO interaction, posted on Biorxiv and for which a revised version was accepted at Nature Plants on November 25th, 2022.

- Chapter II includes Article 2 and unpublished results. Article 2 is a review on *UFO* functions that summarizes published knowledge and puts it into perspective with the results of Article 1. Part of Article 2 can also be read as an introduction. This article will eventually be submitted as a review once Article 1 gets published.

- Chapter III corresponds to Article 3, which is another research article on a fairly independent topic (biochemical and structural analysis of the ALOG transcription factors).

For each article, figure numbering and references are independent from the main file.

INTRODUCTION

I. LEAFY is a key Transcription Factor (TF) for flower development

Flowers are of a paramount importance as the sexual reproductive apparatus of angiosperms. Despite a broad variety of shapes and colors, the flower pattern is overall well conserved. It is constituted of four different concentric whorls: sepals, petals, stamens and carpels. Only the two lasts include reproductive structures (pollen and ovules). In this introduction, I will focus on *Arabidopsis thaliana*, a model organism in plant biology. In Arabidopsis, flowers comprise four sepals, four petals, six stamens and two fused carpels.

The floral transition and the development of the Flower Meristem (FM)

Flowers are transient organs that appear at a precise moment during a plant's life cycle, and then ultimately senesce. The control of flower emergence is linked to meristems, from which they are produced. During the vegetative growth phase, aboveground meristems produce leaves and shoots. The transition to the determinate reproductive state, under the control of different internal and environmental cues (among which for example temperature and photoperiod), is done thanks to the formation of a new type of meristem: the Inflorescence Meristem (IM; Amasino, 2010). Once this transition is performed, this IM gives rise to Floral Meristems (FM; Alvarez-Buylla et al., 2010). Floral meristems develop into mature flowers with reproductive and non-reproductive organs. FMs are determinate and their activity ends after the formation of a flower.

The ABCE model describes floral organ identity acquisition

At the molecular level, this abrupt and irreversible transition from a vegetative to a reproductive phase implies a deep development reprogramming through a robust gene regulatory network. Molecular mechanisms that control the floral development began to be

elucidated during the 90's through the analysis of Arabidopsis and *Antirrhinum majus* homeotic mutants. Analysis of single and multiple mutants lead to the ABCE model that describes how the identity of floral organs is acquired (Figure 1; Irish, 2010).

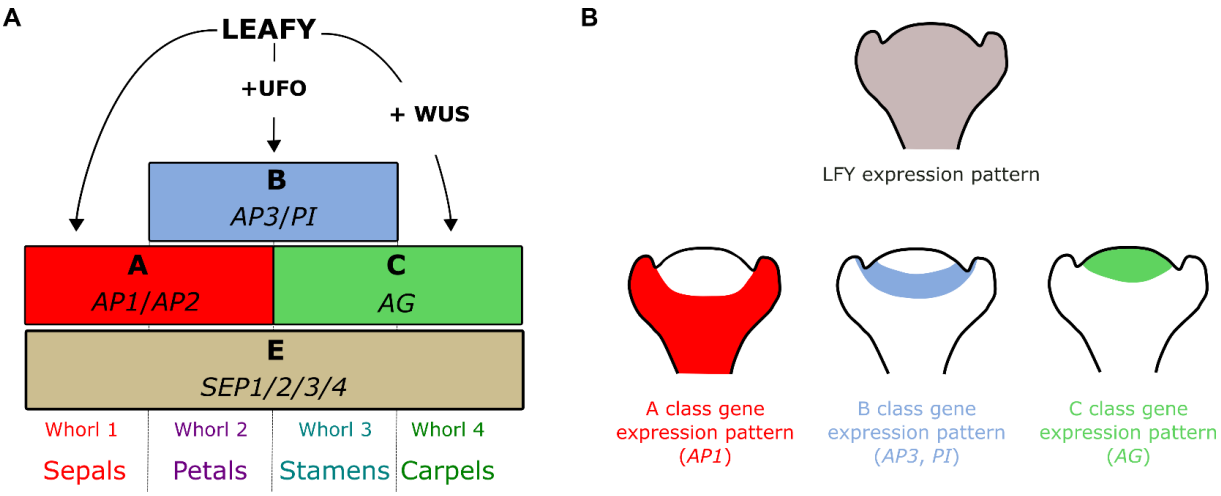

Figure 1: The ABCE model and the acquisition of floral organs identity. (A) APETALA1 *(*AP1*),* PISTILLATA *(*PI*),* APETALA3 *(*AP3*),* AGAMOUS *(*AG*) and* SEPALLATA *(*SEP*) genes encode for MADS TFs and are activated by LFY (directly or with the help of other cofactors).* AP2 *encodes an AP2/ERF transcription factor.* **(B)** *Expression pattern of* LFY *and ABC genes in the young FM.* AP2 *expression is not represented.* AP2 *is expressed in the whole FM (Jofuku et al., 1994) but its activity is restricted to the first and second whorl by the microRNA miR172 (Aukerman and Sakai, 2003).*

In this model, floral organ identity genes are divided into three classes. *A* genes (*APETALA1* and *APETALA2*) control sepals development alone, and petals development together with *B* genes (*APETALA3* and *PISTILLATA*). *B* genes control petals development with *A* genes and stamens development with *C* genes. Only one *C* gene has been described so far in Arabidopsis (*AGAMOUS*); it controls stamens development with *B* genes and carpels development alone. These genes code for TFs that act in combination into discrete meristem domains to specify the identity of floral organs (Figure 1B). Most *ABC* genes encode MADS-Box TFs that are activated only when floral transition has been performed (Irish, 2010). Hence, other upstream regulating factors are required for their activation in the appropriate region of the FM.

LFY is a master regulator TF orchestrating flower development

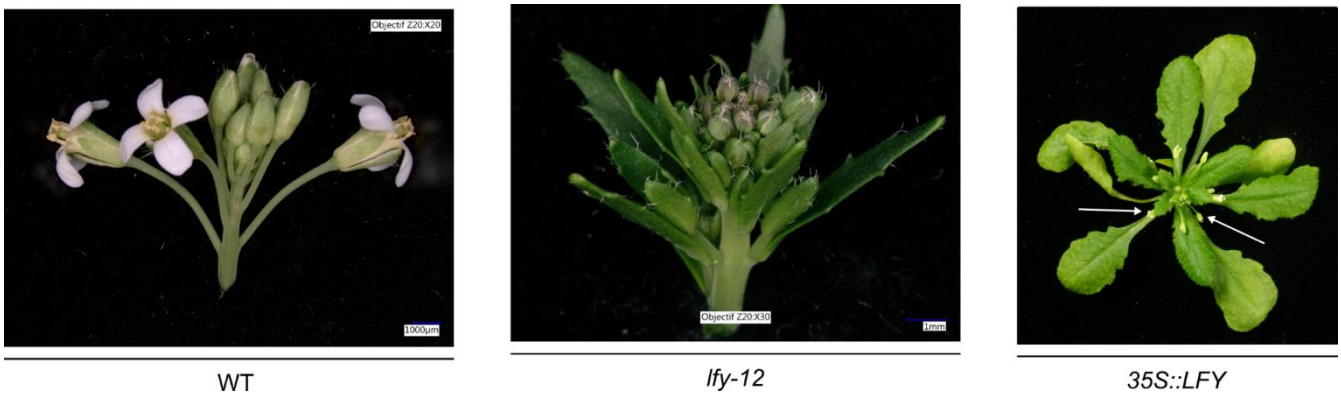

Figure 2: LFY has a crucial role during flowering. *Pictures of a WT inflorescence (left) and of the inflorescence of the* lfy-12 *null mutant (middle). Right picture shows a plant constitutively expressing LFY under the control of the cauliflower mosaic virus (CaMV)* 35S *promoter. Ectopic rosette flowers are indicated by white arrows.*

Genetic analysis has led to the characterization of another major gene, required for FM identity called *LEAFY* (*LFY*). In loss-of-function *lfy* mutants, flowers are converted to shoots or shoot/flower intermediates subtended by leaves (sometimes rudimentary; Figure 2; Weigel et al., 1992). Inversely, ectopic *LFY* overexpression triggers the termination of primary shoots into terminal flowers and the replacement of secondary inflorescence by flowers (Weigel and Nilsson, 1995). Thus, LFY is described as a master regulator of flower development, necessary and somewhat sufficient to trigger FM formation. It is lowly expressed in vegetative tissues and its expression is dramatically increased upon the transition to the reproductive phase, thanks to upstream regulators such as AUXIN RESPONSE FACTOR 5 (ARF5; Yamaguchi et al., 2016), SUPPRESSOR OF OVEREXPRESSION OF CONSTANS1 (SOC1) and AGAMOUS-LIKE 24 (AGL24; Lee et al., 2008).

LFY performs several distinct functions during flower development.

- Determining FM identity: *LFY* is a major FM identity gene, *i.e.* its expression determines the floral developmental program in which the meristem is engaged. In Arabidopsis, another key FM identity gene is the MADS TF *AP1*, activated by LFY (Wagner et al., 1999) but also through independent pathways. To determine FM identity, LFY activates the expression of floral genes

and engages the group of cells in which it is expressed in the flower development program. It has recently been shown that LFY might act as a pioneer TF to perform this function by opening closed chromatin regions for activation (Jin et al., 2021; Lai et al., 2021).

- FM patterning: Once the FM identity is established, a major role of LFY is to activate *ABC* genes determining floral organ identities (Figure 1B). I focused mainly on this function of LFY, notably its role in the activation of the *B* gene *AP3*. LFY expression is uniform in the FM while its *ABC* targets are expressed in precise territories, meaning that its activity varies spatially. Several studies have shown that different spatially-restricted cofactors act with LFY to allow the activation of precise genes within given territories. The functional interaction between LFY and its cofactors is further described below.

LFY performs other functions (like in hormone signaling, repressing defense genes or in the suppression of bract development; Winter et al., 2011) but they will not be detailed here.

Biochemical properties of LFY

Given the importance of LFY during flower development, its molecular functions have been deeply investigated, notably in our team. In Arabidopsis, like in most other angiosperm species, *LFY* is found as a single copy gene (reviewed in Moyroud et al., 2010). This characteristic is quite spectacular as several whole genome duplication events occurred through evolution. The *LFY* gene encodes a plant-specific TF, with no similarity to any other known protein.

In Arabidopsis, LFY is a 50 kDa TF with two highly conserved domains. Analysis of *lfy* mutants showed that the functionality of both domains is required for LFY to fully perform its functions *in planta* (Maizel et al., 2005). The domain at the N-terminus end has been described as a Sterile Alpha Motif (SAM) oligomerization domain and the C-terminal domain is the DNA Binding Domain (DBD). Crystal structures have been obtained for both domains in the team (Hamès et al., 2008; Sayou et al., 2016).

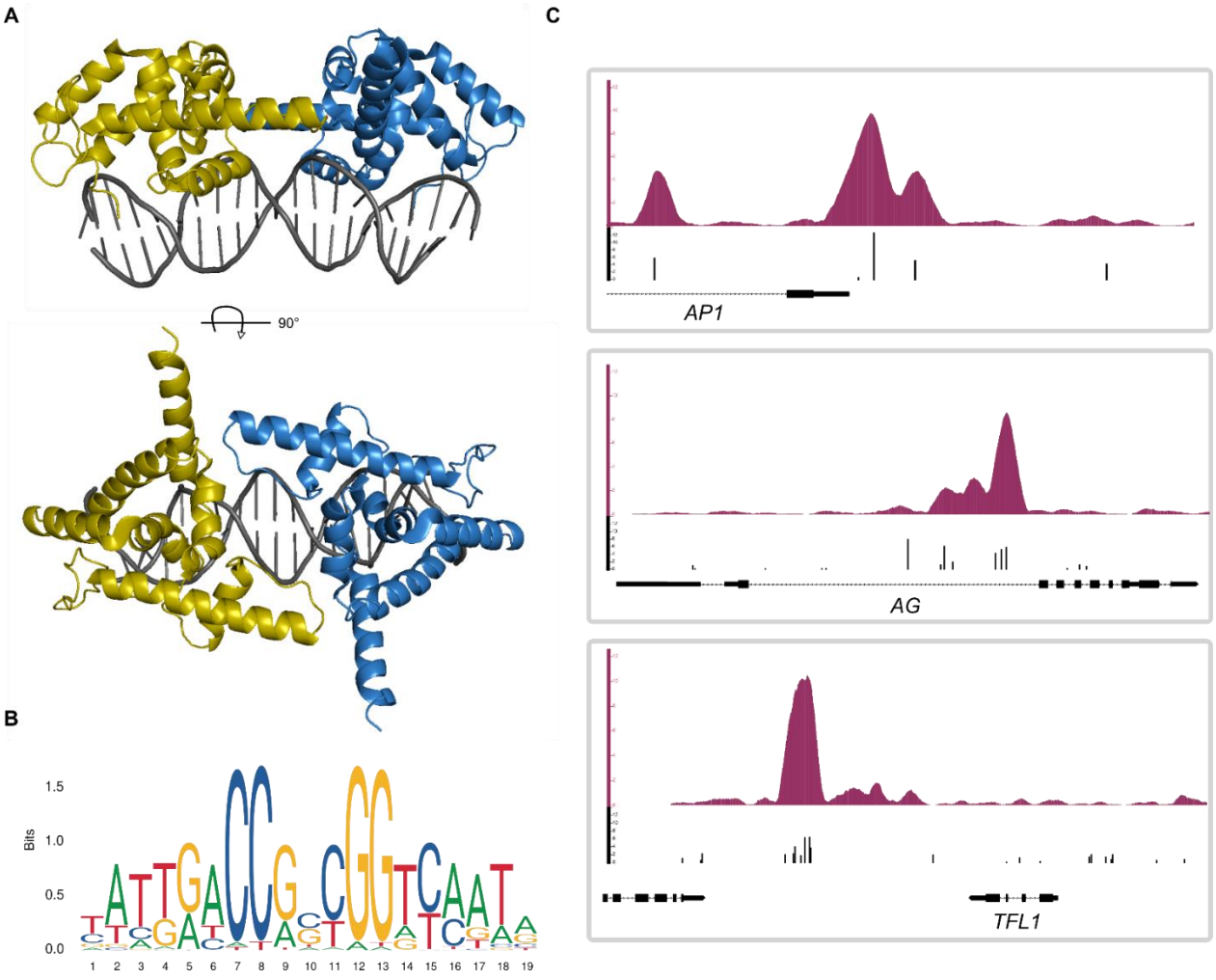

Figure 3. LFY is a well-described TF. (A) *Crystal structure of the LFY DBD (Hamès et al., 2008). LFY DBD monomers are colored in yellow and blue, DNA in grey. A 90° rotation was applied to obtain the bottom picture.* **(B)** *Logo of the motif bound by LFY (downloaded from the JASPAR database).* **(C)** *Integrated Genome Browser (IGB) view of selected genome regions showing ChIP-seq signal in seedlings (Moyroud et al., 2011; top) and predicted LFY binding sites using LFY Position Weight Matrix (bottom).*

The structure of the LFY DBD in complex with DNA revealed the binding mechanism of this TF with its cognate DNA (Figure 3A; Hamès et al., 2008). As described below, the motif bound by LFY is pseudo-palindromic. LFY binds it as a homodimer, each monomer binding one half of the pseudo-palindromic site. The LFY DBD comprises 7 helices connected by short loops, and most residues contacting DNA bases (N287, K303 and R233) are located on helices 2 and 3 (Hamès et al., 2008). Helices 2 and 3 form a helix-turn-helix (HTH) motif, found in several other DBDs. Residues contacting the DNA phosphate backbone are also described. Finally, the

residues implicated in LFY dimerization were identified (H383 and R386), and the effect of their mutation was described *in vitro* and *in planta* (Chahtane et al., 2013).

Genome-wide binding of Arabidopsis LFY is very well described *in vitro* and *in vivo* with DAP-seq and ampDAP-seq (Lai et al., 2021), SELEX (Moyroud et al., 2011) and ChIP-seq data (Goslin et al., 2017; Jin et al., 2021; Sayou et al., 2016; Winter et al., 2011). LFY binds a 19-bp pseudo-palindromic site (Figure 3B), with the positions 7-8 and 12-13 containing the higher information content. The motif is associated with a Position Weight matrix (PWM) summarizing the probability to find a given nucleotide at each position. The PWM can be used to scan a sequence (of a promoter for example) in order to calculate scores predicting LFY binding at each position. Thus, the binding of LFY to its canonical binding site is well described and predictable with bioinformatic models in Arabidopsis.

Analysis of ChIP-seq data revealed that the LFY matrix obtained from genome-wide experiments correctly predicts LFY binding at several loci in the genome. High-score LFY Binding Sites (LFYBS) are found in the regulatory regions of several LFY targets, like in the promoter of *AP1*, *TERMINAL FLOWER1* (*TFL1)* 3' regulatory region or in the second intron of *AG* (Moyroud et al., 2011; Figure 3C).

These binding data are very helpful to understand the regulatory networks in which LFY is implicated. However, the significance of LFY binding in some regions is not yet fully understood.

The biological significance of LFY binding to some loci is not yet understood: the example of the LFY-dependent repression of *LSH* genes in Arabidopsis

Binding of LFY to the regulatory regions of some genes have been associated to a clear regulation. For example, LFY binds to the promoter of *AP1* and directly activates it (Benlloch et al., 2011; Parcy et al., 1998; Wagner et al., 1999).

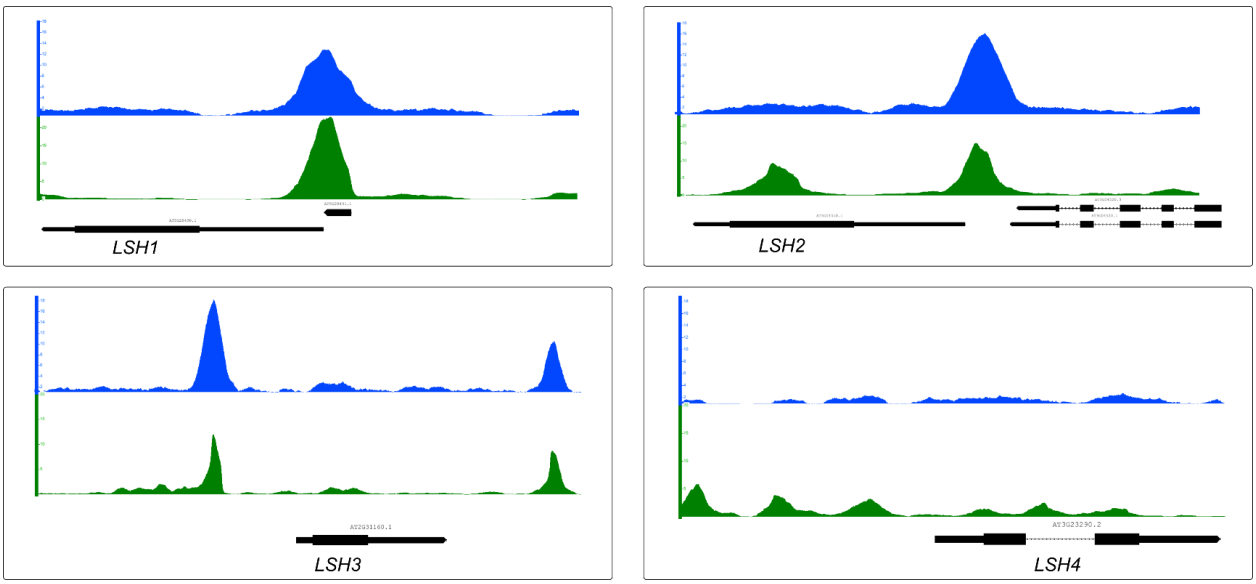

Figure 4: LFY strongly binds the promoter of *LSH1*, *LSH2* and *LSH3 in vitro* and *in vivo*. *Integrated Genome Browser (IGB) view of selected genome regions showing LFY ChIP-seq signals in inflorescence (blue; Goslin et al., 2017) and LFY ampDAP-seq signals (green; Lai et al., 2021). Clear peaks are identified in the promoters of* LSH1*,* LSH2 *and* LSH3 *but not in the promoter of LSH4.*

However, LFY binds hundreds of regions in ChIP, and the significance of such binding has not been studied in most cases. When looking at LFY ChIP-seq data from inflorescences (Goslin et al., 2017), we found massive peaks in the promoter of three genes called *LIGHT SHORT HYPOCOTYL 1* (*LSH1*), *LSH2* and *LSH3* (Figure 4). Canonical LFYBS were identified below these peaks, strongly suggesting direct LFY binding. When looking at non-published transcriptomic and qRT-PCR data, we found that LFY likely negatively regulates these genes. However, the role of this possible regulation has not been described. We especially focused on this regulation in Chapter III. Hence, even if LFY's binding is well described, the consequence of its binding at several loci has not been studied and many LFY-dependent regulations are still to be discovered.

LFY acts with cofactors

LFY is expressed ubiquitously in the young FM where it activates key floral genes. However, this master regulator has to be tightly controlled to express specific genes (like *ABC* genes) in

delineated territories. To spatially regulate its activity, several cofactors specify LFY's transcriptional functions.

A major experiment revealing the different LFY mechanisms of activation was the study of LFY-VP16 (Parcy et al., 1998). The VP16 domain is the activation domain from the viral VP16 protein (Cousens et al., 1989); this domain strongly enhances the ability of the protein fused to it to initiate translation. Hence, LFY-VP16 is an activated form of LFY that strongly induces target genes whenever LFY binds in the genome. While some LFY direct target genes like *AP1* or *AG* are highly expressed in plants expressing *pLFY::LFY-VP16*, others LFY targets like *AP3* are normally expressed (Parcy et al., 1998). The main explanation is that LFY activates some targets directly while other activations require the presence of cofactors, and the addition of the VP16 domain to LFY is not sufficient to bypass their action. This experiment also shows that depending on target genes, LFY acts through different molecular mechanisms. Thus, LFY is a complex TF with a highly adjustable activity.

The fact that LFY does not act alone is further validated by the analysis of LFY ChIP-seq data. In fact, the comparison between ampDAP-seq (*in vitro*) and ChIP-seq (*in vivo*) data revealed that LFY binds several loci in the genome where its presence cannot be explained by LFY direct binding to its canonical LFYBS (Lai et al., 2021). Other factors may recruit LFY to these sites where LFY cannot bind alone. This implies that LFY has several binding mechanisms, likely in cooperation with cofactors. I have particularly focused on this last point.

Several genetic studies focused on identifying LFY cofactors. It has been shown that LFY acts with WUSCHEL (WUS) to activate *AG* in the 3rd and 4th whorls (Lohmann et al., 2001), but the precise molecular mechanism for their joint action is not entirely understood. Another crucial LFY cofactor is UNUSUAL FLORAL ORGANS (UFO). UFO is strictly required for LFY-dependent activation of the *B* gene *AP3* (Lee et al., 1997; Levin and Meyerowitz, 1995; Wilkinson and Haughn, 1995). In that case as well it is not clear how UFO modulates LFY functions.

Hence, even if LFY is a well described TF, several questions about how it performs its functions are not yet answered. In particular, how LFY's activity is modulated by cofactors is not understood at the molecular level. A major part of my PhD was to study the role of UFO, and the next part of the introduction is dedicated to the description of this LFY cofactor.

II. UNUSUAL FLORAL ORGANS (UFO) is an F-box protein playing a crucial role during flower development

In this part, I focus on *Arabidopsis thaliana*; information on other species is further detailed in Chapter II.

UFO is a crucial gene for flower development

UFO affects several developmental steps during flower development

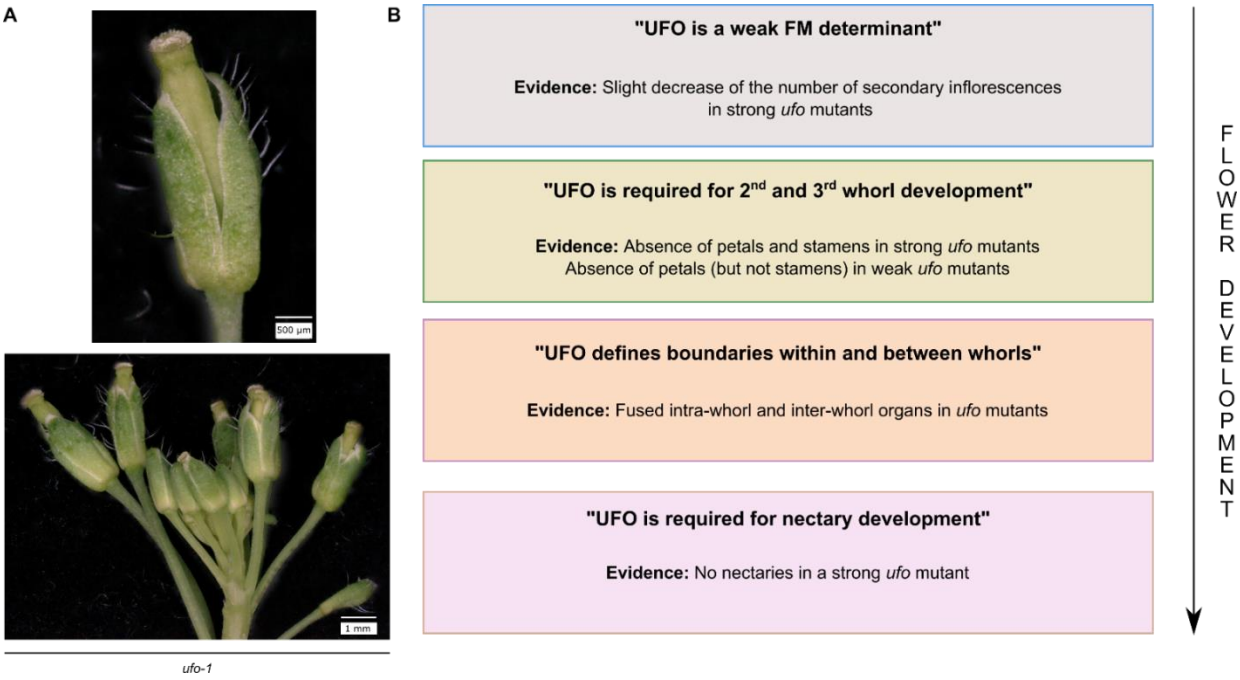

Figure 5: The phenotype of the *ufo* mutant reveals the separable roles of UFO during flower development. (A) *Pictures of* ufo-1 *inflorescence and flowers. Note the absence of petals and stamens.* **(B)** *UFO has several functions during flower development.*

The first Arabidopsis *ufo* mutants were described in the 1990's (Levin and Meyerowitz, 1995; Wilkinson and Haughn, 1995). In Arabidopsis, the most severe phenotypes of *ufo* mutants are observed in flowers (Figure 5A). The phenotype of strong *ufo* mutants is very complex and informative about the multiple functions UFO performs during flower development. A more complete description of *ufo* mutants in several species is provided in Article 2.

The various genetic studies on *UFO* (Durfee et al., 2003; Laufs et al., 2003; Lee et al., 1997; Levin and Meyerowitz, 1995; Wilkinson and Haughn, 1995) were very precise in describing UFO functions and its relations with other floral genes. In Arabidopsis, UFO performs several functions summarized in Figure 5B. The most obvious function of UFO is to allow the development of petals and stamens (2nd and 3rd whorls of flowers), as these organs are not produced in strong *ufo* mutants. UFO performs other functions, and some are revealed only in weak *ufo* mutants or in double mutants (Durfee et al., 2003; Levin and Meyerowitz, 1995). For example, *ap1 ufo* double mutants do not produce flowers contrarily to single *ap1* and *ufo* mutants, showing that the acquisition of the FM identity is impaired when both genes are not functional (Levin and Meyerowitz, 1995). Hence, the role of UFO in FM determination is more important than evidenced by the analysis of the single *ufo* mutant.

UFO is implicated in the transcriptional regulation of major floral genes

The strong phenotype induced by the *UFO* mutation was quickly linked to defects in the expression of key floral genes. For example, the absence of petals and stamens in *ufo* mutants is explained by the dramatic reduction in the expression of *B* genes (*AP3* and *PI*). Accordingly, ectopic *UFO* expression in Arabidopsis results in enlarged *B* genes expression and the production of ectopic petals and stamens (Lee et al., 1997). Overexpressing *AP3* in the strong *ufo-2* mutant was shown to restore the development of petals and stamens, revealing that *AP3* is the major UFO target in Arabidopsis (Krizek and Meyerowitz, 1996).

In addition to *AP3* (and to a lesser extent *PI*; Honma and Goto, 2000), few other genes have been shown to be deregulated in the *ufo* mutant. One of them is *RABBIT EARS* (*RBE*), a gene implicated in petal development. Indeed, *RBE* is not expressed in a *ufo* mutant (Krizek et al., 2006).

However, the role of UFO in transcription regulation is likely very broad. In fact, plants expressing activated (UFO-VP16) or repressive (UFO-SRDX) forms of UFO display strong floral phenotypes (Chae et al., 2008; Risseeuw et al., 2013). In particular, the spectacular development of flowers out of leaves in plants overexpressing UFO-VP16 revealed that UFO potentially has the ability to activate all the genes necessary to launch flower development (Risseeuw et al., 2013). Hence, UFO likely targets many genes in addition to *B* genes, but few

of these targets are known. All these data show that UFO has a clear role in gene regulation during flower development.

UFO is a member of the large F-box protein family

Despite the strong effect of the *UFO* mutation on the transcription of floral genes, the analysis of UFO sequence did not reveal any resemblance with known TFs. In a publication from 1999, it was reported that UFO N-terminal sequence has a strong similarity with a yeast domain that had been recently described at the time, the F-box domain (Samach et al., 1999). UFO was the first F-box protein to be characterized as such in Arabidopsis.

The F-box domain defines the F-box protein family

The F-box domain consists of a conserved 40-50 amino acids domain first discovered in the cyclin-F protein (Chang et al., 1996). This domain is conserved among eukaryotes and it is often found at the N-terminus of proteins. The F-box protein family comprises protein harboring this domain. While there are less than 100 F-box proteins in human or yeast, this family is much broader in plants. In Arabidopsis, the F-box protein family is one of the largest protein family with about 700 members (Gagne et al., 2002), and other plant genomes also contain hundreds of F-box proteins (900 in rice for example; Jain et al., 2007).

The C-terminal part of F-box proteins comprises different kinds of domain

The C-terminal part of F-box proteins is very variable and several types of domain are found (like LRR, WD40, Kelch-repeat etc). The different C-terminal domains were used to define 42 subfamilies in the F-box protein family (Jain et al., 2007). The C-terminal domain strongly

determines the function of F-box proteins because it is an interface for the interaction with other proteins.

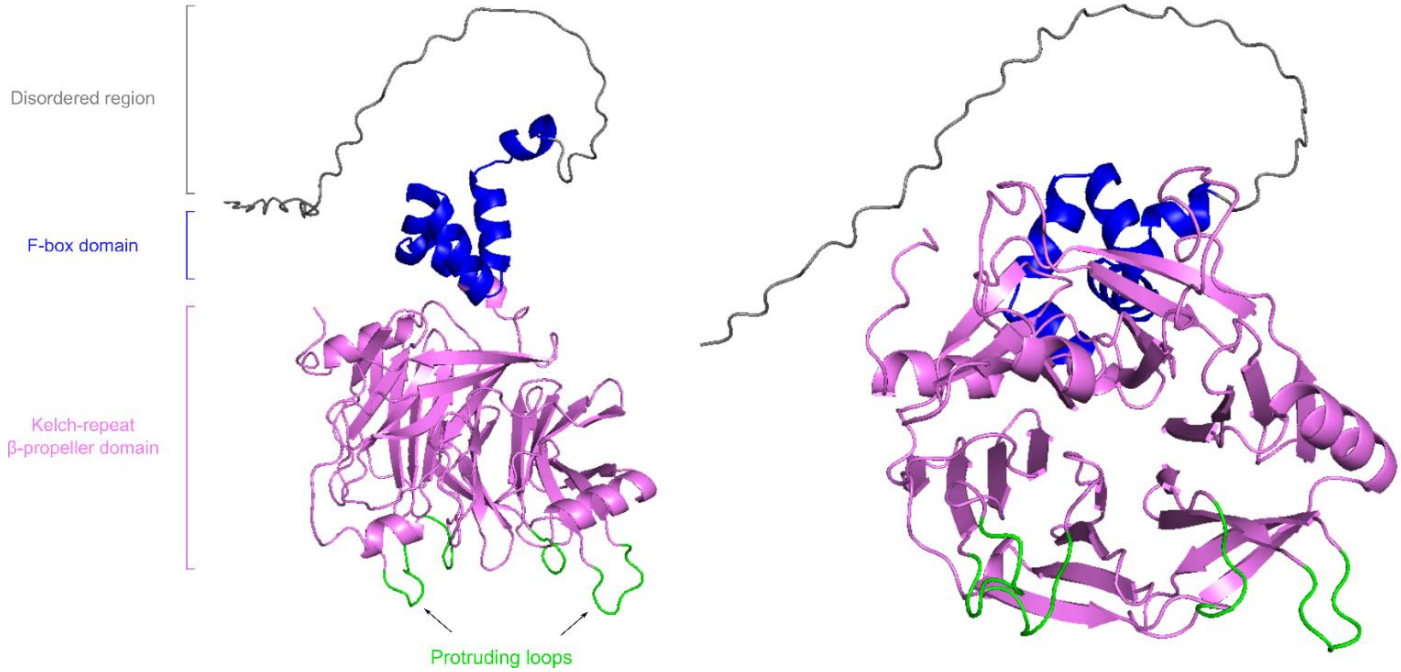

Figure 6: UFO AlphaFold model. *Left picture is a complete view with indicated regions and domains. Right picture is from another angle and shows the central hole of the β-propeller. Loops protruding from the β-propeller with charged residues are colored in green.*

UFO is made of the F-box at its N-terminus and a Kelch-repeat β-propeller domain at the C-terminus. The Kelch motif is a conserved motif of about 50 amino acids forming four antiparallel beta-sheets. The assembly of several Kelch units (more than 4, 6 in the case of UFO) around a central axis forms a β -propeller domain (Figure 6). The Kelch domain is highly represented in plant F-box proteins, and the "Kelch subfamily" has 103 members in Arabidopsis (Schumann et al., 2011).

It has been shown that loops protruding from β-propellers are often implicated in the interaction with other proteins (Adams et al., 2000). The structure of the UFO loops are poorly predicted compared to the core of the β-propeller and their position is difficult to assess precisely. However, these loops contain several exposed charged residues that could contact residues from other proteins.

F-box proteins are implicated in ubiquitination

F-box proteins are part of SCF complexes

The molecular role of F-box proteins was first discovered in yeast. It was shown that F-box proteins are involved in ubiquitination through their implication in the Skp1-Cullin1-F-box (SCF) complex. The SCF complex is a highly conserved complex made of several core subunits including S-phase kinase-associated protein 1 (SKP1; Arabidopsis SKP1-like proteins (ASK) in Arabidopsis), Cullin 1 (CUL1) and RING-box 1 (RBX1).

CUL1 plays the role of a scaffold protein by binding all core SCF subunits. ASK proteins act as adaptors as they interact with both CUL1 and the F-box domain of F-box proteins. In Arabidopsis, there are 21 ASKs proteins, characterized by a specific expression pattern and different affinities toward the various F-box proteins (Gagne et al., 2002). Given the large diversity of the F-box protein family and the various ASK homologs, hundreds of different SCF complexes can theoretically form. UFO F-box domain was shown to bind specific ASKs *in vitro*, notably ASK1, ASK2 and ASK11 (Gagne et al., 2002; Samach et al., 1999).

$SCF^{F\text{-}box}$ complexes act as E3 ligases in ubiquitination reactions

The F-box protein, through its C-terminal domain, recruits target proteins to the SCF complex. It is commonly accepted that the F-box protein gives specificity to the SCF complex by presenting a precise target. Once the target is recruited, the RBX1-bound E2 enzyme directly transfers a ubiquitin molecule to specific lysine residue(s) on the target protein. If this process is repeated, it leads to the formation of a poly-ubiquitin chain on the target protein. The presence of a poly-ubiquitin chain is a tag recognized by the 26S proteasome, leading to the degradation of the poly-ubiquitinated protein. However, the type of ubiquitination (poly or mono-ubiquitination), the type of ubiquitin chain (K48-linked or other) and the site of ubiquitination on a target protein cannot be accurately predicted.

F-box protein in plants: the example of jasmonate signaling and SCF^{COI}

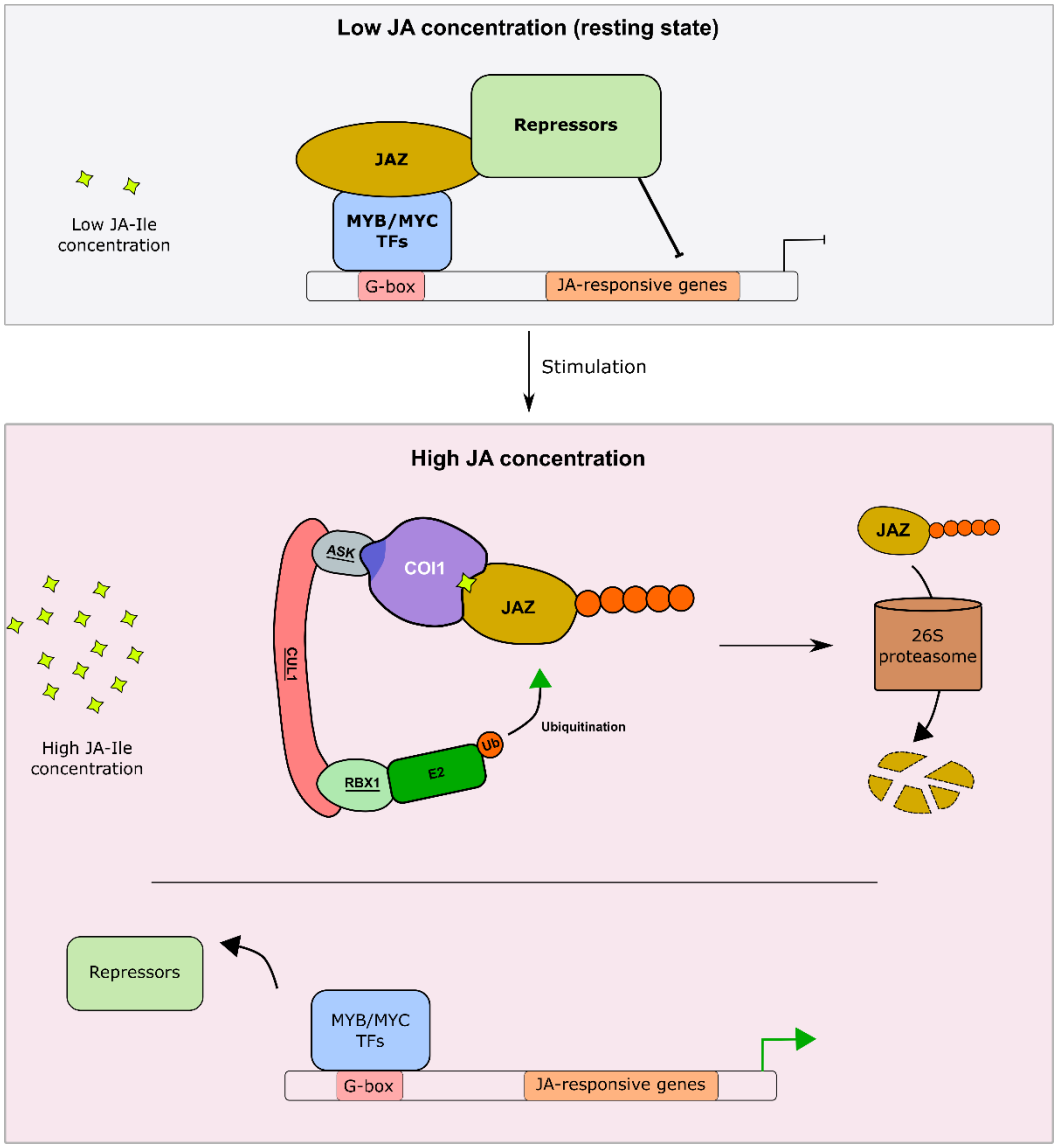

Figure 7: SCF^{COI1} is implicated in jasmonate signaling. *Adapted from Wasternack et al., 2013. See the text for description.*

Since the discovery of the SCF complex, many SCF$^{F\text{-}box}$ complexes have been described in plants, and many of them play crucial roles in plant physiology. The number of processes in which F-box proteins take part is very large: hormone signaling, defense against pathogens, development, light signaling, etc. (reviewed in Stefanowicz et al., 2015). To illustrate this diversity and to present how a canonical F-box protein works, I have selected a famous example showing the role of a canonical F-box in jasmonate signaling.

Jasmonate (JA) is a key hormone for plant response to biotic and abiotic stresses (Wasternack and Hause, 2013). In the absence of the hormone, the jasmonate ZIM-domain (JAZ) proteins interact with MYB/MYC TF and block the activation of JA-responsive genes (Figure 7; Chini et al., 2007; Thines et al., 2007). The presence of JA-Ile (the active form of the hormone) favors the interaction between the F-box protein CORONATIN-INSENSITIVE 1 (COI1) and JAZ proteins through the "molecular glue" mechanism (Sheard et al., 2010). SCF^{COI1} then targets JAZ proteins for degradation, releasing MYB/MYC transcriptional activity. This example shows the canonical function of an F-box within an SCF complex.

Little is known on UFO at the molecular level

Despite its major role in flower development, little is known on UFO molecular functions. UFO likely takes part into an SCF complex because it strongly interacts with several ASK proteins (Samach et al., 1999). Furthermore, there are evidences that this complex is functional *in planta* (see Article 2). Thus, if SCF^{UFO} forms, a major question is which proteins it targets for ubiquitination. Y2H screens were performed to identify putative UFO targets but they did not allow identifying clear targets in Arabidopsis and in other species (Samach et al., 1999; Article 2). Apart from ASK proteins, the only clear UFO interactant is LFY (Chae et al., 2008), and the role of this interaction is further discussed in the next part.

Hence, the role of UFO in transcription regulation and its implication within an E3 ligase complex are well-established. However, the link between these two functions is not straightforward, and in the next part I will present how UFO could modulate transcription by acting as a LFY cofactor through ubiquitination.

III. LFY and UFO regulate transcription together but the molecular mechanism underlying this synergy is unknown

LFY and UFO activate genes together through an unknown molecular mechanism

When the *ufo* mutant was first described, it was noted that *lfy* and *ufo* mutant phenotypes share many similarities. The fact that the *lfy ufo* double mutant is very similar to single *lfy* mutants confirmed the genetic interaction between the two genes (Levin and Meyerowitz, 1995; Wilkinson and Haughn, 1995).

A major characteristic shared by both *lfy* and *ufo* mutants is the strong reduction of the expression of the *B* gene *AP3*. It was shown that LFY and UFO are implicated in the activation of *AP3*, but these experiments did not reveal if this activation is direct or indirect. It has to be noted here that LFY and UFO likely regulate a great number of genes together (see Article 1) but in this introduction I will focus only on *AP3*, their major common target.

A key experiment was the study of the activation of *pAP3::GUS* in seedlings (Parcy et al., 1998). In this tissue, the *AP3* promoter (*pAP3*) is not active, likely because its floral activators are not present. The same staining experiment was then performed with *pAP3::GUS* seedlings harboring a *35S::LFY* or a *35S::UFO* transgene. No staining was observed, revealing that overexpressing *LFY* or *UFO* alone is not sufficient to activate *pAP3*. It also showed that *pAP3* activation by LFY alone (or UFO alone) is not direct and requires other factors. However, overexpressing both *LFY* and *UFO* induced a strong staining in *pAP3::GUS* seedlings. This experiment revealed a major LFY-UFO synergy for the activation of *pAP3*. However, it was not understood with this experiment why *pAP3* activation required both LFY and UFO.

Then, other studies focused on understanding this synergy at the molecular level. Chae et al. proved the physical interaction between LFY and UFO using several *in vivo* and *in vitro* methods (Chae et al., 2008). Mapping of the interaction revealed that it implies LFY DBD and UFO C-terminal Kelch-repeat β-propeller domain in Arabidopsis. Because of the physical interaction between the two proteins, it was proposed that SCF^{UFO} targets LFY for ubiquitination and that a post-translational modification of LFY triggers its ability to activate

AP3. However, clear ubiquitinated forms of LFY have never been convincingly shown (Chae et al., 2008) and the ability of UFO to target LFY for ubiquitination remained to be demonstrated.

In parallel, it was shown that UFO is present in the vicinity of DNA. In fact, a ChIP-qPCR experiment demonstrated that UFO is recruited to *pAP3* in a LFY-dependent manner (Chae et al., 2008). However, it was not known if and how UFO was recruited at specific loci and what was its role on DNA.

Thus, despite several clues, the precise molecular function of UFO was not elucidated. We therefore analyzed the literature to find examples that could help us to design models for the LFY-UFO molecular mechanism.

Cases of F-box proteins acting directly in transcription regulation are well-documented outside plants

In plant, F-box proteins are usually described for their role in ubiquitination pathways (Stefanowicz et al., 2015). The interaction of UFO with a master TF and its putative role in transcription were very puzzling. We carefully analyzed the plant biology literature and we found no example of such case where an F-box directly regulates transcription.

This led us to look at literature in other species. In species like yeast, drosophila or human, the direct role of F-box proteins in transcription regulation is well described and several models are proposed (Geng et al., 2012). These models helped us in designing possible molecular scenarii describing the LFY-UFO synergy. In the next paragraph I present a famous case in human showing how an F-box directly modulates the activity of a transcriptional regulator.

The time clock model and the example of SRC-3 activation

This example is based on the study by Wu et al. (Wu et al., 2007) and shows how an F-box protein triggers the activation of transcription. I have selected this example because it illustrates very well how both proteolytic and non-proteolytic ubiquitination modulate the activity of a transcriptional regulator.

In this paper, authors analyzed the control of the activation of Steroid Receptor Coactivator-3 (SRC-3), a human transcriptional cofactor (Figure 8). First, they show that SRC-3 is phosphorylated at specific residues (S505 and S509) by a kinase called GSK3.

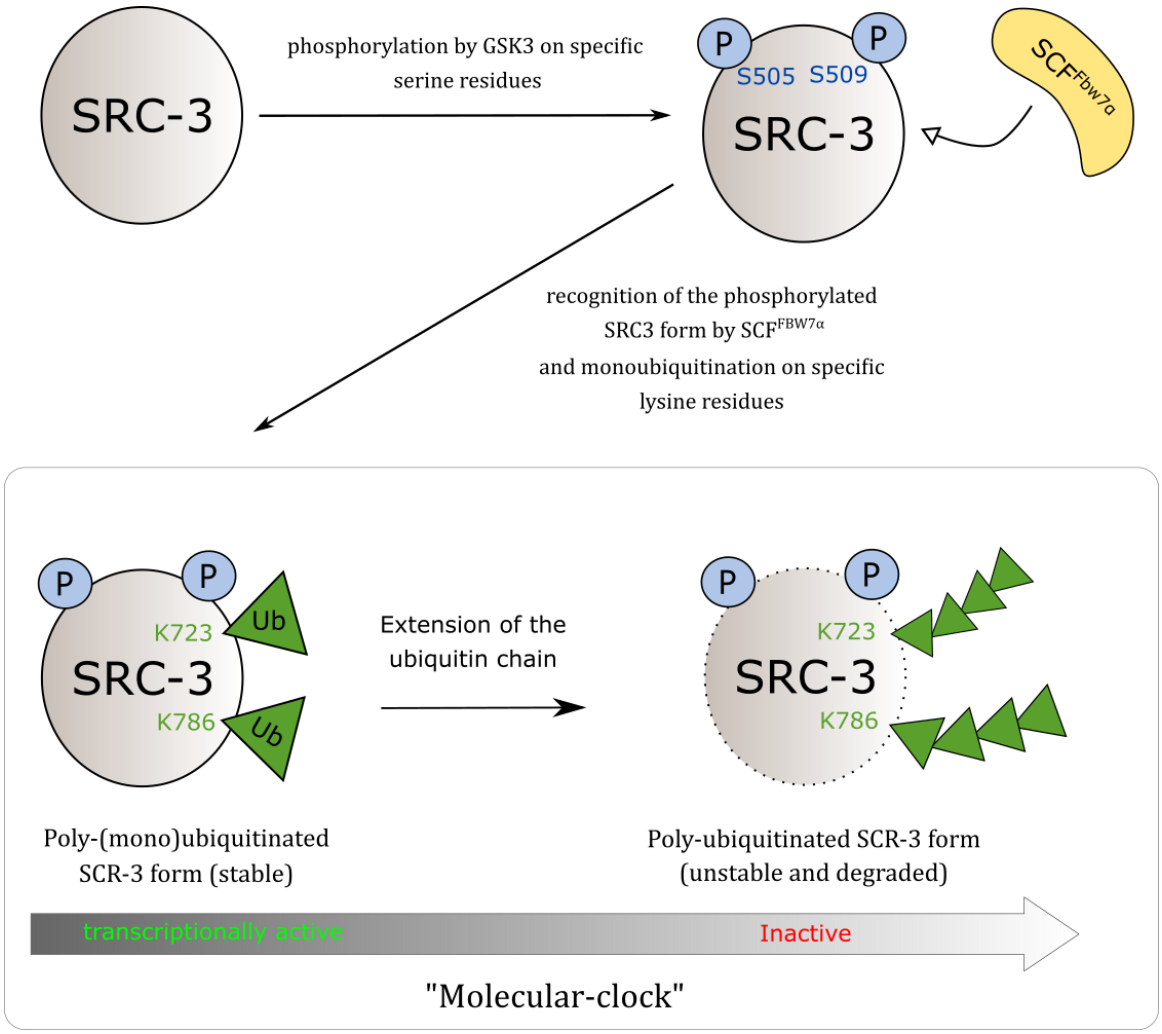

Figure 8: The transcriptional activity of the human SRC-3 coactivator is regulated by phosphorylation and ubiquitination.

Next, they demonstrate that SRC-3 phosphorylation is required for the interaction with a $SCF^{Fbw7\alpha}$ E3 ligase complex. The $SCF^{Fbw7\alpha}$ complex induces a precise SRC-3 ubiquitination pattern, with mono-ubiquitination of specific SRC-3 lysine residues. Only this mono-ubiquitinated form of SCR-3 is transcriptionally active, and the transition from mono-ubiquitination to poly-ubiquitination of SRC-3 is coupled with the progression of transcription.

The elongation of the ubiquitin chains leads to the recognition by the proteasome and the final degradation of SRC-3. The time frame during the transition from a mono-ubiquitinated SRC-3 active form to the poly-ubiquitinated SRC-3 defines a window of activation and explains how a transcriptional cofactor can be regulated by an F-box protein. This model has been called the transcriptional "time clock" model and applies to several other cases.

The role of non-proteolytic and proteolytic ubiquitination in the regulation of transcription

Like in the case of SRC-3, non-proteolytic ubiquitination can deeply affect the activity of a TF or a transcriptional cofactor. The most represented non-proteolytic ubiquitination induced by F-box proteins playing a role in transcription is mono-ubiquitination. Mono-ubiquitination of a TF (or of a cofactor) can change its activity in many different ways. Mono-ubiquitination can activate a TF by making it able to recruit the transcription machinery, by changing its cellular localization (van der Horst et al., 2006), by repressing its degradation or its removal from DNA by other factors (Archer et al., 2008) or by modifying its DNA binding properties, etc. Despite the major impact of mono-ubiquitination on transcription activators or coactivators, no general rule can apply and each case has its own specificity.

Proteolytic control of TFs can also positively regulate their activity. This property appeared counterintuitive when it was first discovered because it was hard to understand how degradation of a TF could favor its activity. Several models have now been proposed to solve this apparent problem (Kodadek et al., 2006). A major answer is that degrading a TF can increase its turnover. Like in the case of SRC-3, it is necessary to remove "spent" molecules (often "marked" as such by phosphorylation) to allow the new ones to perform their function. If these marked molecules are not removed by degradation the molecular mechanism is impeded. Another major role of proteolytic regulation is to degrade repressors. There are examples in the literature showing that the activity of a TF can be activated after the degradation of a repressor by an E3 ligase (McShane and Selbach, 2014). Models for proteolytic control of transcription are often complex, and like for mono-ubiquitination, each case has its own specificities.

Several molecular mechanisms could explain the LFY-UFO synergy

Based on the analysis of the different models described in the literature, we then hypothesized mechanisms that could explain the joint role of LFY and UFO in transcription regulation. In many examples where F-box proteins regulate TF activity, TF phosphorylation is a critical initial step in the molecular mechanism. However, in the case of LFY, no kinases are known to interact with it and LFY phosphorylation has never been described. Hence, even if a LFY phosphorylation is possible, we chose to neglect it in our hypotheses. We also omitted some models because they could not fit available data. For example, LFY ubiquitination by SCF^{UFO} followed by major degradation is unlikely. In fact, the experiment in *pAP3::GUS* seedlings revealed a positive LFY-UFO synergy, meaning that the role of UFO is to activate LFY and not to simply degrade it. The mechanisms we considered also included a role for UFO near DNA because UFO is recruited to DNA in a LFY-dependent manner (Chae et al., 2008). The three mechanisms presented in Figure 9 fit with the data available in the literature.

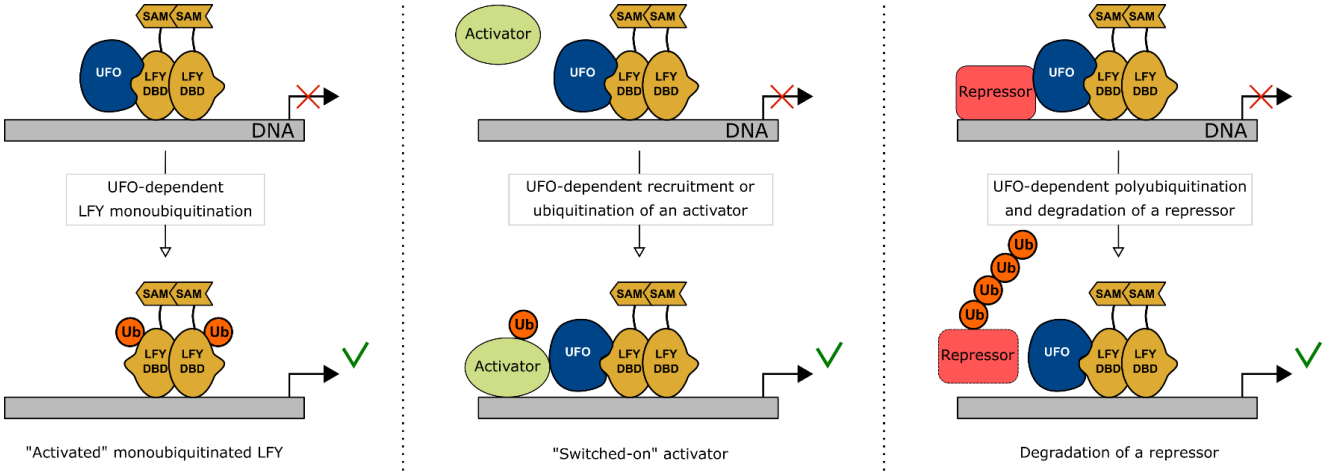

Figure 9: Three possible molecular mechanisms to describe the LFY-UFO synergy. *See the text for description.*

-A first possible mechanism is the activation of transcription by a UFO-dependent LFY mono-ubiquitination. In that case, the addition of a single ubiquitin to LFY could modify its properties like its DNA binding specificity or its ability to interact with other partners. To test this hypothesis, it would have been necessary to prove the existence of a UFO-dependent LFY

ubiquitination and to identify LFY exposed lysine residues where ubiquitination could happen. In that case, mutating these LFY residues should abolish the LFY-UFO synergy.

-Another possibility is that LFY and UFO positively regulate the activity of an unknown regulator. For example, this activator may not interact with LFY or UFO alone but with LFY-UFO, and this could explain the observed LFY-UFO synergy. In this scenario, the SCF^{UFO}-dependent ubiquitination of the activator should increase its transcriptional activity.

-Inversely, it is possible that LFY and UFO negatively regulate a repressor together. In that case, the role of LFY could be to recruit UFO to specific loci in the genome to target this repressor for degradation.

The last two hypotheses were more difficult to test because in addition to prove the role of a SCF^{UFO}-dependent ubiquitination, activator(s) and repressor(s) were to be identified. Thus, we started this project with the goal to test these models.

OBJECTIVES

The goal of my PhD was to decipher the molecular mechanism underlying the LFY-UFO synergy. Several scenarii were proposed in previous studies but the molecular mechanism for the joint role of LFY and UFO remained to be determined. The ability of an F-box protein to directly regulate transcription was never described in plants, and we thought that it might imply an original molecular mechanism.

The first and the second chapters are focused on the molecular bases of the LFY-UFO synergy in transcriptional regulation. In these two chapters, I try to answer different questions:

- **Is UFO-dependent ubiquitination required for the LFY-UFO synergy?**
- **Why is *AP3* specifically activated by LFY-UFO and are there LFY-UFO response elements in its promoter sequence? More generally which genes are regulated by LFY in a UFO-dependent manner?**
- **Which residues of LFY and UFO are implicated in the LFY-UFO interaction and is it possible to find mutations disrupting their synergy?**
- **Is the LFY-UFO interaction conserved and what are its roles in other species?**

The third chapter is independent from the first two and is dedicated to the study of the biochemical properties of ALOG TFs. Indeed, few biochemical data were available on this putative new class of TF. I tried to better characterize their properties by answering the following questions:

- **Are ALOG TFs and what is their DNA binding specificity?**
- **Is it possible to obtain the structure of the ALOG domain?**
- **What are the genes regulated by the ALOG in Arabidopsis and in other species?**

CHAPTER I:

The F-box cofactor UFO redirects the LEAFY floral regulator to novel *cis*-elements

Several studies previously focused on the LFY-UFO interaction, notably on the genetic side. Still, many questions on the molecular mechanism remained unanswered. In previous studies, the main hypothesis was that UFO acts primarily via ubiquitination to regulate LFY activity. In this first chapter, I present most of the results we obtained on the molecular mechanism underlying the LFY-UFO interaction. We show that in Arabidopsis the role of UFO in ubiquitination pathways in mostly dispensable, and that instead UFO acts as a LFY cofactor by forming a transcriptional complex with this TF on newly characterized *cis*-elements.

I. Introduction

The choice of *Arabidopsis thaliana* to study the LFY-UFO interaction

To decipher how LFY and UFO jointly regulate flower development, we chose to work with the model plant *Arabidopsis thaliana*. Other species could have been used to study the LFY-UFO synergy like tomato or petunia where the role of UFO homologs was already analyzed (see Article 2). In fact, UFO is only required for a subset of LFY functions in Arabidopsis (Krizek and Meyerowitz, 1996) while in some other species UFO homologs are strictly required for proper FM or IM development. However, most previous studies were performed in Arabidopsis and many data were already available, especially genomic and structural data.

Genomic data: LFY ChIP-seq and LFY ampDAP-seq data, which are available only in Arabidopsis, were particularly useful to study the LFY-UFO synergy. In fact, their comparison revealed all the loci where LFY binding cannot be solely explained by direct binding to canonical LFYBS (Lai et al., 2021). Hence, we assumed that UFO would allow to understand a fraction of LFY binding to these regions. Nevertheless, available LFY ChIP-seq data also have some limitations. The best dataset was obtained in a ChIP-seq experiment performed with *LFY* overexpressing seedlings (Sayou et al., 2016) At this stage, LFY has no crucial physiological role in Arabidopsis and most of its floral cofactors are not expressed (for example *UFO* is not expressed at this stage except in the SAM; Long and Barton, 1998). Another LFY ChIP-Seq dataset was obtained in *ap1 cauliflower* inflorescences with an inducible version of LFY but the quality of this dataset is lower and the identification of peaks is more difficult (Goslin et al., 2017).

Structural data. The structure of the Arabidopsis LFY DBD (the LFY domain interacting with UFO) was previously obtained in the team (Hamès et al., 2008). Having a structure is particularly useful to predict the effect of precise mutations. We used the LFY DBD structure to select which LFY residues to mutate in order to impair the functional interaction with UFO.

Despite many available data, a main limitation for the study of LFY-UFO in Arabidopsis is the difficulty to perform experiments *in planta*. LFY and UFO are both expressed in meristems, a small tissue that cannot be easily collected in large amounts in Arabidopsis (compared to seedlings for example). LFY is not detectable by Western Blot when expressed under its constitutive promoter with our anti-LFY antibody, and no antibody against UFO is available. In addition, *LFY* (and to a lesser extent *UFO*) induce strong phenotypes *in planta* when overexpressed or mutated (homozygous *lfy-12* -/- plants are sterile, *ufo-1 -/-* plants are male sterile and lines overexpressing *LFY* or *UFO* have a greatly reduced fertility). As only *lfy +/-* and *ufo +/-* heterozygous plants are fully fertile, a lot of genotyping is required at each generation to keep plants of interest. Thus, contrarily to most TFs and F-box proteins, performing biochemical experiments on LFY-UFO with Arabidopsis plant extracts is challenging.

These limitations led us to use other techniques to study the LFY-UFO interaction. Here I present two experiments that were crucial to determine the molecular bases of the LFY-UFO synergy. The first one is a transient assay in Arabidopsis protoplasts that I developed at the beginning of my PhD.

Dual Luciferase Reporter Assay (DLRA) in Arabidopsis protoplasts: a versatile tool to study the LFY-UFO transcriptional activity

To better understand the joint role of LFY and UFO in transcription, we decided to focus on *pAP3*, the best-characterized LFY-UFO target (Hill et al., 1998; Lamb et al., 2002; Parcy et al., 1998). This promoter was extensively studied in previous studies with GUS reporter lines, and several *cis*-elements and domains were already characterized (Hill et al., 1998; Tilly et al., 1998). However, the LFY-UFO response elements were not yet identified and it was not understood why *pAP3* was activated by LFY and UFO together but not by LFY alone (Lamb et al., 2002; Parcy et al., 1998).

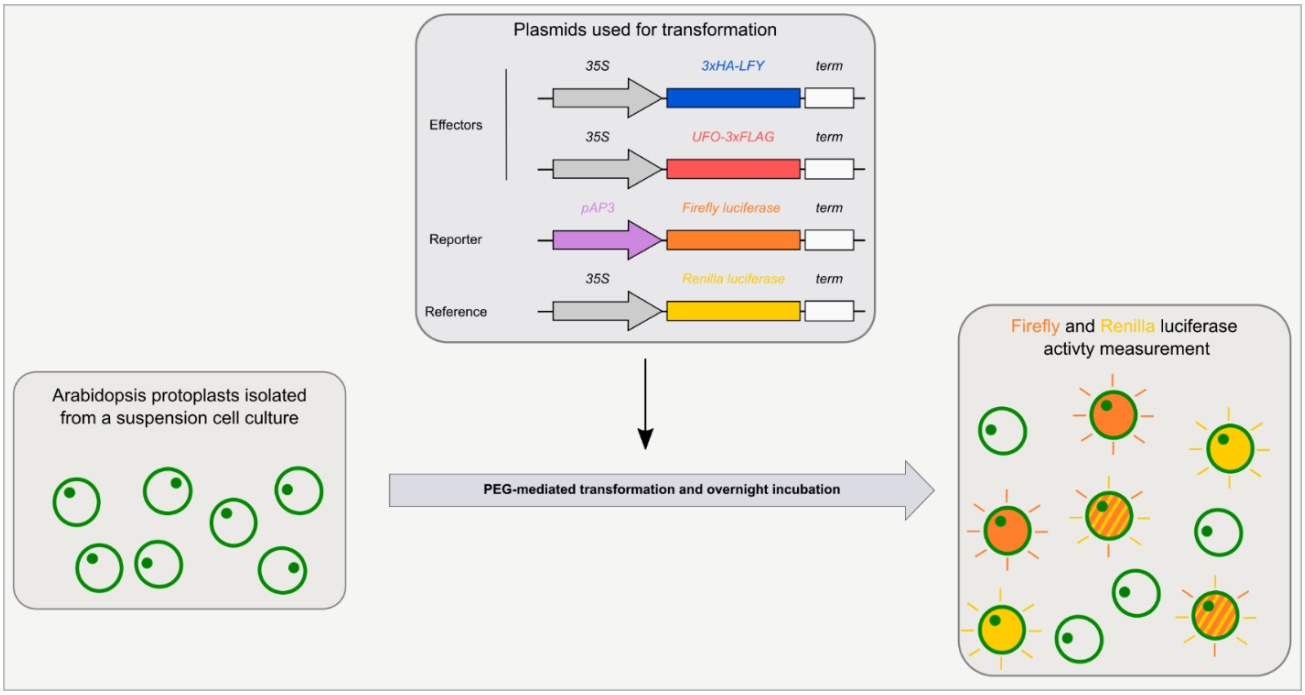

Figure 10: Principle of the Dual Luciferase Reporter Assay in Arabidopsis protoplasts used to study the LFY-UFO transcriptional activity (adapted from Iwata et al., 2011). *Arabidopsis cells from a suspension culture are used to prepare protoplasts. Protoplasts are transformed with a combination of plasmids and after an overnight incubation the activity of the two luciferases is measured.*

It would have been possible to localize *pAP3* LFY-UFO response elements with reporter lines harboring different mutations in the promoter sequence. However, transforming plants is time-consuming and the analysis of several independent transgenic lines is necessary to avoid variability. Thus, to elucidate the transcriptional role of LFY-UFO, we developed a protoplast-based experimental assay. The goal was to design a transient system where both full-length LFY and UFO could be expressed, and in which it could be easy to monitor their synergistic effect on one of their known target.

In plant, popular transient systems are based on protoplasts (isolated cells) or tobacco leaves. We chose to use Arabidopsis protoplasts obtained from a cell suspension culture, as a culture was already available in the institute and because protoplasts are very easy to prepare from cell suspensions. Conditions are also reproducible as the starting material is the same from one experiment to another. Furthermore, protoplasts contain endogenous Arabidopsis

proteins. Compared to other systems like yeast for example, it allows having conditions closer to physiological ones.

In transient assays, the activity of a promoter can be studied by placing it upstream of a reporter gene for which activity can be easily monitored (reporter proteins can be GFP, GUS, luciferase…). We decided to use a dual-luciferase reporter assay, in which the activity of two different luciferases (Firefly and Renilla luciferases) is measured within a single reaction (Figure 10). Firefly luciferase gene is placed under the control of the studied promoter (in our case *pAP3*), while the Renilla luciferase gene is constitutively expressed thanks to the *35S* promoter. The effectors (LFY and UFO in our case) were also overexpressed with the *35S* promoter.

The dual luciferase assay has several advantages. It provides an internal control (the constitutively expressed Renilla luciferase), enabling to assess the transformation efficiency. In fact, with a single reporter gene, high promoter activity can be due to both activation of the studied promoter or high transformation efficiency. Hence, a dual system is less biased and more suitable for precise measurements of a promoter activity. It is also possible with luciferases to measure a broad range of activity with high accuracy (McNabb et al., 2005). Another advantage of this system is that many combinations of effectors/reporter can be tested quickly (effectors alone and reporter alone for example) and with high reproducibility.

However, this assay also has some drawbacks. First, even if protoplasts are prepared from Arabidopsis cells, their cellular context is quite different from meristem cells where LFY and UFO are normally active together. Another strong limitation is that some tested promoters are activated by endogenous protoplasts proteins. For example, we had to use a short 600-bp truncated *pAP1* version to avoid activation of the full-size *pAP1* by endogenous proteins. Finally, effectors are not always highly active in their native form and it is necessary to add an activation domain like the VP16 domain to observe a strong activation.

The protoplast assay allowed us to identify *pAP3 cis*-elements required for the activation by LFY-UFO that we named LFY-UFO Binding Sites (LUBS). Then, it was necessary to complement our results with *in vitro* techniques. However, UFO recombinant protein had never been obtained before. This was a strong limitation for biochemistry experiments and this led us to find a way to obtain the UFO recombinant protein.

Recombinant UFO production and purification in insect cells

Production of recombinant protein is often performed in the bacteria *E. coli* because this system is simple and generally very efficient. In the past, several people in the team tried to express UFO (fused to different common tags like 6xHis or MBP) in bacteria and to purify it. Despite many attempts, these experiments never allowed obtaining recombinant UFO for biochemical experiments. This also explains why there are no experiments with recombinant UFO in the literature. As bacteria are not always able to produce eukaryotic proteins, we then decided to produce UFO in insect cells. We supposed that the presence of a eukaryotic folding machinery in insect cells would help to produce the recombinant UFO protein. Moreover, several publications showed that F-box proteins (like TRANSPORT INHIBITOR RESPONSE 1 (TIR1) or COI1) are well produced in insect cells, especially when co-expressed with ASK1 (Li et al., 2017).

We jointly expressed 6xHis-ASK1 and 6xHis-MBP-UFO in insect cells using the MultiBac system (Geneva Biotech). The initial goal was to purify the complex first by Nickel Sepharose affinity chromatography and then by Dextrin Sepharose affinity chromatography to obtain an equimolar complex. As Dextrin Sepharose affinity chromatography failed, we purified the complex only by Nickel Sepahrose affinity chromatography. After purification, tags were removed by TEV cleavage and the unaggregated ASK1-UFO (or ASK1-UFO-3xFLAG) complex was further purified by Size Exclusion Chromotography and used for *in vitro* experiments.

We also tried to produce and purify the ASK1-UFO-LFY complex with full-length proteins. All proteins were correctly produced but LFY was cleaved after purification (likely between the SAM and the DBD; not shown). We then only produced the stable ASK1-UFO-LFY-DBD complex.

The purification of the ASK1-UFO and ASK1-UFO-LFY-DBD complexes allowed us to perform many *in vitro* experiments like EMSA. However, we were never able to obtain a large amount of the complex (1 or 2 mg maximum and at a low concentration). Thus, it was not possible to perform several experiments like crystallography where large amounts of proteins are needed.

II. Article 1

The F-box protein UFO controls flower development by redirecting the master transcription factor LEAFY to novel *cis*-elements

Philippe Rieu[1], Laura Turchi[1,2], Emmanuel Thévenon[1], Eleftherios Zarkadas[3,4], Max Nanao[5], Hicham Chahtane[1,†], Gabrielle Tichtinsky[1], Jérémy Lucas[1], Romain Blanc-Mathieu[1], Chloe Zubieta[1], Guy Schoehn[3], François Parcy[1*]

[1] Univ. Grenoble Alpes, CEA, CNRS, INRAE, Laboratoire Physiologie Cellulaire et Végétale, IRIG-DBSCI-LPCV, Grenoble, France

[2] Univ. Grenoble Alpes, CNRS, Translational Innovation in Medicine and Complexity, Grenoble, France

[3] Univ. Grenoble Alpes, CNRS, CEA, IBS, F-38000 Grenoble, France

[4] Univ. Grenoble Alpes, CNRS, CEA, EMBL, ISBG, F-38000 Grenoble, France

[5] European Synchrotron Radiation Facility, Structural Biology, Group, Grenoble, France

† Present address: Institut de Recherche Pierre Fabre, Green Mission Pierre Fabre, Conservatoire Botanique Pierre Fabre, Soual, France.

* Corresponding author.

Accepted at Nature Plants on Nov. 25th 2022

Abstract

In angiosperms, flower development requires the combined action of the transcription factor (TF) LEAFY (LFY), and the ubiquitin ligase adaptor F-box protein, UNUSUAL FLORAL ORGANS (UFO), but the molecular mechanism underlying this synergy has remained unknown. Here, we show in transient assays and stable transgenic plants that the connection to ubiquitination pathways suggested by the UFO F-box domain is mostly dispensable. Based on biochemical and genome-wide studies, we establish that UFO instead acts by forming an active transcriptional complex with LFY at newly discovered regulatory elements. Structural characterization of the LFY-UFO-DNA complex by cryo-electron microscopy further demonstrates that UFO performs this function by directly interacting with both LFY and DNA.

Finally, we propose that this complex might have a deep evolutionary origin, largely predating flowering plants. This work reveals a novel mechanism of an F-box protein directly modulating the DNA-binding specificity of a master TF.

Main text

The formation of flowers is key to the reproductive success of angiosperms. Flowers are made of four types of organs (sepals, petals, stamens and carpels) arranged in concentric whorls. The patterning of flower meristems requires the localized induction of the ABCE floral homeotic genes that determine specific floral organ identities. In *Arabidopsis thaliana*, this developmental step is largely controlled by the master transcription factor (TF) LEAFY (LFY) that activates the ABCE genes[1,2]. LFY directly activates the A class gene *APETALA1* (*AP1*) uniformly in the early flower meristem[3,4], while activations of B and C genes are local and require the activity of cofactors. For instance, LFY regulates the C class gene *AGAMOUS* (*AG*) in conjunction with the TF WUSCHEL to specify third (stamen) and fourth whorl (carpel) identities[5]. The activation of the B class gene *APETALA3* (*AP3*), necessary to specify the identity of the second (petal) and third whorls of the flower, requires the combined activity of LFY and the spatially-delineated cofactor UNUSUAL FLORAL ORGANS (UFO)[6–8]. In Arabidopsis, the main function of LFY and UFO is to activate *AP3*[9] but in numerous species (such as rice, wheat, tomato or petunia), their joint role goes well beyond *B* genes activation and is key to floral meristem and inflorescence development[10–13].

At the molecular level, little is known on the nature of LFY-UFO synergy. Unlike most floral regulators, *UFO* does not encode for a TF but for an F-box protein, one of the first to be described in plants[14–16]. UFO is part of a SKP1-Cullin1-F-box (SCF) E3 ubiquitin ligase complex through the interaction of its F-box domain with ARABIDOPSIS SKP1-LIKE (ASK) proteins[15,17]. In addition, its predicted C-terminal Kelch-type β-propeller domain physically interacts with LFY DNA Binding Domain (DBD)[18]. As the control of TF activity through proteolytic and non-proteolytic ubiquitination is a well-described mechanism[19], it was suggested that LFY is targeted for ubiquitination and possibly degradation by the SCF^{UFO} complex. Other data showed that adding a repression or an activation domain to UFO changes its activity and that UFO is recruited at the *AP3* promoter in a LFY-dependent manner, rather suggesting a more direct role of UFO in gene regulation[18,20]. However, direct evidence explaining how UFO

regulates a specific subset of LFY targets was still missing and the molecular mechanism underlying LFY-UFO synergistic action remained elusive.

Here, we show that UFO connection to the SCF complex is largely dispensable for its activity and that an important role of UFO is to form a transcriptional complex with LFY at genomic sites devoid of canonical high-affinity LFY binding sites (LFYBS). Our study presents a unique mechanism by which an F-box protein acts as an integral part of a transcriptional complex.

Results

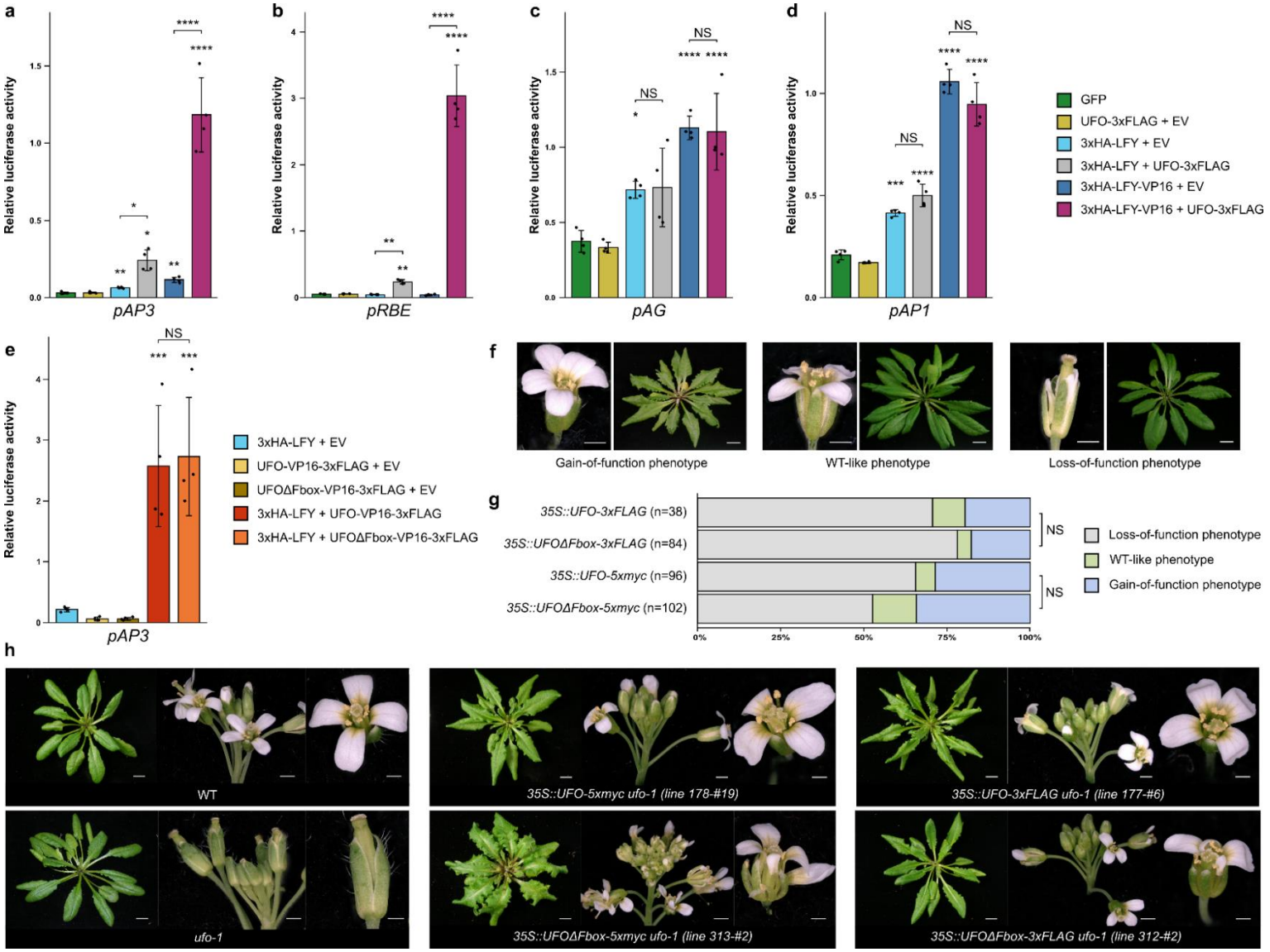

Fig. 1. UFO action is largely independent on its F-box domain. a-e, Promoter activation in Arabidopsis protoplasts, with indicated effectors (right) and promoters (below each graph). EV = Empty Vector. Data are mean ± SD (n = 4 biological replicates). One-way ANOVA with Tukey's multiple comparisons test (**c,d**) or Welch's ANOVA with Games-Howell post-hoc test (**a,b,e**). Stars represent a significant statistical difference compared to GFP (**a-d**) or to 3xHA-LFY+EV (**e**), non-significant (NS) otherwise. Other comparisons are indicated with brackets. (NS: $p > 0.05$,*: $p < 0.05$, **: $p < 0.01$; ***: $p < 0.001$ and ****: $p < 0.0001$). **f,** Representative pictures of the different phenotypic classes obtained in the T1 population of indicated transgenic plants (bars, 1 mm for flowers and 1 cm for rosettes). **g,** Distribution of T1 plants in phenotypic classes as described in (**f**). The distribution of *35S::UFO* and *35S::UFOΔFbox* lines within phenotypic classes is not significantly different (χ^2 tests, NS: $p > 0.05$). n = number of independent lines. **h,** *ufo-1* complementation assay by the *35S::UFO* and *35S::UFOΔFbox* transgenes. Rosette (scale bar, 1 cm), inflorescence (scale bar, 1 mm) and flower (scale bar, 0.5 mm) are shown.

UFO F-box domain is partially dispensable for its floral role. A Dual Luciferase Reporter Assay (DLRA) in Arabidopsis protoplasts was used to study floral promoter activation by LFY and UFO. We used promoter versions known to allow full complementation of mutants or able to recapitulate a WT expression pattern (see Methods). We found that the *AP3* promoter (*pAP3*) was more strongly activated when LFY (or LFY-VP16, a fusion of LFY with the VP16 activation domain) was co-expressed with UFO (or UFO-VP16) than by either effector alone (Fig 1a,e). Similar results were obtained with the promoter of *RABBIT EARS* (*RBE*), another UFO target (Fig. 1b)[22]. We also analyzed the promoters of *APETALA1* (*pAP1*) and *AGAMOUS* (*pAG*), two LFY targets regulated independently of UFO[3,4,21] and that are required for organ identity of the first and second (*AP1*) or third and fourth (*AG*) floral whorls. We found that their activation by LFY and LFY-VP16 were insensitive to UFO (Fig. 1c,d). Thus, the protoplast assay accurately reproduced several floral promoter activation patterns.

We next investigated the involvement of a SCF^{UFO}-dependent ubiquitination pathway in *pAP3* activation by LFY-UFO. We found that, when co-expressed with LFY, N-terminally truncated UFO versions lacking the F-box domain (UFOΔFbox and UFOΔFbox-VP16) activated *pAP3* similarly to the full-length (FL) UFO (Fig. 1e). Thus, the connection of UFO to an SCF complex appears dispensable for the *pAP3* activation in transient protoplast assays. The previously reported inactivity of UFO with an internal deletion of its F-box likely reflects the poor folding of this protein variant rather than the functional importance of the F-box domain (Extended Data Fig. 1a-c)[20].

We also constitutively expressed tagged versions of UFO and UFOΔFbox in Arabidopsis. Irrespective of the presence of the F-box, plants displaying a detectable UFO or UFOΔFbox expression (Extended Data Fig. 1d) showed a typical UFO gain-of-function phenotype (Fig. 1f,g). In addition, both UFO versions complemented the strong *ufo-1* mutant and induced gain-of-function phenotypes (Fig. 1h and Extended Data Fig. 1e,f)[8]. Still, minor defects (such as some missing or misshapen petals and disorganized flowers) were specifically observed in the absence of the F-box, suggesting that this conserved domain might be important for a subset of UFO functions (Fig. 1h and Extended Data Fig. 1g). Overall, UFO and UFOΔFbox have a very similar activity, showing that the role of the F-box domain is largely dispensable and that a ubiquitination-independent mechanism determines the LFY-UFO synergy.

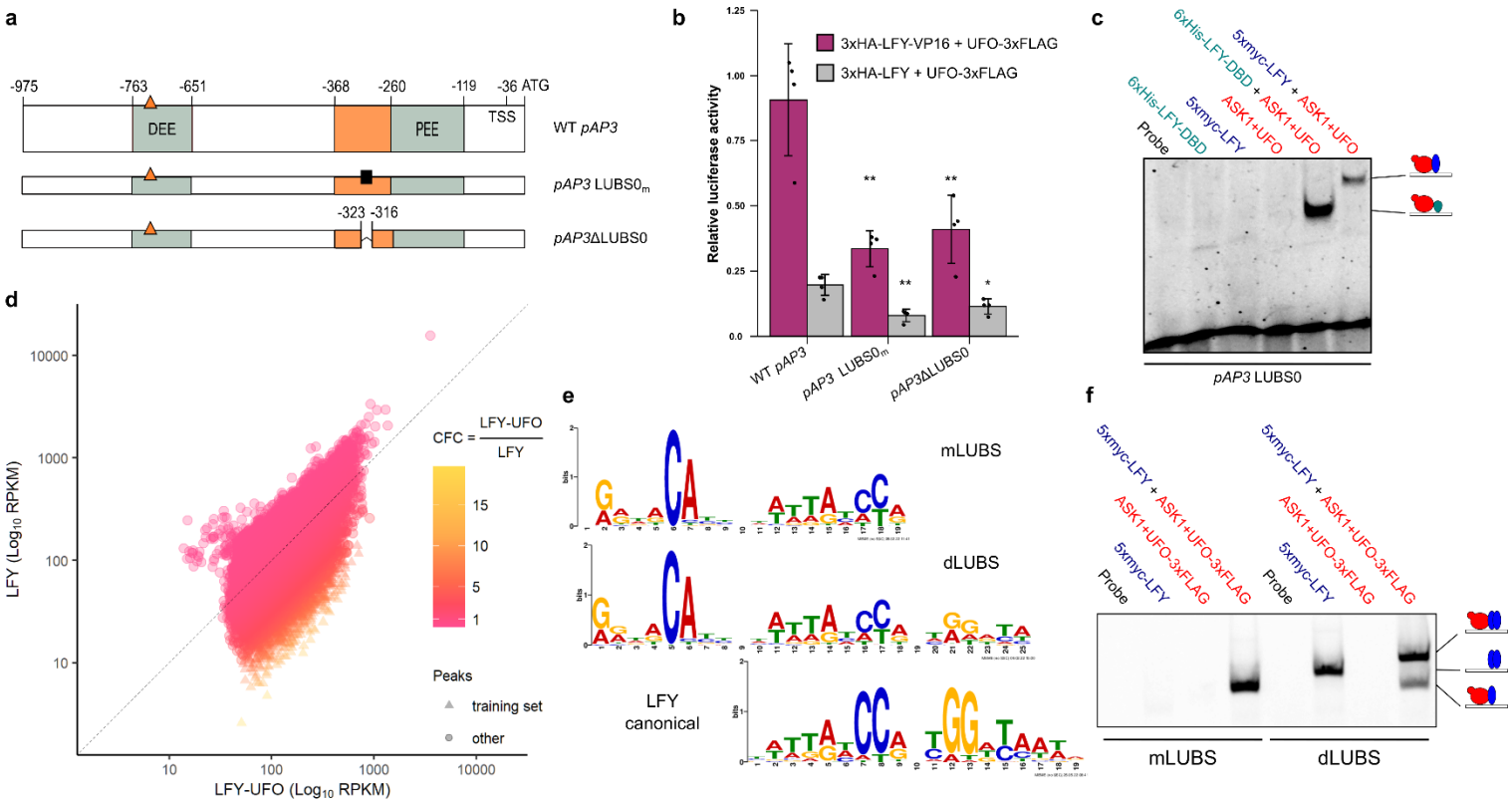

Fig. 2. LFY and UFO together bind a new DNA motif. a, WT *pAP3* with regulatory regions and *cis*-elements (top line). Coordinates are relative to *AP3* start codon. TSS: Transcription Start Site. Orange triangle represents canonical LFYBS. Detailed functional dissection of the 107-bp region and the LUBS0 mutation are described in Extended Data Fig. 3. Other rows show the promoter versions used in (**b**). **b,** *pAP3* activation in Arabidopsis protoplasts. Data are mean ± SD (n = 4 biological replicates). One-way ANOVA with data from the same effector and Tukey's multiple comparisons tests. Stars represent a significant statistical difference compared to WT *pAP3* (*: $p < 0.05$, **: $p < 0.01$). **c,** EMSA with LUBS0 DNA probe and indicated proteins. Size Exclusion Chromatography coupled to Multi-Angle Laser Light Scattering established a mass of 102 ± 3.3 kDa for the ASK1-UFO-LFY-DBD-LUBS0 complex, consistent with a 1:1:1:1 stoichiometry (Extended Data Fig. 3e). Drawings represent the different complexes with FL LFY (blue), LFY-DBD (pale blue) and ASK1-UFO (red) on DNA. **d,** Comparison of peak coverage in LFY and LFY-UFO ampDAP-seq experiments, colored by CFC. LFY-UFO-specific peaks used to build mLUBS and dLUBS motifs in (**e**) are triangle-shaped. **e,** Logos for mLUBS, dLUBS and LFY binding site. The LFY logo was generated using the 600 peaks with the strongest LFY ampDAP-seq signal. **f,** EMSA with mLUBS and dLUBS highest score sequence DNA probes. Drawings represent the different complexes with LFY (blue) and ASK1-UFO (red) on DNA.

LFY and UFO form a transcriptional complex on a new DNA motif. Protoplast assays established that *AP3* and *RBE* promoter sequences contain the information that dictates their specific activation by LFY-UFO. Several regulatory regions driving *AP3* regulation in early floral meristem have been identified, including the Distal and the Proximal Early Elements (DEE and PEE; Fig. 2a)[23,24]. The DEE contains a predicted canonical LFY Binding Site (LFYBS) but in protoplasts, like in plants[24], this site is not sufficient to explain *pAP3* activation (Extended Data Fig. 2). By systematically testing *AP3* promoter variants in the transient assay, we identified a 20-bp DNA element around the PEE important for LFY-UFO-dependent activation but devoid of canonical LFYBS (Fig. 2b and Extended Data Fig. 3a-c). We investigated the possibility that LFY and UFO form a complex on this DNA element using electrophoretic mobility shift assay (EMSA). For this, we mixed either recombinant LFY DNA Binding Domain (DBD, the LFY domain interacting with UFO)[18] or *in vitro*-produced FL LFY, with a reconstituted ASK1-UFO complex. None of the proteins bound the DNA probe alone, but a shift was observed when LFY-DBD or FL LFY were mixed with ASK1-UFO (Fig. 2c). Thus, a presumptive ASK1-UFO-LFY complex was formed on a *pAP3* DNA element (hereafter named LFY-UFO Binding Site 0 or LUBS0) that each partner did not bind on its own. We did note that UFO had a weak affinity for DNA as ASK1-UFO shifted the DNA probe when performing EMSA with low competitor DNA concentrations (Extended Data Fig. 3d). Mutating LUBS0 on various bases provided evidence that the formation of the complex is sequence-specific and suggested a bipartite DNA motif (Extended Data Fig. 3f).

To identify all genome regions possibly targeted by the ASK1-UFO-LFY complex, we performed ampDAP-seq (amplified DNA Affinity Purification sequencing) with a reconstituted ASK1-UFO-LFY complex (Extended Data Fig. 4a,b). We identified numerous genomic regions where LFY binding was strongly enhanced by the presence of ASK1-UFO. For each bound region, we computed the ratio (named Coverage Fold Change or CFC) between the coverage of peaks in the presence or absence of ASK1-UFO (Fig. 2d). Searches for enriched DNA motifs in the 600 regions with the highest CFC (> 4.7) identified two bipartite motifs made of a 6-bp RRNRCA (N=A/C/G/T, R=A/G) sequence, 4 bases of variable sequence and either a monomeric or a dimeric site resembling canonical LFYBS but with more variability (Fig. 2e). Consistent with the presence of a sequence resembling LFYBS, we found that *pAP3* activation in protoplasts

required the LFY amino-acid residues involved in binding to canonical LFYBS (Extended Data Fig. 4c,d).

We named the identified motifs mLUBS and dLUBS for monomeric and dimeric LFY-UFO Binding Sites, respectively (Fig. 2e). Since it is observed specifically with ASK1-UFO, the RRNRCA element will be called UFO Recruiting Motif (URM). dLUBS and to a lesser extent mLUBS Position Weight Matrices (PWM) outperformed LFY canonical PWM showing they reliably predicted binding of ASK1-UFO-LFY (Extended Data Fig. 4e). The LFYBS present within the LUBS of high CFC regions tended to have a lower predicted affinity than those present in regions bound by LFY alone (Extended Data Fig. 4f), explaining why LFY binding to those sequences occurs only with UFO and the URM. Remarkably, we also identified the URM *de novo* from published LFY ChIP-seq data (Extended Data Fig. 4g)[25]. Moreover, we found that the LFY-ChIP-seq performed in inflorescences[25] correlates better with the ASK1-UFO-LFY ampDAP-seq than with the LFY ampDAP-seq (Spearman rank correlation 0.481 vs 0.338 for the first 1000 ChIP-seq peaks), strongly suggesting that many regions are bound *in vivo* by UFO (see examples of such regions in Extended Data Fig. 7b,c).

AmpDAP-seq findings were validated by EMSA with DNA probes corresponding to optimal mLUBS and dLUBS motifs (Fig. 2f and Extended Data Fig. 4h). We observed a complex of slower mobility with dLUBS as compared to mLUBS, consistent with the presence of two LFY molecules on dLUBS. ASK1-UFO also supershifted LFY bound to canonical LFYBS from *pAP1* and *pAP3* DEE (Extended Data Fig. 4i), sometimes (but not systematically) increasing apparent LFY binding.

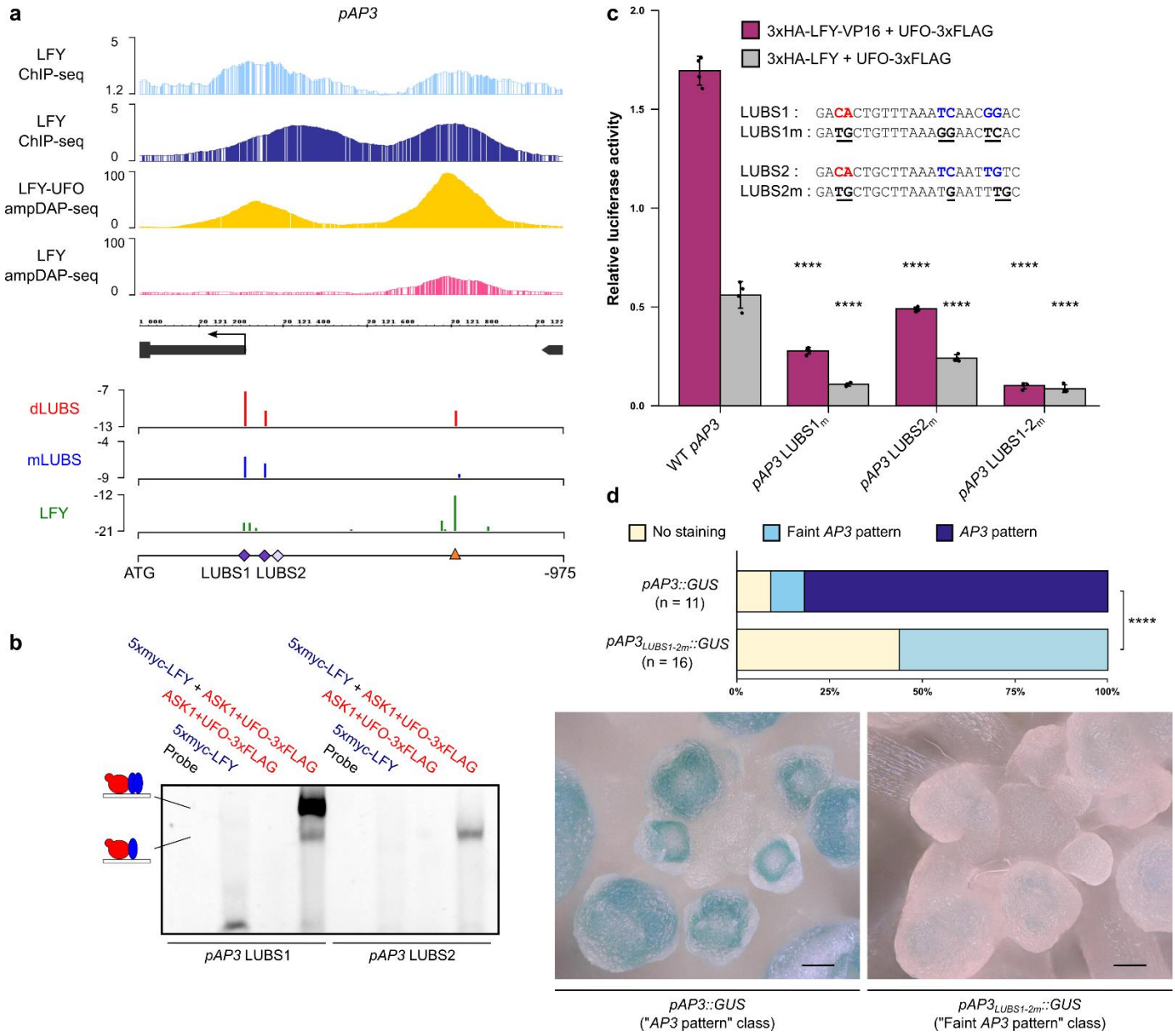

Fig. 3. Functional validation of LUBS. a, Integrated Genome Browser (IGB) view of *pAP3* showing LFY ChIP-seq in inflorescences (light blue)[25] or seedlings (dark blue)[26], LFY-UFO ampDAP-seq (yellow) and LFY ampDAP-seq (pink)[27], y-axis indicates read number range (top). Identification of LUBS in *pAP3* (bottom). Predicted binding sites using dLUBS and mLUBS models and LFY PWM, y-axis represents score values. LUBS1 and LUBS2 are indicated with purple squares, canonical LFYBS as an orange triangle. LUBS0 (light purple square) is not visible because of its low score. **b,** EMSA with *pAP3* LUBS probes. Drawings represent the different complexes involving LFY (blue) and ASK1-UFO (red) on DNA. **c,** *pAP3* activation in Arabidopsis protoplasts. Effect of mutations (underlined) in URM (red) and LFYBS (blue) bases of *pAP3* LUBS were assayed. Data are mean ± SD (n = 4 biological replicates). One-way ANOVA performed with data from the same effector and with Games-Howell post-hoc test. Stars

represent a statistical difference compared to WT promoter (****: $p < 0.0001$). **d,** *In vivo* analysis of *pAP3::GUS* fusions. Percentage of transgenic lines with an *AP3* pattern, a faint *AP3* pattern or absence of staining (top). Pattern distributions are different between the two constructs (χ^2 test, ****: $p < 0.0001$). n = number of independent lines. Representative pictures of plants with an *AP3* pattern (bottom left) and a faint *AP3* pattern (bottom right, scale bar, 50 µm). Note the staining in the ring corresponding to 2nd and 3rd whorl primordia in the left picture.

LUBS are functional regulatory elements. Examination of *pAP3* genomic region in ASK1-UFO-LFY ampDAP-seq revealed a peak that is absent in the experiment performed with LFY alone (Fig. 3a). This peak is roughly located on the PEE and is consistent with LFY ChIP-seq peaks[25,26]. We searched for LUBS under this peak and, to our surprise, we identified several sites predicted to be better than LUBS0 (Fig. 3a). In EMSA, the two highest score sites, LUBS1 and LUBS2, were specifically bound by LFY in the presence of ASK1-UFO (Fig. 3b and Extended Data Fig. 5a). EMSAs performed with a LFY mutant version affected in its ability to dimerize further confirmed the stoichiometry of LFY-UFO complexes on LUBS1 and LUBS2 (Extended Data Fig. 5b). A similar binding was also observed when combining LFY and UFOΔFbox (Extended Data Fig. 5c,d), consistent with the F-box being facultative for LFY-UFO transcriptional activity (Fig. 1). In the protoplast assay, mutating LUBS1 or LUBS2 (or both) significantly reduced *pAP3* activation (Fig. 3c) with a stronger effect of the LUBS1 mutation. Specifically mutating the URM of *pAP3* LUBS1 and LUBS2, that abolished LFY-UFO binding on individual sites in EMSA (Extended Data Fig. 5e), also reduced *pAP3* activation albeit less effectively than mutating the whole LUBS (Extended Data Fig. 5f). Finally, the previously described *pAP3::GUS* staining pattern in the second and third whorls of Arabidopsis early floral meristems was severely reduced when LUBS1 and LUBS2 were mutated, demonstrating the importance of these sites *in vivo* (Fig. 3d and Extended Data Fig. 5g). Similarly, the *RBE* promoter contains an ASK1-UFO-LFY ampDAP-seq peak that is absent with LFY alone (Extended Data Fig. 6a), and the functional importance of the single LUBS identified under this peak was confirmed using EMSA, transient assay in protoplasts and stable reporter constructs in plants (Extended Data Fig. 6b-e).

In addition to *AP3* and *RBE*, LFY and UFO together likely regulate many other genes in Arabidopsis. To identify such potential LFY-UFO targets, we established a list of genes bound (in ampDAP and ChIP) and regulated by LFY-UFO (Extended Data Fig. 7a). This procedure identified the other B gene *PISTILLATA*, previously proposed as a LFY-UFO target but through

an unknown regulatory element that the LUBS model precisely localized (Extended Data Fig. 7b). We also found floral regulators such as *SQUAMOSA PROMOTER BINDING PROTEIN-LIKE 5* and *FD* as well as novel candidates likely regulated by LFY and UFO (Extended Data Fig. 7a,c).

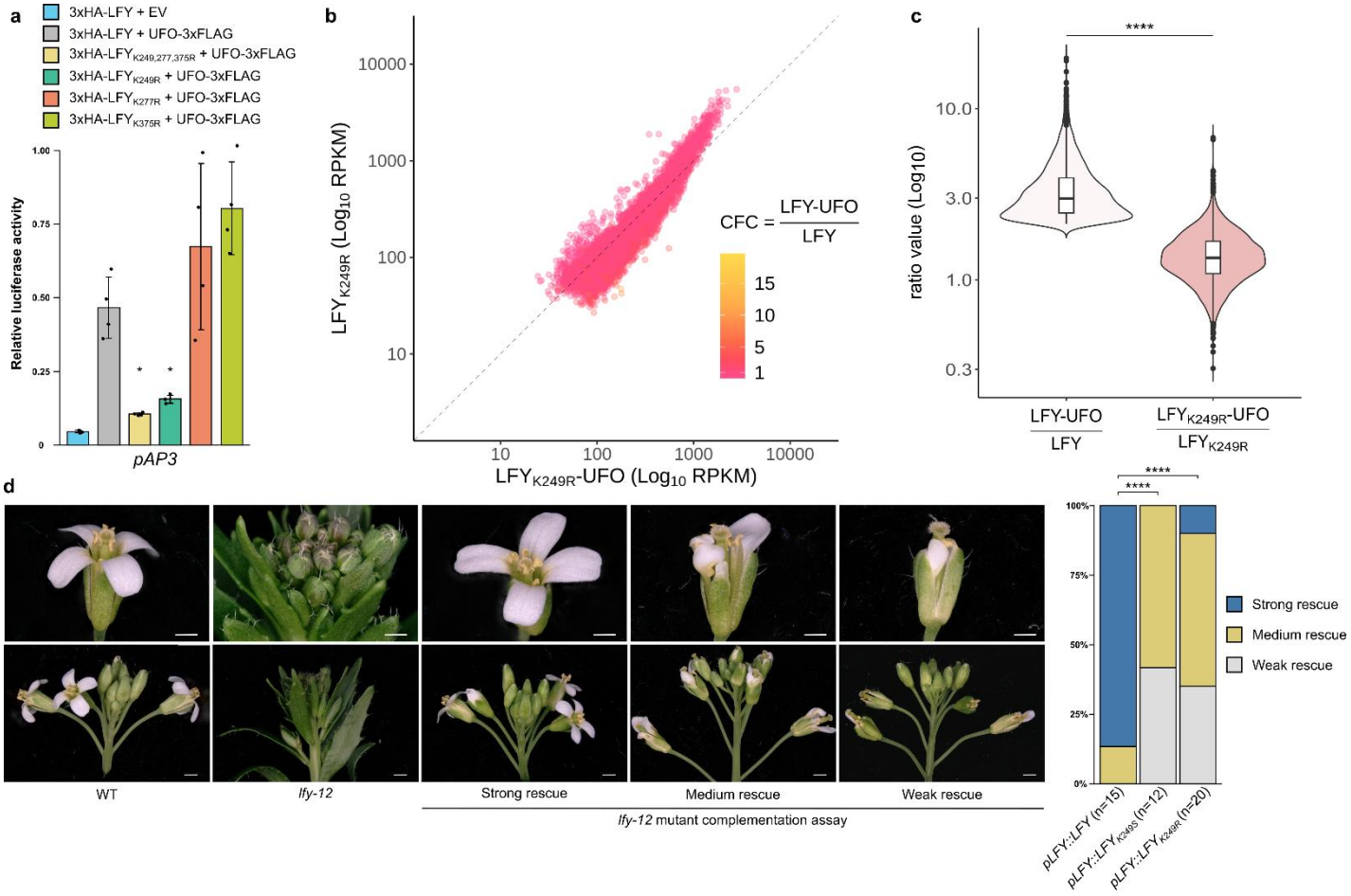

Fig. 4. The LFY K249R mutation disrupts the LFY-UFO synergy. a, *pAP3* activation in Arabidopsis protoplasts. Data are mean ± SD (n = 4 biological replicates). Welch's ANOVA with Games-Howell post-hoc test. Stars indicate a statistical difference compared to 3xHA-LFY+UFO-3xFLAG. (NS: $p > 0.05$,*: $p < 0.05$). **b,** Comparison of peak coverage in LFY_{K249R}-UFO (x-axis) and LFY_{K249R} (y-axis) ampDAP-seq experiments, colored by peak coverage ratio (CFC) as in Fig. 2d. Note that, in contrast to Fig. 2d, the LFY-UFO-specific regions are mostly absent. **c,** Distribution of coverage ratios for LFY and LFY_{K249R} for LFY-UFO-specific regions (20% highest CFC). Wilcoxon's rank sum test (***: $p < 0.0001$). Median (solid line), interquartile range (box edges), ±1.5 × interquartile range (whiskers) and outliers (black dots) are shown. **d,** *lfy-12* mutant complementation assay. Pictures of WT, *lfy-12* mutant and of representative plants of

the different phenotypic complementation classes (left, scale bar 1 mm for top pictures and 1 cm for bottom pictures). Distribution of the different lines within phenotypic complementation classes (right). Plants complemented with LFY_{K249R} and LFY_{K249S} show different complementation patterns compared to plants complemented with LFY (χ^2 tests, ****: $p < 0.0001$). n = number of independent lines.

The LFY K249R mutation specifically affects UFO-dependent LFY functions. In Arabidopsis, LFY performs UFO-dependent and independent functions[3], and we wondered whether they could be uncoupled by introducing specific mutations in LFY. As we were initially looking for LFY ubiquitination mutants, we mutated exposed lysines of LFY-DBD into arginines, and tested the effect of such mutations on LFY-UFO-dependent *pAP3* activation in protoplasts. We found one mutation (LFY K249R; Extended Data Fig. 8a) that strongly reduced *pAP3* activation by LFY-UFO (Fig. 4a) or LFY-VP16-UFO (Extended Data Fig. 8b) without affecting the UFO-independent *pAG* activation (Extended Data Fig. 8c) or the LFY-UFO interaction (Extended Data Fig. 8d). AmpDAP-seq experiments showed that the LFY K249R mutation specifically impaired the binding of LFY-UFO but not that of LFY alone (Fig. 4b,c and Extended Data Fig. 8e-i), revealing that K249 plays a key role in LFY-UFO interaction with the LUBS DNA.

The importance of LFY K249 for UFO-dependent LFY functions was also confirmed using complementation assay of the Arabidopsis *lfy-12* null mutant[28]. *lfy-12* plants expressing LFY_{K249R} or LFY_{K249S} under the control of *LFY* promoter developed flowers with normal sepals and carpels but with defective third and more importantly second whorl organs, resulting in flowers similar to those observed in weak *ufo* mutants (Fig. 4d). When expressed under the constitutive *35S* promoter, LFY_{K249R} triggered ectopic flower formation and early flowering like WT LFY (Extended Data Fig. 8j), consistent with these LFY functions being independent of UFO and thus not affected by the K249R mutation[29].

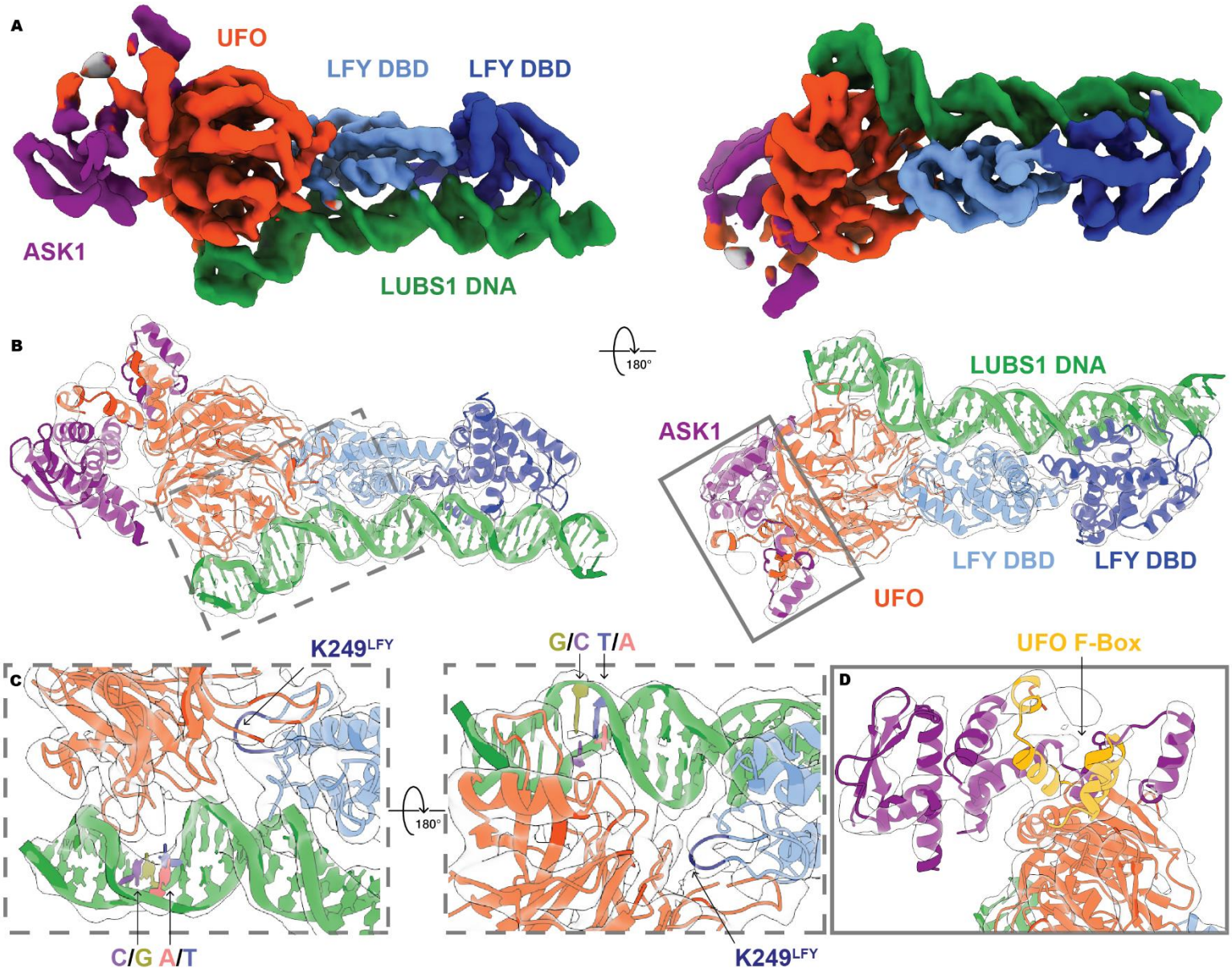

Fig. 5. Structural characterization of the ASK1-UFO-LFY-DNA complex. a, Cryo-EM density map of the ASK1-UFO-LFY-DBD-LUBS1 complex under two angles, colored with regard to the underlying macromolecule (green: LUBS1 DNA; pale and dark blue: LFY-DBD; red: UFO; purple: ASK1). **b,** The same views of the cryo-EM density map in transparent gray with fitted structures of LFY-DBD dimer, UFO, ASK1 and LUBS1 DNA. Same colors as in (**a**). The frames roughly indicate the regions shown in (**c**) and (**d**). **c,** Zoom on the UFO-DNA contact region (left) and on the LFY-UFO interface (right). Only the high-information CA of the URM and its complement is highlighted by filled coloring the rings for each base (red for A, blue for T, pale green for G and purple for C). The LFY-DBD loop containing the K249 residue is highlighted in dark blue. **d,** Zoom on the ASK1-UFO interface, with the UFO F-box highlighted in gold.

Structural characterization of the ASK1-UFO-LFY-DNA complex. In order to understand how the LFY-UFO complex recognizes its cognate DNA binding site and how the K249 mutation impedes this interaction, we purified the ASK1-UFO-LFY-DBD-LUBS1 complex and we structurally characterized it using cryo-electron microscopy (Fig. 5a and Extended Data Fig. 9a-d). A structure at a 4.27 Å resolution was obtained (Extended Data Fig. 9g-i) into which were fit the AlphaFold2 predicted structure for UFO and ASK1, and the LFY-DBD dimer/DNA crystallographic structure[30] (PDB, 2VY1; Fig. 5b and Extended Data Fig. 9e,f). Due to the modest resolution, specific interacting amino acids could not be unambiguously identified. However, the major protein-protein and protein-DNA interaction surfaces were clearly identifiable.

The structure revealed that UFO directly contacts the DNA in the major groove around the URM (Fig. 5c). This binding likely involves basic residues present on loops projecting from the UFO Kelch-type β-propeller and results in a bend of roughly 30 degrees in the DNA double helix (Extended Data Fig. 9f). The structure also shows an interface between UFO and one LFY-DBD monomer (Fig. 5c). The LFY-DBD loop containing the K249 residue lies in this interface and likely interacts with one of the DNA-binding loops of UFO, consistent with the key role of LFY K249 in the ternary complex formation. As expected, ASK1 interacts with UFO F-box domain[15] (Fig. 5D).

These data show how a β-propeller protein is able to modify the specificity of a TF, and offer a structural explanation on how LFY and UFO synergistically recognize a novel DNA element via direct interactions by both proteins with the DNA.

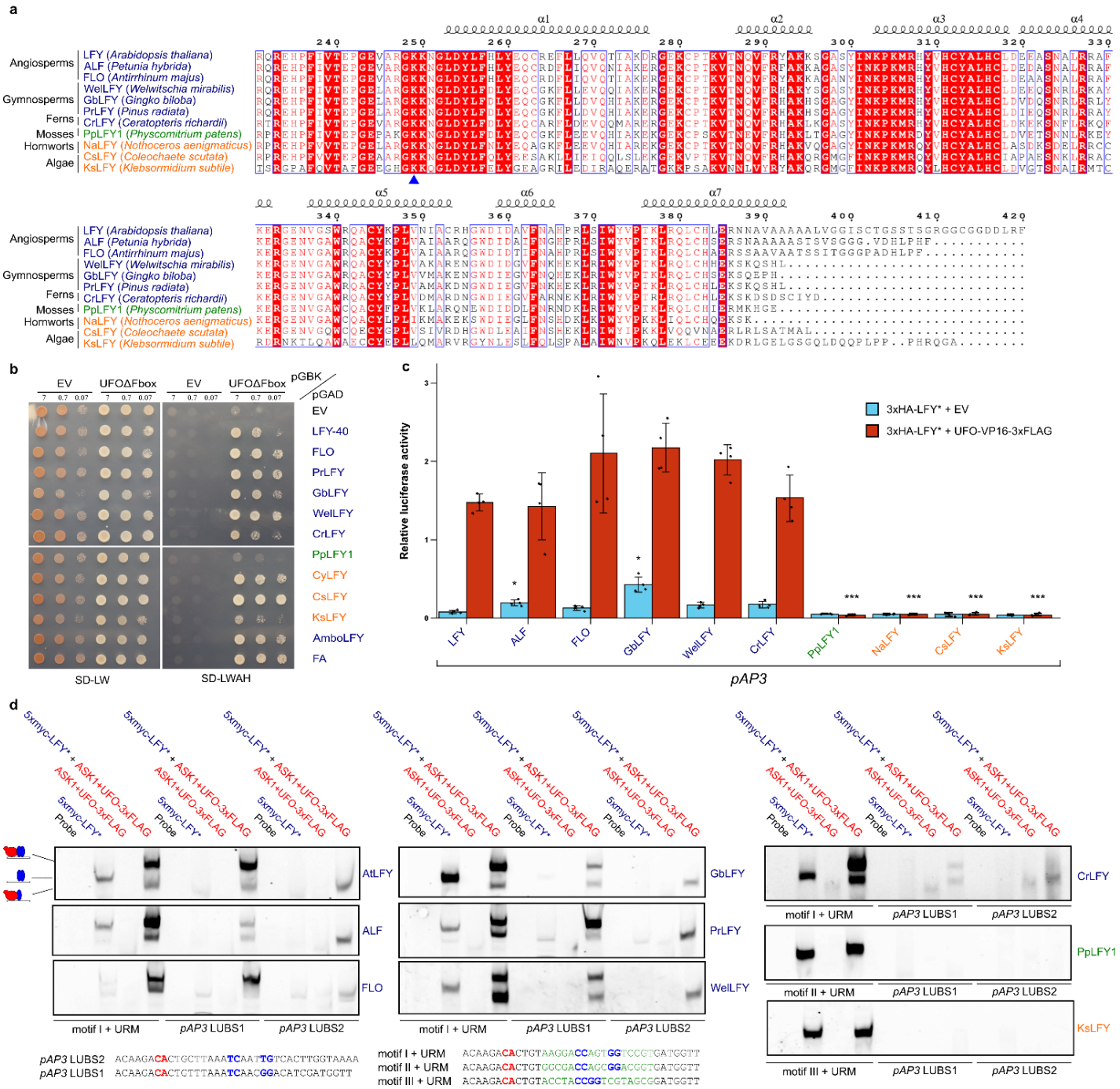

Fig. 6. LFY-UFO interaction is conserved beyond angiosperm species. a, Alignment of LFY DBDs. Amino acid numbering and secondary structure annotation are based on LFY from *A. thaliana*. LFY K249 residue is indicated with a blue triangle. DNA binding specificities are color-coded, type I (blue), II (green) and III (orange). FLO = FLORICAULA; ALF = ABERRANT LEAF AND FLOWER. **b,** Interaction between LFY orthologs and AtUFOΔFbox in Y2H. LFY orthologs are described in (**a**) except CyLFY (*Cylindrocystis sp.*), AmboLFY (*Amborella trichopoda*) and FA (FALSIFLORA; *Solanum lycopersicum*). See Extended Data Fig. 4d for legends. **c,** *pAP3* activation measured by DLRA in Arabidopsis protoplasts. EV = Empty Vector. 3xHA-LFY* refers to the different LFY orthologs indicated under the x-axis. Data represent averages of independent biological replicates and are presented as mean ± SD, each dot representing one biological

replicate (n = 4). Welch's ANOVA with Games-Howell post-hoc test. One-way ANOVA was performed with data from the same effector (described in the legend), and stars represent a statistical difference compared to AtLFY, NS otherwise. (NS: $p > 0.05$,*: $p < 0.05$, **: $p < 0.01$; ***: $p < 0.001$). **d,** EMSA with indicated DNA probes (bottom). URM and LFYBS bases are depicted in red and blue, respectively. *pAP3* LUBS1 sequence was modified to insert the perfect sequence of motif I, II or III[31] (depicted in green): these DNA probes were used as positive controls for binding of LFYs alone and LFY-UFO complex formation. 5xmyc-LFY* refers to the different LFY orthologs indicated next to each EMSA and described in (**a**).

The LFY-UFO complex might have a deep evolutionary origin

As genetic and physical LFY-UFO interactions have been described in diverse angiosperms, we wondered whether the mechanism unraveled for Arabidopsis proteins could also apply to LFY from other species, including non-angiosperm ones. We selected LFY orthologous proteins from several species and with different DNA binding specificities (Fig. 6a). Indeed, through evolution, LFY specificity evolved with three major DNA binding specificities[31]. Type I specificity is the one described in Arabidopsis and valid for other angiosperms, gymnosperms, ferns and the moss *Marchantia polymorpha,* with two half-sites separated by a 3-bp spacer (Fig. 2e). LFY from the moss *Physcomitrium patens* have a type II specificity with specific half-sites (different from type I half-sites) also separated by a 3-bp spacer. Finally, type III specificity is found for LFY from algae and corresponds to a type II motif without the spacer. Because functional UFO homologs have not been identified outside angiosperms, we used Arabidopsis UFO (AtUFO) in all the following experiments.

We tested the interaction of various LFY orthologs with AtUFO in Y2H (Fig. 6b), in DLRA in protoplasts with Arabidopsis *pAP3* (Fig. 6c) and in EMSA (Fig. 6d). In Y2H, all LFYs except LFY from *P. patens* (Type II) interact with AtUFO (Fig. 6b). However only Type I LFY from angiosperms, gymnosperms and ferns form a complex on *pAP3* LUBS and activate *pAP3* in the protoplast assay (Fig. 6c,d). These results suggest that the ability of LFY and UFO to act together by forming a complex is ancient, largely predating the origin of angiosperms. We obtained no evidence that type II and III LFY (from moss and algae) could form a complex with AtUFO on LUBS1 and LUBS2. A detailed and more trustworthy history of the LFY-UFO interaction will await further analyses, notably with the identification of UFO orthologs from non-angiosperm genomes.

Discussion

LFY was long known to interact with UFO to control flower and inflorescence development in numerous angiosperm species. However, the molecular nature of their synergistic action had remained unknown. As UFO encodes an F-box protein taking part in an SCF complex[17,32,33], it was thought to target proteins for a SCF^{UFO}-dependent ubiquitination and possible degradation. LFY was an obvious target candidate but clear evidence of LFY ubiquitination was missing [12,18]. The results we present here suggest that the F-box domain, required for ubiquitination, is dispensable for most UFO-dependent LFY activity. Nevertheless, the high conservation level of UFO F-box sequence in angiosperms, together with slight differences in UFO activity when the F-box is deleted suggest that this domain might still be needed for some elusive facets of UFO function. UFO may work redundantly with other F-box proteins in ubiquitination pathways like with the F-box protein HAWAIIAN SKIRT identified in a genetic screen as an enhancer of *ufo* mutant phenotype[34]. It is thus possible that UFO acts as a moonlighting protein[35] with functions in both transcription and ubiquitination, and these two activities could be related or independent.

The molecular mechanism we discovered here is consistent with most published data on *AP3* and *PI* regulation[18,23,36,37]. However, a detailed understanding of the expression pattern of *AP3* and *RBE* will require further work on other *cis* and *trans*- elements. Why *AP3* is not transcribed in floral stage 0-1 despite the expression of LFY and UFO is unclear[20]. It could be because SUPPRESSOR OF OVEREXPRESSION OF CO 1 (SOC1), AGAMOUS-LIKE 24 (AGL24) and SHORT VEGETATIVE PHASE (SVP) act as early *AP3* repressors as *AP3* mRNA is detected in the floral anlage in a *soc1 svp agl24* mutant[38,39]. Another explanation could be that *AP3* expression requires the *SEPALLATA3* activator [40]. Why *pAP3* is not activated by LFY (or LFY-VP16) alone through the canonical LFYBS is also an open question.

Our work unraveled an unsuspected function unrelated to ubiquitination for UFO: it forms a transcriptional complex with LFY at regulatory sites that are different from the canonical sites bound by a LFY homodimer. UFO was previously proposed to act in transcription, but in the absence of direct evidence that a LFY-UFO complex forms on novel binding sites, it was difficult to understand how UFO controls only a subset of LFY targets. These novel regulatory sites (mLUBS and dLUBS) are made of a low-affinity or half LFYBS (poorly or not bound by LFY alone)

and a motif located at a fixed distance from it and responsible for UFO recruitment. The formation of such a sequence-specific complex is explained at the structural level by the capacity of UFO to interact with both LFY and DNA. The poor ability of UFO to bind DNA alone explains its complete dependence on LFY to perform its transcriptional functions *in planta*[6,20]. Thus, depending on *cis*-elements present in regulatory regions, LFY either binds DNA as a homodimer or requires UFO to form a ternary complex. Mutation of the LFY K249 residue allows uncoupling these two types of binding by specifically disrupting the formation of the LFY-UFO-DNA complex. The position of this residue in the 3D structure at the interface between LFY, UFO and DNA is consistent with the key role of this residue in the complex formation. It is possible that replacing K249 with a bulkier R residue displaces the UFO loops involved in DNA binding without affecting the LFY-UFO interaction. Obtaining a higher-resolution structure will help to understand precisely the interactions occurring in this complex.

Although it might be a common regulatory mechanism, only few cases where non-TF proteins modify TF DNA binding specificity have been described so far (for example Met4 and Met28 modifying the binding of TF Cbf1 in yeast[41], or the herpes simplex virus transcriptional activator VP16 changing specificity of the Oct-1/HCF-1 complex[42]). None of these examples involves an F-box protein or a Kelch-type β-propeller protein and neither of them has been characterized at the structural level. TF DNA binding specificity modification by non-TF proteins offers additional possibilities for a combinatorial control of gene expression and explains how a master regulator such as LFY accesses novel *cis*-elements to perform different functions in distinct territories.

Since LFY and UFO play key roles together in numerous plants species (including ornamental, crops and model plants), our findings expand the molecular understanding of flower and inflorescence development in a large variety of angiosperms. Because the LFY-UFO synergy is observed with LFY orthologs from gymnosperms and ferns as well, we speculate that this complex largely predated the origin of flowers and could have been coopted for flower development from a yet unknown ancestral role.

Acknowledgements

We thank AM. Boisson for preparing suspension cells, X. Lai for ampDAP-seq libraries and technical assistance and R. Koes for sharing data and materials. We gratefully acknowledge C. Marondedze, G. Vachon, M. Le Masson, C. Berthollet, B. Orlando Marchesano and J. Bourenane-Vieira for help with experiments. We thank G. Vert, U. Dolde and R. Dumas for discussion. The electron microscopy facility is supported by the Rhône-Alpes Region, the FRM, the FEDER and the GIS-IBISA. This work used the platforms of the Grenoble Instruct-ERIC center (ISBG; UAR 3518 CNRS-CEA-UGA-EMBL) within the Grenoble Partnership for Structural Biology (PSB), supported by FRISBI (ANR-10-INBS-0005-02). We thank Caroline Mas for assistance and access to the biophysical platform. This work was supported by the GRAL Labex financed within the University Grenoble Alpes graduate school (Ecoles Universitaires de Recherche) CBH-EUR-GS (ANR-17-EURE-0003), the CEA (PhD fellowship to PR) and the ANR-17-CE20-0014-01 Ubiflor project to FP.

Author contributions

FP and PR designed the project. PR performed the plant experiments helped by GT. PR and ET performed the biochemical experiments helped by HC for evolutionary analyses. LT performed the bioinformatics analyses helped by JL and RBM. EZ and GS performed cryo-EM experiments and MN, EZ, CZ and GS analyzed the data. PR and LT assembled the figures. PR and FP wrote the paper with contributions from LT and CZ.

Competing interests

We declare no competing interests.

Methods

Arabidopsis growth. All mutants and transgenic lines are in the *A. thaliana* Columbia-0 accession. Seeds were sown on soil, stratified 3 days at 4 °C, and then grown at 22°C under long-day conditions (16 h light). Transgenic plants were obtained with Agrobacterium tumefaciens C58C1 pMP90 using the floral dip method. Transformants were identified using GFP or Basta selection.

Arabidopsis cell suspension culture. Arabidopsis thaliana (ecotype Columbia-0) cells in suspension cultures were grown under continuous light (90 µmol of photons m-2 s-1) at 21°C with shaking at 135 rpm in Murashige and Skoog (MS) medium supplemented with 30 g/L sucrose and 2 mg/L 2,4-dichlorophenoxyacetic acid (2,4D), pH 5.5. Suspension cells were subcultured every week with a 5-fold dilution. Suspension cells at 4 or 5 days following subculture were used for protoplast preparation.

Cloning. DNA fragments were amplified by PCR with Phusion high fidelity polymerase (NEB). Plasmids were all obtained by Gibson Assembly (GA) with either PCR-amplified or restriction enzyme-digested backbone vectors. We used the 420 aa LFY version. For site-directed mutagenesis, primers containing the desired mutations were used for GA mutagenesis. Plasmids were obtained using DH5α bacteria and were all verified by Sanger sequencing. A list of plasmids and cloning procedures is provided in Supplementary Data 1. Oligonucleotide sequences are listed in Supplementary Data 2.

Yeast-two-hybrid. Coding sequences were cloned in pGADT7-AD or pGBKT7 vectors (Clontech) by GA. Y187 and AH109 yeast strains (Clontech) were transformed with pGADT7-AD or pGBKT7 vectors and selected on plates lacking Leucine (SD-L) or Tryptophan (SD -W), respectively (MP Biomedicals). After mating, yeasts were restreaked on plates lacking Leucin and Tryptophan (SD -L-W) for 2 days. Yeasts were then resuspended in sterile water and OD_{600nm} was adjusted to indicated values for all constructions; two ten-fold dilutions were performed, and 6 µL drops were done on SD -L-W or SD -L-W-A-H (lacking leucine, tryptophan, histidine and adenine) plates. Yeasts were grown at 28°C and pictures were taken at indicated times.

Dual Luciferase Reporter Assay (DLRA) in Arabidopsis protoplasts. Effector plasmids with a 3xHA tag were obtained by cloning indicated genes in the modified pRT104 vector containing a 3xHA N-terminal tag (pRT104-3xHA)[43]. The pRT104 empty plasmid was reengineered to insert a 3xFLAG C-terminal tag. For reporter plasmids, indicated promoter fragments were cloned upstream a Firefly Luciferase gene in pBB174[44]. We used a 975-bp *pAP3* fragment and a 2-kb *pRBE* promoter fragment upstream of the ATG, known to induce a WT pattern in plant[23,45]. *pAG* corresponds to *AG* second intron fused to a minimal *35S* promoter, known to induce a WT pattern in plant[21]. For *pAP1*, we used a 600-bp fragment upstream of the ATG. This version is sufficient to give a WT pattern in plant[46], and the use of longer promoter versions induced a very high background noise in protoplasts. The pRLC reference plasmid contains Renilla Luciferase sequence under the control of the *35S* promoter. Plasmids were obtained in large amounts using NucleoBond Xtra Maxi Plus kit (Macherey-Nagel). Protoplasts were prepared from Arabidopsis Col-0 cell suspension and transformed following the procedure described by Iwata et al.[47]. Cell wall was digested using Onuzuka R-10 cellulase and macerozyme R-10 (Yakult Pharmaceutical). Digested cells were passed through two layers of Miracloth to remove debris, and protoplast concentration was adjusted to 2-5x105 cells/mL. Protoplasts were then PEG-mediated transformed using 10 µg of indicated effector and reporter plasmids and 2 µg of reference plasmid. After 17 h of incubation at RT, protoplasts were lysed. Firefly (F-LUC) and Renilla Luciferase (R-LUC) activities were measured using Dual Luciferase Reporter Assay System (Promega) and a TECAN Spark 10M 96-well plate reader. F-LUC/R-LUC luminescence ratios were calculated with background-corrected values. Four

biological replicates were done for each plasmid combination. All DLRA data were analyzed using R Studio software and are presented as mean ± SD. All statistical methods are indicated within the figure legends. One-way ANOVA was used to analyze experimental data with more than two experimental groups. Welch's ANOVA was performed when the homogeneity of variance assumption was not met. Two-tailed unpaired Student's t-test was used for other data analyses.

Electrophoretic Mobility Shift Assay (EMSA). DNA probes used in EMSA are listed in Supplementary Data 2. Complementary oligos were annealed overnight in annealing buffer (10 mM Tris pH 7.5, 150 mM NaCl and 1 mM EDTA). 4 pmol of double-stranded DNA was then fluorescently labeled with 1 unit of Klenow fragment polymerase (NEB) and 8 pmol Cy5-dCTP (Cytiva) in Klenow buffer during 1 h at 37°C. Enzymatic reaction was stopped with a 10-min incubation at 65°C.
Proteins used in EMSA were obtained by different methods (bacteria, insect cells or TnT). Recombinant proteins (6xHis-LFY-DBD, UFOΔFbox-3xFLAG) and recombinant complexes (ASK1-UFO, ASK1-UFO-3xFLAG) concentration was adjusted to 500 nM for all reactions. All the 5xmyc-tagged proteins were obtained in vitro by TnT. 50 µL TnT reactions were done by mixing for 2 h at 25°C 5 µg of pTNT-5xmyc plasmid containing the gene of interest with TnT SP6 High-Yield Wheat Germ Protein Expression System (Promega). For EMSA with TnT-produced proteins, 5 µL of TnT reaction was used. Recombinant protein buffer or TnT mix was used as control when comparing reactions with multiple proteins.
All binding reactions were performed in 20 µL binding buffer (20 mM Tris pH 7.5, 150 mM NaCl, 1% glycerol, 0.25 mM EDTA, 2 mM MgCl2, 0,01% Tween-20 and 3 mM TCEP) with 10 nM labelled probe. Reactions were supplemented with 140 ng/µL fish sperm DNA (Sigma-Aldrich) for EMSAs performed with in vitro-produced LFY, and 200 ng/µL for EMSAs performed with recombinant 6xHis-LFY-DBD. Binding reactions were incubated for 20 min on ice and then loaded on a 6 % native polyacrylamide gel. Gels were electrophoresed at 90 V for 75 min at 4°C and revealed with an Amersham ImageQuant 800 imager (Cytiva). Uncropped gels are shown in Source data.

Recombinant protein production and purification from bacteria. 6xHis-LFY-DBD was produced in E.Coli Rosetta2 (DE3) cells (Novagen) and purified as previously described [30]. ASK1 was cloned into the pETM-11 expression vector [48], and the resulting plasmid was transformed into E.Coli BL21 cells (Novagen). Bacteria were grown in LB medium supplemented with kanamycin and chloramphenicol at 37°C up to an OD_{600nm} of 0.6. Cells were then shifted to 18°C and 0.4 mM isopropyl b-D-1-thiogalactopyranoside (IPTG) was added. After an overnight incubation, cells were sonicated in UFO buffer (25 mM Tris pH8, 150 mM NaCl, 1 mM TCEP) supplemented with one EDTA-free Pierce Protease Inhibitor Tablets (ThermoFisher). Lysed cells were then centrifuged for 30 min at 15000 rpm. Supernatant was mixed with Ni Sepharose High Performance resin (Cytiva) previously equilibrated with UFO buffer (25 mM Tris pH 8, 150 mM NaCl, 1 mM TCEP). Resin was then washed with UFO buffer containing 20 and 40 mM imidazole. Bound proteins were eluted with UFO buffer containing 300 mM imidazole and dialyzed overnight at 4 °C against UFO buffer without imidazole.

Recombinant protein production and purification from insect cells. The different tagged versions of ASK1, LFY and UFO were cloned in acceptor and donor plasmids (pACEBac1, pIDK and pIDS respectively; Geneva Biotech). Final acceptor plasmids containing the combination

of desired coding sequences were obtained with Cre recombinase (NEB). DH10EmBacY competent cells containing the baculovirus genomic DNA (bacmid) were transformed with final acceptor plasmids. Blue-white selection was used to identify colonies with a recombinant bacmid with acceptor plasmid inserted. Bacmid was then isolated from bacteria and mixed with X-tremeGENE HP DNA Transfection Reagent (Roche) to transfect Sf21 insect cells. 96 h after transfection, supernatant containing the recombinant baculovirus (V0) was collected and used to infect fresh Sf21 cells. When infected cells reached DPA (Day Post Arrest), V1 virus was collected. For large expression, Sf21 cells were infected with either V1 virus or frozen baculovirus-infected cells. The pellet of a 0.75 L culture was sonicated in 50 mL of UFO buffer supplemented with one EDTA-free Pierce Protease Inhibitor Tablets (ThermoFisher). Sonicated cells were centrifuged for 1.5 h at 30 000 rpm, 4 °C. Supernatant was then incubated for 1 h at 4°C with Ni Sepharose High Performance resin (Cytiva) previously equilibrated with UFO buffer. Beads were transferred into a column, and washed with 20 column volumes of UFO buffer, then UFO buffer + 50 mM imidazole. Proteins were eluted with UFO buffer containing 300 mM imidazole. Elution was dialyzed overnight at 4 °C against UFO buffer. TEV protease was added to cleave tags (0.01% w/w). When ASK1 was limiting compared to UFO, recombinant 6xHis-ASK1 from bacteria was added. The following day, elution was repassed on Dextrin Sepharose High Performance (Cytiva) and Ni Sepharose High Performance resins (Cytiva) to remove tags and contaminants. For ASK1-UFO, ASK1-UFO-3xFLAG or UFOΔFbox-3xFLAG, proteins were concentrated with a 30 kDa Amicon Ultra Centrifugal filter (Millipore) and further purified by Size Exclusion Chromatography (SEC). For ASK1-UFO-LFY-DBD complex purification, contaminant DNA was removed by passing proteins on Q Sepharose High Performance resin (Cytiva) pre-equilibrated with UFO buffer. Increasing salt concentrations allowed obtaining DNA-free proteins. Indicated annealed HPLC-purified oligos (Supplementary Data 2) were then added and incubated with proteins on ice for 20 min. Proteins were concentrated with a 30 kDa Amicon Ultra Centrifugal filter (Millipore) and further purified by SEC.

Size Exclusion Chromatography (SEC) and Size Exclusion Chromatography coupled to Multi-Angle Laser Light Scattering (SEC-MALLS). SEC was performed with a Superdex 200 Increase 10/300 GL column (Cytiva) equilibrated with UFO buffer. Unaggregated proteins of interest were frozen in liquid nitrogen and stored at -80°C. SEC-MALLS was performed with a Superdex 200 Increase 10/300 GL column (Cytiva) equilibrated with UFO buffer. For each run, 50 µL containing 1 mg/mL of complex was injected. Separations were performed at RT with a flow rate of 0.5 mL/min. Elutions were monitored by using a Dawn Heleos II for MALLS measurement (Wyatt Technology) and an Optilab T-rEX refractometer for refractive index measurements (Wyatt Technology). Molecular mass calculations were performed using the ASTRA software with a refractive index increment (dn/dc) of 0.185 mL/g.

ampDAP-seq. pTnT-5xmyc-LFY[27] was used to produce 5xmyc-LFY in vitro using TnT SP6 High-Yield Wheat Germ Protein Expression System (Promega). We used the ampDAP-seq libraries described in Lai et al.[27]. ampDAP-seq experiments were performed in triplicates (LFY-UFO) or in duplicates (LFY_{K249R} and LFY_{K249R}-UFO).
A 50 µL TnT reaction producing 5xmyc-LFY was mixed with an excess of recombinant ASK1-UFO-3xFLAG (2 µg) and 20 µL of Pierce Anti-c-Myc Magnetic Beads (ThermoScientific). DAP buffer (20 mM Tri pH 8, 150 mM NaCl, 1 mM TCEP, 0,005% NP40) was added to reach 200 µL. Mix was incubated for 1 h at 4°C on a rotating wheel. Beads were then immobilized and

washed 3 times with 100 µL DAP buffer, moved to a new tube and washed once again. ampDAP-seq input libraries (50 ng) were then added, and protein-DNA mixes were incubated for 1.5 h at 4°C on a rotating wheel. Beads were immobilized and washed 5 times with 100 µL DAP buffer, moved to a new tube and washed 2 more times. Finally, beads were mixed with 30 µL of elution buffer (10 mM Tris pH 8.5) and heated for 10 min at 90°C.
IP-ed DNA fragments contained in the elution were amplified by PCR according to published protocol[49] with Illumina TruSeq primers. Remaining beads were mixed with 20 µL of 1X SDS-PAGE Protein Sample Buffer and WB were performed to check the presence of tagged proteins. PCR products were purified using AMPure XP magnetic beads (Beckman Coulter) following manufacturer's instructions. Library molar concentrations were determined by qPCR using NEBNext Library Quant Kit for Illumina (NEB). Libraries were then pooled with equal molarity. Sequencing was done on Illumina HiSeq (Genewiz) with specification of paired-end sequencing of 150 cycles.

GUS staining. The different promoter versions were cloned upstream *GUS* gene in the pRB14 backbone vector [46]. Transformants were selected with GFP seed fluorescence. The number of independent lines analyzed for each construct is indicated in each figure. GUS staining was performed on the apex of primary inflorescences of T2 plants. Tissues were placed in ice-cold 90% acetone for 20 min at RT, and then rinsed in GUS buffer without X-Gluc (0.2% Triton X-100, 50 mM NaPO4 pH 7.2, 2 mM potassium ferrocyanide, 2 mM potassium ferricyanide). Tissues were transferred in GUS buffer containing 2 mM X-Gluc substrate (X-Gluc DIRECT) and placed under vacuum for 5 min. Samples were then incubated overnight at 37°C unless specified in the legend. Finally, tissues were washed with different ethanol solutions (35%, 50%, and 70%) and pictures were taken with a Keyence VHX-5000 microscope with a VH-Z100R objective. χ^2 tests were used to test for independency between constructs and staining classes.

***In planta* overexpression and mutant complementation assay.** Tagged versions of UFO and UFOΔFbox were cloned under the control of the *35S* promoter in pEGAD[50]. Transformants were selected with Basta treatment. Overexpressing lines with a strong gain-of-function phenotype were crossed to the strong *ufo-1* mutant. Basta-resistant F2 plants were individually genotyped to select *ufo-1 -/-* homozygous plants. For this, a fragment was amplified by PCR with oligos oGT1085 and oPR578 (Supplementary Data 2) and digested with DpnII enzyme (NEB). Based on digestion profile, *ufo-1 -/-* plants were kept and analyzed once they reached flowering.
Mutated versions of LFY were cloned in pETH29[30] or pCA26[51] to express LFY cDNA under the control of its endogenous promoter or the *35S* promoter, respectively. For *lfy-12* complementation assay, heterozygous *lfy-12/+* plants were transformed. Transformants were selected with GFP fluorescence and genotyped with a previously described protocol[46] to select *lfy-12 -/-* plants. Complementation assay was performed with T2 plants and was based on the analysis of the first 10 flowers from the primary inflorescence. Pictures were taken with a Keyence VHX-5000 microscope with a VH-Z20R objective. χ^2 tests were used to test for independency between constructs and complementation classes.

Western Blot. For Western Blots on plant total protein extracts, indicated tissues were crushed in 2X SDS-PAGE Protein Sample Buffer (100 mM Tris pH 6.8, 20% glycerol, 2% SDS, 0.005% Bromophenol blue, and 0.8% w/v dithiothreitol) at a 1:2 w:v ratio and boiled for 5 min.

Samples were then loaded on a 12% acrylamide SDS-PAGE gel. For all WB, transfer was performed with iBlot2 Dry Blotting System (Invitrogen) using default parameters. Membranes were blocked for 1 h at RT with 5% milk TBST and then incubated overnight at 4 °C with 5% milk TBST solution containing HRP-conjugated antibody (1:1000 for anti-FLAG (Sigma-Aldrich; Cat# A8592) and 1:5000 for anti-myc (Invitrogen; Cat# R951-25)). Revelation was performed with Clarity Western ECL substrate (Bio-Rad). Pictures were taken with a ChemiDoc MP Imaging System (BioRad). Uncropped gels are shown in Source Data.

Cryo-EM sample preparation, data collection and data processing. An aliquot of the SEC-purified ASK1-UFO-LFY-LUBS1 complex was thawed on ice (see Supplementary Data 2 for LUBS1 DNA sequence). Subsequently, 3.5 µl of the complex at 1 mg/mL were deposited onto glow-discharged (25 mA, 30 s) C-flat Au grid R 1.2/1.3 300 mesh (Electron Microscopy Sciences), blotted for 5.5 s with force 0, at 20°C and 100% humidity using a Mark IV Vitrobot (FEI, Thermo Fisher Scientific) and plunge-frozen in liquid ethane for specimen vitrification. A dataset of about 1'000 movies of 40 frames was acquired on a 200 kV Glacios (Thermo Fisher Scientific) electron microscope (Supplementary Data 3) at a nominal magnification of 36'000 with a physical pixel size of 1.145 Å.
The raw movies, acquired with SerialEM on a Gatan K2 Summit camera (Supplementary Data 3), were imported to Cryosparc live[52] for motion correction and CTF estimation. The dose-weighted micrographs were used for particle picking with crYOLO 1.7.6 and the general model for low-pass filtered images[53]. Particle coordinates were imported to Cryosparc, where all subsequent steps were performed. After manual inspection, a subset of 761 micrographs was selected based on CTF fit resolution, total and per frame motion, average defocus and relative ice thickness. A raw particle stack of 282'567 images was extracted at 256x256 pixels² box size, binned twice and subjected into 2D classification to remove false positive picks. 207'392 particles from the selected class averages were re-extracted, re-centered at full size and submitted for a second round of 2D classification. All class averages showing clear protein features were selected and the resulting 147'849 particles were used for ab initio reconstruction with 3 classes and subsequent heterogeneous refinement of the resulting volumes. Of those 3 classes, 2 looked like a protein-DNA complex with the most apparent difference being the presence or not of an extra electron density at one edge of the DNA helix. The last class had no recognizable features and was used as a decoy to remove "junk" particles. Each subset and volume of the 2 first classes was refined separately with Non-Uniform refinement [54] resulting into 2 distinct reconstructions of about 4.2 Å resolution, where the DNA model, the crystal structure of LFY-DBD and the AlphaFold2 models of UFO and ASK1 could be unambiguously fitted into the electron density. The second of these classes could fit a LFY-DBD dimer, while in the first class there was density only for the LFY-DBD molecule that directly interacts with UFO (Extended Data Fig. 9d). The unsharpened maps of each reconstruction were used for post-processing with DeepEMhancer[55]. Figures were prepared with Chimera[56] or ChimeraX[57].

Cryo-EM model building. Ideal B-form DNA was generated in Coot[58] and then manually built into the electron density. The resulting model was further refined using phenix.real_space_refine[59]. A single monomer of LFY-DBD was manually placed in the electron density, followed by fitting in ChimeraX[57]. The biological LFY-DBD dimer was then downloaded from the RCSB PDB (2VY1)[30] and used as a guide to place the second LFY monomer, followed by fitting to density in ChimeraX. Alphafold models[60] of ASK1 (uniprot ID: Q39255) and UFO

(uniprot ID: Q39090) were both downloaded from the EBI, preprocessed to remove low confidence regions in phenix.process_predicted_model[61], then placed manually and then fit to density in ChimeraX.

Bioinformatic analyses.

Read mapping and peak calling. Reads processing and peak calling of LFY, LFY-UFO, LFY_{K249R} and LFY_{K249R}-UFO ampDAP-seq data were performed as previously published[62]. Briefly, the quality of sequencing data was analyzed with fastQC v0.11.7 and adapters were removed with NGmerge v0.2_dev[63]. Bowtie2 v2.3.4.1 was used for mapping to the TAIR10 *A. thaliana* reference genome[64]. Reads mapped to a single location and with maximum two mismatches were retained Duplicates were removed with the samtools dedup program v1.8. Bound regions (i.e. peaks) were identified with MACS2 v2.2.7.1, using input DNA from Lai et al. as control[27]. Consensus peaks were selected with MSPC v4.0.0[65] by retaining peaks called in all replicates, and resizing them by ±200 bp around the peak maximum for further analysis.

Analyses of ampDAP-seq experiments. To compare binding in different experiments, peaks were merged according to a previously published procedure[62]. Bound peaks were considered as common if they overlapped by at least 80%, while the remaining non-overlapping portion of either peak was < 50%. Peaks that did not overlap by at least 50% were considered as new peaks. The same procedure was used to assess experimental reproducibility (comparisons between replicates of the same experiment), where peaks were normalized by the number of reads mapped in library (RPKM).
As the fraction of reads mapped in peaks is much lower for LFY than LFY-UFO ampDAP-seq (~25% vs ~40%, respectively), normalizing reads count by all reads mapped along the genome would introduce a bias and estimate the LFY relative coverage (RPKM) towards lower values compared to LFY-UFO. In addition to this consideration, experimental proof from EMSAs suggests that UFO does not strongly affect binding intensity of the complex at canonical LFYBS (which represent most peaks). Hence, reads count at each peak was normalized by the total number of reads mapped within all LFY and LFY-UFO merged peaks. Then, the mean normalized coverage from each experiment, divided by the peak size, was computed for each peak. The same strategy was applied when comparing LFY_{K249R} and LFY_{K249R}-UFO (Fig. 4b), LFY_{K249R} and LFY (Extended Data Fig. 8h) and LFY, LFY-UFO, LFY_{K249R} and LFY_{K249R}-UFO (Fig. 4c). The Coverage Fold Change (CFC) was computed on merged peaks as the ratio between mean normalized peak coverage in LFY-UFO and LFY (Fig. 2d) or mean normalized coverage in LFY_{K249R}-UFO and LFY_{K249R} (Fig. 4b).

Motif search in bound regions. Merged peaks of LFY and LFY-UFO datasets were sorted based on decreasing CFC value. The top 600 peaks (i.e. highest CFC values) were used for a motif search using MEME-ChIP v4.12.0 using options -nmeme 600 -meme-maxsize 600*1000 -meme-nmotifs 1 -dreme-m 0 -noecho and the JASPAR 2018 core plants non-redundant database[66]. For dLUBS, we used options -meme-minw 20 -meme-maxw 30, while for mLUBS we used -meme-minw 16 -meme-maxw 19. To retrieve the LFY motif in Fig. 2e the 600 LFY ampDAP-seq peaks with strongest coverage were fed to MEME-ChIP with options -nmeme 600 -meme-nmotifs 1 --meme-minw 19 -meme-maxw 19 –pal.

Receiver Operating Characteristics (ROC) analysis. From the dataset of merged peak set (peaks found in LFY or in LFY-UFO experiments or in both), peaks were sorted based on decreased

CFC value, the top 20% peaks were selected, and among these, the first 600 used for motif determination were excluded to avoid overfitting, for a total of 3243 final peaks. A negative set of the same size was created using a previously published method, which allows searching for sequences from the A. thaliana genome (TAIR10 reference) with the same GC content and genomic origin as the positive set[67]. Both sets were scanned with dLUBS and mLUBS PWMs as well as with the LFY PWM with dependencies as published previously[68] using an in-house script available on our GitHub page. The ROC plot was then created with the R 'plotROC' package v2.2.1.

LFY in dLUBS within LFY-UFO-specific regions vs LFY in LFY-specific regions. To assess whether the scores of LFYBS within dLUBS were comparable to the scores of canonical LFYBS, we used the peaks from the comparison of LFY vs LFY-UFO ampDAP-seq and resized them (+/-50 bp around the peak maximum). We used the dLUBS matrix to scan the resized sequences and retained the best site per sequence. We then retrieved sequences corresponding to the dLUBS site and computed the score of the LFYBS present in dLUBS using the LFY PWM[68]. The values obtained in the 20% most LFY-UFO-specific sequences (20% highest CFC) is shown in the boxplot. The 20% lowest CFC peaks were scanned with the LFY PWM to generate the box-plot in Extended Data Fig. 4f.

Microarray data analysis. Microarray data were retrieved from AtGenExpress[69] for inflorescence tissue in the *ufo* (ATGE_52A-C) vs Col-0 background (ATGE_29A-C). The 'gcrma' R package was used to adjust probe intensities and convert them to expression measures, and then the 'limma' package was used to fit the model and smooth standard errors. A Benjiamini-Hochberg correction was applied to p-values and fold change (FC) was computed as the ratio between expression inWT versus the *ufo* mutant. Only genes with $|\log2(FC)| > 0.5$ and adjusted p-value < 0.05 were considered as significantly differentially expressed.

ChIP-seq datasets and analysis of ChIP-seq vs ampDAP-seq. We collected the raw data of all available LFY ChIP-seq datasets: GSE141704[70], GSE96806[25], GSE64245[26], GSE24568[68]. Mapping and peakcalling analysis were performed with the same procedure as ampDAP-seq, except that peaks were resized to 600 bp around the peak maximum, and the –q option of MACS2 was set to 0.1. Coverage of the resulting peaks was calculated as the average of normalized read coverage for each replicate. Peaks from the four datasets were merged through a four-way comparison following the same procedure used for ampDAP-seq. Bedtools intersect (v2.30.0) was used with options -wa -f 0.8 -F 0.8 -e to find the peaks common to the merged ChIP-seq peaks and the 20% most LFY-UFO-specific genomic regions (highest CFC value from ampDAP-seq). Peaks were assigned to genes by extending gene regions 3 kb upstream of the TSS and 1 kb downstream of the TTS and using bedtools intersect (options -f 0.8 -F 0.8 –e) to identify genes in the vicinity of peaks. The bound genes obtained were crossed with the list of differentially expressed genes in *ufo* inflorescences.

Identification of the URM from published LFY ChIP-seq data. To test whether the URM could be identified *de novo* (Extended Data Fig. 4g), we collected the 298 regions bound by LFY ChIP-seq data of inflorescence tissue[25] for which the binding intensity was twice greater in vivo relative to in vitro (LFY ampDAP-seq). We resized these regions +/- 55 bp around the ChIP-seq peak maximum. The corresponding sequences were searched with the LFY PWM[68] to identify all LFYBS with a PWM score > -23. Assuming that a recruiting motif should be at a fixed distance

from the LFYBS, we created 140 batches, corresponding to sequences with size ranging from 4 to 10 bp, distant from 1 to 20 bp at both sides of the canonical LFYBS. Each of the 140 batches of sequences was used as input with MEME-ChIP for motif discovery with the motif size constrained to the length of the sequences in a given batch.

Data and code availability

ampDAP-seq data have been deposited at GEO and are publicly available as of the date of publication (GSE204793). All original code has been deposited at github (https://github.com/Bioinfo-LPCV-RDF/LFYUFO_project) and is publicly available as of the date of publication. The cryo-EM structure determined in this study is deposited in the EM data bank under the reference number EMD-15145. The .pdb file of the model is available in Supplementary information. Any additional information required to reanalyze the data reported in this paper is available from the lead contact upon request.

Extended Data Figures

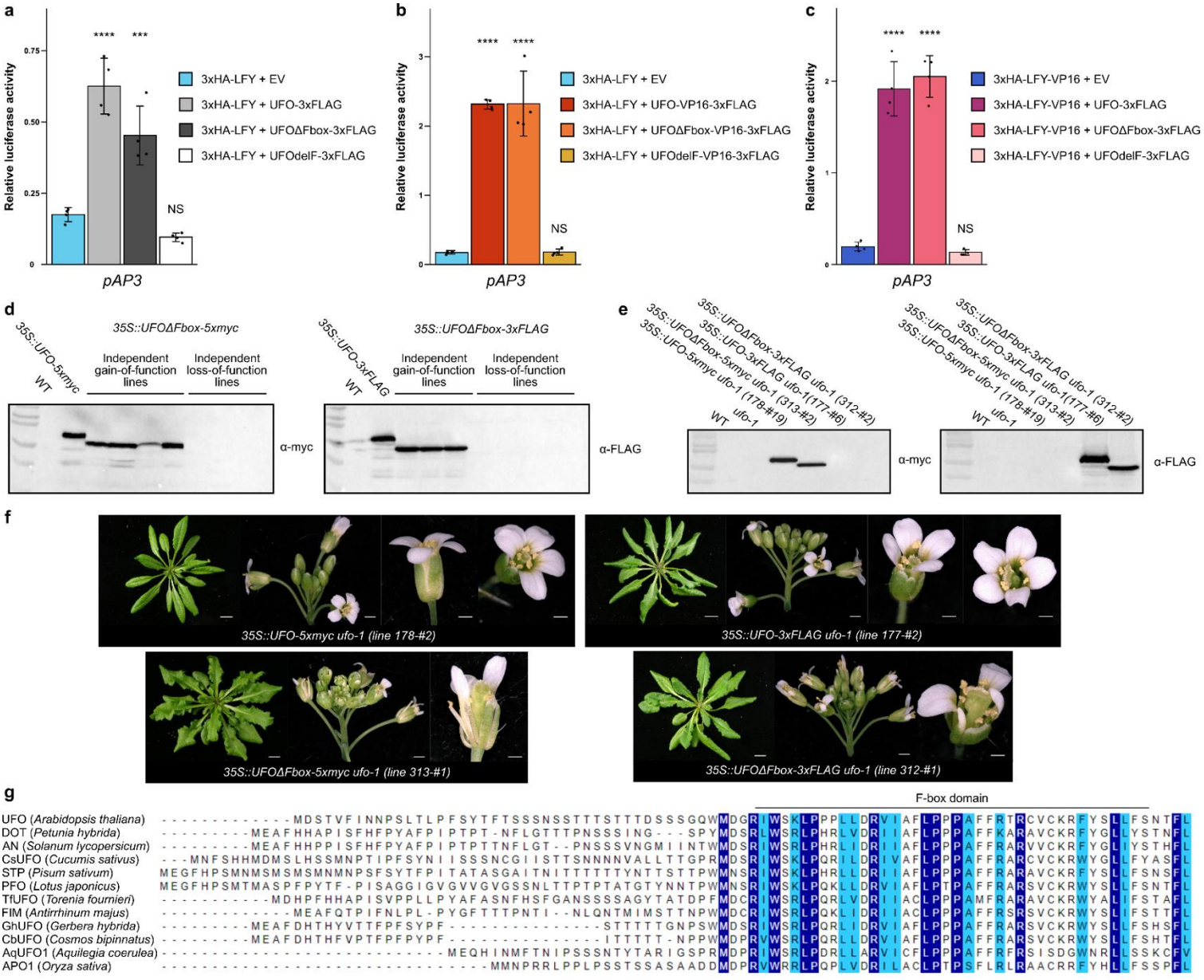

Extended Data Fig. 1. UFO has SCF-dependent and independent functions. a-c, *pAP3* activation measured by DLRA in Arabidopsis protoplasts. EV = Empty Vector (pRT104-3xHA). UFOΔFbox corresponds to a deletion of the whole N-terminal part comprising the F-box domain (aa. 1-90), while UFOdelF corresponds to a previously-described internal deletion in the F-box domain (aa. 50-62)[20]. Data represent averages of independent biological replicates and are presented as mean ± SD, each dot representing one biological replicate (n = 4). One-way ANOVA with Tukey's multiple comparisons test. Stars above bars represent a significant statistical difference compared to 3xHA-LFY + EV or 3xHA-LFY-VP16 + EV negative controls (NS: $p > 0.05$,*: $p < 0.05$, **: $p < 0.01$, ***: $p < 0.001$ and ****: $p < 0.0001$). **d,** Western Blot on protein extracts from independent T1 plants from different phenotypic classes described in Fig. 1g (one independent line per lane). *35S::UFO-5xmyc* (line 178-#19) and *35S::UFO-3xFLAG* (line 177-#6) plants were used as positive controls. Total proteins were extracted from rosette

leaves. Note the difference of molecular weight between UFO and UFOΔFbox. Loss-of-function defects are likely due to silencing of both transgene-encoded UFOΔFbox and endogenous UFO. **e,** Western Blot on protein extracts from F2 plants described in Fig. 1h. Total proteins were extracted from rosette leaves. **f,** *ufo-1* complementation assay with other *35S::UFO* and *35S::UFOΔFbox* lines. Rosette leaves (right, scale bar, 1 cm), inflorescence (middle, scale bar 1 mm) and flower (right, scale bar, 0.5 mm) phenotypes are shown. Primary inflorescences were removed to observe rosette phenotype. For each construct, at least 5 plants were analyzed per line. As in Risseeuw et al, our *35S::UFO* lines displayed relatively milder phenotypes than the *35S::UFO* phenotypes reported by Lee et al.[6,20]. Note that the *35S::UFO-5xmyc* 178-#2 line did not display the serrated leaves phenotype. **g,** Sequence alignment of UFO N-terminal region. The F-box domain is represented[71]. In selected species, presented proteins were identified as UFO homologs and their role was confirmed genetically[7,11,12,16,72–79].

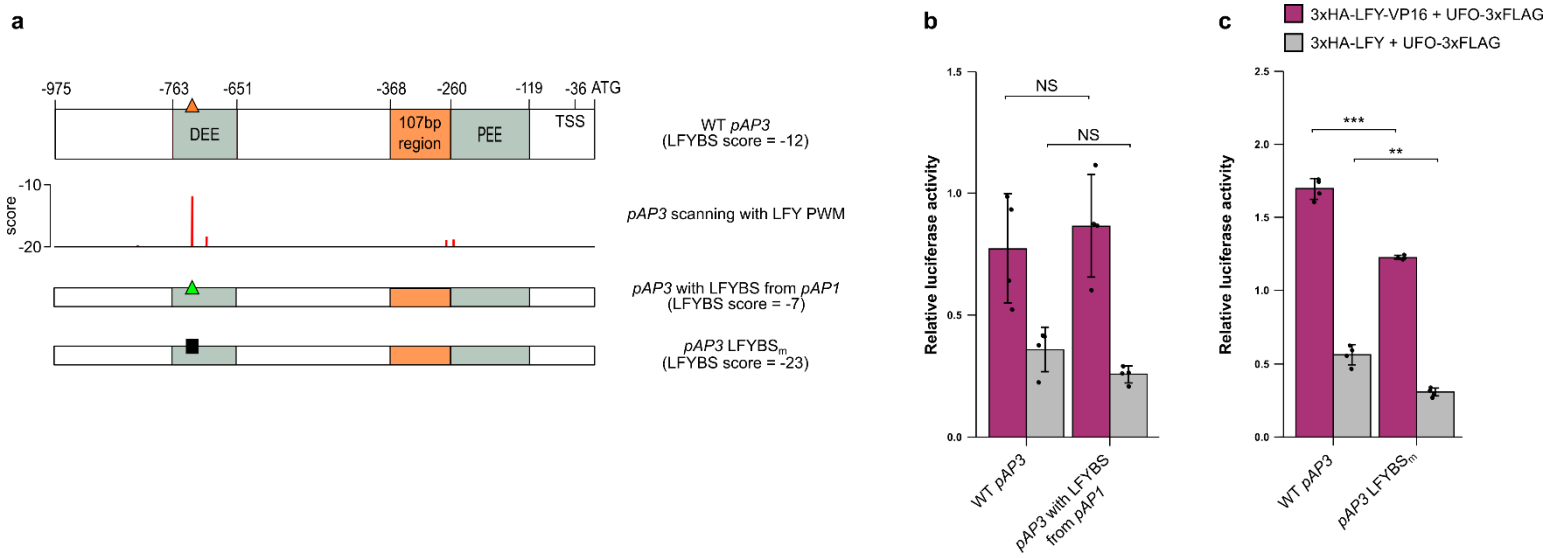

Extended Data Fig. 2. *pAP3* DEE LFYBS is not required for LFY-UFO-dependent *pAP3* activation. **a**, Schematic representation of *pAP3*. Top row represents WT *pAP3* with regulatory regions and *cis*-elements. Orange triangle represents LFYBS. The second row represents the scores for the best LFYBS obtained by scanning WT *pAP3* sequence with LFY PWM[68] (the best binding sites correspond to the less negative score values). Other rows represent the different *pAP3* versions used in (**b**) and (**c**). LFYBS mutation corresponds to the previously described *site1m-site2m* mutation[24]. b,c, *pAP3* activation with promoter versions described in (**a**) and indicated effectors. For bar charts, data represent averages of independent biological replicates and are presented as mean ± SD, each dot representing one biological replicate (n = 4). Unpaired t-tests (b,c). (NS: $p > 0.05$,*: $p < 0.05$, **: $p < 0.01$, ***: $p < 0.001$).

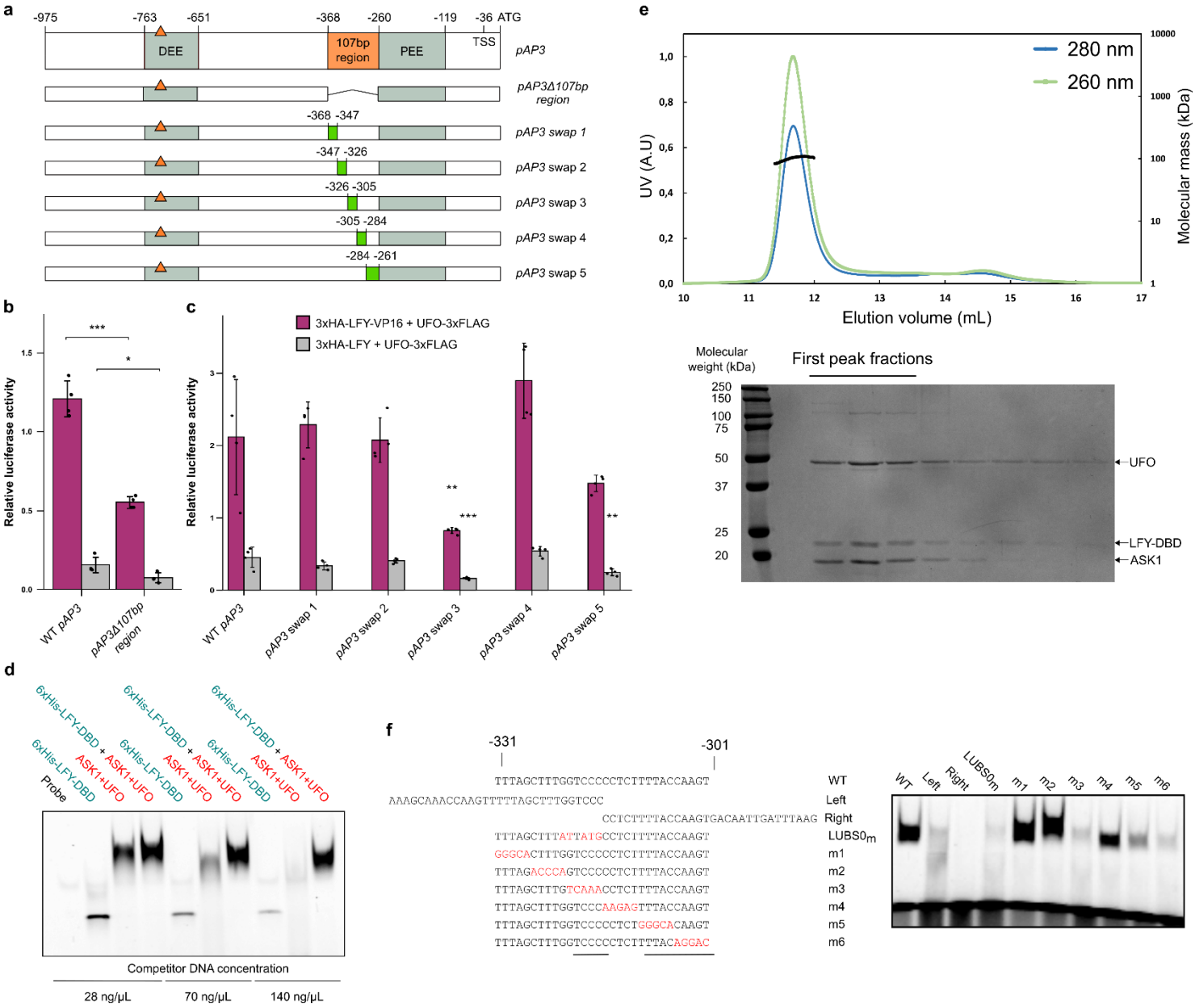

Extended Data Fig. 3. Analysis of *pAP3* activation by LFY-UFO. a, Description of *pAP3*. Top line represents WT *pAP3* with regulatory regions and *cis*-elements. Coordinates are relative to *AP3* start codon. TSS: Transcription Start Site. Orange triangle represents LFYBS. Other rows show the promoter versions used in (**b**) and (**c**). Green rectangles in swapped versions correspond to the same random sequence. **b,c,** *pAP3* LFY-UFO response element mapping with *pAP3* versions described in (**a**) by DLRA in Arabidopsis protoplasts. Data represent averages of independent biological replicates and are presented as mean ± SD, each dot representing one biological replicate (n = 4). One-way ANOVA with Tukey's multiple comparisons test (**c**). One-way ANOVA was performed with data from the same effector, and stars represent a statistical difference compared to WT *pAP3*. Unpaired t-test (**b**). (NS: $p > 0.05$,*: $p < 0.05$, **: $p < 0.01$; ***: $p < 0.001$). **d,** EMSA with ASK1-UFO, LFY-DBD and LUBS0 DNA probe. Different competitor DNA concentrations were tested as indicated. **e,** Molecular mass determination for ASK1-UFO-LFY-DBD in complex with LUBS0 DNA by SEC-MALLS (top). Elution profiles correspond to absorbance at 280 nm and 260 nm (left ordinate axis, A.U:

Arbitrary Unit). The black line shows the molecular mass distribution (right ordinate axis). A mass of 102 ± 3.3 kDa was found for this ASK1-UFO-LFY-DBD-LUBS0 complex, consistent with one copy of each protein per DNA molecule (theoretical mass of 108 kDa). Coomassie-stained SDS-PAGE gel of the different SEC-MALLS fractions (bottom). Each lane corresponds to a 0.5 mL fraction. Molecular weights of the protein standards are indicated (BioRad Precision Plus). Faint bands above UFO likely correspond to contaminants. **f,** EMSA with ASK1-UFO, LFY-DBD and indicated DNA probes. Sequences with coordinates relative to *AP3* start codon (left). Red letters indicate mutated bases. Bars under sequences represent the regions required for ASK1-UFO-LFY-DBD binding. EMSA with described DNA probes (right). Each DNA probe was mixed with the same ASK1-UFO-LFY-DBD protein mix. Note that the LUBS0 mutation also reduced *pAP3* activation in protoplasts (Fig. 2b).

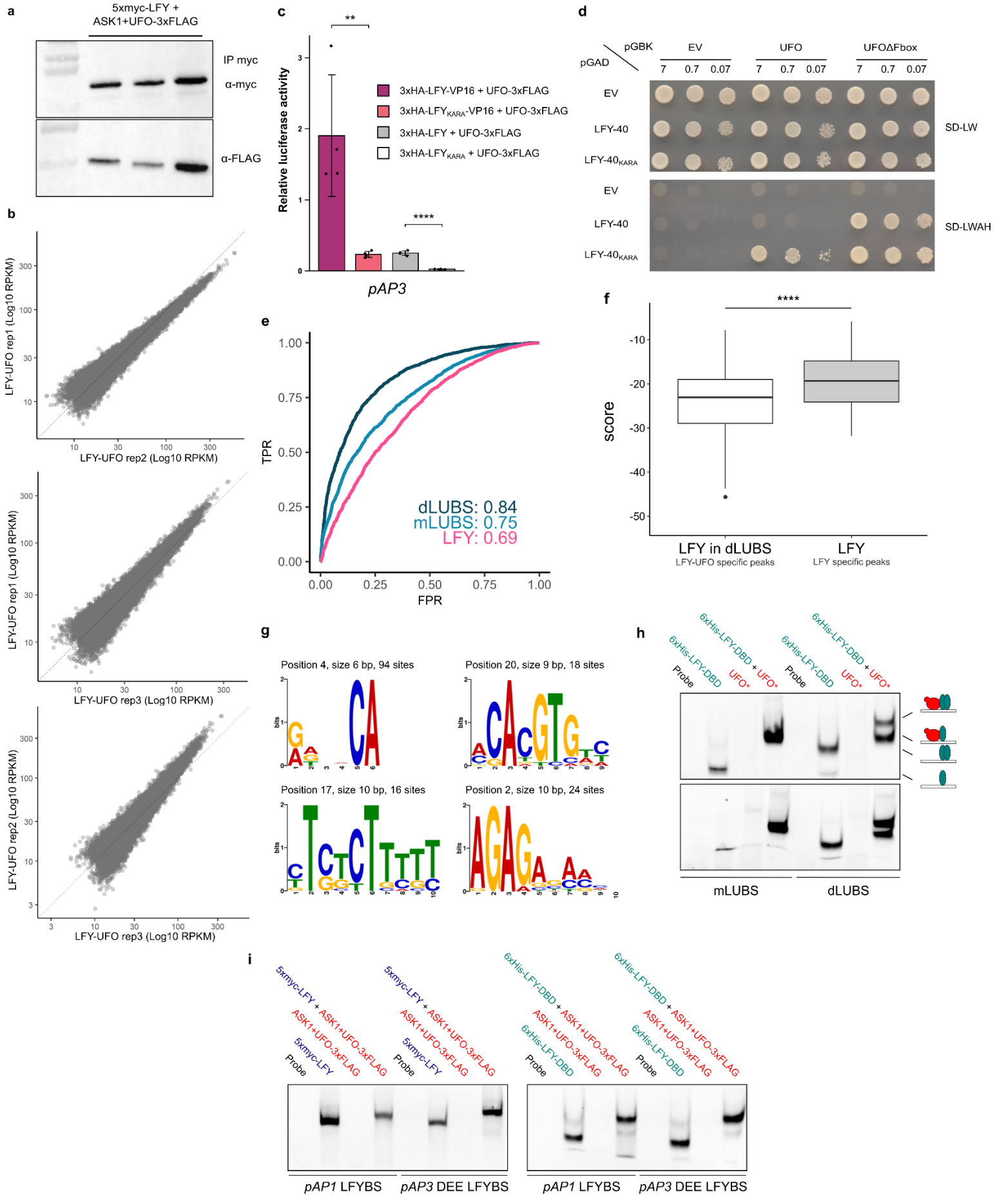
a
5xmyc-LFY +
ASK1+UFO-3xFLAG
IP myc
α-myc
α-FLAG
b
LFY-UFO rep1 (Log10 RPKM)
LFY-UFO rep2 (Log10 RPKM)
LFY-UFO rep3 (Log10 RPKM)
c
Relative luciferase activity
3xHA-LFY-VP16 + UFO-3xFLAG
3xHA-LFY$_{KARA}$-VP16 + UFO-3xFLAG
3xHA-LFY + UFO-3xFLAG
3xHA-LFY$_{KARA}$ + UFO-3xFLAG
pAP3
d
pGBK
pGAD
EV
UFO
UFOΔFbox
LFY-40
LFY-40$_{KARA}$
SD-LW
SD-LWAH
e
TPR
FPR
dLUBS: 0.84
mLUBS: 0.75
LFY: 0.69
f
score
LFY in dLUBS
LFY-UFO specific peaks
LFY
LFY specific peaks
g
Position 4, size 6 bp, 94 sites
Position 20, size 9 bp, 18 sites
Position 17, size 10 bp, 16 sites
Position 2, size 10 bp, 24 sites
h
Probe
6xHis-LFY-DBD
6xHis-LFY-DBD + UFO*
mLUBS
dLUBS
i
5xmyc-LFY
5xmyc-LFY + ASK1+UFO-3xFLAG
6xHis-LFY-DBD
6xHis-LFY-DBD + ASK1+UFO-3xFLAG
pAP1 LFYBS
pAP3 DEE LFYBS

Extended Data Fig. 4. **Genome-wide analysis of LFY-UFO binding. a,** Western Blot after DNA elution during ampDAP-seq experiment. After DNA elution, 20 µL of 1X SDS-PAGE Protein Sample Buffer was added to the remaining beads to run WB. Each lane represents one replicate. **b,** Assessment of experimental reproducibility of ampDAP-seq experiment through the comparison of replicates datasets 2 by 2. **c,** Effect of the LFY KARA mutation (K303A-R233A)[51] on *pAP3* activation in Arabidopsis protoplasts. Data represent averages of independent biological replicates and are presented as mean ± SD, each dot representing one biological replicate (n = 4). Unpaired t-tests (**: $p < 0.01$; ****: $p < 0.0001$). **d,** The LFY KARA mutation (K303A-R233A) does not disrupt LFY-UFO interaction in Yeast-Two-Hybrid (Y2H). EV = Empty Vector. LFY-40 is a LFY version lacking the first 40 aa and better tolerated by yeast cells. Values correspond to the different dilutions (OD = 7, 0.7 and 0.07). Top picture corresponds to the non-selective plate lacking Leucine and Tryptophan (SD -L-W), and bottom picture to the selective plate lacking Leucine, Tryptophan, Histidine and Adenine (SD -L-W-A-H). Pictures were taken at day + 4. **e,** Receiver operating characteristics (ROC) curves for mLUBS, dLUBS and LFY using the top 20% high-CFC LFY-UFO-specific peaks. Area under the curve (AUC) values are shown. TPR: True Positive Rate, FPR: False Positive Rate. **f,** Score distribution of LFY PWM with dependencies[68] within dLUBS (best site on 20% most LFY-UFO-specific genomic regions, high CFC) and in canonical LFYBS (best site on 20% most LFY-specific genomic regions, low CFC). Best sites were selected within ±25 bp around the peak maximum. Wilcoxon rank sum test (****: $p < 0.0001$). Median (solid line), interquartile range (box edges), ±1.5 × interquartile range (whiskers) and outliers (black dot) are shown. **g,** *De novo* identification of URM from LFY ChIP-seq data[25]. Motifs identified at a fixed distance from LFY canonical binding sites in 298 regions harboring high LFY ChIP-seq to LFY ampDAP-seq coverage ratio. The text above each motif gives the motif's start position relative to the canonical LFYBS, its length and the number of sites used to build the motif. **h,** EMSA with mLUBS and dLUBS highest score sequences. 6xHis-LFY-DBD is recombinant. UFO* refers to either recombinant ASK1-UFO-3xFLAG complex (top gel) or *in vitro* produced UFO-3xFLAG (bottom gel). Drawings represent the different types of complexes involving LFY-DBD (pale blue) and ASK1-UFO (red) on DNA. LFY-DBD binds as a monomer as previously reported[30]. The fact that *in vitro* produced UFO-3xFLAG shifts DNA in the presence of LFY indicates that ASK1 is not required for the UFO-LFY-DNA complex formation *in vitro*. **i,** EMSA with DNA probes corresponding to *pAP1* and *pAP3* DEE LFYBS and indicated proteins. Note that probes used here have the same length as those used to study LUBS.

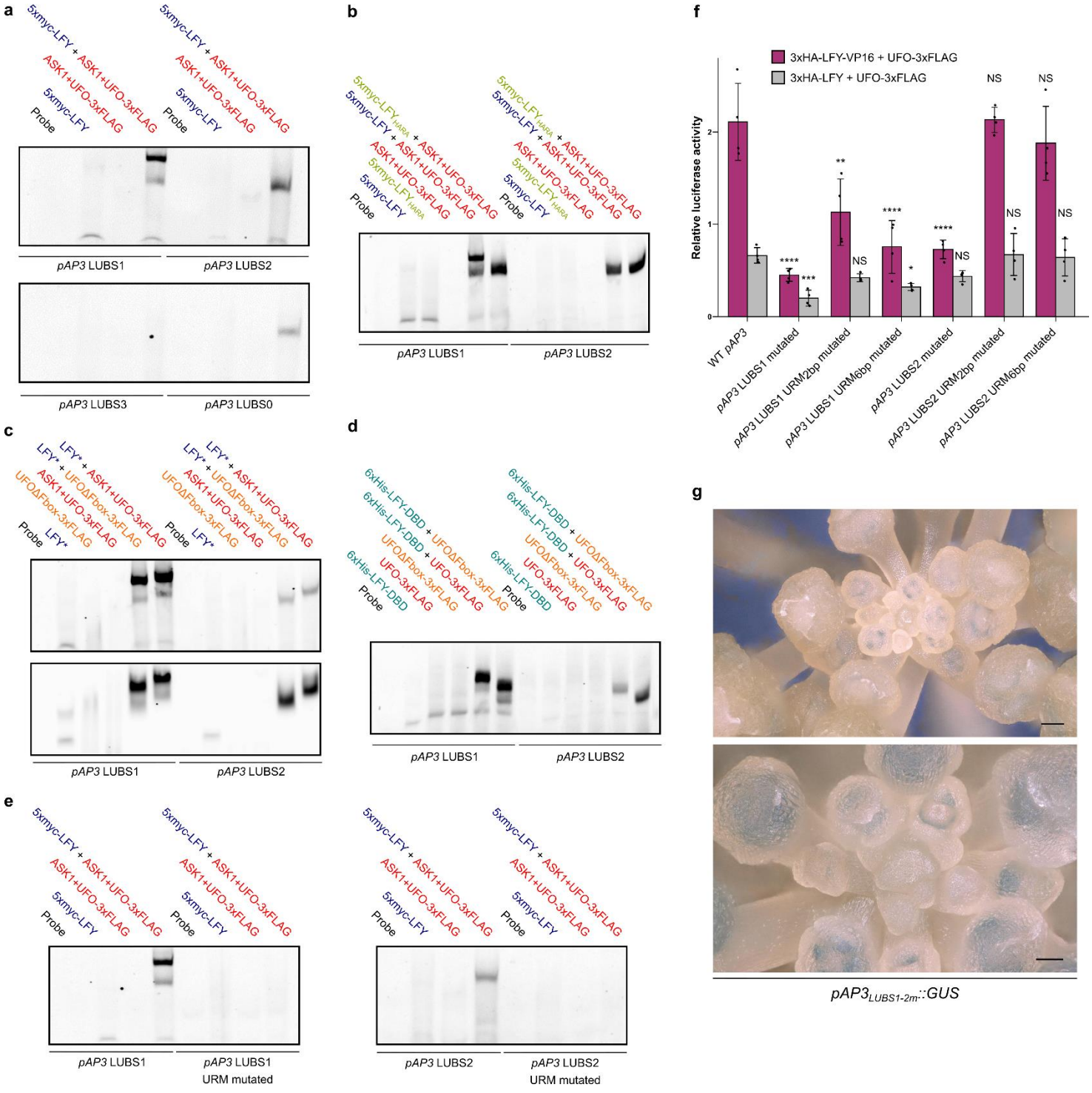

Extended Data Fig. 5. ***pAP3*** **LUBS are required for LFY-UFO-dependent activation. a,** EMSA with indicated probes and proteins. LUBS3 is the third highest-score *pAP3* LUBS. Because LUBS0 is bound with a lower affinity by LFY-UFO compared to LUBS1 and LUBS2, we then focused on LUBS1 and LUBS2. **b,** EMSA with *pAP3* LUBS1 and LUBS2 DNA probes and indicated proteins. $LFY_{H383A-R386A}$ (LFY_{HARA}) is a LFY mutated version affected in its ability to dimerize[30,51]. Note the absence of the complex with a slower mobility on LUBS1 with LFY_{HARA}. **c,** EMSA with *pAP3* LUBS1 and LUBS2 DNA probes and indicated proteins. LFY* refers to either *in vitro*-produced 5xmyc-LFY (top) or recombinant 6xHis-LFY-DBD (bottom). Note the difference of

complex size between UFO and UFOΔFbox. **d,** Same as in (**c**) except that UFO-3xFLAG and UFOΔFbox-3xFLAG were produced *in vitro*. Note that *in vitro* produced UFO-3xFLAG and UFOΔFbox-3xFLAG behave similarly as recombinant UFO versions. **e,** EMSA with indicated proteins and DNA probes corresponding to *pAP3* LUBS1 (left) and LUBS2 (right), WT or with URM mutated. **f,** Promoter activation measured by DLRA in Arabidopsis protoplasts with indicated effectors. Different promoter versions were tested as indicated under x-axis. Either 2 bp (high-informative CA) or 6 bp (whole URM) of *pAP3* LUBS1 and LUBS2 URM were mutated. Data represent averages of independent biological replicates and are presented as mean ± SD, each dot representing one biological replicate (n = 4). One-way ANOVA with Tukey's multiple comparisons tests. One-way ANOVA were performed with data from the same effector and stars represent a statistical difference compared to WT *pAP3* promoter. (NS: $p > 0.05$,*: $p < 0.05$, **: $p < 0.01$, ***: $p < 0.001$ and ****: $p < 0.0001$). **g,** *In vivo* analysis of $pAP3_{LUBS1\text{-}2m}$*::GUS* fusions. Same as in Fig. 3d, except that staining incubation time was increased to 17 h (4h incubation in Fig. 3d). Representative pictures are shown (top scale bar, 100 µm, bottom scale bar, 50 µm). The faint *AP3* pattern suggests that other LUBS (such as LUBS0) may take over but less efficiently. Note that with this staining incubation time, all plants expressing *pAP3::GUS* showed a highly saturated staining.

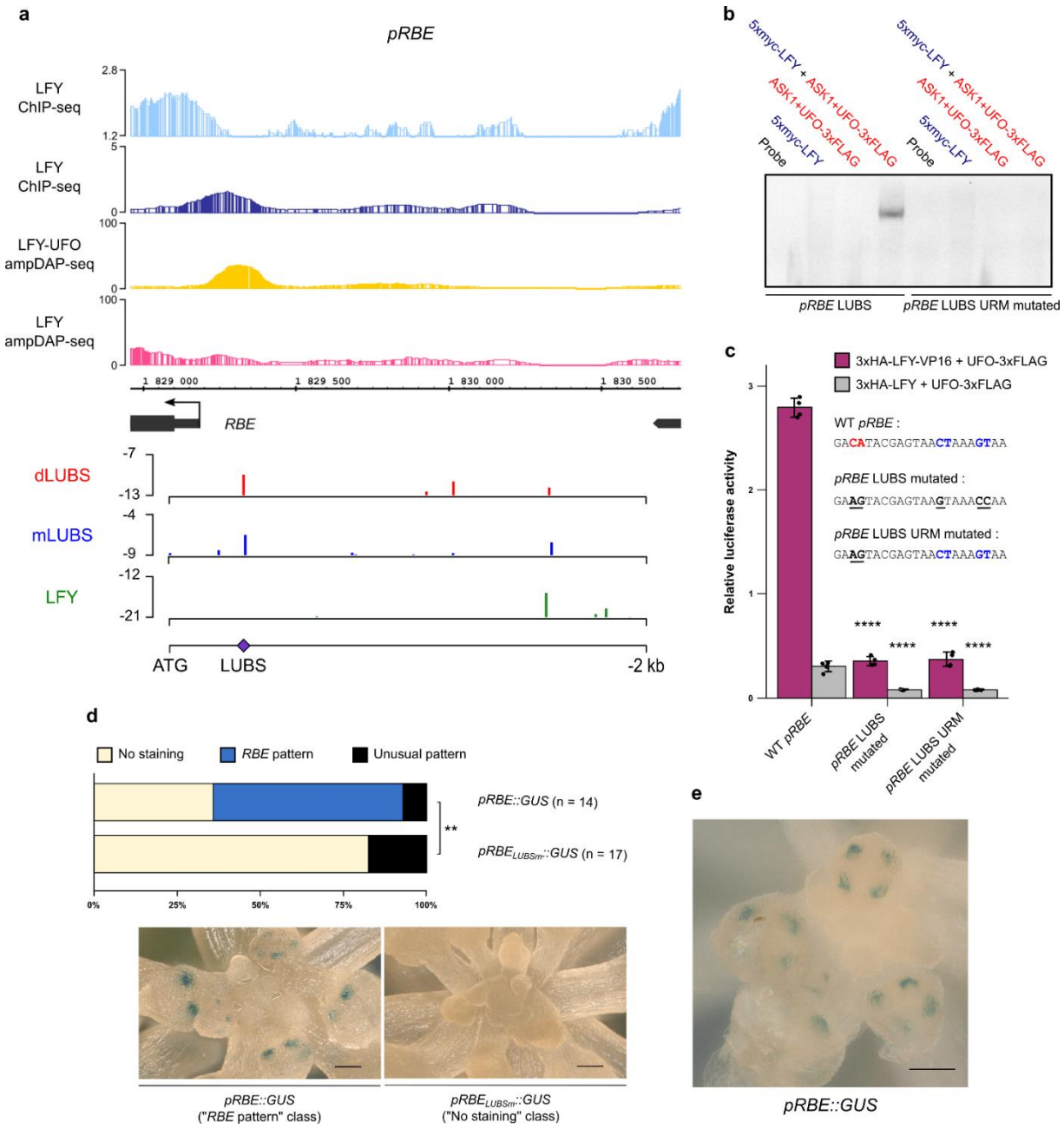

Extended Data Fig. 6. *pRBE* LUBS is required for LFY-UFO-dependent activation. a, IGB view of *pRBE* showing LFY ChIP-seq in inflorescences (light blue)[25] or seedlings (dark blue)[26], LFY-UFO ampDAP-seq (yellow), LFY ampDAP-seq (pink)[27], numbers indicate read number range (top). Identification of LUBS in *pRBE* (bottom). Predicted binding sites using dLUBS and mLUBS models from Fig. 2e and LFY PWM with dependencies[68], y-axis represents score values (bottom). The best binding sites correspond to the less negative score values. Studied LUBS is indicated with a purple square. **b,** EMSA with probes corresponding to *pRBE* LUBS, WT or with URM mutated. **c,** *pRBE* activation in Arabidopsis protoplasts. Effect of mutations (underlined) in URM (red) and in LFYBS (blue) bases of *pRBE* LUBS were assayed. Data represent averages of independent biological replicates and are presented as mean ± SD, each dot representing one biological replicate (n = 4). One-way ANOVA with Tukey's multiple comparisons test. One-way ANOVA were performed with data from the same effector, and stars represent a

statistical difference compared to WT promoters (****: $p < 0.0001$). **d,** *In vivo* analysis of *pRBE::GUS* fusions. The percentage of transgenic lines with *RBE* pattern, unusual pattern or absence of staining was scored (top; χ^2 test, **: $p < 0.01$). n = number of independent lines. Unusual pattern refers to staining in unexpected tissues, each pattern seen in a single line. Representative pictures of plants with no staining (bottom left) and a *RBE* pattern (bottom right) are shown (scale bar, 50 µm). **e,** *In vivo* analysis of *pRBE::GUS* fusions. Same as in (**d**), with another view showing staining in the four petal primordia (scale bar, 50 µm).

a

Gene	Name	Description	Up/Down regulated	LFY ChIP-Seq set
AT1G13260	RAV1	related to ABI3/VP1 1	down	A
AT1G24530	NA	Transducin/WD40 repeat-like superfamily protein	down	B
AT1G34110	NA	Leucine-rich receptor-like protein kinase family protein	up	C; B
AT1G54010	NA	GDSL-like Lipase/Acylhydrolase superfamily protein	down	A
AT1G73805	NA	Calmodulin binding protein-like	down	C; B; A
AT1G74440	NA	Protein of unknown function (DUF962)	down	A
AT1G75450	ATCKX5	cytokinin oxidase 5	up	C; B; D
AT1G76110	NA	HMG (high mobility group) box protein with ARID/BRIGHT DNA-binding domain	up	A
AT1G80840	ATWRKY40	WRKY DNA-binding protein 40	up	C; B; A
AT3G15270	SPL5	squamosa promoter binding protein-like 5	up	A
AT3G20810	NA	2-oxoglutarate (2OG) and Fe(II)-dependent oxygenase superfamily protein	up	A
AT3G28180	ATCSLC04	Cellulose-synthase-like C4	down	B
AT3G54340	AP3	K-box region and MADS-box transcription factor family protein	up	B
AT3G55560	AGF2	AT-hook protein of GA feedback 2	up	C; B; A
AT4G00730	ANL2	Homeobox-leucine zipper family protein / lipid-binding START domain-containing protein	up	A
AT4G02380	AtLEA5	senescence-associated gene 21	down	B
AT4G34160	CYCD3	CYCLIN D3	up	A
AT4G35900	FD	Basic-leucine zipper (bZIP) transcription factor family protein	down	C; B; A
AT5G02540	NA	NAD(P)-binding Rossmann-fold superfamily protein	up	B; D
AT5G20240	PI	K-box region and MADS-box transcription factor family protein	up	A

b

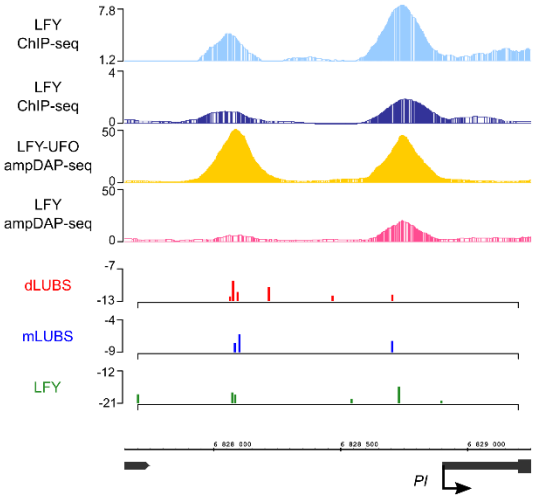

c

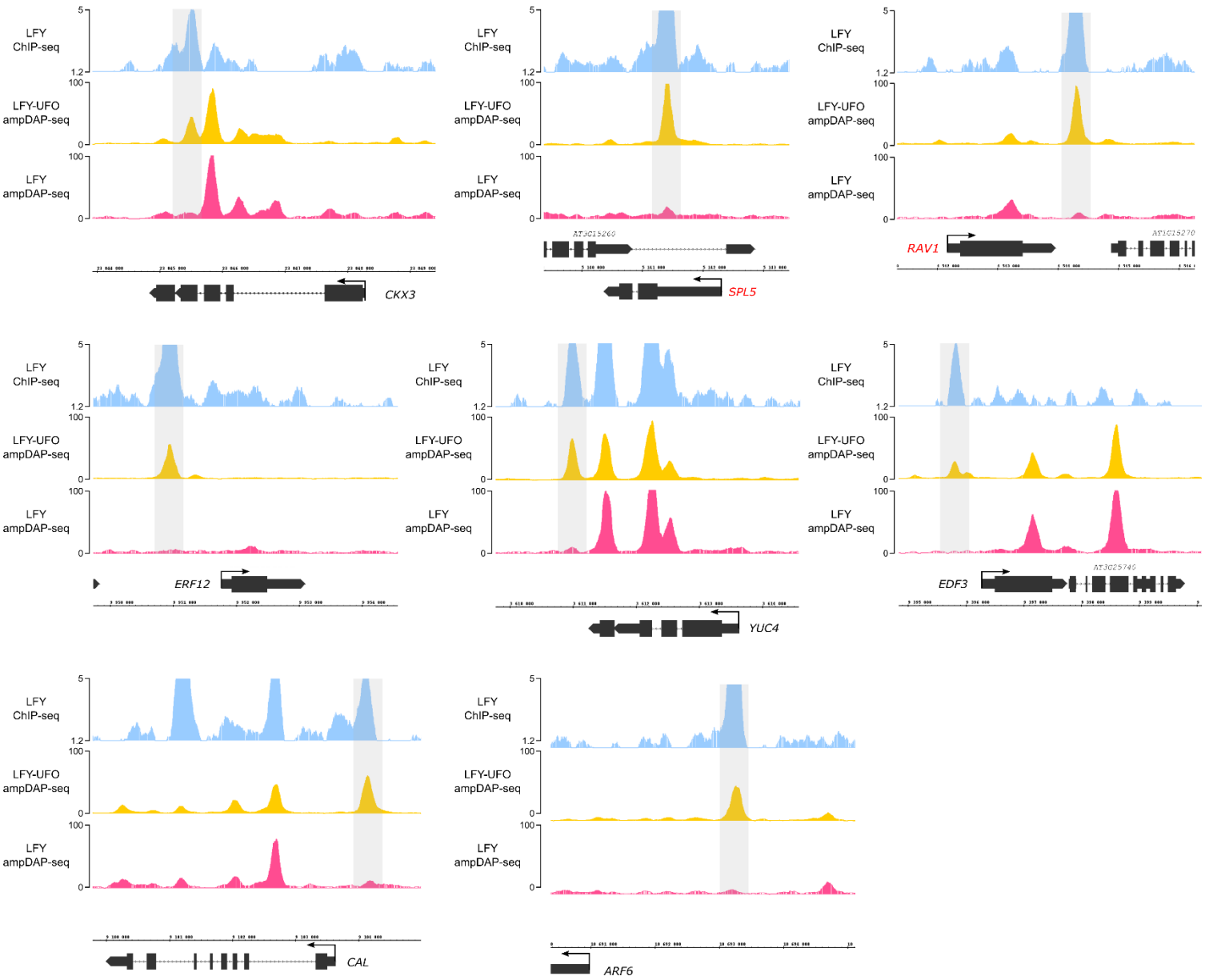

Extended Data Fig. 7. LFY and UFO likely regulate other genes in Arabidopsis. a, List of candidate LFY-UFO target genes selected as i) present in regions specifically bound by LFY-UFO in ampDAP-seq (high CFC) ii) bound *in vivo* in LFY ChIP-seq experiments (A[25]; B[26]; C[68]; D[70]) and iii) deregulated in *ufo* inflorescences[69]. **b,** IGB view of *PISTILLATA* promoter region showing LFY ChIP-seq in inflorescences (light blue)[25] or seedlings (dark blue)[26], LFY-UFO ampDAP-seq (yellow), LFY ampDAP-seq (pink)[27], numbers indicate read number range (top). Predicted binding sites using the dLUBS, mLUBS models from Fig. 2e and LFY PWM with dependencies[68], y-axis represents score values (bottom). **c,** IGB view of selected genes showing LFY ChIP-seq in inflorescences (light blue)[25], LFY-UFO ampDAP-seq (yellow), LFY ampDAP-seq (pink)[27], numbers indicate read number range. Genes in red are deregulated in *ufo* inflorescences[69]. ChIP-seq peaks better explained by LFY-UFO than by LFY alone are shaded in grey.

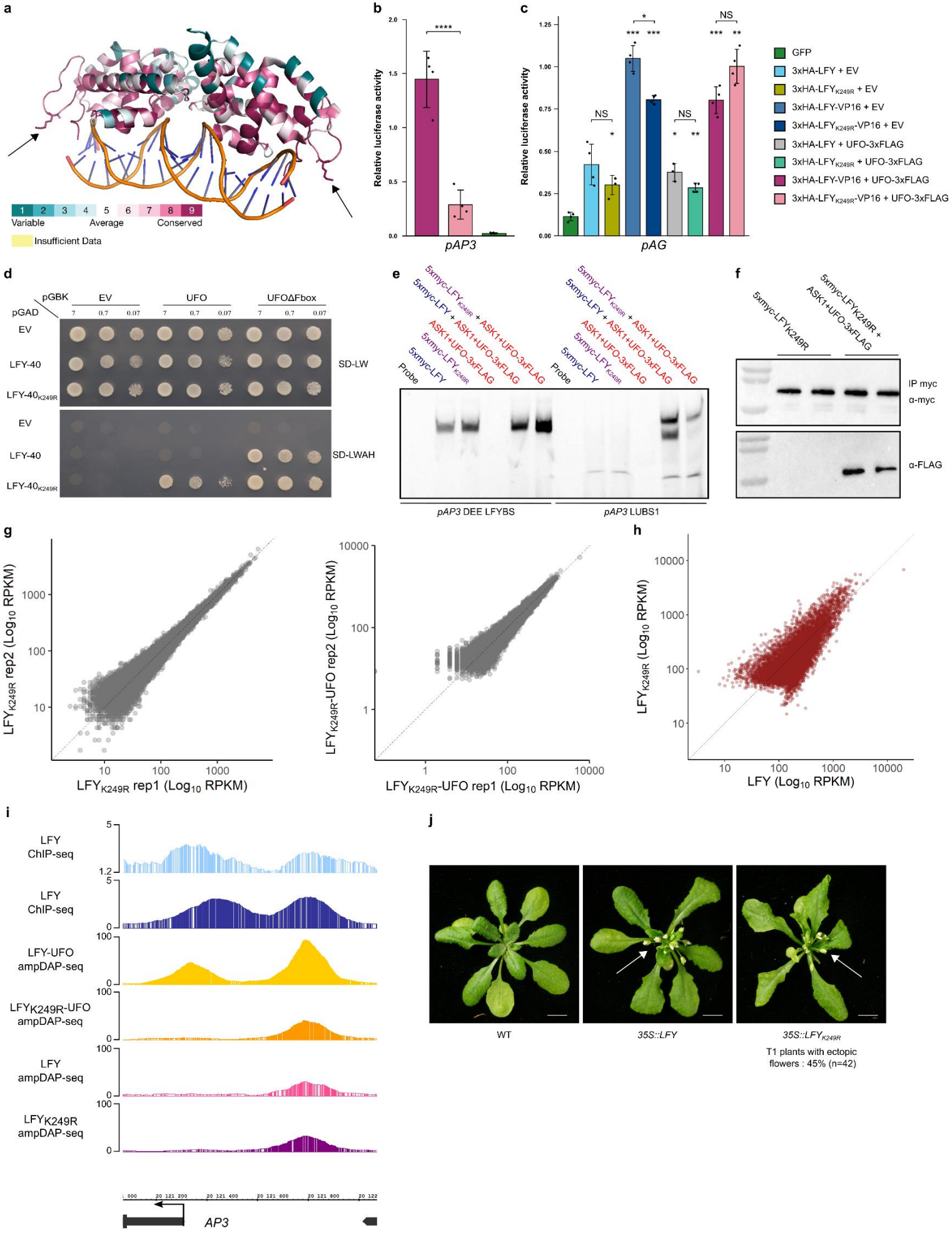
a
1 2 3 4 5 6 7 8 9
Variable
Average
Conserved
Insufficient Data
b
Relative luciferase activity
****
pAP3
c
Relative luciferase activity
NS
pAG
GFP
3xHA-LFY + EV
3xHA-LFY$_{K249R}$ + EV
3xHA-LFY-VP16 + EV
3xHA-LFY$_{K249R}$-VP16 + EV
3xHA-LFY + UFO-3xFLAG
3xHA-LFY$_{K249R}$ + UFO-3xFLAG
3xHA-LFY-VP16 + UFO-3xFLAG
3xHA-LFY$_{K249R}$-VP16 + UFO-3xFLAG
d
pGBK
pGAD
EV
UFO
UFOΔFbox
7
0.7
0.07
LFY-40
LFY-40$_{K249R}$
SD-LW
SD-LWAH
e
Probe
5xmyc-LFY
5xmyc-LFY$_{K249R}$
ASK1+UFO-3xFLAG
pAP3 DEE LFYBS
pAP3 LUBS1
f
5xmyc-LFYK249R
5xmyc-LFYK249R + ASK1+UFO-3xFLAG
IP myc
α-myc
α-FLAG
g
LFY$_{K249R}$ rep2 (Log$_{10}$ RPKM)
LFY$_{K249R}$ rep1 (Log$_{10}$ RPKM)
LFY$_{K249R}$-UFO rep2 (Log$_{10}$ RPKM)
LFY$_{K249R}$-UFO rep1 (Log$_{10}$ RPKM)
h
LFY$_{K249R}$ (Log$_{10}$ RPKM)
LFY (Log$_{10}$ RPKM)
i
LFY ChIP-seq
LFY ChIP-seq
LFY-UFO ampDAP-seq
LFYK249R-UFO ampDAP-seq
LFY ampDAP-seq
LFYK249R ampDAP-seq
AP3
j
WT
35S::LFY
35S::LFY$_{K249R}$
T1 plants with ectopic flowers : 45% (n=42)

Extended Data Fig. 8. The LFY K249 is essential for LFY-UFO-LUBS complex formation. a, Structure of LFY-DBD[30]. Residues were colored by conservation using Consurf with default parameters[80]. K249 residues on each LFY monomer are represented as sticks and indicated with arrows. Note that the K249-containing loop is highly conserved. **b,c,** Promoter activation measured by DLRA in Arabidopsis protoplasts with indicated effectors (right). EV = Empty Vector (pRT104-3xHA). Tested promoters are indicated below each graph. Note that for 3xHA-LFY+UFO-3xFLAG on *pAG* only n = 3 biological replicates are shown. Data represent averages of independent biological replicates and are presented as mean ± SD, each dot representing one biological replicate (n = 4 unless specified). One-way ANOVA with Tukey's multiple comparisons tests (**b**) or Welch's ANOVA with Games-Howell post-hoc test (**c**). In (**c**), stars above bars represent a statistical difference compared to GFP. Other comparisons are indicated with brackets. (NS: $p > 0.05$,*: $p < 0.05$, **: $p < 0.01$, ***: $p < 0.001$ and ****: $p < 0.0001$). **d,** Effect of the LFY_{K249R} mutation on LFY-UFO interaction in Y2H. EV = Empty Vector. LFY-40 is a LFY version lacking the first 40 aa and better tolerated by yeast cells. Values correspond to the different dilutions (OD = 7, 0.7 and 0.07). Top picture corresponds to the non-selective plate lacking Leucine and Tryptophan (SD -L-W), and bottom picture corresponds to the selective plate lacking Leucine, Tryptophan, Histidine and Adenine (SD -L-W-A-H). Pictures were taken at day + 4. **e,** EMSA with DNA probes corresponding to *pAP3* DEE LFYBS and *pAP3* LUBS1 and indicated proteins. *pAP3* DEE LFYBS DNA probe was used as a control for binding on canonical LFYBS. **f,** WB after DNA elution during ampDAP-seq experiment. After DNA elution, 20 µL of 1X SDS-PAGE Protein Sample Buffer was added to the remaining beads to run WB. Each lane represents one replicate. **g,** Reproducibility of ampDAP-seq experiments with LFY_{K249R} (left) and LFY_{K249R}-UFO (right) through the comparison of replicates datasets 2 by 2. **h,** Comparison of peak coverage in LFY_{K249R} (y-axis, this study) and LFY (x-axis)[27] ampDAP-seq experiments. **i,** Integrated Genome Browser (IGB) view of *pAP3* showing LFY ChIP-seq in inflorescences (light blue)[25] or seedlings (dark blue)[26], LFY-UFO ampDAP-seq (yellow; this study), LFY ampDAP-seq (pink)[27] and LFY_{K249R} ampDAP-seq (purple; this study). Numbers indicate read number range. **j,** Pictures of WT and representative transgenic plants expressing *35S::LFY* or *35S::LFY$_{K249R}$* (scale bar, 1 cm). The white arrows indicate ectopic rosette flowers. *35S::LFY* was obtained previously[26]. 42 T1 plants expressing *35S::LFY$_{K249R}$* were analyzed; the percentage of plants with a LFY overexpressing phenotype is comparable to the one obtained with *35S::LFY* [26].

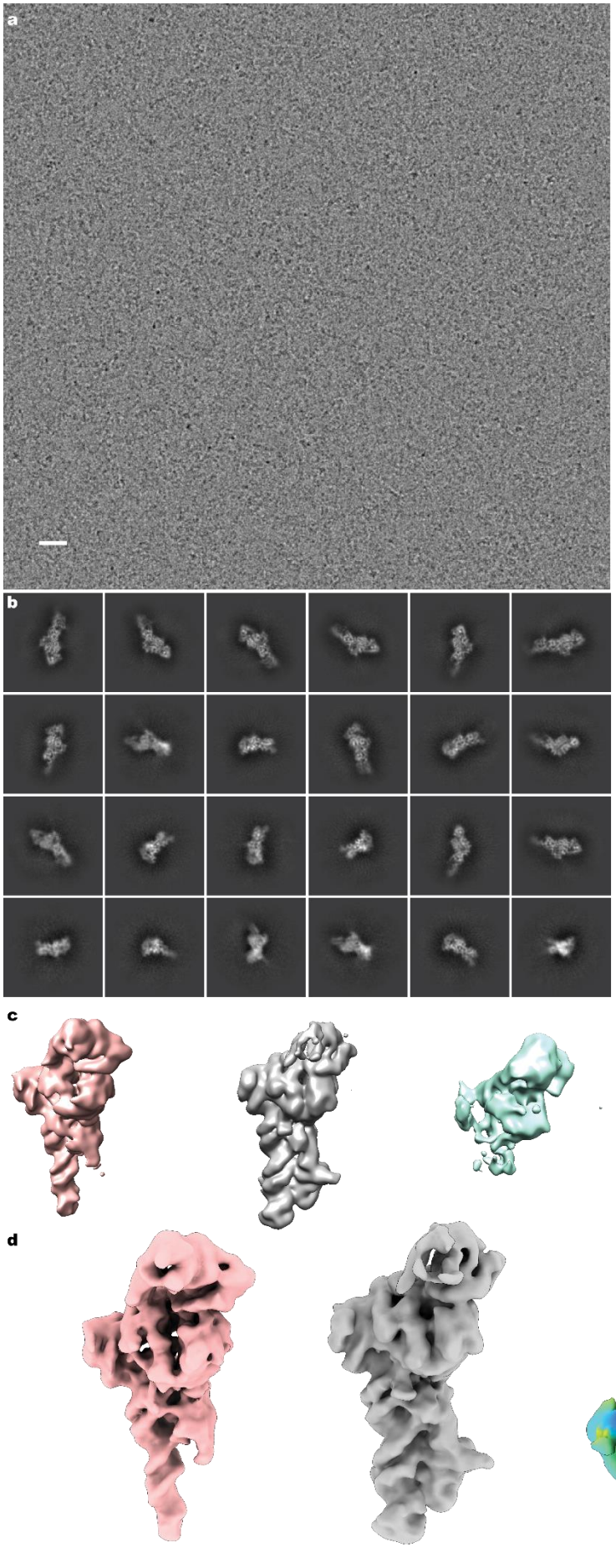
a
b
c
d
e
f
g
h
i
Elevation
Azimuth
# of images
FSC
fsc_noisesub
fsc_nomask
FSC =0.143
4.3Å
6.4Å
Spacial Frequency [1/Å]

Extended Data Fig. 9. UFO binds DNA and LFY DBD. a, A representative micrograph of the ASK1-UFO-LFY-DNA complex in vitreous ice. **b,** Selected 2D class averages of the particles submitted to *ab initio* reconstruction and heterogeneous refinement for 3D classification. **c,** Intermediate reconstructions of the 3D classes after heterogeneous refinement. **d,** Final reconstructions of ASK1-UFO-LFY-DNA complexes (involving either a LFY-DBD monomer (pink) or a LFY-DBD dimer (gray)) after Non-Uniform refinement. **e,** Unprocessed AlphaFold2 model for ASK1 (top, purple; uniprot ID, Q39255), UFO (middle, red; uniprot ID, Q39090) and the LFY-DBD dimer/DNA crystallographic structure (bottom, pale and dark blue for the LFY-DBD dimer and green for the DNA; PDB, 2VY1). **f,** Cryo-EM density map color-coded by fitted molecule. Note the kink on DNA induced by the presence of UFO. **g,** Heat map of the angular distribution of particle projections contributing for the final reconstruction of the complete ASK1-UFO-LFY-DNA complex (with a LFY-DBD dimer). **h,** Gold-standard Fourier shell correlation (FSC) curves. The dotted line represents the 0.143 FSC threshold, which indicates a nominal resolution of 6.4 Å for the unmasked (red) and 4.3 Å for the masked (blue) reconstruction. **i,** View of the post-processed map of the complete ASK1-UFO-LFY-DNA complex, colored according to the local resolution.

References

1. Moyroud, E., Kusters, E., Monniaux, M., Koes, R. & Parcy, F. LEAFY blossoms. *Trends in Plant Science* vol. 15 346–352 (2010).
2. Irish, V. F. The flowering of Arabidopsis flower development. *Plant J.* **61**, 1014–1028 (2010).
3. Parcy, F., Nilsson, O., Busch, M. A., Lee, I. & Weigel, D. A genetic framework for floral patterning. *Nature* **395**, 561–566 (1998).
4. Wagner, D., Sablowski, R. W. M. & Meyerowitz, E. M. Transcriptional activation of APETALA1 by LEAFY. *Science* **285**, 582–584 (1999).
5. Lohmann, J. U. *et al.* A molecular link between stem cell regulation and floral patterning in Arabidopsis. *Cell* **105**, 793–803 (2001).
6. Lee, I., Wolfe, D. S., Nilsson, O. & Weigel, D. A LEAFY co-regulator encoded by UNUSUAL FLORAL ORGANS. *Curr. Biol.* **7**, 95–104 (1997).
7. Levin, J. Z. & Meyerowitz, E. M. UFO: an Arabidopsis gene involved in both floral meristem and floral organ development. *Plant Cell* **7**, 529–548 (1995).
8. Wilkinson & Haughn. UNUSUAL FLORAL ORGANS Controls Meristem Identity and Organ Primordia Fate in Arabidopsis. *Plant Cell* **7**, 1485–1499 (1995).
9. Krizek, B. A. & Meyerowitz, E. M. The Arabidopsis homeotic genes APETALA3 and PISTILLATA are sufficient to provide the B class organ identity function. *Development* **122**, 11–22 (1996).
10. Ikeda-Kawakatsu, K., Maekawa, M., Izawa, T., Itoh, J.-I. & Nagato, Y. ABERRANT PANICLE ORGANIZATION 2/RFL, the rice ortholog of Arabidopsis LEAFY, suppresses the transition from inflorescence meristem to floral meristem through interaction with APO1. *Plant J.* **69**, 168–180 (2012).
11. Lippman, Z. B. *et al.* The Making of a Compound Inflorescence in Tomato and Related

Nightshades. *PLoS Biol.* **6**, e288 (2008).

12. Souer, E. *et al.* Patterning of Inflorescences and Flowers by the F-Box Protein DOUBLE TOP and the LEAFY Homolog ABERRANT LEAF AND FLOWER of Petunia. *Plant Cell Online* **20**, 2033–2048 (2008).

13. Kuzay, S. *et al.* WAPO-A1 is the causal gene of the 7AL QTL for spikelet number per spike in wheat. *PLoS Genet.* **18**, (2022).

14. Ingram, G. C. *et al.* Dual role for fimbriata in regulating floral homeotic genes and cell division in Antirrhinum. *EMBO J.* **16**, 6521–6534 (1997).

15. Samach, A. *et al.* The UNUSUAL FLORAL ORGANS gene of Arabidopsis thaliana is an F-box protein required for normal patterning and growth in the floral meristem. *Plant J.* **20**, 433–445 (1999).

16. Simon, R., Carpenter, R., Doyle, S. & Coen, E. Fimbriata controls flower development by mediating between meristem and organ identity genes. *Cell* **78**, 99–107 (1994).

17. Wang, X. *et al.* The COP9 Signalosome Interacts with SCF UFO and Participates in Arabidopsis Flower Development. *Plant Cell* **15**, 1071–1082 (2003).

18. Chae, E., Tan, Q. K.-G., Hill, T. A. & Irish, V. F. An Arabidopsis F-box protein acts as a transcriptional co-factor to regulate floral development. *Development* **135**, 1235–1245 (2008).

19. Geng, F., Wenzel, S. & Tansey, W. P. Ubiquitin and Proteasomes in Transcription. *Annu. Rev. Biochem.* **81**, 177–201 (2012).

20. Risseeuw, E. *et al.* An activated form of UFO alters leaf development and produces ectopic floral and inflorescence meristems. *PLoS One* **8**, (2013).

21. Busch, M. A., Bomblies, K. & Weigel, D. Activation of a floral homeotic gene in Arabidopsis. *Science* **285**, 585–587 (1999).

22. Krizek, B. A., Lewis, M. W. & Fletcher, J. C. *RABBIT EARS* is a second-whorl repressor of *AGAMOUS* that maintains spatial boundaries in Arabidopsis flowers. *Plant J.* **45**, 369–383 (2006).

23. Hill, T. A., Day, C. D., Zondlo, S. C., Thackeray, A. G. & Irish, V. F. Discrete spatial and temporal cis-acting elements regulate transcription of the Arabidopsis floral homeotic gene APETALA3. *Development* **125**, 1711–1721 (1998).

24. Lamb, R. S., Hill, T. a, Tan, Q. K.-G. & Irish, V. F. Regulation of APETALA3 floral homeotic gene expression by meristem identity genes. *Development* **129**, 2079–2086 (2002).

25. Goslin, K. *et al.* Transcription Factor Interplay between LEAFY and APETALA1/CAULIFLOWER during Floral Initiation. *Plant Physiol.* **174**, 1097–1109 (2017).

26. Sayou, C. *et al.* A SAM oligomerization domain shapes the genomic binding landscape of the LEAFY transcription factor. *Nat. Commun.* **7**, 11222 (2016).

27. Lai, X. *et al.* The LEAFY floral regulator displays pioneer transcription factor properties. *Mol. Plant* **14**, 829–837 (2021).

28. Weigel, D., Alvarez, J., Smyth, D. R., Yanofsky, M. F. & Meyerowitz, E. M. *LEAFY* controls floral meristem identity in *Arabidopsis*. *Cell* **69**, 843–859 (1992).

29. Weigel, D. & Nilsson, O. A developmental switch sufficient for flower initiation in diverse plants. *Nature* **377**, 495–500 (1995).

30. Hamès, C. *et al.* Structural basis for LEAFY floral switch function and similarity with helix-turn-helix proteins. *EMBO J.* **27**, 2628–2637 (2008).

31. Sayou, C. *et al.* A promiscuous intermediate underlies the evolution of LEAFY DNA binding specificity. *Science* **343**, 645–648 (2014).

32. Zhao, D., Yu, Q., Chen, M. & Ma, H. The ASK1 gene regulates B function gene expression in cooperation with UFO and LEAFY in Arabidopsis. *Development* **128**, 2735–2746 (2001).

33. Ni, W. *et al.* Regulation of flower development in arabidopsis by SCF complexes. *Plant Physiol.* **134**, 1574–1585 (2004).

34. Levin, J. Z., Fletcher, J. C., Chen, X. & Meyerowitz, E. M. A genetic screen for modifiers of UFO meristem activity identifies three novel FUSED FLORAL ORGANS genes required for early flower development in Arabidopsis. *Genetics* **149**, 579–595 (1998).

35. Singh, N. & Bhalla, N. Moonlighting Proteins. (2020)

36. Honma, T. & Goto, K. *PISTILLATA transcriptional regulation*. (2000).

37. Tilly, J. J., Allen, D. W. & Jack, T. The CArG boxes in the promoter of the Arabidopsis floral organ identity gene APETALA3 mediate diverse regulatory effects. *Development* **125**, 1647–1657 (1998).

38. Liu, C., Xi, W., Shen, L., Tan, C. & Yu, H. Regulation of floral patterning by flowering time genes. *Dev. Cell* **16**, 711–22 (2009).

39. Gregis, V., Sessa, A., Colombo, L. & Kater, M. M. AGL24 , SHORT VEGETATIVE PHASE , and APETALA1 Redundantly Control AGAMOUS during Early Stages of Flower Development in Arabidopsis. *Plant Cell* **18**, 1373–1382 (2006).

40. Castillejo, C., Romera-Branchat, M. & Pelaz, S. A new role of the Arabidopsis SEPALLATA3 gene revealed by its constitutive expression. *Plant J.* **43**, 586–596 (2005).

41. Siggers, T., Duyzend, M. H., Reddy, J., Khan, S. & Bulyk, M. L. Non-DNA-binding cofactors enhance DNA-binding specificity of a transcriptional regulatory complex. *Mol. Syst. Biol.* **7**, 555 (2011).

42. Babb, R., Huang, C., Aufiero, D. J. & Herr, W. DNA Recognition by the Herpes Simplex Virus Transactivator VP16: a Novel DNA-Binding Structure. *Mol. Cell. Biol.* **21**, 4700–4712 (2001).

43. Chahtane, H. *et al.* LEAFY activity is post-transcriptionally regulated by BLADE ON PETIOLE2 and CULLIN3 in Arabidopsis. *New Phytol.* **220**, 579–592 (2018).

44. Blanvillain, R. *et al.* The Arabidopsis peptide kiss of death is an inducer of programmed cell death. *EMBO J.* **30**, 1173–1183 (2011).

45. Takeda, S., Matsumoto, N. & Okada, K. RABBIT EARS, encoding a SUPERMAN-like zinc finger protein, regulates petal development in Arabidopsis thaliana. *Development* **131**, 425–34 (2004).

46. Benlloch, R. *et al.* Integrating long-day flowering signals: A LEAFY binding site is essential for proper photoperiodic activation of APETALA1. *Plant J.* **67**, 1094–1102 (2011).

47. Iwata, Y., Lee, M. H. & Koizumi, N. Analysis of a transcription factor using transient assay in Arabidopsis protoplasts. *Methods Mol. Biol.* **754**, 107–117 (2011).

48. Dümmler, A., Lawrence, A. M. & de Marco, A. Simplified screening for the detection of soluble fusion constructs expressed in E. coli using a modular set of vectors. *Microb. Cell Fact.* **4**, 34

(2005).

49. Bartlett, A. *et al.* Mapping genome-wide transcription-factor binding sites using DAP-seq. *Nat. Protoc.* **12**, 1659–1672 (2017).

50. Cutler, S. R., Ehrhardt, D. W., Griffitts, J. S. & Somerville, C. R. Random GFP::cDNA fusions enable visualization of subcellular structures in cells of Arabidopsis at a high frequency. *Proc. Natl. Acad. Sci. U. S. A.* **97**, 3718 (2000).

51. Chahtane, H. *et al.* A variant of LEAFY reveals its capacity to stimulate meristem development by inducing *RAX1*. *Plant J.* **74**, 678–689 (2013).

52. Punjani, A., Rubinstein, J. L., Fleet, D. J. & Brubaker, M. A. cryoSPARC: algorithms for rapid unsupervised cryo-EM structure determination. *Nat. Methods 2017 143* **14**, 290–296 (2017).

53. Wagner, T. *et al.* SPHIRE-crYOLO is a fast and accurate fully automated particle picker for cryo-EM. *Commun. Biol. 2019 21* **2**, 1–13 (2019).

54. Punjani, A., Zhang, H. & Fleet, D. J. Non-uniform refinement: adaptive regularization improves single-particle cryo-EM reconstruction. *Nat. Methods 2020 1712* **17**, 1214–1221 (2020).

55. Sanchez-Garcia, R. *et al.* DeepEMhancer: a deep learning solution for cryo-EM volume post-processing. *Commun. Biol. 2021 41* **4**, 1–8 (2021).

56. Pettersen, E. F. *et al.* UCSF Chimera--a visualization system for exploratory research and analysis. *J. Comput. Chem.* **25**, 1605–1612 (2004).

57. Pettersen, E. F. *et al.* UCSF ChimeraX: Structure visualization for researchers, educators, and developers. *Protein Sci.* **30**, 70–82 (2021).

58. Emsley, P., Lohkamp, B., Scott, W. G. & Cowtan, K. Features and development of Coot. *Acta Crystallogr. D. Biol. Crystallogr.* **66**, 486–501 (2010).

59. Afonine, P. V. *et al.* Real-space refinement in PHENIX for cryo-EM and crystallography. *Acta Crystallogr. Sect. D, Struct. Biol.* **74**, 531 (2018).

60. Jumper, J. *et al.* Highly accurate protein structure prediction with AlphaFold. *Nat. 2021 5967873* **596**, 583–589 (2021).

61. Terwilliger, T. C. *et al.* Improved AlphaFold modeling with implicit experimental information. *bioRxiv* 2022.01.07.475350 (2022) doi:10.1101/2022.01.07.475350.

62. Lai, X. *et al.* Genome-wide binding of SEPALLATA3 and AGAMOUS complexes determined by sequential DNA-affinity purification sequencing. *Nucleic Acids Res.* **48**, 9637–9648 (2020).

63. Gaspar, J. M. NGmerge: merging paired-end reads via novel empirically-derived models of sequencing errors. *BMC Bioinformatics* **19**, 536 (2018).

64. Berardini, T. Z. *et al.* The Arabidopsis Information Resource: Making and Mining the 'Gold Standard' Annotated Reference Plant Genome. *Genesis* **53**, 474 (2015).

65. Jalili, V., Matteucci, M., Masseroli, M. & Morelli, M. J. Using combined evidence from replicates to evaluate ChIP-seq peaks. *Bioinformatics* **31**, 2761–2769 (2015).

66. Machanick, P. & Bailey, T. L. MEME-ChIP: motif analysis of large DNA datasets. *Bioinformatics* **27**, 1696–1697 (2011).

67. Stigliani, A. *et al.* Capturing Auxin Response Factors Syntax Using DNA Binding Models. *Mol. Plant* **12**, 822–832 (2019).

68. Moyroud, E. *et al.* Prediction of Regulatory Interactions from Genome Sequences Using a Biophysical Model for the *Arabidopsis* LEAFY Transcription Factor. *Plant Cell* **23**, 1293–1306 (2011).

69. Schmid, M. *et al.* A gene expression map of Arabidopsis thaliana development. *Nat. Genet. 2005 375* **37**, 501–506 (2005).

70. Jin, R. *et al.* LEAFY is a pioneer transcription factor and licenses cell reprogramming to floral fate. *Nat. Commun. 2021 121* **12**, 1–14 (2021).

71. Gagne, J. M., Downes, B. P., Shiu, S. H., Durski, A. M. & Vierstra, R. D. The F-box subunit of the SCF E3 complex is encoded by a diverse superfamily of genes in Arabidopsis. *Proc. Natl. Acad. Sci. U. S. A.* **99**, 11519–11524 (2002).

72. Zhang, S. *et al.* Proliferating floral organs (pfo), a Lotus japonicus gene required for specifying floral meristem determinacy and organ identity, encodes an F-box protein. *Plant J.* **33**, 607–619 (2003).

73. Zhao, Y. *et al.* Evolutionary co-option of floral meristem identity genes for patterning of the flower-like asteraceae inflorescence. *Plant Physiol.* **172**, 284–296 (2016).

74. Chen, Y. *et al.* CsUFO is involved in the formation of flowers and tendrils in cucumber. *Theor. Appl. Genet.* **3**, (2021).

75. Ikeda, K., Ito, M., Nagasawa, N., Kyozuka, J. & Nagato, Y. Rice ABERRANT PANICLE ORGANIZATION 1, encoding an F-box protein, regulates meristem fate. *Plant J.* **51**, 1030–1040 (2007).

76. Li, F. *et al.* Reduced expression of CbUFO is associated with the phenotype of a flower-defective cosmos bipinnatus. *Int. J. Mol. Sci.* **20**, 2503 (2019).

77. Sasaki, K. *et al.* Mutation in Torenia fournieri Lind. UFO homolog confers loss of TfLFY interaction and results in a petal to sepal transformation. *Plant J.* **71**, 1002–1014 (2012).

78. Sharma, B. *et al.* Homologs of LEAFY and UNUSUAL FLORAL ORGANS Promote the Transition From Inflorescence to Floral Meristem Identity in the Cymose Aquilegia coerulea. *Front. Plant Sci.* **10**, (2019).

79. Taylor, S., Hofer, J. & Murfet, I. Stamina pistilloida, the pea ortholog of Fim and UFO, is required for normal development of flowers, inflorescences, and leaves. *Plant Cell* **13**, 31–46 (2001).

80. Ashkenazy, H. *et al.* ConSurf 2016: an improved methodology to estimate and visualize evolutionary conservation in macromolecules. *Nucleic Acids Res.* **44**, W344–W350 (2016).

III. Complementary results

In Article 1, results are presented without respecting the chronological order in which they were obtained. For this reason, and because of length constraints for publication, the rationale of some experiments is not straightforward. In this part, I explain the reason why we performed some experiments based on the literature. I also present an alternative hypothesis we had when we began to decipher the LFY-UFO molecular mechanism. Other complementary results related to Article 1 are presented in Chapter II.

A close look at *pAP3*: a clue to understand the LFY-UFO synergy

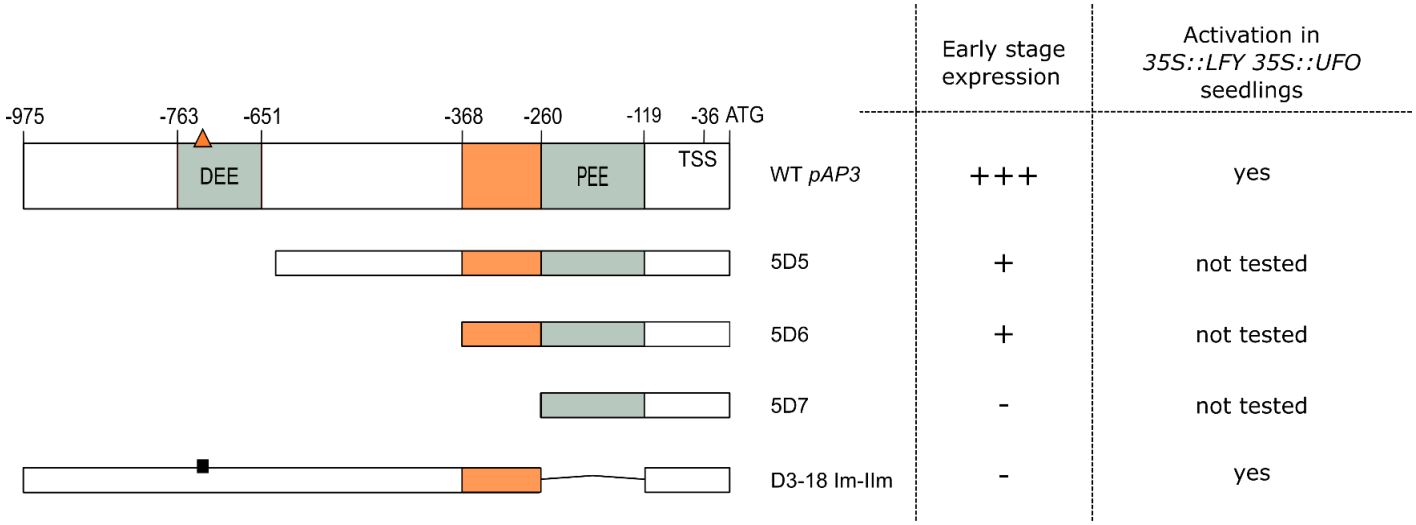

Figure 11. Summary of previous results suggesting the importance of the *pAP3* 107-bp region. *WT pAP3 with regulatory regions and cis-elements is represented in the top row. Coordinates are relative to AP3 start codon. TSS: Transcription Start Site. The orange rectangle represents the 107-bp region. Orange triangle represents canonical LFYBS and the black square a mutated version of this site. Other rows represent different constructs tested by Hill et al. Their activation during early stages of flower development is reported in the middle column (Hill et al., 1998). The activation of the different constructs in 35S::LFY 35S::UFO seedlings is reported in the right column (Parcy et al., 1998; Lamb et al. 2002).*

As mentioned before, we decided to tackle the molecular basis of the LFY-UFO synergy by trying to understand why *pAP3* is activated by LFY-UFO and not by LFY alone. In Article 1, we first focused on a *pAP3* region that we called the "107-bp region" (orange rectangle in Figure

11). Figure 11 explains why, based on previous published results, we thought this region may contain LFY-UFO response elements. In particular, activation of the *D3-18 ImIIm* construct (a *pAP3* version deleted of the PEE and with a mutated canonical LFYBS) in *35S::LFY 35::UFO* seedlings led us to believe that *pAP3* LFY-UFO response elements were not in the PEE (Lamb et al., 2002). LFY ChIP-seq data also showed a peak on this region that cannot be explained by LFY direct binding (see Article 1 Figure 3a). We then proceeded with the functional characterization of this promoter region and the LFY-UFO DNA binding model derived from the ampDAP-seq experiment allowed to identify several additional LUBS.

When we found thanks to protoplast assays that *pAP3* contains some elements recognized only by LFY-UFO, we formulated several hypotheses to explain this result. One of them, not described in Article 1, is presented in the next paragraph.

The hypothesis of another partner binding both LFY-UFO and *pAP3*

Using the protoplast assay, we identified the 107-bp region as a *pAP3* region important for LFY-UFO-dependent activation. Because this sequence is not bound by LFY alone (Lamb et al., 2002), one of our hypotheses was that another endogenous TF(s) recruits both LFY and UFO to this site but not LFY alone (Figure 12A and Figure 9).

To identify this putative partner(s), we performed two screens in yeast in collaboration with the team of Luis Oñate-Sánchez at the CBGP in Madrid. In general, yeast screens are performed with a home-made library prepared from cDNA. However, using an already-characterized TF library allows skipping the cloning step and ensures that all interactions are properly tested, which reduces the probability of obtaining false positives. In their team, they work with a large collection of yeast that had been transformed with vectors containing a precise Arabidopsis TF (Sánchez-Montesino and Oñate-Sánchez, 2018). The yeast library covers most Arabidopsis TFs. Moreover, all the vectors were manually cloned and are known not to induce self-activation. Hence, these conditions are optimal to obtain reliable candidates. I thank them for accepting to collaborate with us and for allowing me to perform this experiment in their lab.

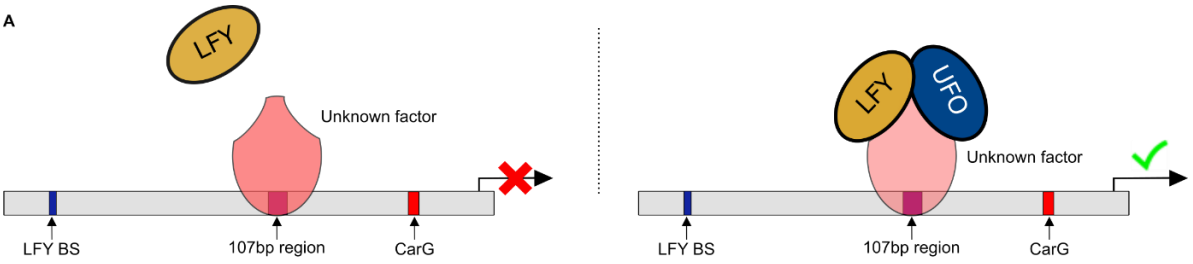

B

Legend
4 = Strong
3 = Medium
2 = Weak
1 = Just above background

Y1H screen (107bp region as bait)

Strength	AgI	ID
2	At4g18390	TCP2
4	At1g53230	TCP3

Y2H screen (UFO as bait)

Strength	AgI	ID
1	At5g23260	TT16
2	AT5G53420	CCT motif
2	At4g30980	LRL2
1	At1g67260	TCP1
1	At4g18390	TCP2
4	At1g53230	TCP3
4	At3g45150	TCP16
2	At4g37180	Homeodomain-like
2	At1g01060	LHY
1	At2g23340	DEAR3
1	At3g04420	NAC048
1	At5g24520	TTG1
1	AT5G52830	WRKY27
2	At5g64750	ABR1
3	At1g19490	bZIP
1	At3g57980	Bromodomain
2	At1g29160	DOF

Figure 12: Some TCP TFs bind UFO and the *pAP3* 107-bp region in yeast. (A) *Drawings representing a possible mechanism for LFY-UFO-dependent pAP3 activation. In this scenario, an unknown TF binds the 107-bp region but does not interact with LFY alone. When UFO is present, the formation of a complex involving LFY-UFO and the unknown factor would induce pAP3 activation.* **(B)** *Yeast screen results. Genes written in red are those for which interaction was reconfirmed after the initial screen.*

Y1H (Yeast-One-Hybrid) screen with the 107-bp region as bait

We performed an Y1H screen with the *pAP3* 107-bp region as bait. The goal was to find which TFs bind this region (and could recruit LFY-UFO). We expected the best candidates to be broadly-expressed TFs, *i.e.* expressed in protoplasts.

Y2H (Yeast-Two-Hybrid) screen with full-length UFO as bait

We also did an Y2H screen with full-length UFO as bait. The objective was to determine which TF(s) could interact with UFO (and possibly recruit it to the *pAP3* 107-bp region). This screen was also a good opportunity to find new UFO interactants, as very few of them have been characterized so far (see Article 2).

First, we performed all the preliminary experiments to check that our constructs for both screens did not induce self-activation and we tested several 3-aminotriazole (3-AT) concentrations to reduce background noise. Once we found good conditions, I performed the two screens in Madrid with the help of Gerardo Carrera. We identified several candidates in both screens that were subsequently retested to confirm the interactions (Figure 12B). Some TCP (TEOSINTE BRANCHED1-CYCLOIDEA-PROLIFERATING CELL NUCLEAR ANTIGEN FACTOR1) were found TFs in both screens, notably TCP3. TCPs form a family of plant-specific TFs with more than 20 members in Arabidopsis, and these TFs are implicated in very diverse physiological processes (Li, 2015). The identification of TCP3 in the Y1H screen is consistent with the presence of a high-score TCP BS within the 107-bp region. The physical interaction between UFO and some TCPs was more surprising but was reconfirmed.

However, Y2H techniques are prone to false positive and TCP are often found as bait in Y2H screens (73 interactants for TCP3 in the BioGRID database). We tested some TCPs (notably TCP3 and TCP4) in the protoplast assay and we never found them able to activate *pAP3*, with or without UFO (not shown). We did not go any further with this "TCP hypothesis" because at the same time we found the formation of the LFY-UFO complex on LUBS through ampDAP-seq. However, TCPs are implicated in flower development (Nag et al., 2009) and the existence of a functional UFO-TCP interaction is possible.

IV. Discussion

The discussion of this chapter is succinct as Article 2 can be considered as a general discussion of this first chapter.

LFY and UFO form a transcriptional complex

In this chapter, the molecular basis of the LFY-UFO interaction in Arabidopsis have been characterized at several levels. We have shown that the main role of UFO is to form a transcriptional complex with LFY. Using cryoEM, we confirmed that LFY and UFO interact and together bind a precise DNA motif. We also showed that UFO binds DNA when in complex with LFY.

At the transcriptional level, the discovery of the LUBS motif explains why LFY requires UFO for the activation of specific genes. If a promoter contains one or several canonical LFYBS (like in *pAP1* or *AG* second intron), LFY does not require UFO because it binds DNA on its own. However, other promoters do not contain canonical LFYBS but LUBS. In that case, UFO is required for the LFY-UFO complex to bind these *cis*-elements. Based on our LUBS model and available transcriptomic data, we infer that the LFY-UFO complex regulates a broad set of genes in Arabidopsis and we propose new targets.

Our results are mostly in agreement with previous studies

We confronted our results on the LFY-UFO interaction with available data from the literature. The role of UFO as a LFY transcriptional cofactor able to bind DNA is consistent with the strong phenotype induced by the addition of a repressive (Chae et al., 2008; Risseeuw et al., 2013) or an activation (Risseeuw et al., 2013) domain to UFO *in planta*. We also explain the fact that UFO overexpression in a *lfy* mutant background does not induce a strong phenotype (Lee et al., 1997; Risseeuw et al., 2013) by the poor ability of UFO to bind DNA alone.

Our luciferase assays in protoplasts are also in agreement with results obtained with *pAP3::GUS* reporter lines (Hill et al., 1998; Tilly et al., 1998). Furthermore, some previously unexplained results like the activation of the *pAP3 D3-18 ImIIm* construct in *35S::LFY 35S::UFO* seedlings (Figure 11; Lamb et al., 2002) can be explained by our LUBS model. In that precise case, despite the PEE deletion (which comprises LUBS1), other LUBS like LUBS0 and LUBS2 may be sufficient for promoter activation in the LFY-UFO overexpression context.

The only point on which we disagree with previous studies is about the role of UFO F-box domain. Most previous studies on LFY-UFO were performed with the assumption that UFO regulates LFY transcriptional activity through ubiquitination. However, despite some indirect results, this hypothesis had never been demonstrated. Our results are particularly in opposition with one study in which a UFO version with a deletion in the F-box domain (UFOdelF) was shown to induce loss-of-function phenotypes when overexpressed *in planta* (Risseeuw et al., 2013). This was interpreted as the inability of UFOdelF to ubiquitinate target proteins. However, in our case, we deleted the whole F-box domain and we found that UFOΔFbox induced a gain-of-function phenotype when overexpressed in a Col-0 WT

background. This apparent difference raises the question of the role of UFO in ubiquitination pathways, which is further discussed in the next chapter.

Hence, the formation of a LFY-UFO complex likely explains a major part of their synergy. In the next chapter, the case of other species is discussed and other complementary results are presented.

CHAPTER II:

The LFY-UFO interaction in land plants and future perspectives

In the first chapter, I focused of the LFY-UFO interaction in Arabidopsis with a mechanistic point of view (Article 1). However, *UFO* was also studied in other angiosperms where it has some crucial functions. In this chapter I will present the role of this gene in other species than Arabidopsis, and I will show some ongoing experiments.

I. Introduction

First *UFO* mutants were described early, and in the 1990s *UFO* was cloned in model species. Since then, *UFO* has been studied in several angiosperms species and many genetic data are available, notably precise descriptions of *ufo* mutant phenotypes. These numerous studies are of great interest to understand the functions of *UFO* and to figure out which one are conserved or specific to given species. In all angiosperm species examined to date, *UFO* is always a crucial floral gene, regulating separable processes during this developmental step. However, even if the floral role of *UFO* is conserved, *UFO* does not always fulfill the same floral functions across species.

How UFO homologs perform their functions at the molecular level in other species remained, like in Arabidopsis, very elusive. UFO homologs were known to regulate the activation of specific floral genes but the molecular mechanism was unknown. The hypothesis of UFO regulating LFY activity through ubiquitination also prevailed for other species than Arabidopsis (Souer et al., 2008).

In addition to the conserved floral role of *UFO*, a common denominator between all plant species is the existence of a LFY-UFO interaction. Indeed, genetic and/or physical interactions between LFY and UFO were always identified whenever they were tested. This likely reflects the existence and the functionality of the LFY-UFO complex in all angiosperms. In the figure 6 of Article 1, we also present results suggesting the existence of LFY-UFO complexes in non-flowering plants like gymnosperm or ferns.

All these observations led us to write a review on the role of *UFO* in land plants. The vast literature on *UFO* was never compiled, and we thought that it would be interesting for the flower development community to rediscover these data at the light of the identification of

the LFY-UFO complex on LUBS. In this review, we also propose several hypotheses for the UFO mode of action across species and we pinpoint future challenges.

Then, in the second part of this chapter, I present other experiments that are not published and that could be used for future studies on the LFY-UFO interaction.

II. Article 2

Title

UFO in land plants: it is more than activating B genes

Authors

Philippe Rieu and François Parcy.

Univ. Grenoble Alpes, CEA, CNRS, INRAE, Laboratoire Physiologie Cellulaire et Végétale, IRIG-DBSCI-LPCV, Grenoble, France

Abstract

In angiosperms, the development of flowers is a crucial developmental step that requires the activation of a complex genetic network. Over the last decades, genetic studies have revealed the key role of specific genes during this process. One of them is *UNUSUAL FLORAL ORGANS* (*UFO*): in all angiosperm species examined to date, UFO regulates crucial processes such as meristem identity transitions and organ identity acquisition. While most floral regulators are transcription factors, *UFO* represents an exception by encoding an F-box protein. Recent advances on the molecular function of UFO have shown that UFO acts as a transcriptional cofactor redirecting the LEAFY floral regulator to novel *cis*-elements. Nearly 30 years after this gene was first cloned, we summarize here its various roles across species, we examine past results in the light of novel findings and we pinpoint key questions to answer in the future.

Introduction

During the vegetative development of angiosperms, the Shoot Apical Meristem (SAM) produces vegetative tissues such as leaves and shoots. Upon the perception of external and internal cues, flowering is initiated and the SAM is converted into an Inflorescence Meristem (IM). The IM then produces determinate Flower meristems (FM) that ultimately give rise to flowers. The meristem identity transitions require a deep genetic reprogramming, with the precise spatiotemporal activation of floral genes. Genetic pathways controlling flower development have been studied extensively and several key floral regulators have been identified (Denay et al., 2017; Sablowski, 2015).

These central regulators include the transcription Factor (TF) LEAFY (LFY). LFY orchestrates flower development by activating numerous floral genes (such as *ABCE* homeotic genes) in precise territories through diverse molecular mechanisms (reviewed in Moyroud et al., 2010). Downstream of LFY (and of several other floral meristem identity genes), *ABCE* genes encode TFs specifying floral organ identities, and their role is summarized in the ABCE model of floral development (Alvarez-Buylla et al., 2010; Irish, 2010).

This review will focus on *UNUSUAL FLORAL ORGANS* (*UFO*), another key floral regulator in most angiosperms. Defects of *ufo* mutants were described early (Baur 1930; Helm, 1951; Monti and Devreux, 1969), and molecular cloning of *UFO* was achieved in the 1990s in the *Antirrhinum majus* and *Arabidopsis thaliana* model plants (Simon et al., 1994; Wilkinson and Haughn, 1995). Since then, *ufo* mutants have been isolated and described in numerous angiosperms species.

A first characteristic shared by all *ufo* mutants is the complexity (and sometimes variability) of the mutant phenotypes (Levin and Meyerowitz, 1995; Simon et al., 1994; Taylor et al., 2001; Wilkinson and Haughn, 1995). The impairment of numerous developmental steps by the *UFO* mutation shows that this gene fulfills several separable roles during plant development.

The goal of this review is to present which developmental processes are impacted by UFO across angiosperm species and how UFO performs its functions at the molecular level, notably its role as a LFY cofactor.

A) UFO controls various facets of plant development

1. UFO has a minor role before flowering

In most eudicots, *UFO* mutations do not affect the vegetative development. In species such as petunia (*Petunia hybrida*), tomato (*Solanum lycopersicum*) or *Gerbera hybrida*, *UFO* is not expressed before flowering (Lippman et al., 2008; Souer et al., 2008; Zhao et al., 2016). In some other species, *UFO* is expressed in vegetative tissues but without apparent role (Lee et al., 1997; Pouteau et al., 1998). For example, in Arabidopsis, *UFO* RNA is first detected at the heart stage of embryo development (Long and Barton, 1998; Reddy, 2008), and later *UFO* is expressed in the Shoot Apical Meristem (SAM) periphery where it might work redundantly with other genes to specify domains (Lee et al., 1997). In some eudicot species, UFO has a clear role during vegetative development: compound leaves development is affected in the pea (*Pisum sativum*) *stamina pistilloida* (*stp*) mutant (Taylor et al., 2001), and in cucumber (*Cucumis sativus*) *csufo* mutant tendrils are misshapen (Chen et al., 2021).

In monocots, *ufo* mutants have been described in rice (*Oryza sativa*; *aberrant panicle organization 1* (*apo1*); Ikeda et al., 2005) and recently in wheat (*Triticum aestivum; wheat ortholog from APO1* (*wapo1*); Kuzay et al., 2022). During vegetative development, *APO1* is expressed in the SAM where it fulfills several roles like negatively affecting the number of leaves and branches produced (Ikeda-Kawakatsu et al., 2009; Ikeda et al., 2005, 2007).

The ability of UFO to affect the vegetative development might be ancient because it concerns distant species like rice and pea. Like for other floral regulators, the role of UFO during vegetative development could derive from an ancestral function that has been latter lost in several species.

2. UFO affects the meristem identity transitions and consequently the inflorescence architecture

UFO most important role is during flower development, as all *ufo* mutants are affected at this stage. Upon flowering, the IM is converted into or produces a FM: where and when Floral Meristem Identity (FMI) is acquired ultimately determines the inflorescence architecture. UFO

affects the FMI acquisition, and its role in species representing three major inflorescence types will be detailed (Figure 1).

Raceme

In species with a raceme inflorescence, the IM grows indefinitely and produces lateral meristems on its flank, giving secondary inflorescences and flowers. In Arabidopsis, some *ufo* defects like a slight increase of the number of secondary inflorescences and the presence of a bract or a filamentous structure subtending the most basal flowers show that FMI acquisition is moderately delayed and weaker when *UFO* is not functional (Levin and Meyerowitz, 1995; Wilkinson and Haughn, 1995). The arrangement of some central floral organs in a spiral phyllotaxy (typical of shoot meristem) rather than in a whorled pattern observed in *Antirrhinum fimbriata* (*fim*) mutants also reveals a reduction of floral identity (Ingram et al., 1997; Simon et al., 1994). However, *UFO* overall weakly contributes to FMI in species with a raceme inflorescence. In those species, the main FM determinant is *LFY*: flower development is completely abolished in *lfy* mutants and the onset of flowering is associated with the sharp increase in *LFY* expression. Accordingly, overexpressing *UFO* in Arabidopsis has no effect on FMI (Lee et al., 1997). In other species like pea (Taylor et al., 2001) or *Torenia fournierii* (Sasaki et al., 2012) the FMI acquisition is also lowly affected by the *UFO* mutation.

In species in which *UFO* is a partial FM determinant, *UFO* works with other genes to specify FMI. Arabidopsis *ufo apetala1* (*ap1*) or Antirrhinum *fim squamosa* (*squa*, *AP1* homolog in Antirrhinum) double mutants do not produce flowers but only shoot-like structures with a spiral arrangement of leaves or sepals and a deformed gynoecium (Levin and Meyerowitz, 1995; Simon et al., 1994; Wilkinson and Haughn, 1995). Thus, even if *LFY* is the main FM determinant in those species, in the absence of *AP1*, *UFO* is necessary for complete FMI determination. Similarly, mutating both *FILAMENTOUS FLOWER* (*FIL*) and *UFO* leads to the absence of flowers in Arabidopsis, a phenotype not observed with single mutants (Levin and Meyerowitz, 1995). Thus, *UFO* likely has a deeper implication in FMI determination in Arabidopsis or Antirrhinum than initially thought, but this role is “masked” by other pathways.

Cyme

In cyme inflorescences, the apical meristem terminates by forming a flower and a new IM develops laterally to form the next unit, leading to a sympodial branching pattern. Petunia and tomato are two *Solanaceae* species with a cyme inflorescence where *UFO* homologs, respectively *DOUBLE TOP* (*DOT*) and *ANANTHA* (*AN*), play a key role. *DOT* and *AN* are not expressed in the IM and their expression strictly coincides with the development of flowers. In petunia *dot* and tomato *an* mutants, the IM is never transformed into a FM and flowers are not produced. The IM grows indefinitely, producing hyper-branched inflorescences (Allen and Sussex, 1996; Lippman et al., 2008; Souer et al., 2008). Inversely, *DOT* overexpression triggers early flowering and induces termination of flowering with a solitary flower (Souer et al., 2008). Such solitary flower is also observed when *AN* is expressed precociously during inflorescence development, showing that *AN* expression timing determines inflorescence architecture in tomato (MacAlister et al., 2012). Thus, in these species with a cyme inflorescence, *UFO* appears like a major FMI determinant. However in the cymose plant *Aquilegia coerulea*, *AqUFO* downregulation appears to only delay the FMI acquisition without abolishing the production of FM (Sharma et al., 2019).

Panicle

In many grass species, inflorescence is organized as a panicle, with spikelets, small branches containing flowers, attached to lateral branches. Upon flowering, the IM produces primary branches and finally aborts. Primary branch meristem gives rise to secondary branches and spikelet meristems. Finally, spikelet meristems give FMs. In rice, the main phenotype observed in the *apo1* mutant is a highly reduced inflorescence branching, with a strong decrease of the number of primary and secondary branches (Ikeda et al., 2005). Hence, IM and branch meristems change identity precociously when *APO1* is not functional and prematurely terminate into flowers. Conversely, dominant *apo1-D* mutants expressing *APO1* at higher levels have hyper-branched inflorescences (Ikeda-Kawakatsu et al., 2009). Similar results were found in wheat (a grass developing a spike inflorescence): *WAPO1* mutation reduces spikelet number per spike while a higher *WAPO1* expression level increases it (Kuzay et al., 2022; Wittern et al., 2022). Thus, one of the main roles of *UFO* in these species with a panicle

inflorescence is to promote IM/branch meristem identity. Since inflorescence architecture determines the number of spikelets, ultimately affecting the number of flowers and the grain yield, it is not surprising that *APO1* was identified in several QTL analyses in monocots crops (Muqaddasi et al., 2019; Ookawa et al., 2010; Tsukahara et al., 2015; Yano et al., 2015).

In species with other types of inflorescences, *UFO* also deeply affects the FMI acquisition. For example, in *Gerbera hybrida* or *Cosmos bipinnatus*, two species with a capitula inflorescence, the main FM determinant is not *LFY* but *UFO*, with *LFY* expressed quite uniformly in the capitulum and the localized onset of *UFO* expression coinciding with flower emergence (Li et al., 2019; Zhao et al., 2016). Thus, *UFO* specifies different kinds of meristem identities: it promotes more or less strongly FMI in eudicots and represses it in monocots. Despite differences across species, the role of *UFO* during flower meristem development is likely ancient because it is observed in a wide variety of angiosperms.

3. *UFO* specifies identity and determinacy of certain floral organs and has other roles during flower development

Once FM identity is established, specific FM territories acquire a given identity, later developing into different floral organs. UFO plays several roles in the FM, in correlation with its highly dynamic expression pattern (Figure 2). In species in which FM identity is strongly impaired by the *UFO* mutation (i.e. not producing flowers), UFO functions in the FM were evidenced through the analysis of weak or partial revertant mutants.

Promoting floral organ identities and determinacy

Promoting specific floral organ identities is a major role of UFO in most angiosperm. In most eudicots species UFO is required for the determination of 2nd and 3rd whorl identities. In strong *ufo* mutants, petals and stamens never develop properly and these two whorls often have several complex abnormalities (like the presence of filaments, various other floral organs or mosaic combinations; Levin and Meyerowitz, 1995; Simon et al., 1994; Taylor et al., 2001; Wilkinson and Haughn, 1995). Petals are generally homeotically replaced by sepals and stamens by carpels. Accordingly, overexpressing *UFO* in Arabidopsis or *DOT* in petunia induces

the formation of supernumerary petals and stamens and the transformation of leaves into petals, respectively (Lee et al., 1997; Souer et al., 2008). UFO specifies these local identities during early stages of FM development thanks to its specific expression pattern ("cup-shape" phase in stage 3 Arabidopsis flowers; Figure 2). Interestingly, it has been shown in Arabidopsis with partial UFO restoration that petal primordia require a higher dose of UFO compared to stamen primordia for their correct development (Laufs, 2003). In weak eudicots *ufo* mutants, partial loss of identity of the 2nd and 3rd whorl is the main mutant phenotype, showing the strong implication of UFO in promoting their identity. Thus, specifying 2nd and 3rd whorl identities is a conserved role of UFO in eudicots. In some eudicot species like Antirrhinum, the identity of the 4th whorl is also affected by the *UFO* mutation (Simon et al., 1994).

An important characteristic of the FM is that its growth is determinate (*i.e.* produces a defined number of whorls and organs). FM cells are thus committed to a specific fate. Noticeably, the identity and determinacy of the 4th whorl is necessary to ensure the termination of flower development. In some eudicot species, UFO also affects FM determinacy, as evidenced by the production of ectopic flowers at the expense of specific floral tissues in *ufo* mutants. Ectopic flower production is observed at a low frequency in pea or Antirrhinum basal *ufo* mutant flowers (Simon et al., 1994; Taylor et al., 2001) but in the *Lotus japonicus proliferating floral organs* (*pfo*) mutant it concerns all flowers, leading to a severe mutant phenotype (Dong et al., 2005; Zhang et al., 2003). A strong floral indeterminacy is also observed in the strawberry (*Fragaria vesca*) *extra floral organs* (*efo*) mutant (Shahan et al., 2018). Production of these ectopic flowers shows that cells of specific primordia keep meristematic features, reiterating endlessly the whole floral program.

In monocots, *ufo* mutant flowers also have defects related to floral organ identity and determinacy, but in a different way compared to eudicot *ufo* mutants. Lodicules (2nd whorl organs) have several abnormalities in the wheat *wapo1* mutant (Kuzay et al., 2022) while in the *apo1* rice mutant their number is increased compared to WT (Ikeda et al., 2005). However, in both *apo1* and *wapo1*, the 3rd and 4th whorls are deeply affected: stamens are absent or replaced by lodicules and carpels are formed indeterminately (Ikeda et al., 2005; Kuzay et al., 2022). This strong effect of *WAPO1* on floral organs may explain why despite its positive action on spikelet number in wheat, high *WAPO1* expression level is not correlated with an increased grain yield (Wittern et al., 2022). Thus, in monocots, *UFO* mainly controls the identity and the

determinacy of the 3rd and 4th whorls. This major difference between monocots and dicots shows that UFO specifies different floral organ identities across species.

Establishing FM patterning and boundaries

Another role of UFO throughout flower development is to delineate territories and to maintain boundaries. The correct arrangement of floral organs in a whorled pattern requires that the different type of primordia receive precise information of identity and positioning. Filaments (aborted organs), inter-whorl mosaic organs and intra-whorl fused organs are observed in several eudicots and monocots *ufo* mutants like in Arabidopsis, Antirrhinum or wheat (Ingram et al., 1997; Kuzay et al., 2022; Levin and Meyerowitz, 1995). Thus, *UFO* delineates territories in the flower primordia and specifies boundaries between whorls and between organs throughout flower development. This cadastral role of UFO is likely linked to its precise expression pattern in the FM (Figure 2).

Promoting petal growth

Finally, UFO promotes petal primordia initiation and/or proliferation. This late role, not discernable in strong *ufo* mutants, was proposed in Arabidopsis based on the analysis of weak *ufo* mutants and transient *UFO* activation at different developmental stages (Durfee et al., 2003; Laufs et al., 2003). This function is independent of 2nd whorl identity acquisition because expressing *UFO* in early steps of flower development only is not enough to generate mature petals (Laufs et al., 2003). UFO performs this role from stage 4 in Arabidopsis when it is expressed at the base of petals. The expression of *UFO* at the base of petals in late stages in several species may indicate that this function is conserved.

Development of nectaries

In late stages, Arabidopsis *UFO* also controls the development of nectaries, small glands producing a sugar-rich liquid at the base of stamens (Baum et al., 2001). Nectaries are not present in the *ufo* mutant, and overexpressing *B* genes in the *ufo* mutant background restores

the development of petals and stamen but is not sufficient to restore the presence of nectaries, showing the direct role of *UFO* in controlling the development of these organs (Baum et al., 2001).

4. The transcription of a broad set of floral genes is affected by the *UFO* mutation

Soon after the description of phenotypes in Antirrhinum or Arabidopsis, the floral defects observed in *ufo* mutants were linked to defects in the expression of floral genes (Levin and Meyerowitz, 1995; Simon et al., 1994; Wilkinson and Haughn, 1995). The correlation between observed phenotypes and defects in the expression of key floral genes in *ufo* mutants shows that *UFO* has the ability, direct or indirect, to affect their transcription.

Activation of genes specifying FM and IM identities

In eudicots, UFO first main role is to specify FM identity. Overexpressing an activated form of UFO (UFO-VP16, a translational fusion between UFO and the strong activation domain from the viral transcription factor VP16) in Arabidopsis, tobacco (*Nicotiana tabacum*) or rapeseed (*Brassica napus*) induces the spectacular formation of ectopic FM on leaves (Risseeuw et al., 2013), revealing that UFO has the ability to activate all the genes required for FM development. Major UFO targets for determining FM identity are likely the *SEPALLATA* (*SEP*) *E* genes (Chen et al., 2021; Souer et al., 2008), but other targets are still to be discovered. In monocots, *UFO* promotes IM identity, and in agreement with this role, several crucial floral genes (such as *MADS1*, *MADS3* and *MADS58*) were shown to be differentially expressed in the IM of *APO1* overexpressing lines (Yano et al., 2015).

Activation of genes specifying floral organ identities

UFO second major role is to determine floral organ identities. UFO performs this role by positively regulating *B* genes in eudicots (Honma and Goto, 2000; Levin and Meyerowitz, 1995; Sasaki et al., 2012; Simon et al., 1994; Wilkinson and Haughn, 1995). UFO-dependent *B* genes

activation was demonstrated in most eudicots species, showing a strong conservation of this function. In Arabidopsis, overexpressing the *B* gene *APETALA3* (*AP3*) in *ufo* is sufficient to restore normal petal and stamen development (Krizek and Meyerowitz, 1996), showing that *AP3* is the major UFO target. Other genes have been shown to be downregulated in *ufo* mutants and likely explain some observed phenotypes. In Antirrhinum, the *C* gene *PLENA* (determining 4th whol identity) is strongly downregulated in *fim* (Simon et al., 1994) and in Arabidopsis *RABBIT EARS* (*RBE*, a gene involved in petal development) is not expressed in a *ufo* mutant (Krizek et al., 2006).

In monocots, expression of homeotic genes is also strongly altered in *ufo* mutants. In agreement with observed phenotypes in rice, the *C* gene *MADS3* is downregulated in *apo1* but not the *B* gene *SUPERWOMAN1* (Ikeda et al., 2005). In wheat, both *B* and *C* genes (but not *E* genes) are downregulated in *wapo1* (Kuzay et al., 2022). Thus, UFO is a major actor in the activation of floral genes. The role of UFO in transcription regulation in concert with LFY is further discussed below.

5. UFO as a cell cycle regulator?

UFO was proposed to regulate cell growth or division in several species (Lee et al., 1997; Levin and Meyerowitz, 1995; Samach et al., 1999; Wilkinson and Haughn, 1995). In fact, the production of supernumerary or fused organs a well as filaments in *ufo* mutants is likely caused by cell division defects (Levin and Meyerowitz, 1995; Samach et al., 1999). Furthermore, IM size is perturbed in several *ufo* mutants; UFO affects it negatively in Arabidopsis and positively in rice (Hepworth et al., 2006; Ikeda-Kawakatsu et al., 2009; Samach et al., 1999). The increase of IM size (*i.e.* increased cell division) by APO1 in rice explains its positive role on inflorescence branching (Ikeda-Kawakatsu et al., 2009). Whether UFO regulates cell division directly by targeting cell cycle regulators or indirectly through its role in transcription is unknown.

B) UFO regulation and expression pattern

1. *UFO* expression is tightly regulated

UFO expression pattern in meristems is very well delineated (Figure 2). In species in which *UFO* is the main FM determinant like petunia or tomato, precise expression of *UFO* is peculiarly crucial (Kusters et al., 2015; Lippman et al., 2008; Souer et al., 2008). This implies a precise regulation, and several *ufo* mutant phenotypes are caused by alterations in the *UFO* promoter sequence (Durfee et al., 2003; Ingram et al., 1997). Analysis of the *DOT* and *UFO* promoters showed that their sequence carry the information for the precise spatio-temporal activation (Kusters et al., 2015). Interestingly, it was shown that *pDOT* (or *pUFO*) induced the same expression pattern when expressed in either Arabidopsis or petunia. Hence, some *cis*-elements are recognized by conserved regulators between the two species (Kusters et al., 2015).

Finally, functional comparisons between *pDOT* and *pAN* promoters showed that both promoters induced the same expression pattern in petunia (Kusters et al., 2015). Sequence comparison between the two promoters allowed identifying conserved blocks; comparison between a large set of promoter sequence from related species could help to identify *cis*-elements and to propose upstream regulators.

2. Few UFO upstream regulators are known

Only a few *UFO* upstream regulators have been proposed to date. SHOOT MERISTEMLESS (STM) is a direct *UFO* activator during embryo development (Long and Barton, 1998) and throughout development in Arabidopsis (Roth et al., 2018). During flower development, AP3 positively regulates *UFO* expression (Wuest et al., 2012) and PETAL LOSS also activates *UFO* after stage 4 (PTL; Takeda et al., 2022). In tomato, a clear *AN* regulator is the ALOG protein TERMINATING FLOWER (TMF; MacAlister et al., 2012). TMF represses *AN* expression and allows its gradual activation upon flowering. A mechanism involving TMF phase separation on the *AN* promoter was recently proposed (Huang et al., 2021b, 2022). In petunia, a crucial *DOT* activator is the WOX-protein EVERGREEN, but this activation is indirect and may implicate another unknown factor (Rebocho et al., 2008).

Other proposed regulations were based mainly on *UFO* reduced or delayed expression in mutants. For example, AP1 is required for *UFO* expression beyond stage 3 in Arabidopsis (Lee et al., 1997) and SQUA likely activates *FIM* in early stages (Simon et al., 1994). In some species, LFY is also an *UFO* upstream regulator (see below). However, the action of yet unknown regulators has to be taken into account to understand precisely the regulation of *UFO* in time and space. For example, describing which factor(s) restricts *UFO* expression to a cup-shape domain in the young FM in eudicots would be a major step forward in the understanding of floral patterning.

3. UFO protein expression domain in flowers is poorly described

UFO expression pattern was described only with RNA *in situ* hybridization and the protein expression domain in inflorescences and floral tissues is not described. In Antirrhinum, it was shown with *fim* periclinal chimeras that FIM activates genes in regions where it is not transcribed (Schultz et al., 2001). Similarly, UFO negatively affects bract development in Arabidopsis without being expressed in this tissue (Hepworth et al., 2006). UFO protein is thus possibly mobile and active outside its expression domain. A DOT gradient within the FM was proposed by Souer et al. to explain the different needs of UFO in each tissue (Souer et al., 2008). UFO mobility could also explain why, across related species, UFO has the same function despite slight differences of expression pattern. Further microscopy data (by immulocalization or fluorescent reporters) are required to better characterize UFO protein expression domain in meristems.

C) Molecular role of the UFO protein

1. UFO is an F-box protein

The analysis of UFO protein sequence revealed that *UFO*, despite its deep implication in transcription, does not encode for a TF but for an F-box protein (Samach et al., 1999). In Arabidopsis, the F-box gene family comprises about 700 genes involved in very diverse physiological processes (Gagne et al., 2002; Stefanowicz et al., 2015). At the molecular level, F-box proteins are part of Skp1–Cullin–F-box protein (SCF) complexes. First described in yeast,

SCF complexes act as ubiquitin E3 ligase, targeting proteins for proteasome-dependent degradation. The F-box domain is required for the interaction with ARABIDOPSIS SKP1-LIKE (ASK) proteins, core SCF subunits. F-box proteins confer specificity to SCF complexes by recruiting target proteins thanks to the large variety of domain they harbor in addition to the F-box domain. UFO C-terminal region contains a Kelch-repeat β-propeller domain.

2. Formation and functionality of the SCF^{UFO} complex

The formation of an SCF^{UFO} complex was demonstrated *in vitro* and *in planta*. Interaction between UFO F-box domain and ASK proteins was confirmed genetically (Ni et al., 2004; Zhao et al., 1999, 2001) and/or biochemically in several species (Ingram et al., 1997; Samach et al., 1999; Souer et al., 2008). The ASK family comprises several members (21 in Arabidopsis) and UFO preferentially interacts with specific ones (like ASK1, ASK2 or ASK11 in Arabidopsis; Gagne et al., 2002). UFO also interacts genetically with other SCF core subunits like CULLIN1 (CUL1), and CUL1 is co-immunoprecipitated with UFO *in planta* (Wang et al., 2003). Several lines of evidence show that the SCF^{UFO} complex is functional in plant. Arabidopsis mutants (notably *ask1* mutants) or RNAi lines targeting any core subunits of the SCF complex exhibit altered floral organs in 2nd and 3rd whorls similar to those observed in ufo mutants (Liu et al., 2004; Ni et al., 2004; Zhao et al., 1999). Finally, a decrease of COP9 SIGNALOSOME (CSN) complex activity (a regulator of SCF complexes) in Arabidopsis impairs some UFO functions (like *AP3* activation), revealing that CSN likely regulates UFO through the SCF complex in which it is implied (Wang et al., 2003). Thus, SCF^{UFO} likely targets proteins for ubiquitination, but these targets are yet poorly described. LFY was an obvious candidate, and the possibility of a SCF^{UFO}-dependent LFY ubiquitination is discussed below. Other proteins may be targeted for ubiquitination, and some were proposed in Antirrhinum but were never characterized (Wilkinson et al., 2000). Obtaining a complete UFO interactome would help to identity putative targets, but Y2H screens performed with FIM, UFO or DOT as bait yielded nearly only ASK proteins as interactants (Ingram et al., 1997; Samach et al., 1999; Souer et al., 2008).

3. UFO F-box domain is partially dispensable in Arabidopsis

In contrast to a previous study (Risseeuw et al., 2013), we found that overexpressing a truncated UFO version lacking the F-box domain (*i.e.* unable to participate to an SCF complex) in a strong *ufo* mutant largely complemented the mutant phenotype, with the development of petals and stamens. Hence, the connection of UFO to an E3 ligase complex is partially dispensable in Arabidopsis, and another molecular role outside ubiquitination explains UFO function. Still, in the absence of the F-box domain, complemented *ufo* plants retained some mutant defects (such as absent or misshapen petals). This observation together with the high conservation of the UFO F-box domain across species suggests that the F-box domain (and thus the connection to the SCF complex) has a function *in planta*.

It is possible that UFO acts redundantly with other F-box proteins in ubiquitination pathways. A genetic screen performed with *ufo* as a starting population in Arabidopsis identified three mutants enhancing *ufo* phenotype named *FUSED FLORAL ORGANS 1* to *3* (Levin et al., 1998). The *ufo ffo1* double mutant (but not single mutants) does not produce flowers but only filamentous structures. *FFO1* corresponds to *HAWAIIAN SKIRT* (*HWS*), a gene encoding an F-box protein very similar to UFO (González-Carranza et al., 2007, 2017). HWS is implicated in the microRNA pathway (González-Carranza et al., 2017) and, for this, strictly functions through an E3 ligase complex. HWS targets are yet unknown (Lang et al., 2018) and it can be hypothesized that HWS and UFO work redundantly in ubiquitination pathways. Redundancy between UFO and other F-box proteins could explain why UFO's role as an E3 ligase is not easily discernable in Arabidopsis. Moreover, the function of SCF^{UFO} could be more important in other species than in Arabidopsis. While the role of UFO as a part of an E3 ligase remains unclear, we have recently proposed another function for UFO outside ubiquitination that could explain its role in transcription regulation.

4. UFO and LFY together form a transcriptional complex of deep evolutionary origin

LFY and UFO interact genetically and physically

Initial genetic studies in numerous species reported that *ufo* and *lfy* mutants share many similarities (Levin and Meyerowitz, 1995; Simon et al., 1994; Taylor et al., 2001). For example, in rice, a mutant was called *apo2* because of its phenotypic resemblance with the *apo1* mutant, and it was later found that *APO2* corresponds to the *LFY* homolog in rice (also called *RICE FLORICAULA LEAFY* or *RFL*; Ikeda-Kawakatsu et al., 2012; Kyozuka et al., 1998). The analyses of *lfy ufo* double mutants revealed the genetic interaction between the two genes in several species (Levin and Meyerowitz, 1995; Simon et al., 1994; Souer et al., 2008; Taylor et al., 2001; Wilkinson and Haughn, 1995). The epistatic relation between LFY and UFO was confirmed anytime it was tested, showing its high conservation in angiosperms.

A first hypothesis regarding the LFY-UFO genetic interaction would be that one gene transcriptionally regulates the other one. Despite some regulations reported in Antirrhinum (Simon et al., 1994), tomato (Lippman et al., 2008) or rice (Ikeda-Kawakatsu et al., 2012), overall, transcriptional regulation does not explain epistasis between the two genes and no general rule can be defined across species.

Instead, it was shown in diverse species that LFY and UFO act at the same level and that the two proteins physically interact (Chae et al., 2008; Ikeda-Kawakatsu et al., 2012; Sasaki et al., 2012; Souer et al., 2008; Zhao et al., 2016). Some of the mutations in *LFY* (Selva et al., 2021) or *UFO* (Sasaki et al., 2012) that induce a phenotype *in planta* impair the LFY-UFO interaction, revealing its importance *in vivo*. Mapping of the interaction domains showed that in some species like Arabidopsis or Gerbera, interaction implies LFY C-terminal DNA-Binding-Domain (DBD) and UFO Kelch-repeat β-propeller domain (Chae et al., 2008; Zhao et al., 2016). However, in petunia, DOT interacts with ABERRANT LEAF AND FLOWER (ALF, the LFY homolog in petunia) N-terminal domain (Souer et al., 2008). This result is quite striking since ALF-LFY and DOT-UFO share a high degree of homology. Hence, even if the interaction is conserved, the mode of interaction may have evolved and this could account for differences of activity.

Does SCF^{UFO} target LFY for ubiquitination?

Because UFO interacts with LFY, it was long though that SCF^{UFO} regulates LFY activity through ubiquitination. In fact, TF regulation through ubiquitination is a well-described mechanism (Geng et al., 2012; Kodadek et al., 2006) and proteasome-mediated degradation was shown to be required for LFY-UFO activity in seedlings (Chae et al., 2008). However, LFY protein level is unaltered in a strong *ufo* mutant (Chae et al., 2008) and specific LFY mono- or poly-ubiquitination are insufficiently described in Arabidopsis or petunia (Chae et al., 2008; Souer et al., 2008). The hypothesis of a SCF^{UFO}-dependent LFY ubiquitination cannot be ruled out but further investigations are needed.

The LFY-UFO complex binds specific cis-elements

As LFY is a TF, the role of UFO as a transcriptional cofactor was studied extensively. Arabidopsis or petunia plants overexpressing both *LFY* and *UFO* (but not single proteins) do not survive beyond the seedling stage (Parcy et al., 1998; Souer et al., 2008) because of the ectopic activation of many floral genes (Souer 2008). This experiment showed that LFY and UFO act synergistically to activate transcription anytime they are present together (Parcy 1998; Souer 2008). Moreover, adding an activation or a repression domain to UFO changes its activity in Arabidopsis, suggesting a role for UFO nearby DNA (Chae et al., 2008; Risseeuw et al., 2013).

It was also shown that UFO is recruited on DNA in a LFY-dependent manner (Chae et al., 2008). In agreement with these data, we recently found that LFY and UFO together form a transcriptional complex able to access new loci (named LFY-UFO Binding Sites or LUBS) that LFY poorly accesses on its own. LUBS comprise a low-affinity canonical LFY Binding Site (comprising either a monomeric or a dimeric LFY site) located at a fixed distance from a UFO Recruiting Motif (URM). The presence of those two features is required for LFY-UFO complex binding on LUBS. Structure of the LFY-UFO complex revealed that UFO Kelch-repeat β-propeller domain contacts both DNA (at the URM) and LFY, explaining its role as a LFY cofactor. This characteristic of the Kelch-repeat β-propeller domain is particularly interesting as this domain is highly represented in plant F-box proteins (Gagne et al., 2002).

The LFY-UFO synergy likely has a deep evolutionary origin

The formation of a LFY-UFO complex is likely conserved because the LFY-UFO genetic interaction is a common denominator between all angiosperms. Moreover, we found that LFY orthologs from gymnosperms and ferns functionally interact with Arabidopsis UFO in a transient assay. Thus, LFY and UFO likely had an ancestral joint role before the development of flower plants, latter coopted for this process. Deciphering the history of the LFY-UFO complex will be a challenge for the future. Indeed, UFO homologs from non-angiosperm species have not been described yet and the identification of the correct UFO homologs is not straightforward because of the large diversity of the F-box gene family.

5. The LFY-UFO complex likely has multiple target genes

The identification of LUBS allows revisiting all the UFO-dependent regulations reported in early studies. In Arabidopsis, *AP3* was the best described LFY-UFO target (Hill et al., 1998; Lamb et al., 2002; Parcy et al., 1998) and we identified several high-affinity LUBS in its promoter that are crucial for activation. A proposed mechanism for *pAP3* early activation in Arabidopsis is detailed in Figure 3B. We also identified a LUBS in the promoter of *PI* that could explain the partial involvement of UFO in *PI* activation (Honma and Goto, 2000). A functional LUBS was also found in the promoter of *RBE*, another known UFO target (Krizek et al., 2006). Thus, the binding of the LFY-UFO complex to LUBS *cis*-elements likely explains a major part of the role of UFO in transcription regulation.

In Arabidopsis, a species in which UFO is not the main FM determinant, UFO was proposed to target only a small subset of genes (Krizek and Meyerowitz, 1996). By crossing expression and binding data, we found that several other genes are likely targeted by LFY-UFO, among which the floral regulators *SQUAMOSA PROMOTER BINDING PROTEIN LIKE 5* (*SPL5*) and *FD*. Thus, the list of LFY-UFO target genes in Arabidopsis may be broader than initially detected.

If the molecular mechanism for the LFY-UFO complex unraveled in Arabidopsis is valid in other species, it could allow understanding multiples crucial regulations during flower development. For example, in species in which UFO is the main FM determinant, LUBS should be found in the regulatory regions of major floral genes, and this would explain the key role of UFO in FM

determination. Additional RNA- or ChIP-seq data would be helpful to determine precisely which genes UFO regulates at each developmental stage.

6. LFY and UFO interplay: who needs whom?

UFO functions completely rely on LFY

LFY-UFO synergistic role raises the question of their relative dependence. UFO does not seem to have any LFY-independent functions, even in species in which UFO is the main FM determinant. The complete absence of gain-of-function phenotype of Arabidopsis, petunia or rice plants overexpressing UFO in a *lfy* mutant background shows that UFO performs most of its activity in a LFY-dependent manner (Ikeda-Kawakatsu et al., 2012; Lee et al., 1997; Souer et al., 2008). UFO dependence on LFY to perform its functions is likely explained by the poor ability of UFO to bind DNA on its own (Chae et al., 2008). Determining UFO genome-wide DNA binding in planta would reveal whether UFO DNA binding is strictly LFY-dependent. The possible role of UFO as an E3 ligase could be LFY-dependent or independent.

LFY has UFO-dependent and UFO-independent functions

On the opposite, LFY has UFO-dependent and -independent functions (Parcy et al., 1998). In Arabidopsis, LFY directly activates some targets alone like *AP1* (Parcy et al., 1998; Wagner et al., 1999) or with other cofactors (like with WUSCHEL (WUS) for *AGAMOUS* (*AG*) activation; Lohmann et al., 2001). These activations require LFY direct binding to canonical LFYBS present in the regulatory elements of these genes, independently of UFO. In Arabidopsis like in several eudicot species, UFO acts as a partially dispensable LFY cofactor and mainly provides spatial specificity for LFY-dependent activation of *B* genes (Parcy et al., 1998). Remarkably, LFY UFO-dependent and -independent functions can be decoupled in Arabidopsis by mutating a single amino acid located in the LFY-UFO interface.

However, in species in which UFO is the main FM determinant, LFY apparently performs most of its functions in a UFO-dependent manner. In petunia, ectopic *ALF* expression does not lead to a phenotype while overexpressing both *ALF* and *DOT* induces growth arrest at the seedling

stage (Souer et al., 2008). Interestingly, *FALSIFLORA* (*FA*; *LFY* homolog in tomato) overexpression results in early flowering and single-flower primary inflorescences, maybe by activating *AN* (MacAlister et al., 2012). Thus, determining whether LFY has UFO-independent functions in those species is difficult.

Why LFY requires UFO at different degrees remains unclear, and differences between species are difficult to understand. A first explanation could be that LFY-UFO complexes form differently, as evidenced by the different interacting domains between Arabidopsis and petunia. In Arabidopsis, LFY could have evolved to bypass the need of UFO, while in petunia DOT would have remained indispensable for ALF activity. This hypothesis is unlikely because ALF-LFY and UFO-DOT are highly similar and interchangeable (Souer et al., 2008).

A second explanation could be that LFY-UFO complexes from different species act in a same fashion but target different genes. Gene activations may require LFY alone or the LFY-UFO complex depending on the *cis*-elements regulating their expression. In that case, evolution of target cis-elements rather than evolution of the LFY-UFO complex would explain differences between species.

7. UFO (or the LFY-UFO complex) works with other pathways

At the genetic level, interaction of UFO with other regulatory pathways has been widely examined. It revealed that UFO (or the LFY-UFO complex) acts with several other pathways during flower development. As mentioned before, the analysis of double mutants showed that UFO (or likely the LFY-UFO complex) works other pathways to determine FMI in species like Arabidopsis or Antirrhinum. Furthermore, the different LFY-UFO targets (like *AP3*, *PI* and *RBE* in Arabidopsis) have very distinct expression patterns, meaning that in addition to LFY-UFO, other genes regulate their spatiotemporal expression. For example, UFO acts with AP1 and in parallel to SEP3 to activate *AP3* in Arabidopsis (Castillejo et al., 2005; Ng and Yanofsky, 2001). In petunia, it was proposed that ALF-DOT associates with the WUS homolog TERMINATOR to regulate *C* gene expression (Souer et al., 2008). Moreover, it was shown in rice that the HECT-domain E3 ligase LARGE2 stabilizes the APO1-APO2 complex and positively regulates its activity (Huang et al., 2021a).

Most of these interactions have been demonstrated at the genetic level. Hence, a future challenge is to dig these genetic interactions; for example, it would be relevant to test the physical interaction between UFO and MADS TF.

D) Conclusion and perspectives

In angiosperms, three major features distinguish the FM from the shoot: its growth is determinate, it produces floral organs and these organs are arranged in a whorled pattern. UFO is a major floral gene as it has the ability to affect these three features. During flower development, UFO has several roles and acts sequentially, notably to promote precise meristem and floral organ identities. Certain UFO functions are highly conserved across species, showing that they appeared early during evolution. In basal land plant species like *Physcomitrium patens*, analysis of *lfy* mutants revealed a role for LFY in the regulation of cell division (Tanahashi et al., 2005). Reverse genetics could help widening the collection of *ufo* mutants to non-flowering plants and shedding light on *UFO* ancestral functions.

At the molecular level, UFO was recently demonstrated to act as a transcriptional coactivator by forming a complex with LFY. Through its interactions with both DNA and LFY, UFO brings LFY to specific loci where LFY cannot bind on its own. The LFY-UFO complex plays a crucial role in the flower development of all angiosperm species, and describing LFY-UFO complexes from different species (notably their structure, the motif they bind and the genes they regulate) will expand current models of flower development. Furthermore, it was recently proposed that LFY is a pioneer TF (Jin et al., 2021; Lai et al., 2021), opening closed chromatin regions during early flower development. UFO may help LFY in reshaping the chromatin status in meristems to allow the activation of floral genes.

The role of UFO in ubiquitination pathways is also intriguing and several questions are not yet answered. Proteins having two functions (also called protein moonlighting; Singh and Bhalla, 2020) is common and UFO may act both in transcription and ubiquitination. These two functions may work cooperatively and their relative importance may vary across species. For example, it can be hypothesized that LFY recruits UFO at specific loci to specifically degrade other regulators through its E3 ligase activity. UFO may also ubiquitinate histones at precise locations in the genome.

Finally, the ability of LFY-UFO to trigger flower development ectopically (especially with VP16-activated forms) could be used as a biotechnology tool to regenerate plants quickly by decreasing the time to flowering.

E) Figures

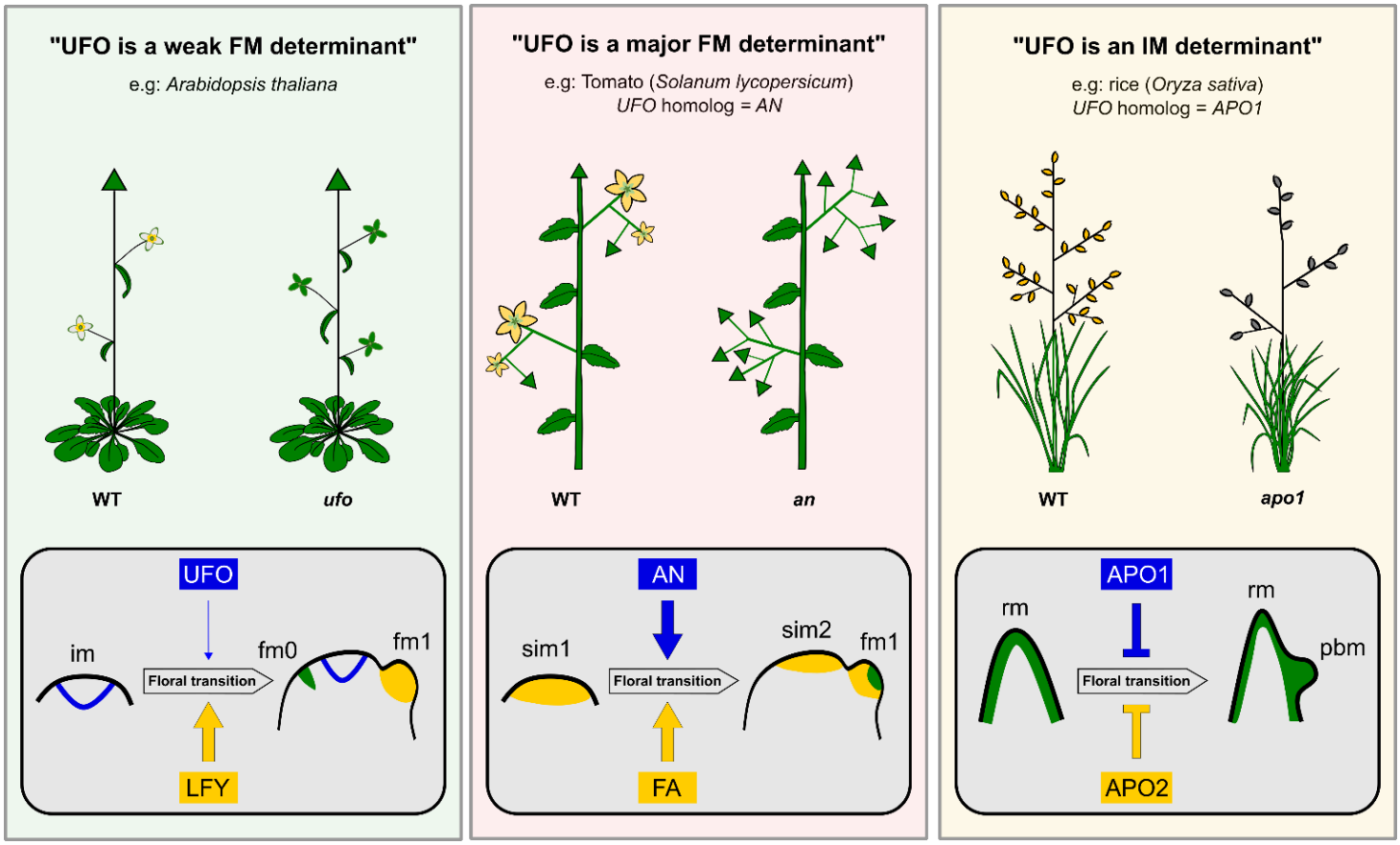

Figure 1: UFO promotes different meristem fates across species. Top part represents the *ufo* mutant phenotype in indicated species. Drawings are not exhaustive and only highlight some *ufo* phenotypes. Arrows represent indeterminate meristems. Boxes below describe *UFO* (blue) and *LFY* (yellow) expression pattern during the floral transition, overlap is in green. Relative contribution of each gene to floral transition is depicted with thin or wide arrows. See Figure 2 for a complete expression pattern of each gene. In Arabidopsis *UFO* specifies FM identity when it is expressed in the IM (Hepworth et al., 2006; Lee et al., 1997). However, it has to be noted that in other species like Antirrhinum, FIM is not expressed in the IM (Ingram et al., 1997; Simon et al., 1994). IM, inflorescence meristem; FM, flower meristem; SIM, sympodial inflorescence meristem; RM rachis meristem; PBM, primary branch meristem.

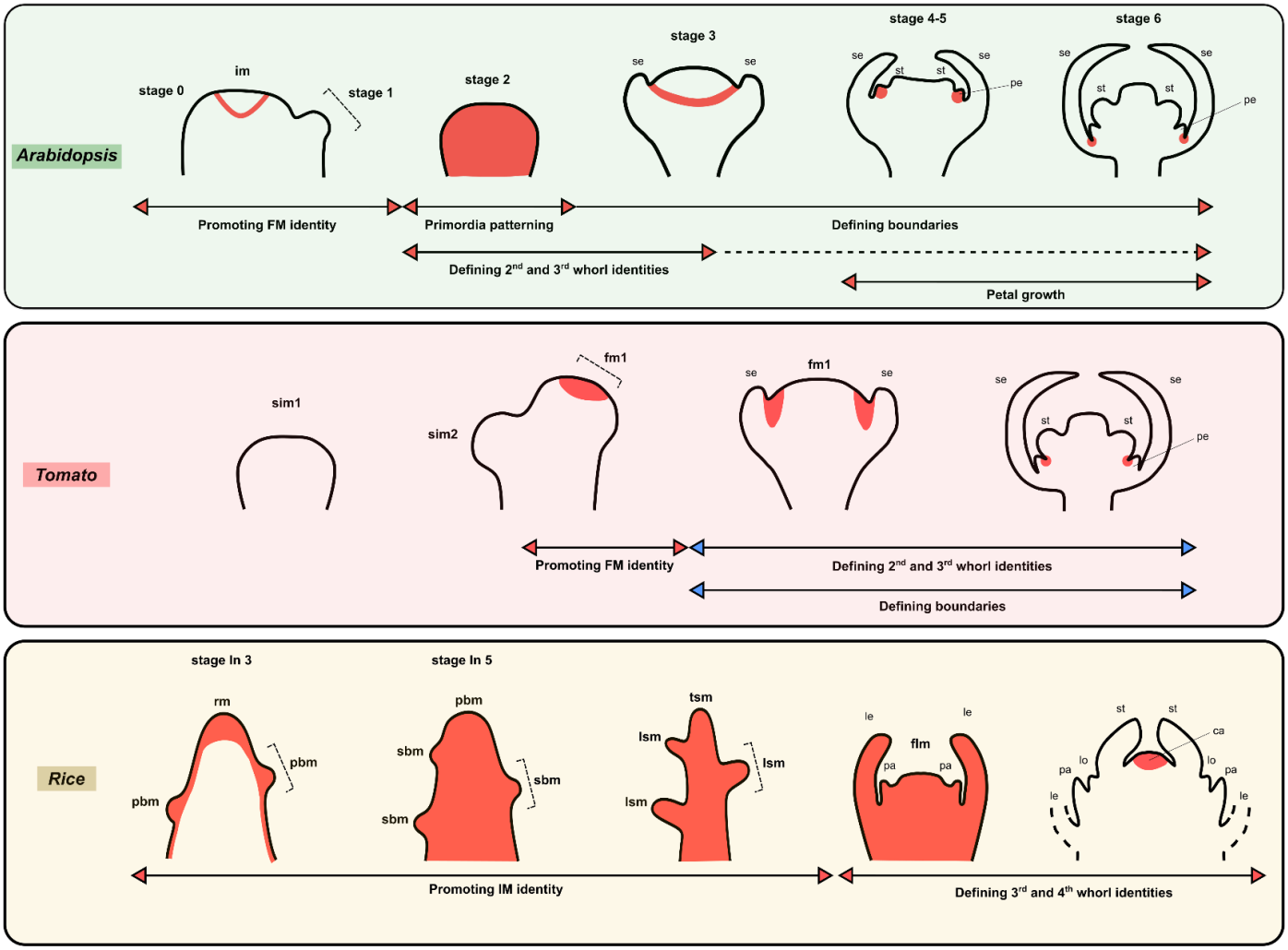

Figure 2: UFO has a dynamic expression pattern and separable roles during flower development. *UFO* expression domain in Arabidopsis (top), tomato (middle) and rice (bottom). Dashed segments indicate a zoom for the following drawing. Plain double-sided red arrows represent UFO functions that are well-documented. In the top panel, dashed line represents the same role but with weaker intensity. In the middle panel, plain double-sided blue arrows represent AN roles that are strongly suggested (by phenotypes or expression pattern) but that have not been rigorously demonstrated (notably at which stages it is performed). Flower development stages in Arabidopsis and rice are according to (Smyth et al., 1990) and (Ikeda et al., 2004), respectively. im, inflorescence meristem; fm, floral meristem, sim, sympodial inflorescence meristem; rm, rachis meristem, pbm, primary branch meristem; sbm, secondary branch meristem; tsm, terminal spikelet meristem; lsm, lateral spikelet meristem; flm, floret meristem; se, sepal; st, stamen; pe, petal; le, lemma; pa, palea; lo, lodicule; ca, carpel.

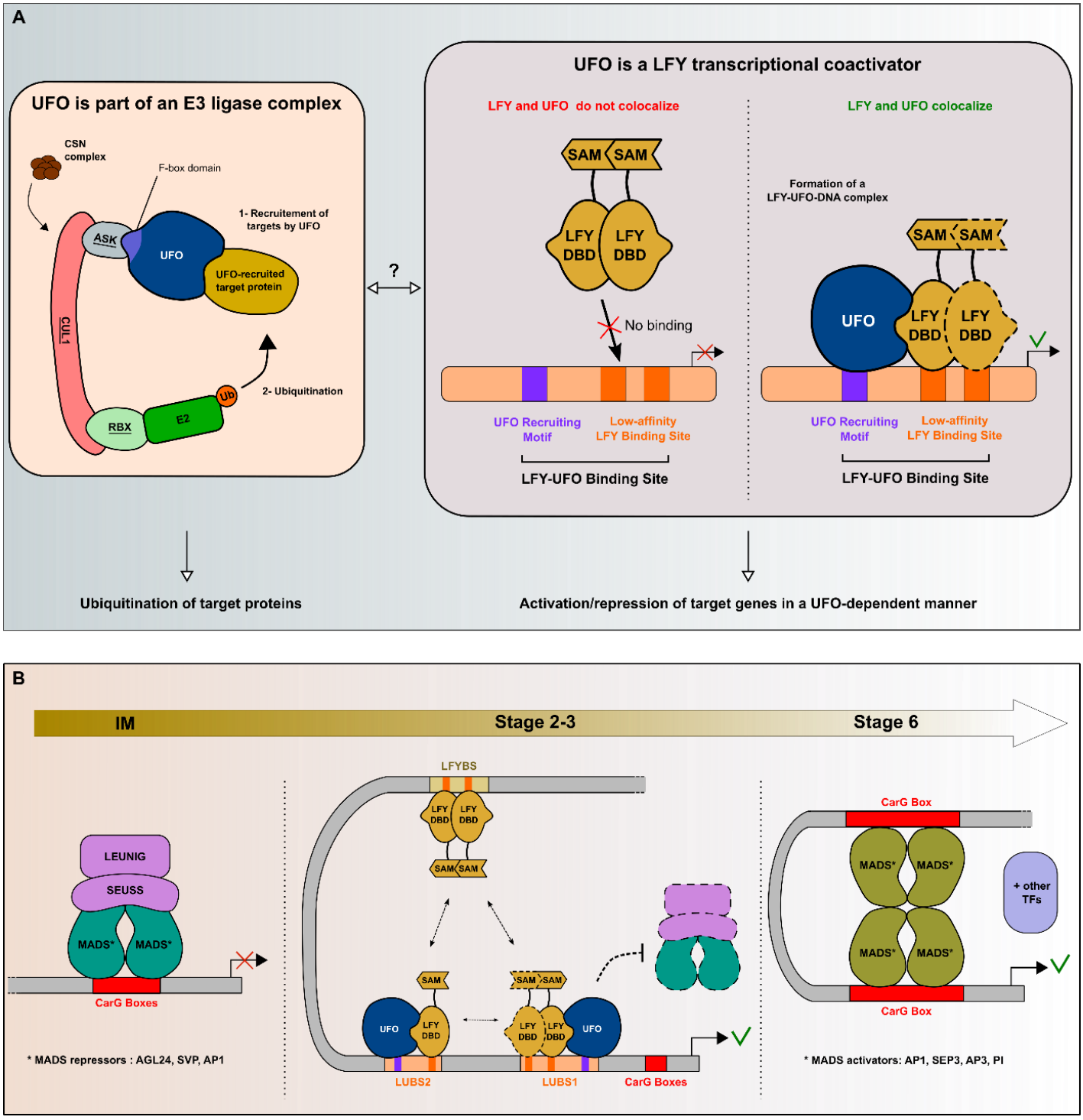

Figure 3: UFO is part of an E3 ligase complex and is a LFY transcriptional cofactor. (**A**) UFO is part of an SCF complex (left). SCF complex core subunits are underlined. In SCF^{UFO}, UFO recruits target proteins for ubiquitination. The CSN complex is a regulator of SCF^{UFO}. UFO is a LFY transcriptional co-activator (right). When LFY does not colocalize with UFO, it does not bind LUBS because of the low affinity of the LFY Binding Site. When LFY and UFO are present together, the formation of a transcriptional complex on LUBS sites allows activation of specific target genes. The relation between the different UFO functions (transcriptional cofactor and component of an E3 ligase complex) are not yet described. (**B**) The *AP3* promoter (*pAP3*) is the

best-characterized LFY-UFO target in Arabidopsis. *pAP3* is not activated in *lfy* and *ufo* mutant backgrounds (Hill et al., 1998; Lamb et al., 2002) and both LFY and UFO are necessary and sufficient for its activation (Parcy et al., 1998). During vegetative and early flower development, *AP3* locus is kept silent thanks to repressive epigenetic marks (Gómez-Mena et al., 2001). Release of this repression is regulated by several mechanisms (Carles and Fletcher, 2009; Sacharowski et al., 2015), notably by LFY-dependent recruitment of chromatin remodelers (Wu et al., 2012). In the IM and during very early flowering stages, *pAP3* CarG boxes (notably CarG3; Tilly et al., 1998) are bound by a repressive complex comprising CarG-bound MADS TFs like SHORT VEGETATIVE PHASE (SVP), AGAMOUS LIKE24 (AGL24) or AP1 in complex with LEUNIG and SEUSS repressors (Franks et al., 2002; Gregis et al., 2006, 2009; Liu and Meyerowitz, 1995). From stage 2, LFY and UFO activate *pAP3* by binding LUBS. It is not known whether UFO associates with a LFY monomer or a LFY dimer *in planta*. The different LUBS-bound complexes may interact, notably through LFY SAM oligomerization domain (Sayou et al., 2016). The repressive complex is removed from CarG boxes at this stage, and UFO may help to degrade specific subunits through the SCF^{UFO} complex. *pAP3* also contains a relatively high-score canonical LFYBS that acts only as an enhancer element (Lamb et al., 2002). The LFY dimer bound to this site may enhance transcription by interacting with LFY-UFO complexes. Later on, thanks to UFO, CarG boxes are bound by positive MADS regulators like AP1 (Ng and Yanofsky, 2001), SEP3 (Castillejo et al., 2005) and AP3 (self-activation; Jack et al., 1994). In addition to LFY-UFO, other TFs like AINTEGUMENTA also regulate *AP3* (Krizek, 2009). DBD, DNA Binding Domain; SAM, Sterile Alpha Motif; LFYBS, LFY Binding Site; URM, UFO Recruiting Motif; LUBS, LFY-UFO Binding Site.

F) References

Allen, K.D., and Sussex, I.M. (1996). *Falsiflora* and *anantha* control early stages of floral meristem development in tomato (*Lycopersicon esculentum* Mill.). Planta *200*, 254–264. https://doi.org/10.1007/BF00208316.

Alvarez-Buylla, E.R., Benítez, M., Corvera-Poiré, A., Chaos Cador, Á., de Folter, S., Gamboa de Buen, A., Garay-Arroyo, A., García-Ponce, B., Jaimes-Miranda, F., Pérez-Ruiz, R. V., et al. (2010). Flower Development. Arab. B. 8, e0127. https://doi.org/10.1199/tab.0127.

Baum, S.F., Eshed, Y., and Bowman, J.L. (2001). The Arabidopsis nectary is an ABC-independent floral structure. Development 128, 4657–4667. https://doi.org/10.1242/DEV.128.22.4657.

Carles, C.C., and Fletcher, J.C. (2009). The SAND domain protein ULTRAPETALA1 acts as a trithorax group factor to regulate cell fate in plants. Genes Dev. 23, 2723–2728. https://doi.org/10.1101/GAD.1812609.

Castillejo, C., Romera-Branchat, M., and Pelaz, S. (2005). A new role of the Arabidopsis *SEPALLATA3* gene revealed by its constitutive expression. Plant J. 43, 586–596. https://doi.org/10.1111/j.1365-313X.2005.02476.x.

Chae, E., Tan, Q.K.-G., Hill, T.A., and Irish, V.F. (2008). An Arabidopsis F-box protein acts as a transcriptional co-factor to regulate floral development. Development 135, 1235–1245. https://doi.org/10.1242/dev.015842.

Chen, Y., Wen, H., Pan, J., Du, H., Zhang, K., Zhang, L., Yu, Y., He, H., and Cai, R. (2021). CsUFO is involved in the formation of flowers and tendrils in cucumber. Theor. Appl. Genet. 3. https://doi.org/10.1007/s00122-021-03811-4.

Denay, G., Chahtane, H., Tichtinsky, G., and Parcy, F. (2017). A flower is born: an update on Arabidopsis floral meristem formation. Curr. Opin. Plant Biol. 35, 15–22. https://doi.org/10.1016/J.PBI.2016.09.003.

Dong, Z.C., Zhao, Z., Liu, C.W., Luo, J.H., Yang, J., Huang, W.H., Hu, X.H., Wang, T.L., and Luo, D. (2005). Floral patterning in *Lotus japonicus*. In Plant Physiology, (American Society of Plant Biologists), pp. 1272–1282.

Durfee, T., Roe, J.L., Sessions, R.A., Inouye, C., Serikawa, K., Feldmann, K.A., Weigel, D., and Zambryski, P.C. (2003). The F-box-containing protein UFO and AGAMOUS participate in antagonistic pathways governing early petal development in Arabidopsis. Proc. Natl. Acad. Sci. U. S. A. 100, 8571–8576. https://doi.org/10.1073/pnas.1033043100.

Franks, R.G., Wang, C., Levin, J.Z., and Liu, Z. (2002). SEUSS, a member of a novel family of plant regulatory proteins, represses floral homeotic gene expression with LEUNIG. Development 129, 253–263. https://doi.org/10.1242/DEV.129.1.253.

Gagne, J.M., Downes, B.P., Shiu, S.H., Durski, A.M., and Vierstra, R.D. (2002). The F-box subunit of the SCF E3 complex is encoded by a diverse superfamily of genes in Arabidopsis. Proc. Natl. Acad. Sci. U. S. A. 99, 11519–11524. https://doi.org/10.1073/pnas.162339999.

Geng, F., Wenzel, S., and Tansey, W.P. (2012). Ubiquitin and Proteasomes in Transcription. Annu. Rev. Biochem. 81, 177–201. https://doi.org/10.1146/annurev-biochem-052110-120012.

Gómez-Mena, C., Piñeiro, M., Franco-Zorrilla, J.M., Salinas, J., Coupland, G., and Martínez-Zapater, J.M. (2001). *early bolting in short days*: An Arabidopsis Mutation That Causes Early Flowering and Partially Suppresses the Floral Phenotype of *leafy*. Plant Cell 13, 1011–1024. https://doi.org/10.1105/TPC.13.5.1011.

González-Carranza, Z.H., Rompa, U., Peters, J.L., Bhatt, A.M., Wagstaff, C., Stead, A.D., and Roberts, J.A. (2007). *HAWAIIAN SKIRT*: An F-Box Gene That Regulates Organ Fusion and Growth in Arabidopsis. Plant Physiol. 144, 1370–1382. https://doi.org/10.1104/PP.106.092288.

González-Carranza, Z.H., Zhang, X., Peters, J.L., Boltz, V., Szecsi, J., Bendahmane, M., and Roberts, J.A. (2017). *HAWAIIAN SKIRT* controls size and floral organ number by modulating *CUC1* and *CUC2* expression. PLoS One 12, e0185106. https://doi.org/10.1371/JOURNAL.PONE.0185106.

Gregis, V., Sessa, A., Colombo, L., and Kater, M.M. (2006). AGL24, SHORT VEGETATIVE PHASE, and APETALA1 redundantly control *AGAMOUS* during early stages of flower development in Arabidopsis. Plant Cell 18, 1373–1382. https://doi.org/10.1105/tpc.106.041798.

Gregis, V., Sessa, A., Dorca-Fornell, C., and Kater, M.M. (2009). The Arabidopsis floral meristem identity genes *AP1*, *AGL24* and *SVP* directly repress class *B* and *C* floral homeotic genes. Plant J. 60, 626–637. https://doi.org/10.1111/j.1365-313X.2009.03985.x.

Helm, J. (1951). Vergleichende Betrachtungen über die Entwicklung der Infloreszenz beiLycopersicum esculentum Mill. und bei einer Röntgenmutante. Der Züchter 1951 213 21, 89–95. https://doi.org/10.1007/BF00710588.

Hepworth, S.R., Klenz, J.E., and Haughn, G.W. (2006). UFO in the Arabidopsis inflorescence apex is required for floral-meristem identity and bract suppression. Planta 223, 769–778. https://doi.org/10.1007/s00425-005-0138-3.

Hill, T.A., Day, C.D., Zondlo, S.C., Thackeray, A.G., and Irish, V.F. (1998). Discrete spatial and temporal *cis*-acting elements regulate transcription of the Arabidopsis floral homeotic gene *APETALA3*. Development 125, 1711–1721. https://doi.org/10.1242/dev.125.9.1711.

Honma, T., and Goto, K. (2000). The Arabidopsis floral homeotic gene *PISTILLATA* is regulated by discrete *cis*-elements responsive to induction and maintenance signals. Development 127, 2021–2030. https://doi.org/10.1242/dev.127.10.2021.

Huang, L., Hua, K., Xu, R., Zeng, D., Wang, R., Dong, G., Zhang, G., Lu, X., Fang, N., Wang, D., et al. (2021). The LARGE2-APO1/APO2 regulatory module controls panicle size and grain number in rice. Plant Cell 33, 1212–1228. https://doi.org/10.1093/PLCELL/KOAB041.

Huang, X., Chen, S., Li, W., Tang, L., Zhang, Y., Yang, N., Zou, Y., Zhai, X., Xiao, N., Liu, W., et al. (2021). ROS regulated reversible protein phase separation synchronizes plant flowering. Nat. Chem. Biol. 1–9. https://doi.org/10.1038/s41589-021-00739-0.

Huang, X., Xiao, N., Zou, Y., Xie, Y., Tang, L., Zhang, Y., Yu, Y., Li, Y., and Xu, C. (2022). Heterotypic transcriptional condensates formed by prion-like paralogous proteins canalize flowering transition in tomato. Genome Biol. 23, 1–21. https://doi.org/10.1186/S13059-022-02646-6/FIGURES/6.

Ikeda-Kawakatsu, K., Yasuno, N., Oikawa, T., Iida, S., Nagato, Y., Maekawa, M., and Kyozuka, J. (2009). Expression level of *ABERRANT PANICLE ORGANIZATION1* determines rice inflorescence form through control of cell proliferation in the meristem. Plant Physiol. 150, 736–747. https://doi.org/10.1104/pp.109.136739.

Ikeda-Kawakatsu, K., Maekawa, M., Izawa, T., Itoh, J.-I., and Nagato, Y. (2012). *ABERRANT PANICLE ORGANIZATION 2/RFL*, the rice ortholog of Arabidopsis *LEAFY*, suppresses the transition from inflorescence meristem to floral meristem through interaction with *APO1*. Plant J. 69, 168–180. https://doi.org/10.1111/j.1365-313X.2011.04781.x.

Ikeda, K., Sunohara, H., and Nagato, Y. (2004). Developmental Course of Inflorescence and Spikelet in Rice. Breed. Sci. 54, 147–156. https://doi.org/10.1270/jsbbs.54.147.

Ikeda, K., Nagasawa, N., and Nagato, Y. (2005). *ABERRANT PANICLE ORGANIZATION 1* temporally regulates meristem identity in rice. Dev. Biol. 282, 349–360. https://doi.org/10.1016/j.ydbio.2005.03.016.

Ikeda, K., Ito, M., Nagasawa, N., Kyozuka, J., and Nagato, Y. (2007). Rice *ABERRANT PANICLE ORGANIZATION 1*, encoding an F-box protein, regulates meristem fate. Plant J. 51, 1030–1040. https://doi.org/10.1111/j.1365-313X.2007.03200.x.

Ingram, G.C., Doyle, S., Carpenter, R., Schultz, E.A., Simon, R., and Coen, E.S. (1997). Dual role for *fimbriata* in regulating floral homeotic genes and cell division in *Antirrhinum*. EMBO J. 16, 6521–6534. https://doi.org/10.1093/emboj/16.21.6521.

Irish, V.F. (2010). The flowering of Arabidopsis flower development. Plant J. 61, 1014–1028. https://doi.org/10.1111/j.1365-313X.2009.04065.x.

Jack, T., Fox, G.L., and Meyerowitz, E.M. (1994). Arabidopsis homeotic gene *APETALA3* ectopic expression: Transcriptional and posttranscriptional regulation determine floral organ identity. Cell 76, 703–716. https://doi.org/10.1016/0092-8674(94)90509-6.

Jin, R., Klasfeld, S., Zhu, Y., Fernandez Garcia, M., Xiao, J., Han, S.K., Konkol, A., and Wagner, D. (2021). LEAFY is a pioneer transcription factor and licenses cell reprogramming to floral fate. Nat. Commun. 2021 121 12, 1–14. https://doi.org/10.1038/s41467-020-20883-w.

Kodadek, T., Sikder, D., and Nalley, K. (2006). Keeping Transcriptional Activators under Control. Cell 127, 261–264. https://doi.org/10.1016/j.cell.2006.10.002.

Krizek, B. (2009). *AINTEGUMENTA* and *AINTEGUMENTA-LIKE6* Act Redundantly to Regulate Arabidopsis Floral Growth and Patterning. Plant Physiol. 150, 1916–1929. https://doi.org/10.1104/PP.109.141119.

Krizek, B.A., and Meyerowitz, E.M. (1996). The Arabidopsis homeotic genes *APETALA3* and *PISTILLATA* are sufficient to provide the B class organ identity function. Development 122, 11–22. https://doi.org/10.1242/DEV.122.1.11.

Krizek, B.A., Lewis, M.W., and Fletcher, J.C. (2006). *RABBIT EARS* is a second-whorl repressor of *AGAMOUS* that maintains spatial boundaries in Arabidopsis flowers. Plant J. 45, 369–383. https://doi.org/10.1111/j.1365-313X.2005.02633.x.

Kusters, E., Pina, S. Della, Castel, R., Souer, E., and Koes, R. (2015). Changes in *cis*-regulatory elements of a key floral regulator are associated with divergence of inflorescence architectures. Dev. 142, 2822–2831. https://doi.org/10.1242/dev.121905.

Kuzay, S., Lin, H., Li, C., Chen, S., Woods, D.P., Zhang, J., Lan, T., von Korff, M., and Dubcovsky, J. (2022). *WAPO-A1* is the causal gene of the 7AL QTL for spikelet number per spike in wheat. PLoS Genet. 18. https://doi.org/10.1371/JOURNAL.PGEN.1009747.

Kyozuka, J., Konishi, S., Nemoto, K., Izawa, T., and Shimamoto, K. (1998). Down-regulation of *RFL*, the *FLO/LFY* homolog of rice, accompanied with panicle branch initiation. Proc. Natl. Acad. Sci. U. S. A. 95, 1979–1982. https://doi.org/10.1073/pnas.95.5.1979.

Lai, X., Blanc-Mathieu, R., GrandVuillemin, L., Huang, Y., Stigliani, A., Lucas, J., Thévenon, E., Loue-Manifel, J., Turchi, L., Daher, H., et al. (2021). The LEAFY floral regulator displays pioneer transcription factor properties. Mol. Plant 14, 829–837. https://doi.org/10.1016/J.MOLP.2021.03.004.

Lamb, R.S., Hill, T. a, Tan, Q.K.-G., and Irish, V.F. (2002). Regulation of *APETALA3* floral homeotic gene expression by meristem identity genes. Development 129, 2079–2086. https://doi.org/https://doi.org/10.1242/dev.129.9.2079.

Lang, P.L.M., Christie, M.D., Dogan, E.S., Schwab, R., Hagmann, J., van de Weyer, A.-L., Scacchi, E., and Weigel, D. (2018). A Role for the F-Box Protein HAWAIIAN SKIRT in Plant microRNA Function. Plant Physiol. 176, 730–741. https://doi.org/10.1104/pp.17.01313.

Laufs, P., Coen, E., Kronenberger, J., Traas, J., and Doonan, J. (2003). Separable roles of *UFO* during floral development revealed by conditional restoration of gene function. Development *130*, 785–796. https://doi.org/10.1242/DEV.00295.

Lee, I., Wolfe, D.S., Nilsson, O., and Weigel, D. (1997). A LEAFY co-regulator encoded by *UNUSUAL FLORAL ORGANS*. Curr. Biol. 7, 95–104. https://doi.org/10.1016/S0960-9822(06)00053-4.

Levin, J.Z., and Meyerowitz, E.M. (1995). *UFO*: an Arabidopsis gene involved in both floral meristem and floral organ development. Plant Cell 7, 529–548. https://doi.org/10.1105/tpc.7.5.529.

Levin, J.Z., Fletcher, J.C., Chen, X., and Meyerowitz, E.M. (1998). A genetic screen for modifiers of *UFO* meristem activity identifies three novel *FUSED FLORAL ORGANS* genes required for early flower development in Arabidopsis. Genetics 149, 579–595. https://doi.org/https://doi.org/10.1093/genetics/149.2.579.

Li, F., Lan, W., Zhou, Q., Liu, B., Chen, F., Zhang, S., Bao, M., and Liu, G. (2019). Reduced expression of *CbUFO* is associated with the phenotype of a flower-defective *Cosmos bipinnatus*. Int. J. Mol. Sci. 20, 2503. https://doi.org/10.3390/ijms20102503.

Lippman, Z.B., Cohen, O., Alvarez, J.P., Abu-Abied, M., Pekker, I., Paran, I., Eshed, Y., and Zamir, D. (2008). The Making of a Compound Inflorescence in Tomato and Related Nightshades. PLoS Biol. 6, e288. https://doi.org/10.1371/journal.pbio.0060288.

Liu, Z., and Meyerowitz, E.M. (1995). *LEUNIG* regulates *AGAMOUS* expression in Arabidopsis flowers. Development 121, 975–991. https://doi.org/10.1242/DEV.121.4.975.

Liu, F., Ni, W., Griffith, M.E., Huang, Z., Chang, C., Peng, W., Ma, H., and Xie, D. (2004). The *ASK1* and *ASK2* Genes Are Essential for Arabidopsis Early Development. Plant Cell 16, 5–20. https://doi.org/10.1105/tpc.017772.

Lohmann, J.U., Hong, R.L., Hobe, M., Busch, M.A., Parcy, F., Simon, R., and Weigel, D. (2001). A molecular link between stem cell regulation and floral patterning in Arabidopsis. Cell 105, 793–803. https://doi.org/10.1016/S0092-8674(01)00384-1.

Long, J.A., and Barton, M.K. (1998). The development of apical embryonic pattern in Arabidopsis. 3035, 3027–3035. .

MacAlister, C.A., Park, S.J., Jiang, K., Marcel, F., Bendahmane, A., Izkovich, Y., Eshed, Y., and Lippman, Z.B. (2012). Synchronization of the flowering transition by the tomato *TERMINATING FLOWER* gene. Nat. Genet. 44, 1393–1398. https://doi.org/10.1038/ng.2465.

Monti, L.M., and Devreux, M. (1969). *Stamina pistilloida*: a new mutation induced in pea. Theor. Appl. Genet. 39, 17–20. https://doi.org/10.1007/BF00283080.

Moyroud, E., Kusters, E., Monniaux, M., Koes, R., and Parcy, F. (2010). LEAFY blossoms. Trends Plant Sci. 15, 346–352. https://doi.org/10.1016/j.tplants.2010.03.007.

Muqaddasi, Q.H., Brassac, J., Koppolu, R., Plieske, J., Ganal, M.W., and Röder, M.S. (2019). *TaAPO-A1*, an ortholog of rice *ABERRANT PANICLE ORGANIZATION 1*, is associated with total spikelet number per spike in elite European hexaploid winter wheat (Triticum aestivum L.) varieties. Sci. Rep. 9. https://doi.org/10.1038/S41598-019-50331-9.

Ng, M., and Yanofsky, M.F. (2001). Activation of the Arabidopsis *B* Class Homeotic Genes by *APETALA1*.

Ni, W., Xie, D., Hobbie, L., Feng, B., Zhao, D., Akkara, J., and Ma, H. (2004). Regulation of flower development in arabidopsis by SCF complexes. Plant Physiol. 134, 1574–1585. https://doi.org/10.1104/pp.103.031971.

Ookawa, T., Hobo, T., Yano, M., Murata, K., Ando, T., Miura, H., Asano, K., Ochiai, Y., Ikeda, M., Nishitani, R., et al. (2010). New approach for rice improvement using a pleiotropic QTL gene for lodging resistance and yield. Nat. Commun. 1. https://doi.org/10.1038/NCOMMS1132.

Parcy, F., Nilsson, O., Busch, M.A., Lee, I., and Weigel, D. (1998). A genetic framework for floral patterning. Nature 395, 561–566. https://doi.org/10.1038/26903.

Pouteau, S., Nicholls, D., Tooke, F., Coen, E., and Battey, N. (1998). Transcription pattern of a *FIM* homologue in Impatiens during floral development and reversion. Plant J. 14, 235–246. https://doi.org/10.1046/j.1365-313X.1998.00114.x.

Rebocho, A.B., Bliek, M., Kusters, E., Castel, R., Procissi, A., Roobeek, I., Souer, E., and Koes, R. (2008). Role of *EVERGREEN* in the Development of the Cymose Petunia Inflorescence. Dev. Cell 15, 437–447. https://doi.org/10.1016/J.DEVCEL.2008.08.007.

Reddy, G.V. (2008). Live-imaging stem-cell homeostasis in the Arabidopsis shoot apex. Curr. Opin. Plant Biol. 11, 88–93. https://doi.org/10.1016/j.pbi.2007.10.012.

Risseeuw, E., Venglat, P., Xiang, D., Komendant, K., Daskalchuk, T., Babic, V., Crosby, W., and Datla, R. (2013). An activated form of UFO alters leaf development and produces ectopic floral and inflorescence meristems. PLoS One 8. https://doi.org/10.1371/journal.pone.0083807.

Roth, O., Alvarez, J.P., Levy, M., Bowman, J.L., Ori, N., and Shani, E. (2018). The KNOXI Transcription Factor SHOOT MERISTEMLESS Regulates Floral Fate in Arabidopsis. Plant Cell 30, 1309–1321. https://doi.org/10.1105/tpc.18.00222.

Sablowski, R. (2015). Control of patterning, growth, and differentiation by floral organ identity genes. J. Exp. Bot. 66, 1065–1073. https://doi.org/10.1093/jxb/eru514.

Sacharowski, S.P., Gratkowska, D.M., Sarnowska, E.A., Kondrak, P., Jancewicz, I., Porri, A., Bucior, E., Rolicka, A.T., Franzen, R., Kowalczyk, J., et al. (2015). SWP73 Subunits of Arabidopsis SWI/SNF Chromatin Remodeling Complexes Play Distinct Roles in Leaf and Flower Development. Plant Cell 27, 1889–1906. https://doi.org/10.1105/TPC.15.00233.

Samach, A., Klenz, J.E., Kohalmi, S.E., Risseeuw, E., Haughn, G.W., and Crosby, W.L. (1999). The *UNUSUAL FLORAL ORGANS* gene of Arabidopsis thaliana is an F-box protein required for normal patterning and growth in the floral meristem. Plant J. 20, 433–445. https://doi.org/10.1046/j.1365-313x.1999.00617.x.

Sasaki, K., Yamaguchi, H., Aida, R., Shikata, M., Abe, T., and Ohtsubo, N. (2012). Mutation in *Torenia fournieri* Lind. UFO homolog confers loss of TfLFY interaction and results in a petal to sepal transformation. Plant J. 71, 1002–1014. https://doi.org/10.1111/j.1365-313X.2012.05047.x.

Sayou, C., Nanao, M.H., Jamin, M., Posé, D., Thévenon, E., Grégoire, L., Tichtinsky, G., Denay, G., Ott, F., Peirats Llobet, M., et al. (2016). A SAM oligomerization domain shapes the genomic binding landscape of the LEAFY transcription factor. Nat. Commun. 7, 11222. https://doi.org/10.1038/ncomms11222.

Schultz, E., Carpenter, R., Doyle, S., and Coen, E. (2001). The gene *fimbriata* interacts non-cell autonomously with floral regulatory genes. Plant J. 25, 499–507. https://doi.org/10.1046/j.1365-313x.2001.00977.x.

Selva, C., Shirley, N.J., Houston, K., Whitford, R., Baumann, U., Li, G., and Tucker, M.R. (2021). HvLEAFY controls the early stages of floral organ specification and inhibits the formation of multiple ovaries in barley. Plant J. 108, 509–527. https://doi.org/10.1111/TPJ.15457.

Shahan, R., Zawora, C., Wight, H., Sittmann, J., Wang, W., Mount, S.M., and Liu, Z. (2018). Consensus Coexpression Network Analysis Identifies Key Regulators of Flower and Fruit Development in Wild Strawberry. Plant Physiol. 178, 202–216. https://doi.org/10.1104/PP.18.00086.

Sharma, B., Meaders, C., Wolfe, D., Holappa, L., Walcher-Chevillet, C., and Kramer, E.M. (2019). Homologs of *LEAFY* and *UNUSUAL FLORAL ORGANS* Promote the Transition From Inflorescence to Floral Meristem Identity in the Cymose *Aquilegia coerulea*. Front. Plant Sci. 10. https://doi.org/10.3389/fpls.2019.01218.

Simon, R., Carpenter, R., Doyle, S., and Coen, E. (1994). *Fimbriata* controls flower development by mediating between meristem and organ identity genes. Cell 78, 99–107. https://doi.org/10.1016/0092-8674(94)90576-2.

Singh, N., and Bhalla, N. (2020). Moonlighting Proteins. https://doi.org/10.1146/annurev-genet-030620.

Smyth, D.R., Bowman, J.L., and Meyerowitz, E.M. (1990). Early flower development in Arabidopsis. Plant Cell 2, 755–767. https://doi.org/10.1105/TPC.2.8.755.

Souer, E., Rebocho, A.B., Bliek, M., Kusters, E., de Bruin, R.A.M., and Koes, R. (2008). Patterning of Inflorescences and Flowers by the F-Box Protein DOUBLE TOP and the LEAFY Homolog ABERRANT LEAF AND FLOWER of Petunia. Plant Cell Online 20, 2033–2048. https://doi.org/10.1105/tpc.108.060871.

Stefanowicz, K., Lannoo, N., and Van Damme, E.J.M. (2015). Plant F-box Proteins – Judges between Life and Death. CRC. Crit. Rev. Plant Sci. 34, 523–552. https://doi.org/10.1080/07352689.2015.1024566.

Takeda, S., Hamamura, Y., Sakamoto, T., Kimura, S., Aida, M., and Higashiyama, T. (2022). Non-cell-autonomous regulation of petal initiation in Arabidopsis thaliana. Development https://doi.org/10.1242/DEV.200684.

Tanahashi, T., Sumikawa, N., Kato, M., and Hasebe, M. (2005). Diversification of gene function: homologs of the floral regulator *FLO/LFY* control the first zygotic cell division in the moss *Physcomitrella patens*. Development 132, 1727–1736. https://doi.org/10.1242/DEV.01709.

Taylor, S., Hofer, J., and Murfet, I. (2001). *Stamina pistilloida*, the pea ortholog of *Fim* and *UFO*, is required for normal development of flowers, inflorescences, and leaves. Plant Cell 13, 31–46. https://doi.org/10.1105/tpc.13.1.31.

Tilly, J.J., Allen, D.W., and Jack, T. (1998). The CArG boxes in the promoter of the Arabidopsis floral organ identity gene *APETALA3* mediate diverse regulatory effects. Development 125, 1647–1657. https://doi.org/10.1242/dev.125.9.1647.

Tsukahara, K., Sawada, H., Kohno, Y., Matsuura, T., Mori, I.C., Terao, T., Ioki, M., and Tamaoki, M. (2015). Ozone-Induced Rice Grain Yield Loss Is Triggered via a Change in Panicle Morphology That Is Controlled by *ABERRANT PANICLE ORGANIZATION 1* Gene. PLoS One 10. https://doi.org/10.1371/JOURNAL.PONE.0123308.

Wagner, D., Sablowski, R.W.M., and Meyerowitz, E.M. (1999). Transcriptional activation of *APETALA1* by LEAFY. Science 285, 582–584. https://doi.org/10.1126/science.285.5427.582.

Wang, X., Feng, S., Nakayama, N., Crosby, W.L., Irish, V., Deng, X.W., and Wei, N. (2003). The COP9 Signalosome Interacts with SCF UFO and Participates in Arabidopsis Flower Development. Plant Cell 15, 1071–1082. https://doi.org/10.1105/tpc.009936.

Wilkinson, and Haughn (1995). *UNUSUAL FLORAL ORGANS* Controls Meristem Identity and Organ Primordia Fate in Arabidopsis. Plant Cell 7, 1485–1499. https://doi.org/10.1105/tpc.7.9.1485.

Wilkinson, M., de Andrade Silva, E., Zachgo, S., Saedler, H., and Schwarz-Sommer, Z. (2000). *Choripetala* and *despenteado*: General regulators during plant development and potential floral targets of FIMBRIATA-mediated degradation. Development 127, 3725–3734. .

Wittern, L.M., Barrero, J.M., Bovill, W.D., Verbyla, K.L., Hughes, T., Swain, S.M., Steed, G., Webb, A.A.R., Gardner, K., Greenland, A., et al. (2022). Overexpression of the *WAPO-A1* gene increases the number of spikelets per spike in bread wheat. Sci. Reports 2022 121 12, 1–15. https://doi.org/10.1038/s41598-022-18614-w.

Wu, M.F., Sang, Y., Bezhani, S., Yamaguchi, N., Han, S.K., Li, Z., Su, Y., Slewinski, T.L., and Wagner, D. (2012). SWI2/SNF2 chromatin remodeling ATPases overcome polycomb repression and control floral organ identity with the LEAFY and SEPALLATA3 transcription factors. Proc. Natl. Acad. Sci. U. S. A. 109, 3576–3581. https://doi.org/10.1073/PNAS.1113409109/SUPPL_FILE/PNAS.201113409SI.PDF.

Wuest, S.E., O'Maoileidigh, D.S., Rae, L., Kwasniewska, K., Raganelli, A., Hanczaryk, K., Lohan, A.J., Loftus, B., Graciet, E., and Wellmer, F. (2012). Molecular basis for the specification of floral organs by APETALA3 and PISTILLATA. Proc. Natl. Acad. Sci. U. S. A. 109, 13452–13457. https://doi.org/10.1073/PNAS.1207075109/SUPPL_FILE/SD04.XLSX.

Yano, K., Ookawa, T., Aya, K., Ochiai, Y., Hirasawa, T., Ebitani, T., Takarada, T., Yano, M., Yamamoto, T., Fukuoka, S., et al. (2015). Isolation of a Novel Lodging Resistance QTL Gene Involved in Strigolactone Signaling and Its Pyramiding with a QTL Gene Involved in Another Mechanism. Mol. Plant 8, 303–314. https://doi.org/10.1016/j.molp.2014.10.009.

Zhang, S., Sandal, N., Polowick, P.L., Stiller, J., Stougaard, J., and Fobert, P.R. (2003). *Proliferating floral organs* (*pfo*), a Lotus japonicus gene required for specifying floral meristem determinacy and organ identity, encodes an F-box protein. Plant J. 33, 607–619. https://doi.org/10.1046/j.1365-313X.2003.01660.x.

Zhao, D., Yang, M., Solava, J., and Ma, H. (1999). The *ASK1* gene regulates development and interacts with the UFO gene to control floral organ identity in Arabidopsis. Dev. Genet. 25, 209–223. https://doi.org/10.1002/(SICI)1520-6408(1999)25:3<209::AID-DVG4>3.0.CO;2-O.

Zhao, D., Yu, Q., Chen, M., and Ma, H. (2001). The *ASK1* gene regulates B function gene expression in cooperation with *UFO* and *LEAFY* in Arabidopsis. Development 128, 2735–2746. https://doi.org/10.1242/dev.128.14.2735.

Zhao, Y., Zhang, T., Broholm, S.K., Tähtiharju, S., Mouhu, K., Albert, V.A., Teeri, T.H., and Elomaa, P. (2016). Evolutionary co-option of floral meristem identity genes for patterning of the flower-like asteraceae inflorescence. Plant Physiol. 172, 284–296. https://doi.org/10.1104/pp.16.00779.

III. Complementary results

In this part, I present some results that are not published and I also introduce ongoing experiments on the LFY-UFO synergy.

AP3 activation likely involves complex interactions between regulators

AP3 activation could be a particular case of LFY-UFO activation

In Article 1, we show that *pAP3* contains several LUBS that are required for LFY-UFO activation, and in Article 2 we propose a model for the activation of this promoter. Despite these results, we are far from explaining *pAP3* activation in detail and many questions remain. More generally, it is difficult to understand with the data we have so far why specific promoters like *pAP3* are strongly activated by LFY-UFO. I propose that *pAP3* is a special case in which the structure of the promoter and the action of other precise cofactors strongly favors activation by LFY-UFO. As presented below, several results suggest a complex mechanism for *pAP3* activation with interactions between diverse regulators bound to different *cis*-elements.

Interaction between pAP3 LUBS for the LFY-UFO activation

An interesting feature of *pAP3* is the presence of several LUBS in close proximity in its sequence (Article 1 Figure 3a). In the protoplast assay, we found that combining LUBS mutations strongly reduced *pAP3* activation (Article 1 Figure 3c). It is thus likely that several LFY-UFO complexes bind this LUBS-rich region. The juxtaposition of several LFY-UFO complexes may increase activation and could explain why *pAP3* is a major LFY-UFO target. It will be interesting to analyze other LFY-UFO-regulated genes to see if several LUBS are present in their regulatory sequence and if it exists a preferential distance between functional LUBS.

pAP3 canonical LFYBS may interact with LUBS to increase AP3 activation

pAP3 canonical LFYBS is a *cis*-elements with a very puzzling role. Despite its relatively high-score, this canonical LFYBS is only an enhancer element as deleting it (Hill et al., 1998) or

mutating it (Lamb et al., 2002; Article 1 Extended Data Fig. 2) in plants or in protoplasts only reduces *pAP3* activity. Moreover, why the LFY-VP16 activated form does not induce *pAP3* through this canonical LFYBS *in planta* (Parcy et al., 1998) or in protoplasts remains unexplained.

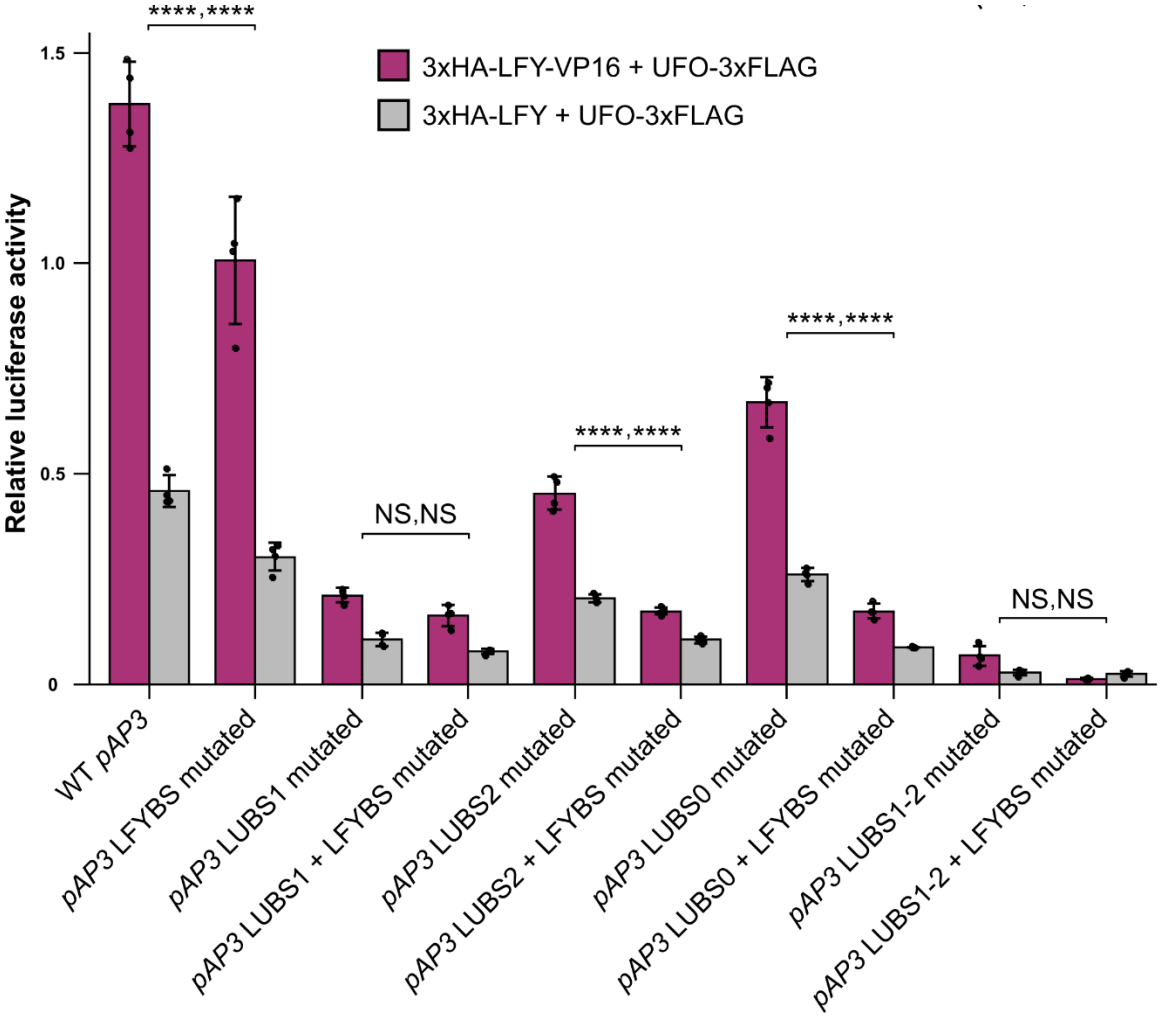

Figure 13. *pAP3* LUBS and the canonical LFYBS likely act synergistically in LFY-UFO-dependent activation. *Promoter activation measured by DLRA in Arabidopsis protoplasts with indicated effectors. Different promoter versions were tested as indicated under x-axis. Data represent averages of independent biological replicates and are presented as mean ± SD, each dot representing one biological replicate (n = 4). One-way ANOVA with Tukey's multiple comparisons tests. One-way ANOVA were performed with data from the same effector and brackets represent relevant comparisons between promoters. (NS: p > 0.05,*: p <0.05, **: p < 0.01, ***: p < 0.001 and ****: p < 0.0001).*

We found that combining LUBS mutations and LFYBS mutation strongly reduced *pAP3* activation in protoplasts (Figure 13). Hence, it is possible that LUBS-bound LFY-UFO complexes interact with LFYBS-bound LFY. This could be achieved through LFY SAM oligomerizaton domain and *pAP3* looping, as we found that the LFY-UFO complex has the ability to bend DNA (Article 1 Extended Data Figure 9f). The formation of such a loop on *pAP3* may explain the high activation of this precise promoter by LFY-UFO and the role of the canonical LFYBS as an enhancer element. It could be interesting to explore if LFY-UFO-regulated promoters present the same structure with LUBS in close proximity to canonical LFYBS.

pAP3 CarG boxes are bound by general repressors in early flowering stages

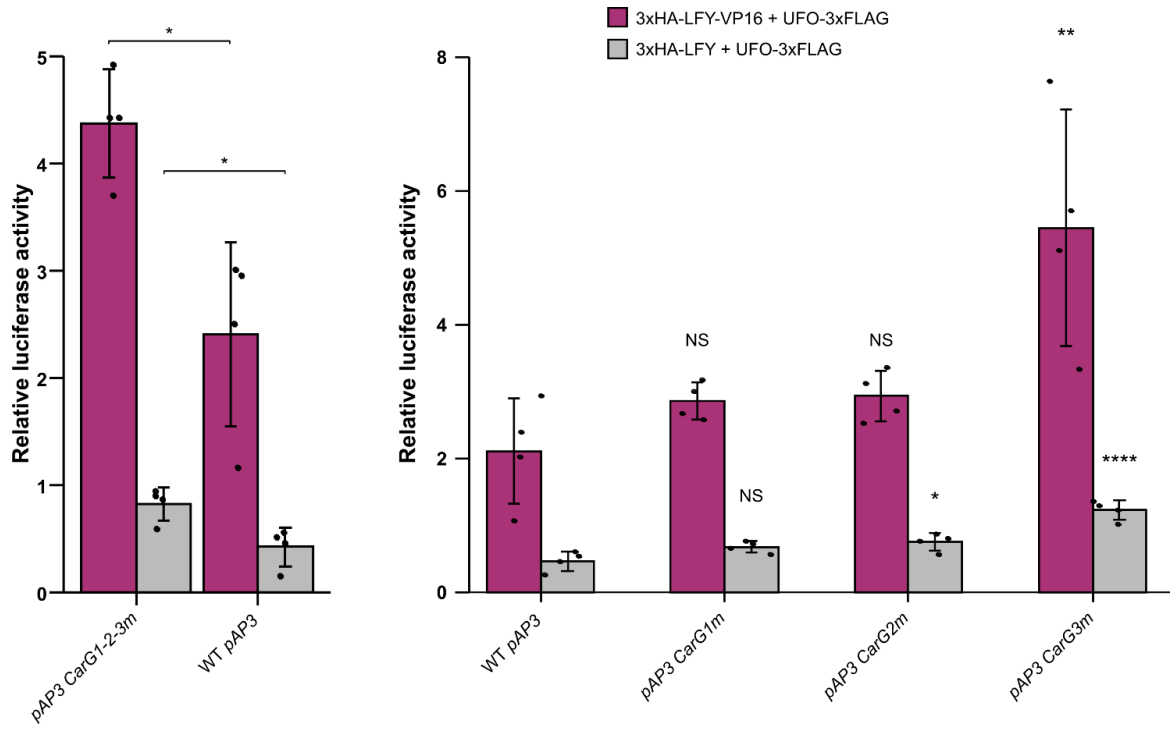

Figure 14. *pAP3* CarG box 3 is bound by repressors in protoplasts. *Promoter activation measured by DLRA in Arabidopsis protoplasts with indicated effectors. Different promoter versions were tested as indicated under the x-axis. CarG boxes are numbered as in Hill et al., 1998. Data represent averages of independent biological replicates and are presented as mean ± SD, each dot representing one biological replicate (n = 4). Left graph: Unpaired t-tests (*: p <0.05). Right graph: One-way ANOVA with Tukey's multiple comparisons tests. One-way ANOVA were performed with data from the same effector and stars represent a significant statistical difference compared to WT pAP3. (NS: p > 0.05,*: p <0.05, **: p < 0.01, ***: p < 0.001 and ****: p < 0.0001).*

Apart from the canonical LFYBS and LUBS, other *cis*-elements regulate *pAP3* activation, notably CarG boxes (the motif recognized by MADS TFs). In *pAP3*, these CarG boxes are located near LUBS1 and LUBS2. It has been shown that *pAP3* CarG boxes are bound by negative MADS regulators in the early flower meristem like SOC1, AGL24 and SVP (Gregis et al., 2006, 2009; Liu et al., 2009). Accordingly, mutating *pAP3* CarG box 3 increases *pAP3* activation in early stages of flower development (Tilly et al., 1998). In later stages of flower development, *pAP3* CarG boxes are bound by an activator MADS quartet involving AP3 (Jack et al., 1994).

We observed that mutating CarG boxes (and notably CarG3) in protoplasts also induced a higher *pAP3* activation by LFY-UFO (Figure 14). Thus, CarG box-bound repressors might be broadly expressed MADS TFs, present both in the early FM and in protoplasts.

It is possible that LUBS-bound LFY-UFO complexes interact with MADS TFs to regulate *AP3* expression. Thus, it could be relevant to investigate the existence of an interaction between UFO and MADS TFs, as previously suggested (Ng and Yanofsky, 2001) but never tested.

Performing LFY and UFO ChIP-Seq

In Article 1, we obtained the sequence bound by LFY-UFO by performing ampDAP-seq with a reconstituted ASK1-UFO-LFY complex. However, this *in vitro* experiment lacks the complexity of *in vivo* regulations and LFY-UFO binding in several regions of the genome can only be hypothesized. Hence, it is not possible with our ampDAP-seq data to know how deeply UFO affects LFY binding *in vivo*. To address this limitation, I designed a LFY and a UFO ChIP-seq experiment (Figure 15).

Despite the fact that we have a ChIP-grade antibody for LFY, in our hand it was not possible to perform ChIP-seq when *LFY* is expressed under its constitutive promoter, and previous LFY ChIP experiments were done in *LFY* overexpressing plants (*35S::LFY* seedlings or *35S::LFY-GR* inflorescences). Because *LFY* induces a strong phenotype when overexpressed, I chose to perform the ChIP experiment in *35S::LFY-GR* plants. In these plants, the LFY-GR protein is overexpressed but remains inactive in the cytoplasm until induction. Upon DEX treatment, LFY-GR is transferred to the nucleus where it is active (Wagner et al., 1999). The use of *35S::LFY-GR* plants allows working on inflorescences (Winter et al., 2011), where LFY and UFO

are normally active. I crossed *35S::LFY-GR* plants to the strong *ufo-2* mutant (single recessive mutant). Because *ufo-2* plants are male sterile, I kept *ufo-2 +/-* plants in the F2 generation. Among these plants I selected lines that are *35S::LFY-GR +/+* (with 100% Kan^R seedlings). After segregation, F3 plants are either *ufo-2 +/+* or *ufo-2 +/-* plants, and have a WT (75%) or a *ufo* (25%) phenotype. The *ufo* phenotype is easy to spot by eye, making it possible to select the two populations for ChIP based only to the phenotype.

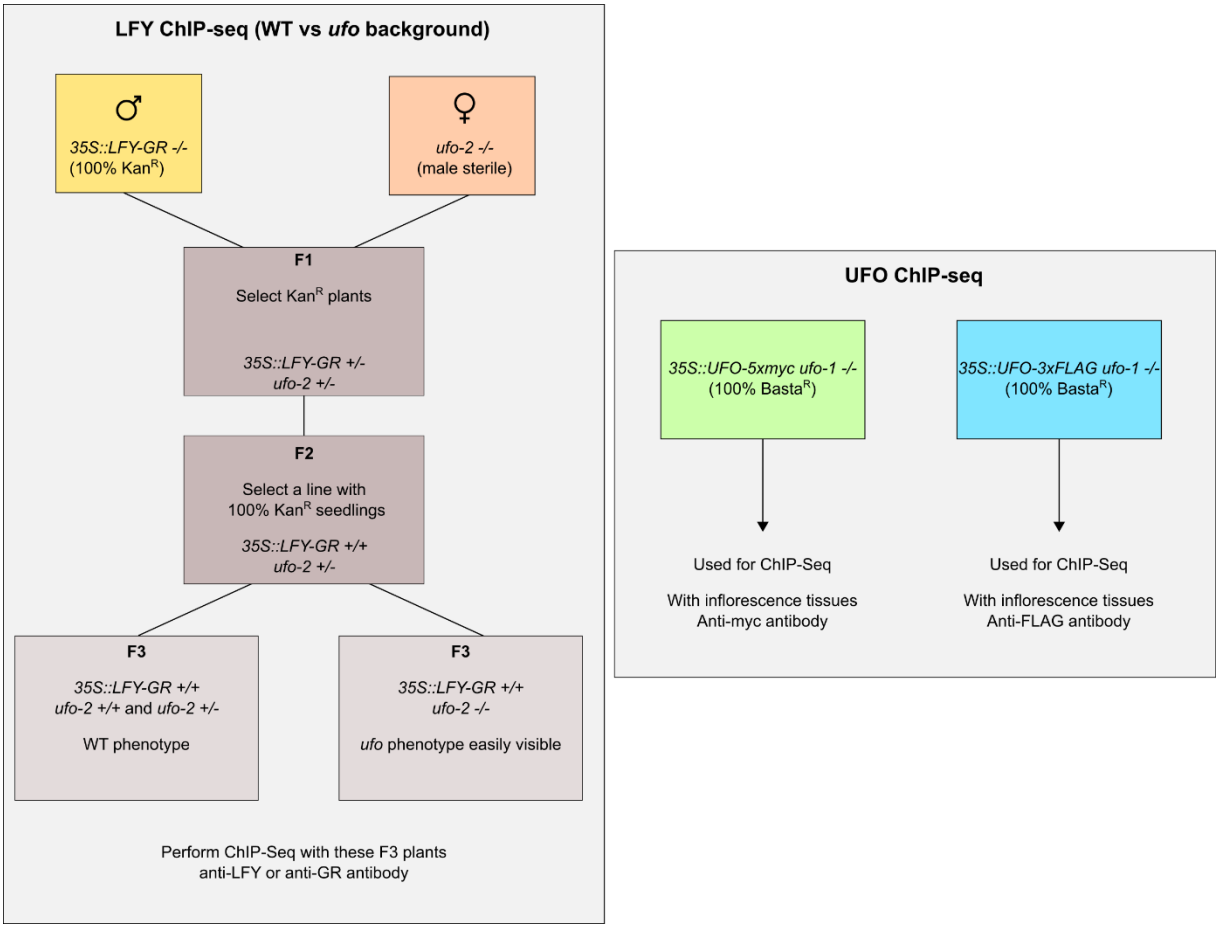

Figure 15: *Design of the LFY ChIP-seq (left) and UFO ChIP-seq (right) experiments.*

I also planned to perform UFO ChIP-Seq. Several UFO tagged lines are described in Article 1 (*35S::UFO-3xFLAG ufo-1 -/-* and *35S::UFO-5xmyc ufo-1 -/-*). In these transgenics, tagged versions of UFO are detected by Western Blot (Article 1 Extended Data Figure 1) and can be IPed (not shown). Furthermore, these lines show a clear *UFO* gain-of-function phenotype. Hence, these plants can be used for ChIP-Seq. It would have been interesting to cross these lines to the strong *lfy-12* mutant to test the effect of *LFY* mutation on UFO binding. However,

it was already shown that UFO is completely inactive *in planta* when *LFY* is not functional (no UFO gain-of-function phenotype in a *lfy* mutant background; Lee 1997; Chae 2008; Risseeuw 2013). Because this cross implies many genotyping steps at each generation, it was not performed.

All seeds were sent to our collaborator M. Schmid at the University of Umea (Sweden). I also tried to perform the ChIP-Seq experiment myself. However, due to time constraints and technical difficulties, I did not manage to obtain high quality DNA at the end of the experiment.

Determining UFO and HAWAIIAN SKIRT (HWS) interactomes by *in planta* proximity labelling

A major question that remains unanswered is the role of UFO in ubiquitination pathways. Indeed, we showed that UFO acts mainly through a transcriptional complex and that its connection to ubiquitination pathways is dispensable. The hypothesis we present in Article 2 is that UFO has a role in ubiquitination but acts redundantly with other F-box proteins. With this assumption, it is expected to complement the *ufo* mutant with the *35S::UFOΔFbox* transgene as UFOΔFbox performs the transcriptional activity and other F-box proteins working in parallel to UFO are still active.

A first objective to understand the role of UFO in ubiquitination pathways would be to identify possible F-box proteins working redundantly with UFO. In Article 1, we propose HWS as a strong candidate because the genetic interaction between *UFO* and *HWS* is clearly established (Levin et al., 1998). Moreover, HWS protein sequence is close to UFO, and HWS strictly functions within an E3 ligase complex (removing the HWS F-box makes it inactive; Lang et al., 2018). However, when performing a BLAST with UFO protein sequence as query in Arabidopsis, several other F-box are found (already characterized like LEAF CURLING RESPONSIVENESS or uncharacterized). Hence, several F-box proteins other than HWS may act redundantly with UFO. Obtaining mutants of these candidates (alone or in combination with *ufo*) could help to reveal interesting phenotypes.

To understand if UFO acts as a classical F-box protein within an SCF complex, its potential targets have to be determined. In fact, these targets are not yet characterized in any species.

Y2H screens performed with UFO and UFO homologs from several species as bait did not identify many clear interactants. In yeast, full-length UFO does not interact with LFY in Y2H and only a truncated UFO version lacking the F-box domain does (Chae et al., 2008). This led us to believe that yeast-based methods are not adapted to find the UFO interactome. Other techniques exist to obtain a protein interactome, like for example IP-MS (Immunoprecipitation-Mass Spectrometry). In this experiment, the protein of interest is IPed (with a specific antibody or with an antibody against a common tag), and proteins pull-downed together with the protein of interest are identified by MS. This technique has been widely used to detect the targets of F-box proteins. Because the interaction of F-box proteins with their targets does not require the F-box domain, this domain is often removed to avoid target protein degradation (also called the "decoy model"; Feke et al., 2019).

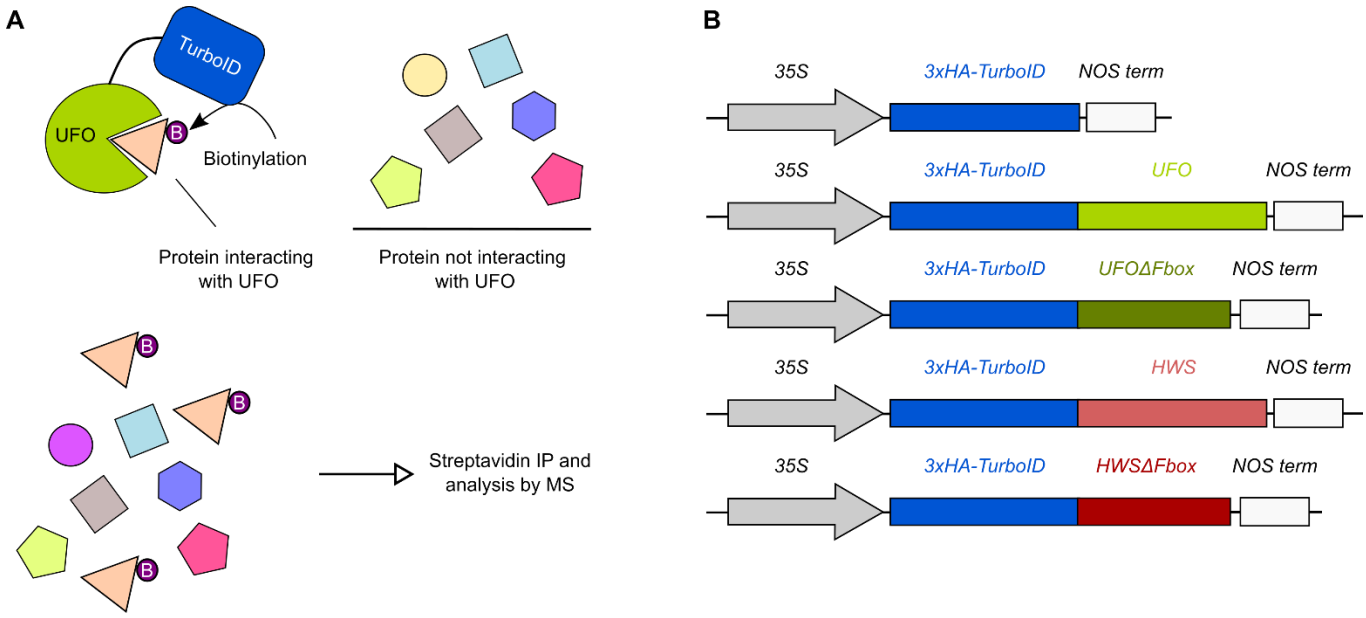

Figure 16. Experimental design to obtain UFO interactome by proximity labelling. (A) *Principle of proximity labelling (adapted from Branon et al., 2018). The TurboID biotin ligase is fused to UFO and biotinylate proteins in close proximity to UFO upon biotin treatment. Biotinylated proteins are then IPed and identified by MS.* **(B)** *Constructs transformed in Arabidopsis Col-0 plants.*

I did not choose IP-MS to identify UFO interactants because the required amount of protein for detection by MS is quite high and hard to reach with floral tissues. I decided to use another technique to obtain UFO interactome called proximity labelling (Figure 16A; Branon et al.,

2018). In this experiment, plants are transformed to express a biotin ligase (TurboID) fused to the protein of interest. Upon biotin treatment, the biotin ligase adds biotin to the proteins in its close proximity, *i.e*. proteins interacting with the protein of interest. Biotinylated proteins are then IPed and identified by MS. The amount of IPed protein after proximity labelling should be more important because interactants are IPed directly and not through their interaction with UFO.

I have transformed WT Col-0 plants to perform proximity labelling with UFO and HWS, as well as their ΔFbox versions (Figure 16). Due to time constraints, I did not characterize these plants. Once transformants will be isolated, it will be necessary to identify the best conditions for biotin ligation (temperature, treatment time, buffer, biotin concentration etc; Mair et al., 2019).

Obtaining a high-resolution structure of the ASK1-UFO-LFY DBD-DNA complex

In the Figure 4 of Article 1 we show that a LFY mutation (K249R) alters the functional interaction with UFO on LUBS. This experiment was useful to demonstrate that LFY has UFO-dependent and UFO-independent functions.

We also tested the effect of mutations on UFO exposed residues, but these results are not presented in Article 1. Based on UFO predicted structure (Figure 6), we selected some conserved charged residues on the loops protruding from the Kelch-repeat β-propeller domain. We hypothesized that these residues could be involved in the interaction with LFY (and latter with DNA when we found that UFO binds DNA). We mutated arginine and lysine residues to serine, and we tested these UFO mutated versions in the protoplast assay. We found that some UFO mutated versions were strongly affected in their ability to activate *pAP3* with LFY (Figure 17). The cryoEM data latter revealed that these residues are likely located at the UFO-DNA interface. This experiment will have to be repeated (with VP16 versions for example) and complemented with EMSAs, but it is possible that we have identified some UFO DNA-contacting residues.

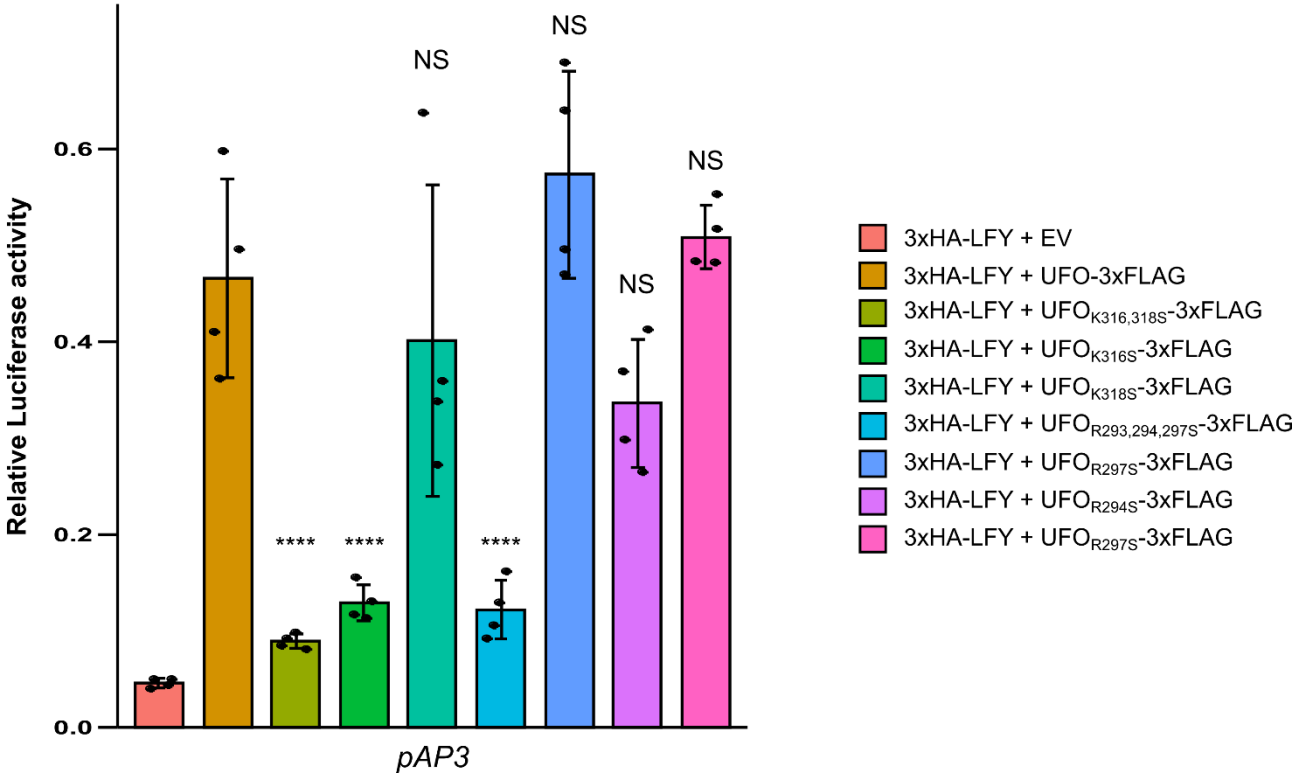

Figure 17. Some UFO residues are required for LFY-UFO-dependent pAP3 activation. *pAP3 activation in Arabidopsis protoplasts, with indicated effectors (right). EV = Empty Vector. Data are mean ± SD (n = 4 biological replicates). One-way ANOVA with Tukey's multiple comparisons test. Stars represent a significant statistical difference compared 3xHA-LFY+ UFO-3xFLAG, non-significant (NS) otherwise. (NS: p > 0.05; ****: p <0.0001).*

Obviously, obtaining a high-resolution cryoEM map will be crucial to build a complete model of the complex. It will allow to precisely position LFY and UFO residues, notably those contacting DNA and those implied in the interaction between the two proteins. The cryoEM experiment presented in the Figure 5 of Article 1 was performed with *pAP3* LUBS1 DNA which is a dLUBS (*i.e.* bound by a LFY DBD dimer). A problem we met is that it exists a mix of two complexes (involving either a LFY DBD monomer or dimer) on cryoEM grids. In addition, there were some problems of particle preferential orientation. To circumvent some of these limitations, we are now reconstituting the ASK1-UFO-LFY DBD-DNA complex with other DNA oligos. We chose oligos corresponding to the mLUBS and dLUBS perfect sequences (see Article 1 Figure 2f). With these oligos, the affinity of LFY-UFO for DNA should be increased. We are reconstituting these complexes at the moment and we will test them in cryoEM.

CHAPTER III:

Biochemical and structural characterization of ALOG-domain TFs

Even if there are obvious connections, this chapter is relatively independent from the first two and deals with another project, focused on the biochemical and structural characterization of the plant ALOG TF family.

I. Introduction

LFY ChIP-seq experiments in Arabidopsis revealed thousands of LFY-bound regions but the significance of these regions (are they truly regulatory?) has, in many cases, not been studied. By exploring LFY ChIP-seq data, we found that LFY strongly binds the promoter of *LSH1*, *LSH2* and *LSH3*, 3 genes belonging to the *Arabidopsis LSH Oryza G1* (*ALOG*) family (Figure 4). These LFY peaks are massive and we wondered whether they were associated with a clear LFY-dependent regulation. By analyzing non-published transcriptomic data, we found that LFY likely negatively regulates *LSH1*, *LSH2* and *LSH3* in the Arabidopsis early FM.

LSH genes were first identified through the study of Arabidopsis activation-tagged lines showing hypersensitivity to continuous light (Zhao et al., 2004). In Arabidopsis, this family comprises 10 genes with very similar protein sequences. Their role in this species is not entirely clear as single *lsh* mutants have no phenotype (Takeda et al., 2011), likely because of genetic redundancy. Some *LSH* genes are expressed in the IM and likely negatively regulate the FM identity acquisition as overexpressing *LSH3* or *LSH4* induces the formation of ectopic meristems (Takeda et al., 2011). A close look at their expression profile showed that LSH are expressed in the boundary regions where they could act as repressors inhibiting cell differentiation (Cho and Zambryski, 2011; Takeda et al., 2011).

To better understand the role of *ALOG* genes, we examined available data in other species. In tomato, the ALOG protein TERMINATING FLOWER (TMF) represses the precocious transition to the FM by repressing the expression of the *UFO* homolog *ANANTHA* (*AN*; MacAlister et al., 2012). In rice, several *alog* mutants have been described like *long sterile lemma1* (*g1*; Yoshida et al., 2009), *tawawa1* (*taw1*; Yoshida et al., 2013) and *triangular hull 1* (*th1*; Li et al., 2012). These genes are involved in several processes like inflorescence architecture for *TAW1* and sterile lemma identity for *G1* (Yoshida et al., 2009; Yoshida et al., 2013).

Hence, the floral function of *ALOG* genes and their role at the crossroad between LFY and UFO pathways led us to study the properties of these proteins. When reading the literature, we realized that very few data were available on their biochemical properties. The DNA motif they bind was not described, preventing from proposing target genes and precisely identifying *cis*-elements. Thus, we decided to better characterize this family of TFs.

II. Article 3

The results we obtained are presented as a paper draft. The structural part is less polished because results were obtained just before the redaction of this draft.

Title

Biochemical and structural characterization of ALOG transcription factors

Authors

Philippe Rieu, Emmanuel Thévénon, Jérémy Lucas, Mahmoud Rizk, Renaud Dumas, Max Nanao, Chloe Zubieta, François Parcy.

Introduction

Proper gene activation is crucial in the development of living organisms. Transcription Factors (TFs) play a key role in this process by activating or repressing target genes, and plant genomes contain a high proportion of genes encoding TFs (Riechmann et al., 2000). Plant TFs have been classified according to the properties of their DNA Binding Domain (DBD; Blanc-Mathieu 2022). Some plant TFs families are shared with other eukaryotes while others are specific to plants.

TFs are characterized by their DNA binding specificity. This fundamental property has been established for most TF families in plants but remains poorly characterized for a few of them. Also, the structure of DBD and the structural basis for their DNA binding have been elucidated

for many, but not all, plant TFs. One of such family where these key data are missing is the *ALOG* (*Arabidopsis LIGHT-DEPENDENT SHORT HYPOCOTYLS 1 (LSH1) and Oryza G1*) gene family. This conserved gene family is present in land plants as well as in some algae (Iyer and Aravind, 2012; Naramoto et al., 2020). In land plants, *ALOG* genes are often found in several copies like in *Arabidopsis thaliana* where the LSH family comprises 10 members (Zhao et al., 2004).

ALOG have been shown to play crucial developmental roles in diverse plant species. In *Marchantia polymorpha*, *ALOG* genes *LATERAL ORGAN SUPPRESSOR 1* (*LOS1*) and *LOS2* are implicated in meristem maintenance and lateral organ development (Naramoto et al., 2019, 2020). In tomato, the *ALOG* gene *TERMINATING FLOWER* (*TMF*) plays a key role in flowering by preventing the precocious expression of the *UNUSUAL FLORAL ORGAN* (*UFO*) homolog *ANANTHA* (*AN*; MacAlister et al., 2012). In rice, several *ALOG* genes have been characterized such as *LONG STERILE LEMMA1* (*G1*; Yoshida et al., 2009), *TAWAWA1* (*TAW1*; Yoshida et al., 2013) or *TRIANGULAR HULL 1* (*TH1*; Li et al., 2012). They play diverse roles such as controlling the panicle and the sterile lemma architectures. In pea, *SYMMETRIC PETALS 1* (*SYP1*) is a regulator of floral organ internal asymmetry (He et al., 2020). In Arabidopsis, the role of LSH is less clear since single *lsh* mutants display no obvious phenotype (Takeda et al., 2011). LSH3 and LSH4 are active in the boundary regions of shoot organs under the transcriptional control of CUP-SHAPED COTYLEDON 1 and 2 TFs (CUC1-2; Cho and Zambryski, 2011; Takeda et al., 2011). Moreover, constitutive expression of LSH results in the inhibition of leaf growth and the production of ectopic meristems in flowers (Takeda et al., 2011). Overall, these phenotypes suggest that Arabidopsis LSHs specifically repress organ formation in boundary regions and the floral meristem identity acquisition.

Even if the role of ALOG has been established in several species, very little is known on how these proteins act at the molecular level. Their role as TFs is commonly accepted and it has been shown in rice and tomato that ALOGs act as transcriptional repressors (Huang et al., 2021; Peng et al., 2017). A mechanism was proposed for TMF-dependent *AN* repression including phase separation on the *AN* promoter (Huang et al., 2021, 2022). DNA binding was observed only for the tomato TMF protein but the motif recognized within the *AN* promoter region was not precisely identified (Huang et al., 2021). The ALOG DNA binding specificity was

not established in any species, preventing from identifying *cis*-elements in target genes and novel regulated candidates.

At the molecular level, ALOGs proteins share a common overall organization. The conserved ALOG domain, proposed to be the DBD (Iyer and Aravind, 2012), is flanked by non-conserved disordered regions of variable lengths. Based on sequence and structure similarity, it was shown that the ALOG domain likely originates from the DBD of bacterial recombinases found in mobile elements (Iyer and Aravind, 2012). The originality of ALOG DBDs compared to that of recombinases lies in the presence of a putative zinc ribbon between predicted helices 2 and 3. The role of this element is unknown, but it was shown that mutating tomato TMF zinc ribbon cysteines affects its DNA binding properties (Huang et al., 2021). How ALOGs bind DNA is unknown, and for this reason the precise role of the predicted helices and the zinc ribbon remains unclear.

Here, we identify the ALOG-bound motif using *in vitro* genomic binding assays and we show that this motif is highly conserved over a large evolutionary distance. Based on structural and biochemical assays, we propose that the DNA binding mechanism is likely more complex than what was originally hypothesized based on the comparison with the DBD from recombinases.

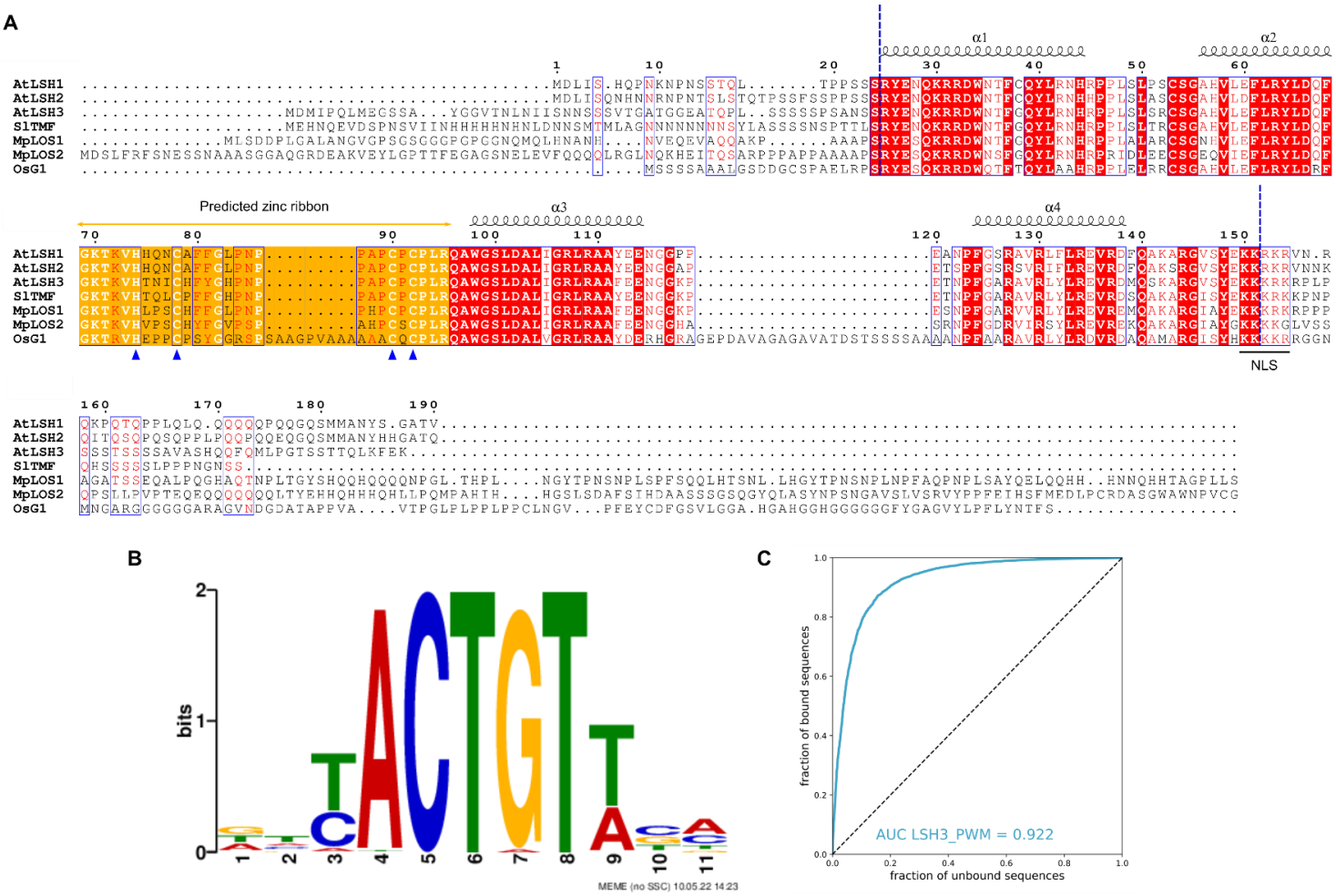

Figure 1. Determination of ALOG binding specificity by ampDAP-seq. (**A**) Alignment of studied ALOG proteins. Blue dotted lines indicate the limits of the ALOG domain. The predicted zinc ribbon is highlighted in orange. Blue triangles represent the key histidine and cysteine residues of the zinc ribbon. NLS = Nuclear Localization Signal. Note that N and C-terminal regions are not conserved. Numbers are relative to AtLSH1. At = *Arabidopsis thaliana*, Sl = *Solanum lycopersicum*, Mp = *Marchantia polymorpha*, Os = *Oryza Sativa*. (**B**) Logo obtained for LSH3 in ampDAP-seq. The logo was generated using the 600 peaks with the strongest LSH3 ampDAP-seq signal. (**C**) Receiver operating characteristic (ROC) curve for LSH3 using all peaks except those used to build the logo. The value of the Area Under the Curve (AUC) is indicated.

Identification of the ALOG DNA-binding specificity

To gain insight into their DNA binding properties, we studied ALOG TFs from various plant species (Figure 1A). We chose ALOG candidates that were already characterized, and/or genes whose mutation induce a phenotype *in vivo*. We also selected OsG1 as it contains two insertions not found in other ALOG proteins (Huang et al., 2021). To establish their DNA

binding specificity, we performed amplified DNA Affinity Purification sequencing (ampDAP-seq; O'Malley 2016) with Full Length (FL) *in vitro*-produced ALOG proteins and Arabidopsis genomic DNA. AmpDAP-seq was performed in triplicates and yielded highly reproducible results (Figure S1). Motif search in ALOG-bound regions allowed to identify a 7-bp YACTGTW (Y=T/C, W=A/T) motif for all the tested ALOG proteins (Figure 1B and S1). Several positions of this motif display a high information content, strongly suggesting specific contacts between ALOG residues and DNA bases at these positions.

The Position Weight Matrix (PWM) corresponding to this motif reliably predicted ALOG protein binding (Figure 1C and S1). The motif did not show any symmetry, suggesting binding by an ALOG monomer. Analysis of spacing between ALOG binding sites in bound genomic regions did not reveal any common distance enrichment, corroborating the hypothesis of binding by an ALOG monomer (Figure S2). Some ALOG proteins may bind two sites with a specific spacing, but this feature is not conserved and might be protein-specific.

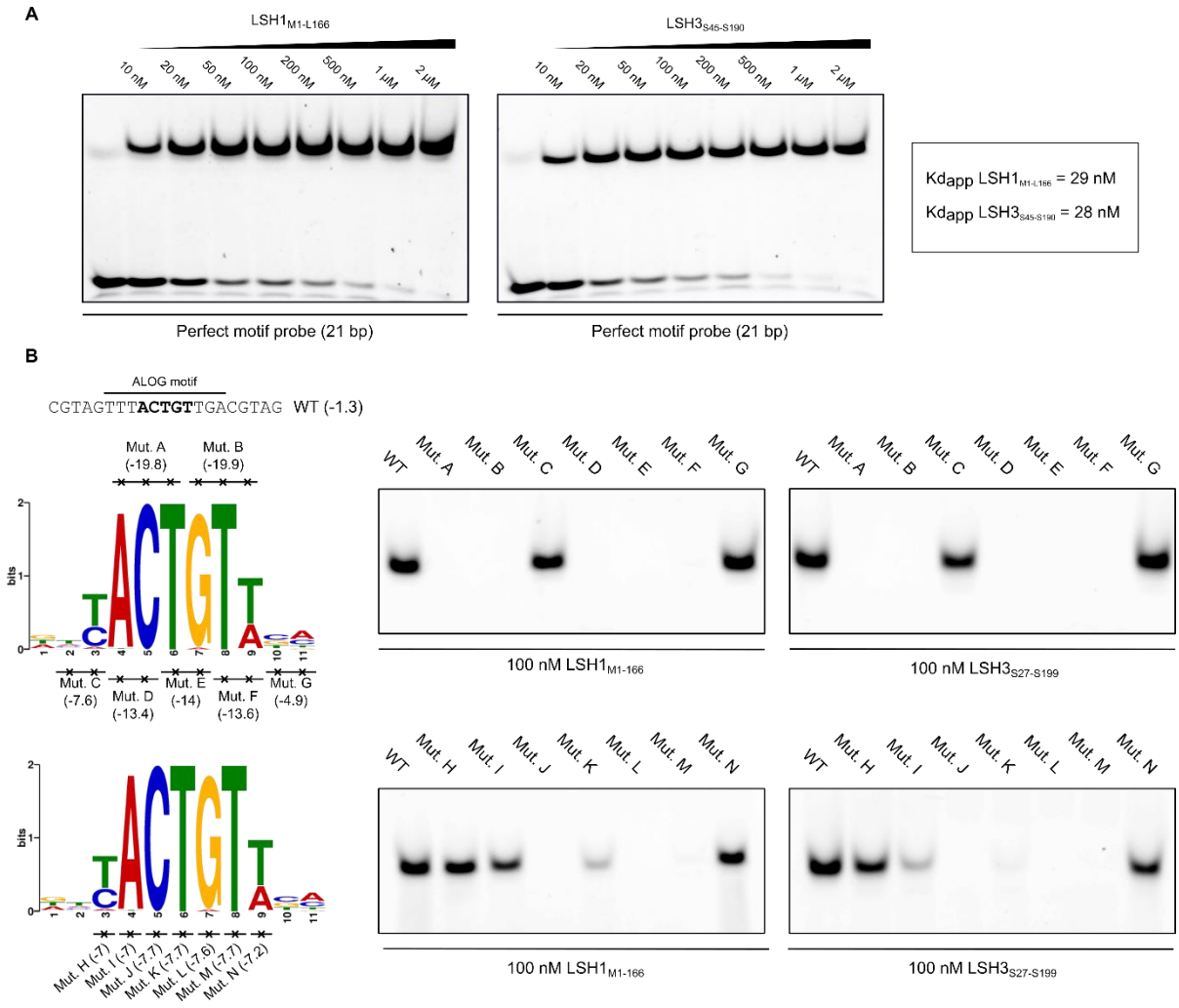

Figure 2. Interaction between the YACTGTW sequence and ALOG proteins in EMSA. (**A**) EMSA with ALOG highest score sequence DNA probe and indicated proteins (left). $LSH1_{M1\text{-}L166}$ and $LSH3_{S45\text{-}S190}$ are truncated versions comprising indicated residues. The apparent Kd was calculated for $LSH1_{M1\text{-}L166}$ and $LSH3_{S45\text{-}S190}$ based on the analysis of 3 independent EMSAs (right). (**B**) EMSA with $LSH1_{M1\text{-}L166}$, $LSH3_{S27\text{-}S199}$ and indicated DNA probes. The same WT probe (top left) was mutated at precise positions as indicated next to the LSH3 logos (bottom left). Scores between brackets were obtained by scanning each DNA probe sequence with the LSH3 PWM. EMSA with described DNA probes (right). Each DNA probe was mixed with the same protein.

The YACTGTW sequence is bound by ALOG proteins with a high affinity and specificity *in vitro*.

We then tested whether the motif identified in ampDAP-seq could be validated using Electrophoretic Mobility Shift Assay (EMSA). First, we found that *in vitro*-produced FL proteins and truncated recombinant versions comprising only the ALOG domain behaved similarly

(Figure S3A), showing that the binding specificity is fully conferred by the ALOG domain and not impacted by the N- and C-terminal disordered regions. For this reason, we then characterized ALOG biochemical properties using their isolated DBDs.

We used a DNA probe of optimal affinity according to LSH3 PWM (Figure 2A). We observed a single shifted band with LSH1 or LSH3 DBDs, indicative of a single protein-DNA complex. Based on EMSAs, we estimated the apparent Kd for LSH1 and LSH3 DBDs to be below 50 nM, a rather high affinity for TF/DNA.

By systematically mutating bases of the motif (Figure 2B), we found that, overall, mutations at the highly-informative positions of the motif strongly reduced binding of LSH1 and LSH3 DBDs. Thus, the YACTGTW motif identified by ampDAP-seq is validated as the sequence bound by ALOG proteins.

It had been previously shown that ALOG homodimerize in Yeast-Two-Hybrid (Y2H; Xu 2016; Peng 2017). Because our ampDAP-seq experiment revealed little signs of homodimerization on DNA, we wanted to test homodimerization using an independent method. Thus, we performed co-immunoprecipitation (co-IP). In our co-IP conditions (the same as ampDAP-seq ones), we did not observe any self-interaction between ALOGs (Figure S3B). We also performed EMSA by mixing two LSH3 versions of different molecular weights. We observed the same complex as those obtained with single proteins and no intermediate band corresponding to an LSH3 heterodimer (Figure S3C). Thus, we concluded that ALOG proteins bind the YACTGTW motif as monomers.

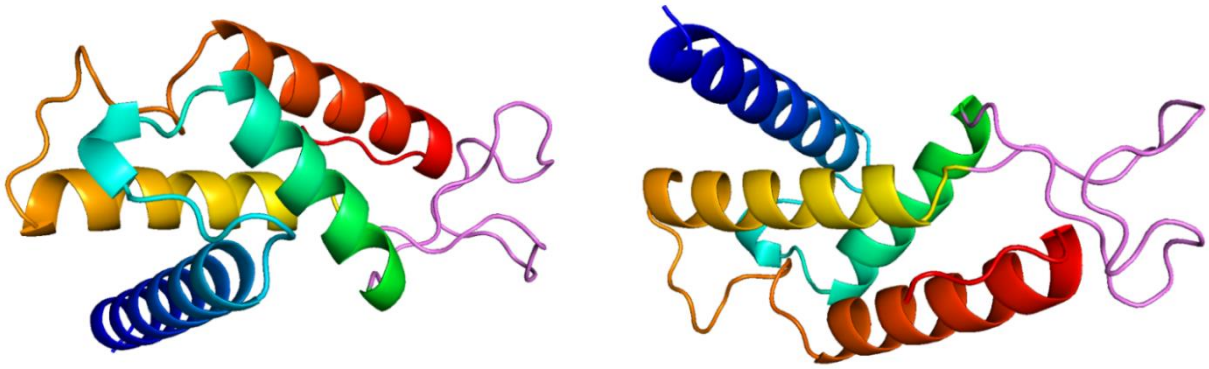

Figure 3. Structure of LSH3 DBD. A 180° rotation along the x-axis was applied to obtain the second picture. Helices are individually colored: helix 1 (blue), helix 2 (green), helix 3 (yellow) and helix 4 (red). Residues of the zinc ribbon are represented in pink.

We aimed at gaining structural insights on the ALOG DBD. For this, we first mapped the minimal domain binding DNA (Figure S4A). This experiment revealed that deleting the conserved putative NLS (comprising a stretch of basic amino acids) abolished DNA binding. We also found that some additives affected the binding affinity *in vitro* (Figure S4B). In particular, we found that Zn^{2+} strongly reduced LSH3 binding when present at high concentration (Figure S4C). Inversely, the polyamine spermidine slightly facilitated LSH3 binding (Figure S4D).

We then performed crystallization tests with a LSH3 DBD ($LSH3_{S45\text{-}S190}$). For this, the purified DBD and the DNA probe corresponding to the high-affinity sequence described before were directly mixed. We obtained crystals that allowed to solve the structure of the protein alone without DNA at 3.2 Å resolution (Figure 3).

The structure revealed the spatial arrangement of the 4 helices of the ALOG domain. Some density was also clearly visible between the histidine and cysteine residues of the zinc ribbon, revealing the presence of a Zn^{2+} ion (not shown).

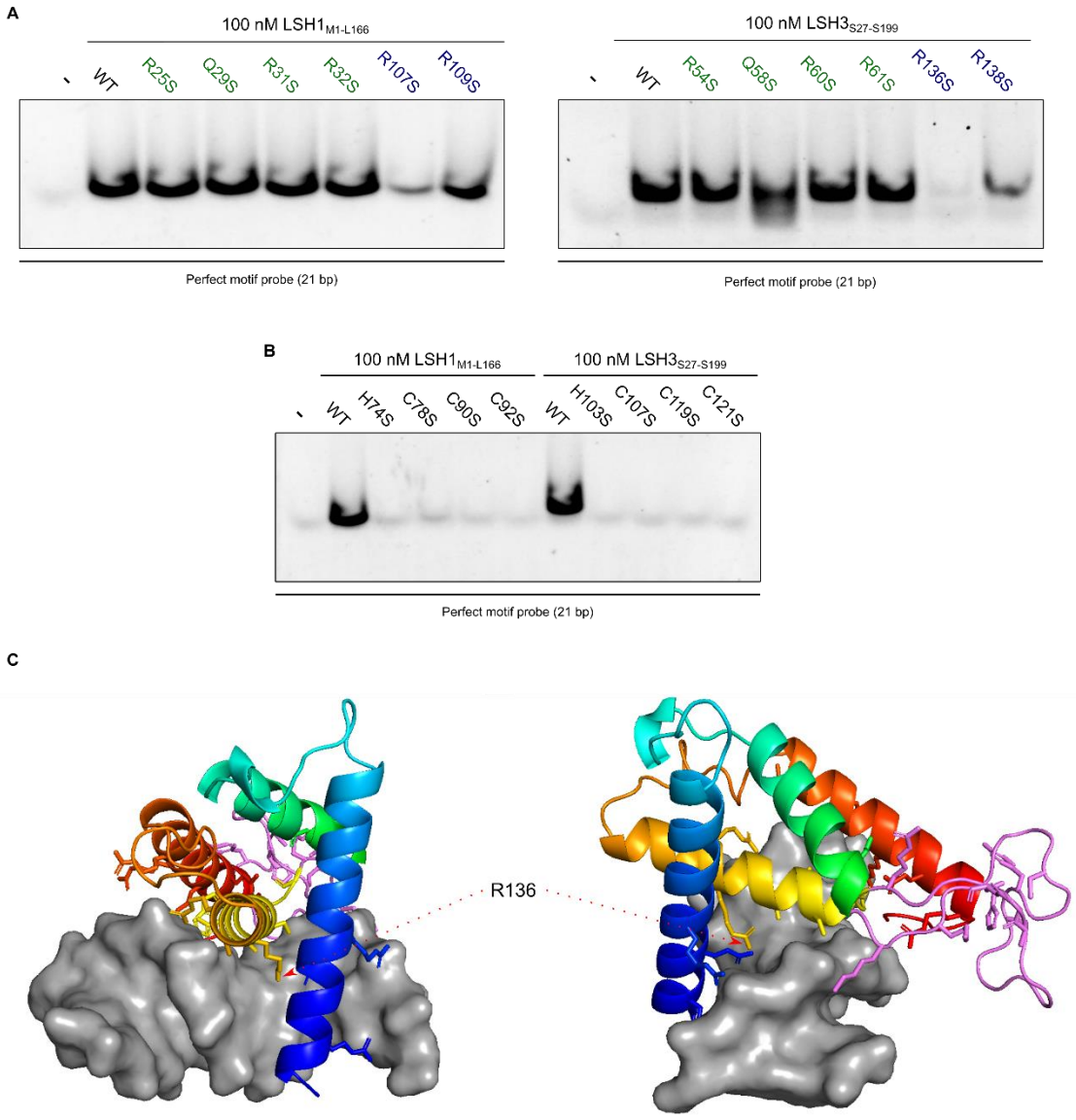

Figure 4. Determination of LSH3 key residues for DNA binding. (A) EMSA with indicated proteins and DNA probes. Mutations highlighted in green and blue are located in helices 1 and 3, respectively. (**B**) Same as in (A) except that mutations affect residues of the zinc ribbon coordinating the Zn^{2+} ion. (**C**) Model for LSH3 binding to DNA. Same colors as in Figure 3, DNA is in grey. The R136 residue is indicated with red arrows

Identification of LSH3 key residues for DNA binding suggests an original binding mechanism

Based on the structure comparison with the DBD of recombinases in complex with DNA, it was proposed that major DNA-contacting residues would be located on helices 1 and 3 (Iyer and Aravind, 2012). To test this assumption, we mutated several residues from helices 1 and 3 and

we evaluated the effect of such mutations in EMSA. We found that none of the mutations in residues from helix 1 impaired DNA binding (Figure 4A).

However, some residues from helix 3 were required for DNA binding as mutating them strongly reduced DNA binding (notably LSH3 R136, Figure 4A). Thus, the mechanism for ALOG binding to DNA is somewhat different from what is predicted based on the comparison with the DBD of recombinases.

The main difference of the ALOG domain compared to the DBD of bacterial recombinase is the insertion of a zinc ribbon between helices 2 and 3. We thus wanted to understand its role for DNA binding. For this, we mutated the canonical cysteine and histidine residues of the zinc ribbon. We found that all the mutated versions of LSH1 and LSH3 DBDs completely lost their ability to bind their cognate DNA in EMSA (Figure 4B) suggesting that the zinc ribbon either directly contacts DNA or, more likely, is key for the positioning of the DNA-binding helices.

Finally, we proposed a model for LSH3 DNA-binding mechanism (Figure 4C). This model was initially built based on the alignment of LSH3 DBD with the DBD of a recombinase in complex with DNA (Ghosh et al., 2007). Based on EMSA results, the LSH3 DBD was then positioned so that major contacts with DNA bases imply residues from helix 3, notably R136. In this model, helix 3 dives into the DNA major groove while residues from helix 1 are mainly engaged in interactions with the DNA phosphate backbone. It appears from this model that other residues from helix 4 could engage contacts with DNA. This model, even if incomplete, could be used to pinpoint LSH3 residues involved in DNA binding.

Discussion

ALOG proteins play key developmental roles in multiple plants ranging from bryophytes to flowering plants. They were proposed to act as transcription factors but their molecular properties were poorly characterized. In this study, we determined the DNA binding specificity of ALOG proteins. We found that the bound motif is the same for ALOG proteins from evolutionary distant organisms, showing that a strong selective pressure was applied on this feature over several hundred million years. In particular, the two insertions within the rice G1 protein sequence did not change DNA binding specificity. Even if the identified motif is similar

for all tested ALOG proteins, it has been shown in Marchantia that LOS1 and LOS2 have different functions (Naramoto et al., 2020). Moreover, G1 and TAW1 cannot complement a *los1* mutant while LOS1 can complement a rice *g1* mutant (Naramoto et al., 2020). Thus, other features than the DNA binding specificity explain the properties of ALOG proteins *in vivo*.

A characteristic of ALOG proteins that is likely crucial for their function *in vivo* is their ability to undergo phase separation, reported for tomato ALOG proteins (Huang et al., 2021, 2022). This property was shown to be dependent on the redox conditions and intrinsic ALOG properties, notably their disordered regions and their ability to form inter-molecular disulfide bonds. The different tomato ALOG homologs were recently shown to have distinct phase separation and transcriptional regulation capabilities (Huang et al., 2022). This could explain the differences of *in vivo* activity between ALOG proteins mentioned before.

In our case, all our experiments were performed in reducing conditions, and we never observed phase separation for LSH1 or LSH3 DBDs. It was previously proposed that cysteine residues of the zinc ribbon were required for the formation of TMF inter-molecular disulfide bonds (Huang et al., 2021). However, based on our structure, we think that the phenotype induced by the mutation of TMF cysteines is rather due to a disruption of the zinc ribbon. Hence, we propose that the ability to undergo phase separation is not conferred by the ALOG domain and not required for DNA binding. Further work is required to understand the role of disordered regions and the biochemical properties they confer to each ALOG proteins.

In this study, we investigated the structural basis of ALOG DNA binding. LSH3 DBD structure revealed that the zinc ribbon indeed coordinates a Zn^{2+} ion. Based on our biochemical assays, it appears that the zinc ribbon is key for the DNA binding properties of ALOG proteins. The insertion of the zinc ribbon during evolution likely conferred new properties to ALOG proteins compared to the DBD of recombinases from where they originate. The insertion of the zinc ribbon could have resulted in a change in the DNA binding mechanism (and the DNA binding specificity) through the modification of the arrangement of helices. In agreement with this point, we found that key LSH3 DBD residues for DNA binding are located on helix 3 (like R136) and not helix 1 as previously proposed. Obtaining the structure of the ALOG domain in complex with DNA will be valuable to decipher the exact binding mechanism.

The determination of the ALOG motif will allow to identify *cis*-elements in the regulatory sequence of target genes, notably those previously proposed like the rice *SHORT VEGETATIVE PHASE* (*SVP*) gene subfamily (Yoshida et al., 2013). ampDAP-seq data will also be valuable to compare with ChIP-seq data once they will be available. It will help to know if ALOG binding is more complex *in vivo*, with the presence of specific a spacing between BS for example. Finally, another question to answer is the link between ALOG proteins and their interactants. The genetic and/or physical interaction of ALOG proteins with BLADE ON PETIOLE (BOP) homologs was reported in tomato and pea (He et al., 2020; Xu et al., 2016) but the molecular significance of this interaction remains to be understood.

Acknowledgments

We thank Miguel Blazquez for *Marchantia polymorpha* gDNA and advices, Michel Hernould for *Solanum lycopersicum* gDNA and Veronica Gregis for rice gDNA.

Author contributions

FP and PR designed the project. PR performed the biochemical experiments helped by ET and RD. JL performed the bioinformatics analyses. CZ, MN and MZ performed the crystallization tests and analyzed the data, RD proposed the DBD/DNA model. PR assembled the figures. PR and FP wrote the paper.

Supplementary Information

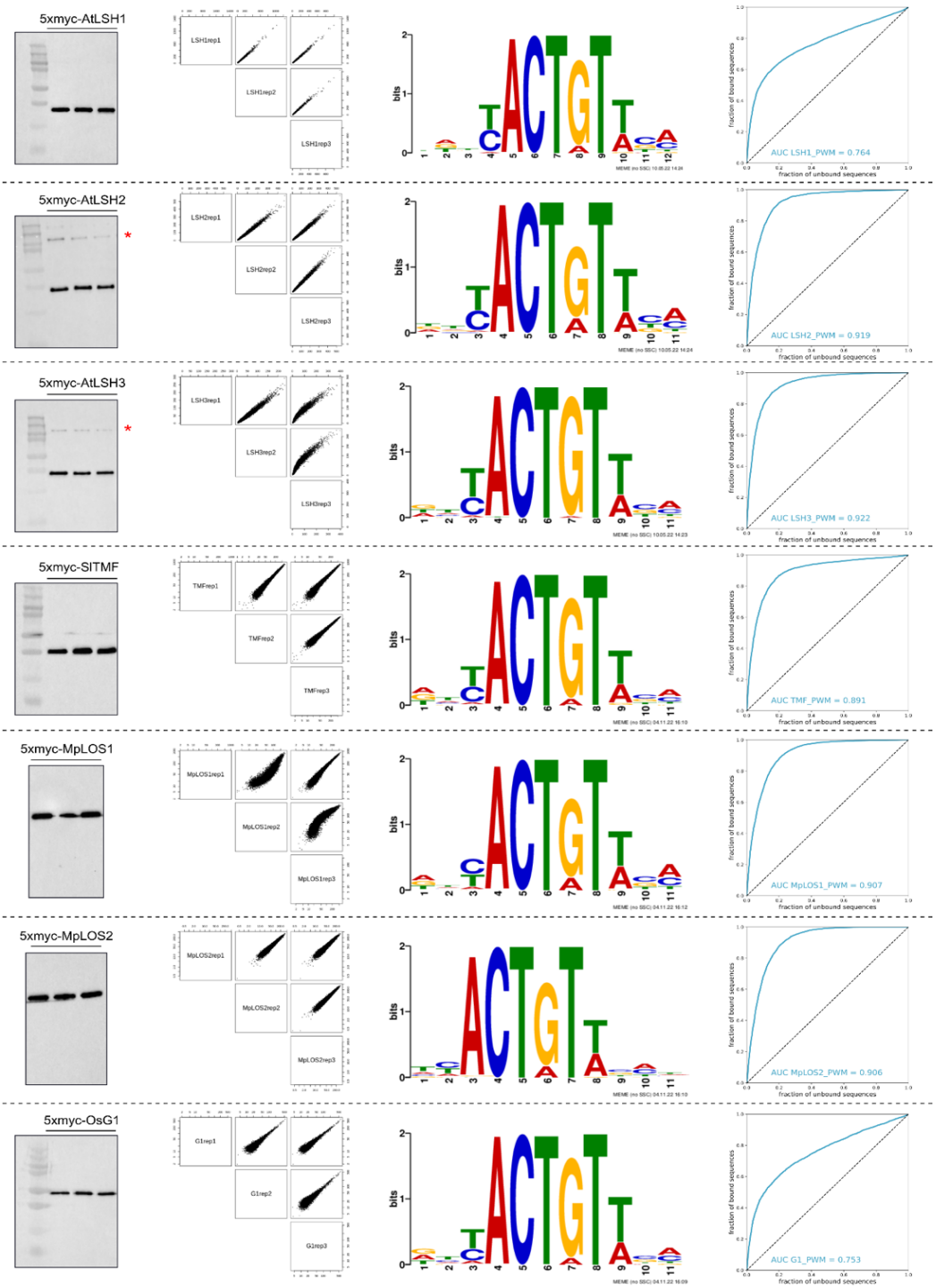

Figure S1. AmpDAP-seq results for all tested ALOG proteins. Each line summarizes the data for one protein. Western Blots (WB) performed after DNA elution during ampDAP-seq experiment are shown in the first column (20 µL of 1X SDS-PAGE Protein Sample Buffer was added to the remaining beads to run WB). Each lane represents one replicate. WB revealed with an anti-myc antibody. Red stars indicate probable contaminants. The second column shows the experimental reproducibility of ampDAP-seq experiments through the comparison of replicate datasets 2 by 2. The motif generated using the 600 peaks with the strongest ampDAP-seq signal is reported in the third column. The last column represents the ROC curve using all peaks except those used to build the logo, and AUC is indicated.

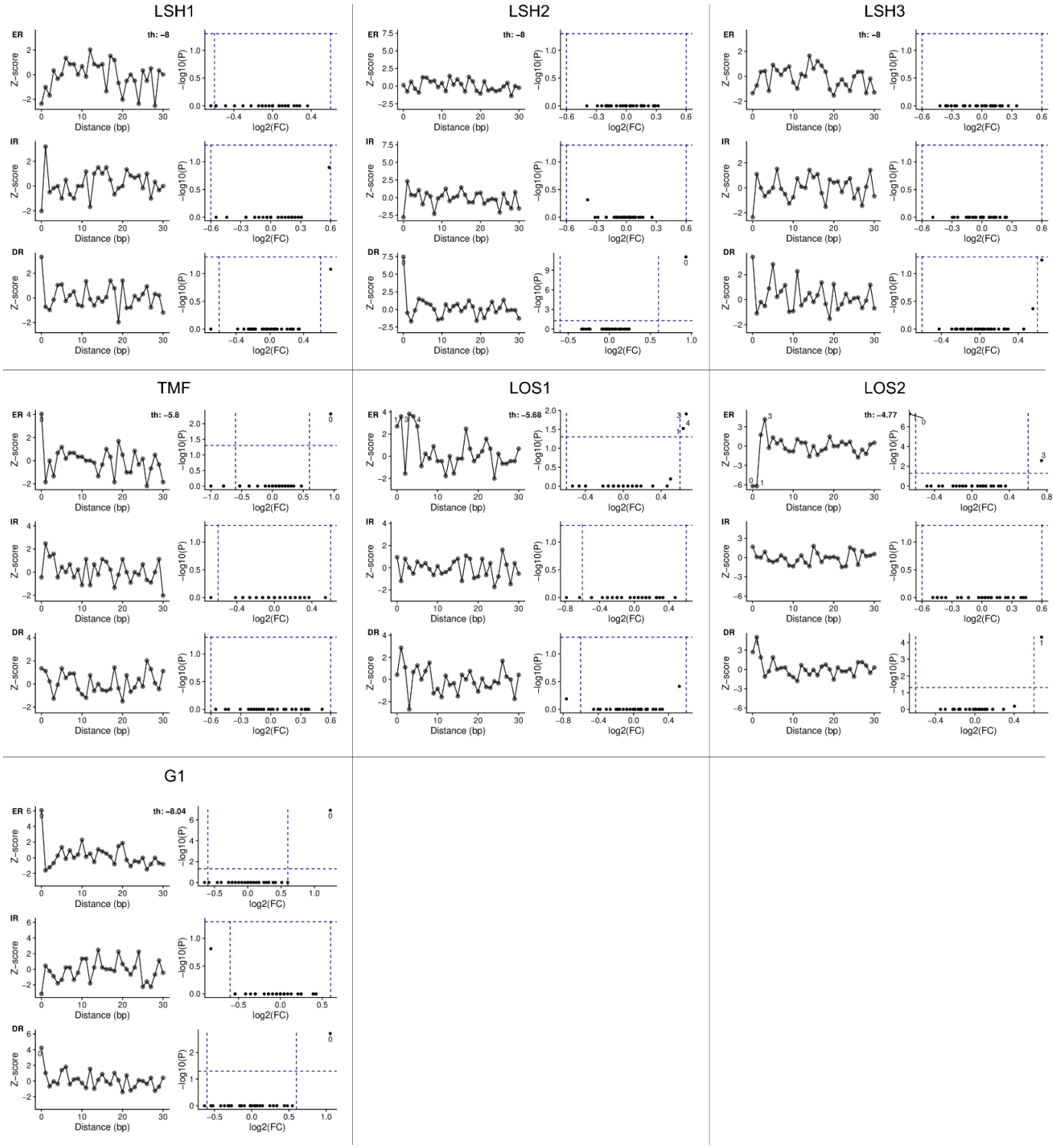

Figure S2. Distribution of spacings between ALOG Binding Sites (BS) using PWM models. ER = Everted Repeat, IR = Inverted Repeat, DR = Direct Repeat. For each bound regions, the analysis was performed on all detected peaks with sites selected as those with a calculated BS score above the threshold ("th"). The used PWM is the one generated for each protein and tested with a ROC. For each protein, the left graphs represent the Z-score as a function of the distance between sites oriented with a given conformation (ER, IR or DR; Ho Sui et al., 2005). The Z-score restitutes the enrichment for each spacing between BS. The right graphs show the enrichment of each spacing (FC = Fold Change) and its associated p-value. Blue dotted lines

represent the significance thresholds. We considered a conformation as truly enriched for a TF when both significance thresholds were reached. Some proteins show a clear spacing preference like ER_0 for TMF and G1 and DR_0 for LSH2. However, these spacings are not found for other ALOG proteins and likely do not represent a general feature of the ALOG domain. These properties might be specific to each protein and should be further tested individually. Moreover, it has to be noted that the Arabidopsis genome used in ampDAP-seq is not perfectly adapted for the study of ALOG proteins other than LSHs.

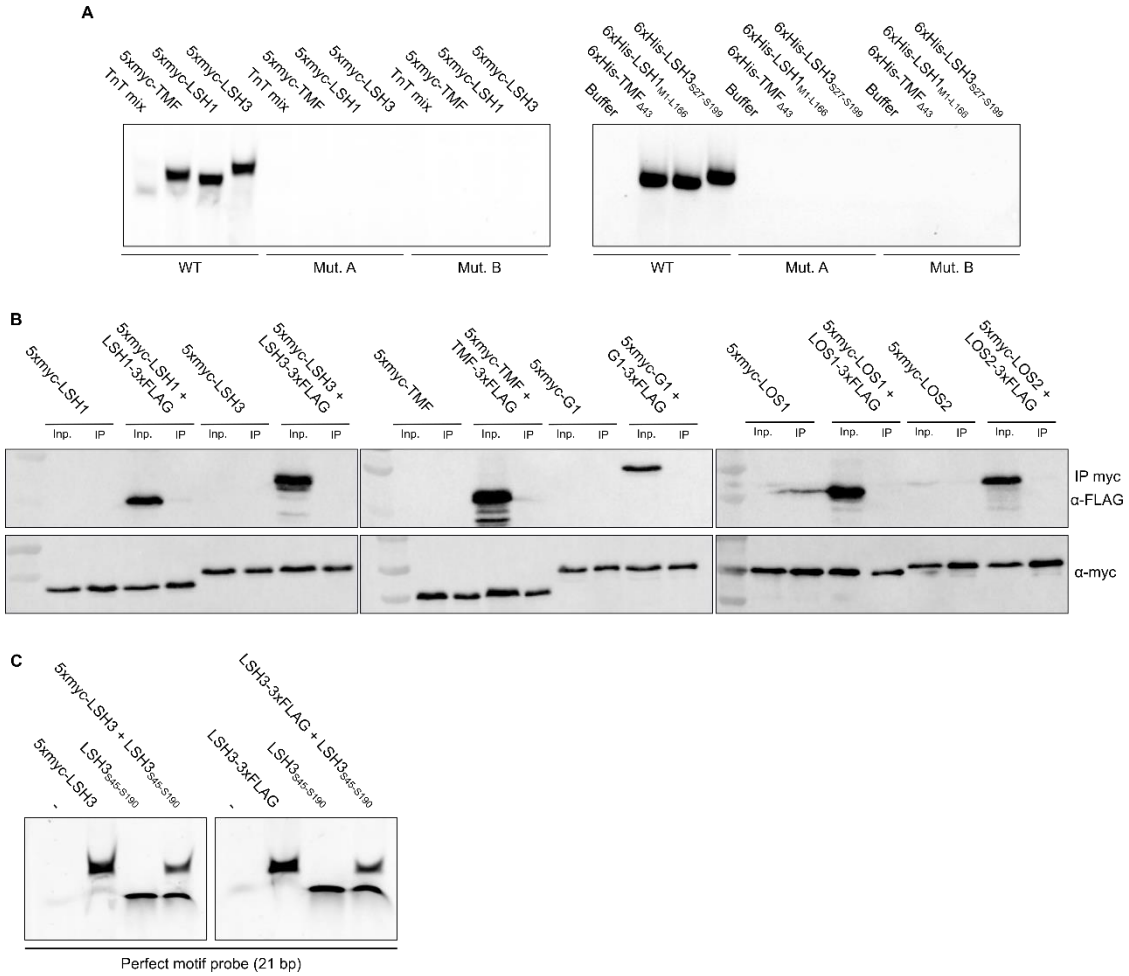

Figure S3. (**A**) EMSA with indicated proteins and DNA probes. The different probes are described in Figure 2B. 5xmyc-tagged proteins are FL and were *in vitro*-produced while 6xHis-tagged proteins are recombinant and comprise only the ALOG domain. $TMF_{\Delta 43}$ corresponds to a TMF truncated versions lacking the first 43 aa. (**B**) co-IP with indicated *in vitro*-produced proteins. (**C**) EMSA with indicated proteins and DNA probes. 5xmyc-LSH3 and LSH3-3xFLAG are *in vitro*-produced FL versions while $LSH3_{S45\text{-}S190}$ is recombinant. When two LSH3 versions were mixed, the amount of each protein was half the amount used for reactions with the protein alone. Note that no LSH3 heterodimer is observed.

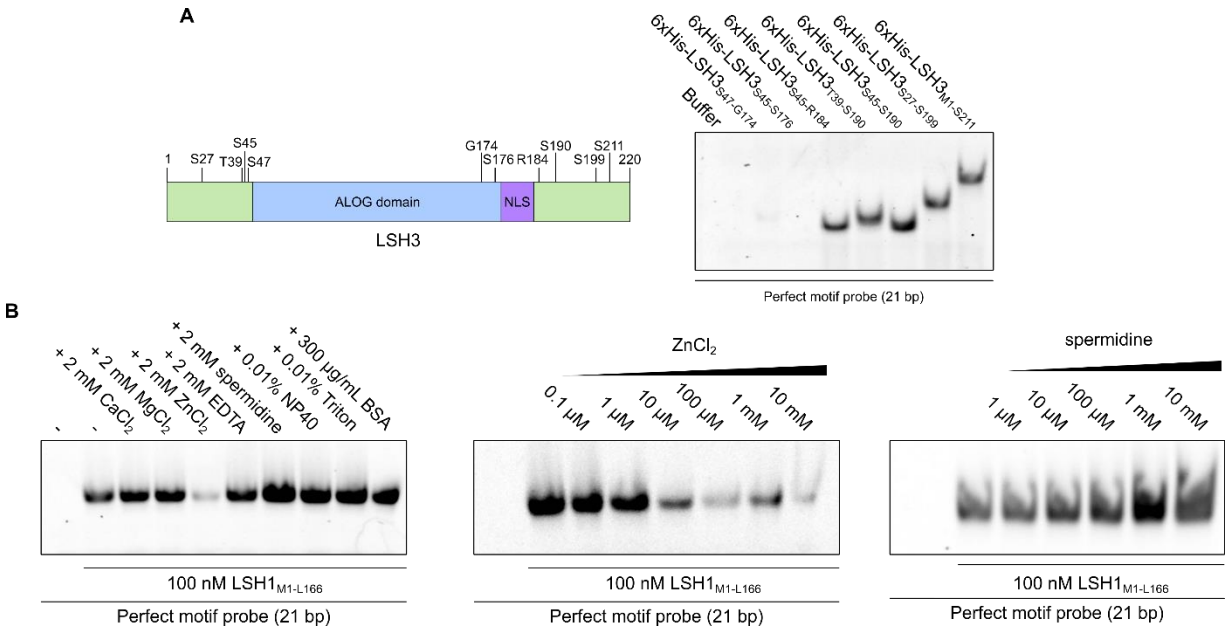

Figure S4. Preliminary tests for crystallographic assays. (A) Determination of the minimal LSH3 truncated version to observe DNA binding. Schematic of LSH3 with relevant residues (left). Drawing is not at scale. EMSA with indicated truncated versions (right). Proteins concentration was 100 nM. Each protein was mixed with the same DNA-containing solution. (**B**) Effect of several additives on LSH3 DNA binding *in vitro*. Buffer B (see Methods) was supplemented with indicated compounds (left). $ZnCl_2$ (middle) and spermidine (right) were further studied with a concentration range.

Material and Methods

Cloning. All genes were amplified from gDNA with a Phusion high fidelity polymerase (NEB) or a platinum SuperFi II polymerase (ThermoFisher) when the GC content was over 70%. All cloning were performed by Gibson Assembly and clones were checked by Sanger sequencing. Mutations were introduced by Gibson Assembly.

ampDAP-seq. All coding sequences were cloned in the pTNT-5xmyc vector (Lai et al., 2021). We used the ampDAP-seq libraries described in Lai et al. (Lai et al., 2021). ampDAP-seq experiments were performed in triplicates following a previously-described protocol (Bartlett et al., 2017).

ALOG recombinant protein production and purification from bacteria. All genes were cloned in the pETM11 vector containing an N-terminal 6xHis tag and a TEV cleavage site (Dummler 2005). Plasmids were transformed in *E. coli* Rosetta2 (DE3) cells (Novagen). Bacteria were grown in LB medium at 37 °C up to an OD_{600nm} of 0.6. Cells were then shifted to 20 °C and 0.4 mM isopropyl b-D-1-thiogalactopyranoside (IPTG) was added. After a 3 h incubation at 20 °C, cells were collected by centrifugation and sonicated in Buffer 1 (25 mM Tris pH8, 600 mM

NaCl, 1 mM TCEP) supplemented with one EDTA-free Pierce Protease Inhibitor Tablets (ThermoFisher). Lysed cells were then centrifuged for 30 min at 15000 rpm. Supernatant was mixed with Ni Sepharose High Performance resin (Cytiva) previously equilibrated with Buffer 1. Resin was washed with Buffer 1 containing 35 mM imidazole and bound proteins were eluted with Buffer 1 containing 300 mM imidazole. Eluted proteins were mixed with TEV protease (0.01% w/w) and dialyzed overnight at 4 °C against Buffer 1.

The following day, elution was loaded again on Ni Sepharose High Performance resins (Cytiva) to remove tags and contaminants. Contaminant DNA was removed by passing proteins on Q Sepharose High Performance resin (Cytiva) pre-equilibrated with Buffer 1. DNA-free proteins (260/280 ratio below 0.6) were recovered in the flow-through and further purified by Size Exclusion Chromatography (SEC) with Superdex 200 Increase 10/300 GL column (Cytiva) equilibrated with Buffer 2 (25 mM Tris pH8, 150 mM NaCl, 1 mM TCEP).

EMSA. Complementary oligos were annealed overnight in annealing buffer (10 mM Tris pH 7.5, 150 mM NaCl and 1 mM EDTA). We used either TAMRA-labeled oligos (Macrogen) or complementary oligos with an overhanging G that we labelled with Cy5-dCTP. For this, 4 pmol of double-stranded DNA was labeled with 1 unit of Klenow fragment polymerase (NEB) and 8 pmol Cy5-dCTP (Cytiva) in Klenow buffer during 1 h at 37 °C. Enzymatic reaction was then stopped with a 10-min incubation at 65 °C. The type of oligo used in each experiment (Cy5 or TAMRA labelled) is indicated in each figure legend.

Binding reactions were performed in 20 µL with different binding buffers as indicated in each figure legend. We used mainly buffer A (10 mM HEPES pH 7.5, 300 µg/mL BSA, 140 ng/µL fish sperm DNA (Sigma-Aldrich), 100 µM spermidine, 0.25 % CHAPS, 1.5 mM TCEP, 0.8 % glycerol) and buffer B (25 mM Tris pH 8, 150 mM NaCl, 1 mM TCEP, 140 ng/µL fish sperm DNA, 0.8 % glycerol) when indicated in the figure legend. Different additives were also used as indicated in each figure legend. Proteins were added at indicated concentrations. Binding reactions were incubated for 20 min on ice and then loaded on a 6 % native polyacrylamide gel. Gels were electrophoresed at 90 V for 75 min at 4 °C and revealed with an Amersham ImageQuant 800 imager (Cytiva).

Estimations of Kd was based on the quantifications of binding experiments from Figure 2A and 2 other independent EMSAs for each protein. Kd were estimated with Kaleidagraph using a Michaelis-Menten model.

co-IP. Myc- and FLAG-tagged versions of the different ALOG proteins were produced by TnT (Promega). 25 µL of TnT reactions producing indicated proteins were mixed with Buffer 1 to reach 150 µL and rotated at 4 °C during 1 h. 10 µL of pre-washed anti-myc beads were then added and incubated with the proteins for 1 h at 4 °C on a rotating wheel. Beads were then washed 4 times with Buffer 1. 1X protein Blue was then added to the beads, and beads were boiled for 5 min at 95 °C. Western Blots were then performed and revealed with HRP-conjugated anti-myc and anti-FLAG antibodies.

Crystallization. For crystallization, LSH was purified as described above except that SEC was performed in Buffer 2 supplemented with 1 mM spermidine (Alfa Aesar). Protein was then concentrated to 5.3 mg/mL. Complementary HPLC-purified oligos were resuspended to 10 mM in 1X annealing buffer (25 mM Tris pH8, 150 mM NaCl) and annealed. Protein and DNA duplexes were mixed in a molar ratio of 1.1:1.

References

Bartlett, A., O'Malley, R.C., Huang, S.S.C., Galli, M., Nery, J.R., Gallavotti, A., and Ecker, J.R. (2017). Mapping genome-wide transcription-factor binding sites using DAP-seq. Nat. Protoc. *12*, 1659–1672. https://doi.org/10.1038/nprot.2017.055.

Cho, E., and Zambryski, P.C. (2011). *ORGAN BOUNDARY1* defines a gene expressed at the junction between the shoot apical meristem and lateral organs. Proc. Natl. Acad. Sci. U. S. A. *108*, 2154–2159. https://doi.org/10.1073/pnas.1018542108.

Ghosh, K., Guo, F., and Van Duyne, G.D. (2007). Synapsis of loxP Sites by Cre Recombinase. J. Biol. Chem. 282, 24004–24016. https://doi.org/10.1074/JBC.M703283200.

He, L., Lei, Y., Li, X., Peng, Q., Liu, W., Jiao, K., Su, S., Hu, Z., Shen, Z., and Luo, D. (2020). *SYMMETRIC PETALS 1* Encodes an ALOG Domain Protein that Controls Floral Organ Internal Asymmetry in Pea (*Pisum sativum L.*). Int. J. Mol. Sci. *21*, 4060. https://doi.org/10.3390/ijms21114060.

Ho Sui, S.J. (2005). oPOSSUM: identification of over-represented transcription factor binding sites in co-expressed genes. Nucleic Acids Res. *33*, 3154–3164. https://doi.org/10.1093/nar/gki624.

Huang, X., Chen, S., Li, W., Tang, L., Zhang, Y., Yang, N., Zou, Y., Zhai, X., Xiao, N., Liu, W., et al. (2021). ROS regulated reversible protein phase separation synchronizes plant flowering. Nat. Chem. Biol. *17*, 549–557. https://doi.org/10.1038/s41589-021-00739-0.

Huang, X., Xiao, N., Zou, Y., Xie, Y., Tang, L., Zhang, Y., Yu, Y., Li, Y., and Xu, C. (2022). Heterotypic transcriptional condensates formed by prion-like paralogous proteins canalize flowering transition in tomato. Genome Biol. *23*, 1–21. https://doi.org/10.1186/s13059-022-02646-6.

Iyer, L.M., and Aravind, L. (2012). ALOG domains: provenance of plant homeotic and developmental regulators from the DNA-binding domain of a novel class of DIRS1-type retroposons. Biol. Direct *7*, 39. https://doi.org/10.1186/1745-6150-7-39.

Lai, X., Blanc-Mathieu, R., GrandVuillemin, L., Huang, Y., Stigliani, A., Lucas, J., Thévenon, E., Loue-Manifel, J., Turchi, L., Daher, H., et al. (2021). The LEAFY floral regulator displays pioneer transcription factor properties. Mol. Plant *14*, 829–837. https://doi.org/10.1016/J.MOLP.2021.03.004.

Li, X., Sun, L., Tan, L., Liu, F., Zhu, Z., Fu, Y., Sun, X., Sun, X., Xie, D., and Sun, C. (2012). *TH1*, a DUF640 domain-like gene controls lemma and palea development in rice. Plant Mol. Biol. *78*, 351–359. https://doi.org/10.1007/s11103-011-9868-8.

MacAlister, C.A., Park, S.J., Jiang, K., Marcel, F., Bendahmane, A., Izkovich, Y., Eshed, Y., and Lippman, Z.B. (2012). Synchronization of the flowering transition by the tomato terminating flower gene. Nat. Genet. *44*, 1393–1398. https://doi.org/10.1038/ng.2465.

Naramoto, S., Jones, V.A.S., Trozzi, N., Sato, M., Toyooka, K., Shimamura, M., Ishida, S., Nishitani, K., Ishizaki, K., Nishihama, R., et al. (2019). A conserved regulatory mechanism mediates the convergent evolution of plant shoot lateral organs. PLOS Biol. *17*, e3000560. https://doi.org/10.1371/journal.pbio.3000560.

Naramoto, S., Hata, Y., and Kyozuka, J. (2020). The origin and evolution of the ALOG proteins, members of a plant-specific transcription factor family, in land plants. J. Plant Res. *133*, 323–329.

https://doi.org/10.1007/s10265-020-01171-6.

Peng, P., Liu, L., Fang, J., Zhao, J., Yuan, S., and Li, X. (2017). The rice TRIANGULAR HULL1 protein acts as a transcriptional repressor in regulating lateral development of spikelet. Sci. Rep. *7*, 13712. https://doi.org/10.1038/s41598-017-14146-w.

Riechmann, J.L., Heard, J., Martin, G., Reuber, L., Jiang, C.-Z., Keddie, J., Adam, L., Pineda, O., Ratcliffe, O.J., Samaha, R.R., et al. (2000). Arabidopsis Transcription Factors: Genome-Wide Comparative Analysis Among Eukaryotes. Science *290*, 2105–2110. https://doi.org/10.1126/science.290.5499.2105.

Takeda, S., Hanano, K., Kariya, A., Shimizu, S., Zhao, L., Matsui, M., Tasaka, M., and Aida, M. (2011). CUP-SHAPED COTYLEDON1 transcription factor activates the expression of *LSH4* and *LSH3*, two members of the ALOG gene family, in shoot organ boundary cells. Plant J. *66*, 1066–1077. https://doi.org/10.1111/j.1365-313X.2011.04571.x.

Xu, C., Park, S.J., Van Eck, J., and Lippman, Z.B. (2016). Control of inflorescence architecture in tomato by BTB/POZ transcriptional regulators. Genes Dev. *30*, 2048–2061. https://doi.org/10.1101/gad.288415.116.

Yoshida, A., Suzaki, T., Tanaka, W., and Hirano, H.Y. (2009). The homeotic gene long sterile lemma (*G1*) specifies sterile lemma identity in the rice spikelet. Proc. Natl. Acad. Sci. U. S. A. *106*, 20103–20108. https://doi.org/10.1073/pnas.0907896106.

Yoshida, A., Sasao, M., Yasuno, N., Takagi, K., Daimon, Y., Chen, R., Yamazaki, R., Tokunaga, H., Kitaguchi, Y., Sato, Y., et al. (2013). *TAWAWA1*, a regulator of rice inflorescence architecture, functions through the suppression of meristem phase transition. Proc. Natl. Acad. Sci. U. S. A. *110*, 767–772. https://doi.org/10.1073/pnas.1216151110.

Zhao, L., Nakazawa, M., Takase, T., Manabe, K., Kobayashi, M., Seki, M., Shinozaki, K., and Matsui, M. (2004). Overexpression of *LSH1*, a member of an uncharacterised gene family, causes enhanced light regulation of seedling development. Plant J. *37*, 694–706. https://doi.org/10.1111/J.1365-313X.2003.01993.X.

DISCUSSION

I. Several possible approaches to better understand the LFY-UFO synergy

Mechanistic approach: describing the LFY-UFO complex in details

In Article 1, we have described the Arabidopsis LFY-UFO complex using a structural approach. It allowed us to understand the role of UFO as a LFY cofactor, notably through its ability to bind both LFY DBD and a precise DNA motif that we called the URM. However, our cryoEM map is incomplete and it will be necessary to repeat this experiment to obtain a model of the complex with sufficient resolution to precisely localize the side chains and their interactions. For this, the ASK1-UFO-LFY-DNA complex could be reconstituted with another DNA molecule of higher affinity or with LFY and UFO homologs from other species.

We also revealed that LFY and UFO activate *pAP3* through its LUBS *cis*-elements. However, we are far from understanding in detail the activation of this promoter. Indeed, the molecular mechanism is likely very complex and may imply elegant mechanisms like promoter looping, interaction between different regulators and on-promoter protein ubiquitination and degradation.

Finally, the role of UFO in ubiquitination pathways remains very fuzzy. Indeed, the model we propose does not totally fit with observations from the literature and the significance of the link between UFO and the SCF complex remains to be determined. This could be tackled by determining which proteins UFO targets for ubiquitination and which F-box proteins acts redundantly with UFO.

Genomic approach: characterizing UFO genome-wide binding

We performed ampDAP-seq with the Arabidopsis LFY-UFO complex and it allowed us to identify the LUBS motif. In Arabidopsis, a future plan will be to perform UFO ChIP-seq to

determine to which loci UFO is associated *in vivo*. LFY ChIP-seq obtained in a WT or a *ufo* mutant background should also reveal to which extent UFO affects LFY binding *in vivo*. For other species than Arabidopsis, performing ampDAP-seq with LFY and UFO homologs could be a good way to know if the complex forms and if the bound motif is the same.

It could also be interesting to cross binding data with transcriptomic data. In fact, the list of UFO-regulated genes is not well characterized in most angiosperm species. For this, RNA-seq could be performed in *ufo* mutants or *UFO* overexpressing lines. The advantage of this approach is that it is less technical than ChIP and that it can be easily be performed in multiple species.

Evolutionary approach: deciphering the history of *UFO*

In Article 2, we focused on angiosperm species because it is the only group for which we have genetic data on the role of *UFO*. However, we speculate that the LFY-UFO complex is active not only in angiosperm species but also in non-flowering plants. An obvious next step is to describe the role of UFO in non-angiosperm species. The function of UFO could be studied in species where the role of LFY has already been documented like ferns (*Ceratopteris richardii*; Plackett 2018) or moss (*Physcomitrium patens*; Tanhashi 2005*)*. One of the difficulties will be to find the right UFO homologs as plant genomes contain hundreds of F-box proteins. Mutating the best candidate genes by CRISPR-Cas9 could allow finding mutants with interesting phenotypes.

Biotechnology approach: making the most of the LFY-UFO synergy

The deep impact of *UFO* on flower development makes it a good candidate gene for breeding and biotechnology. In monocots, the strong effect of *UFO* on panicle architecture is already selected in breeding programs. In species where *UFO* is the main flower determinant like petunia or tomato, monitoring where and when *UFO* is expressed is a way to control flowering time and inflorescence architecture.

In other species like Arabidopsis, *UFO* is not the main flower determinant but the VP16 activated form of UFO has the ability to trigger flowering from leaves when overexpressed (Risseeuw 2013). Designing a system in which LFY and UFO-VP16 would be placed under the control of an inducible promoter could allow to trigger flowering "at will". More generally, this feature could be used in several species to regenerate plants more quickly by decreasing the time to flowering.

II. Deciphering the role of ALOG TFs *in vivo* with obtained biochemical data

The data we obtained on the biochemical characterization of ALOGs are presented in Chapter III. We identified the DNA motif bound by several ALOG proteins, proving their role as TFs. We also performed biochemical and structural analyses to better understand how the ALOG DBD binds DNA.

An obvious follow-up of this study would be to obtain the structure of the ALOG domain in complex with DNA. In the experiment we performed, we directly mixed the LSH3 DBD with DNA but we did not obtain crystals containing the complex. A better alternative would have been to reconstitute the complex in SEC. However, despite several attempts, I never obtained the complex by this method. No shift of elution volume was observed when mixing LSH3 DBD and DNA compared to the experiment with single components. This implies that either the complex cannot form in SEC or that the elution volume of the complex is the same as the one of single molecules. We are now working on optimizing crystallization conditions, notably with other DNAs molecules, to obtain crystals of the complex.

Our study on ALOG TFs is mainly based on *in vitro* results. These data should now be used to understand the role of ALOGs *in vivo.* A first application is the identification of target genes. We are currently doing these analyses in collaboration with the team of Martin Kater and Veronica Gregis at the University of Milan. Several floral targets have been identified and could explain the role of LSH TFs in Arabidopsis.

Another point that could be investigated is the position of ALOG TFs in flower development regulatory networks. We have identified clear LFY binding sites in the promoter of *LSH1*, *2* and

3, but we do not know yet if this regulation is conserved in other species. The ALOG protein TMF was also shown to repress the *UFO* homolog *ANANTHA* in tomato, it could be interesting to investigate if ALOG TFs also repress UFO in other species.

MATERIAL AND METHODS

This section is very short as methods are thoroughly described in Article 1 and Article 3. In both manuscripts, I wrote methods so that it should possible to repeat the main experiments without further reading. In this section, I wrote only the methods for the complementary results presented in Chapter II.

DLRA in Arabidopsis protoplasts

Mutated version of *pAP3* and UFO were obtained by multiple-fragment Gibson Assembly. Primers used to insert mutations are indicated in the following table. *pAP3* and UFO versions with multiple mutations were obtained by performing multiple-fragment Gibson Assembly with fragments containing single mutations. The DLRA in Arabidopsis protoplasts was then performed as described in Article 1.

Plasmid	Backbone vector digestion	Oligos for mutation
pAP3 CarG1$_m$ in pBB174 (pPR170)	EcoRI-XhoI	**oPR341**: AAAAATCAGTTTACATAGATCAAAAATTTATC **oPR342**: GATAAATTTTTGATCTATGTAAACTGATTTTT
pAP3 CarG2$_m$ in pBB174 (pPR171)	EcoRI-XhoI	**oPR343**: TGAACTTAGCTTTCATGCATTAGGCA **oPR344**: TGCCTAATGCATGAAAGCTAAGTTCA
pAP3 CarG3$_m$ in pBB174 (pPR172)	EcoRI-XhoI	**oPR345**: GCAATACTTTGGATTGTTAGTAACTCAA **oPR346**: TTGAGTTACTAACAATCCAAAGTATTGC
UFO K316S in pRT104-3xFLAG (pPR135)	NcoI-SacI	**oPR264**: GCAGCTGTTGAGATCAGCAAGTTGAAC **oPR265**: GTTCAACTTGCTGATCTCAACAGCT
UFO K318S in pRT104-3xFLAG (pPR136)	NcoI-SacI	**oPR266**: GTTGAGAAAAGCTCGTTGAACGTTCCCAA **oPR267**:TTGGGAACGTTCAACGAGCTTTTCTCAAC
UFO R293S in pRT104-3xFLAG (pPR124)	NcoI-SacI	**oPR258**: CAAGCTCCGATGAGCAGATTTCTCAGATCTC **oPR259**: GAGATCTGAGAAATCTGCTCATCGGAGCTTG
UFO R294S in pRT104-3xFLAG (pPR125)	NcoI-SacI	**oPR260**:TCAAGCTCCGATGAGGAGCTTTCTCAGATCTCCA **oPR261**:TGGAGATCTGAGAAAGCTCCTCATCGGAGCTTGA
UFO R297S in pRT104-3xFLAG (pPR126)	NcoI-SacI	**oPR262**: AGGAGATTTCTCAGCTCTCCAAGCTT **oPR263**: AAGCTTGGAGAGCTGAGAAATCTCCT

Plants for LFY and UFO ChIP-seq

The *35S::LFY-GR* plants (Ler ecotype) were described previously (Wagner et al., 1999). Plants containing this transgene were selected on ½ MS plates supplemented with 50 ug/ml kanamycin. *35S::LFY-GR* plants were crossed to the strong *ufo-2* mutant (Ler ecotype; Wilkinson and Haughn, 1995). For *ufo-2* genotyping, a PCR product was amplified from gDNA with oligos oPR579 (GTGAGTTGGGTCTCCGAAGAAGC) and oGT1086 (AGACTCCAGGAAATGGAAGTGT). The PCR product was then digested with the *AflIII* restriction enzyme (new recognition site created by the *ufo-2* mutation; Lee et al., 1997).

Plants for UFO and HWS proximity labelling

The different plasmids were obtained by Gibson Assembly as described in the following table. Plasmids were than transformed in *Agrobacterium tumefaciens* C58C1 pMP90. Arabidopsis Col-0 plants were then transformed using the floral dip method (Clough and Bent, 1998).

Plasmid	pEGAD backbone vector digestion	Oligos for insert amplification
35S::3xHA-TurboID (pPR375)	AgeI-BamHI	**oPR734**: ACACGGGGACTCTAGCGCTAATGTTCCCATATGACGTTCCAG **oPR747**: TCAGTTATCTAGATCCGGTGCTACTTTTCGGCAGACCGCA
35S::3xHA-TurboID-UFO (pPR376)	AgeI-BamHI	**oPR734**+**oPR735** (TurboID-UFO insert) **oPR735**:TCAGTTATCTAGATCCGGTGTCAACAGACTCCAGGAAATGGAAG
35S::3xHA-TurboID-UFOΔFbox (pPR377)	AgeI-BamHI	**oPR734**+**oPR748** (TurboID insert); **oPR749**+**oPR735** (UFOΔFbox insert) **oPR748**: CATtccatggagagcagcaagCTTTTCGGCAGACCGCAGA **oPR749**: GAAAAGcttgctgctctccatggaATGCTACAACTACTTCCTCTCCGACAC
35S::3xHA-TurboID-HWS (pPR378)	AgeI-BamHI	**oPR734**+**oPR736** (TurboID insert); **oPR737**+**oPR738** (HWS insert) **oPR736**: CTGCTTCCATCCATGGCTTTTCGGCAGAC **oPR737**: AAAGCCATGGATGGAAGCAGAAACGTCTTGGA **oPR738**: TCAGTTATCTAGATCCGGTGCTAAGGAGCAATCTCGAGTCTTG
35S::3xHA-TurboID-HWSΔFbox (pPR379)	AgeI-BamHI	**oPR734**+**oPR750** (TurboID insert); **oPR751**+**oPR738** (HWSΔFbox insert) **oPR750**: GGCCTTTGGGACATCCATGGCTTTTCGGCAGACCGCAGA **oPR751**: GGTCTGCCGAAAAGCCATGGATGTCCCAAAGGCCTTGGT

REFERENCES

Adams, J., Kelso, R., and Cooley, L. (2000). The kelch repeat superfamily of proteins: propellers of cell function. Trends Cell Biol. *10*, 17–24. https://doi.org/10.1016/S0962-8924(99)01673-6.

Alvarez-Buylla, E.R., Benítez, M., Corvera-Poiré, A., Chaos Cador, Á., de Folter, S., Gamboa de Buen, A., Garay-Arroyo, A., García-Ponce, B., Jaimes-Miranda, F., Pérez-Ruiz, R. V., et al. (2010). Flower Development. Arab. B. *8*, e0127. https://doi.org/10.1199/tab.0127.

Amasino, R. (2010). Seasonal and developmental timing of flowering. Plant J. *61*, 1001–1013. https://doi.org/10.1111/j.1365-313X.2010.04148.x.

Archer, C.T., Delahodde, A., Gonzalez, F., Johnston, S.A., and Kodadek, T. (2008). Activation Domain-dependent Monoubiquitylation of Gal4 Protein Is Essential for Promoter Binding in Vivo. J. Biol. Chem. *283*, 12614–12623. https://doi.org/10.1074/jbc.M801050200.

Aukerman, M.J., and Sakai, H. (2003). Regulation of flowering time and floral organ identity by a MicroRNA and its *APETALA2*-like target genes. Plant Cell *15*, 2730–2741. https://doi.org/10.1105/TPC.016238.

Benlloch, R., Kim, M.C., Sayou, C., Thévenon, E., Parcy, F., and Nilsson, O. (2011). Integrating long-day flowering signals: A *LEAFY* binding site is essential for proper photoperiodic activation of APETALA1. Plant J. *67*, 1094–1102. https://doi.org/10.1111/j.1365-313X.2011.04660.x.

Branon, T.C., Bosch, J.A., Sanchez, A.D., Udeshi, N.D., Svinkina, T., Carr, S.A., Feldman, J.L., Perrimon, N., and Ting, A.Y. (2018). Efficient proximity labeling in living cells and organisms with TurboID. Nat. Biotechnol. *36*, 880–887. https://doi.org/10.1038/nbt.4201.

Chae, E., Tan, Q.K.-G., Hill, T.A., and Irish, V.F. (2008). An Arabidopsis F-box protein acts as a transcriptional co-factor to regulate floral development. Development *135*, 1235–1245. https://doi.org/10.1242/dev.015842.

Chahtane, H., Vachon, G., Le Masson, M., Thévenon, E., Périgon, S., Mihajlovic, N., Kalinina, A., Michard, R., Moyroud, E., Monniaux, M., et al. (2013). A variant of LEAFY reveals its capacity to stimulate meristem development by inducing *RAX1*. Plant J. *74*, 678–689. https://doi.org/10.1111/tpj.12156.

Chang, B., Partha, S., Hofmann, K., Lei, M., Goebl, M., Harper, J.W., and Elledge, S.J. (1996). SKP1 connects cell cycle regulators to the ubiquitin proteolysis machinery through a novel motif, the F-box. Cell *86*, 263–274. https://doi.org/10.1016/S0092-8674(00)80098-7.

Chini, A., Fonseca, S., Fernández, G., Adie, B., Chico, J.M., Lorenzo, O., García-Casado, G., López-Vidriero, I., Lozano, F.M., Ponce, M.R., et al. (2007). The JAZ family of repressors is the missing link in jasmonate signalling. Nature *448*, 666–671. https://doi.org/10.1038/nature06006.

Cho, E., and Zambryski, P.C. (2011). *ORGAN BOUNDARY1* defines a gene expressed at the junction between the shoot apical meristem and lateral organs. Proc. Natl. Acad. Sci. U. S. A. *108*, 2154–2159. https://doi.org/10.1073/pnas.1018542108.

Clough, S.J., and Bent, A.F. (1998). Floral dip: a simplified method forAgrobacterium-mediated transformation ofArabidopsis thaliana. Plant J. 16, 735–743. https://doi.org/10.1046/j.1365-313x.1998.00343.x.

Cousens, D.J., Greaves, R., Goding, C.R., and O'Hare, P. (1989). The C-terminal 79 amino acids

of the herpes simplex virus regulatory protein, Vmw65, efficiently activate transcription in yeast and mammalian cells in chimeric DNA-binding proteins. EMBO J. *8*, 2337–2342. https://doi.org/10.1002/J.1460-2075.1989.TB08361.X.

Durfee, T., Roe, J.L., Sessions, R.A., Inouye, C., Serikawa, K., Feldmann, K.A., Weigel, D., and Zambryski, P.C. (2003). The F-box-containing protein UFO and AGAMOUS participate in antagonistic pathways governing early petal development in Arabidopsis. Proc. Natl. Acad. Sci. U. S. A. *100*, 8571–8576. https://doi.org/10.1073/pnas.1033043100.

Feke, A., Liu, W., Hong, J., Li, M.W., Lee, C.M., Zhou, E.K., and Gendron, J.M. (2019). Decoys provide a scalable platform for the identification of plant e3 ubiquitin ligases that regulate circadian function. Elife *8*. https://doi.org/10.7554/ELIFE.44558.

Gagne, J.M., Downes, B.P., Shiu, S.H., Durski, A.M., and Vierstra, R.D. (2002). The F-box subunit of the SCF E3 complex is encoded by a diverse superfamily of genes in Arabidopsis. Proc. Natl. Acad. Sci. U. S. A. *99*, 11519–11524. https://doi.org/10.1073/pnas.162339999.

Geng, F., Wenzel, S., and Tansey, W.P. (2012). Ubiquitin and Proteasomes in Transcription. Annu. Rev. Biochem. *81*, 177–201. https://doi.org/10.1146/annurev-biochem-052110-120012.

Goslin, K., Zheng, B., Serrano-Mislata, A., Rae, L., Ryan, P.T., Kwaśniewska, K., Thomson, B., Ó'Maoiléidigh, D.S., Madueño, F., Wellmer, F., et al. (2017). Transcription Factor Interplay between LEAFY and APETALA1/CAULIFLOWER during Floral Initiation. Plant Physiol. *174*, 1097–1109. https://doi.org/10.1104/PP.17.00098.

Gregis, V., Sessa, A., Colombo, L., and Kater, M.M. (2006). *AGL24* , *SHORT VEGETATIVE PHASE* , and *APETALA1* Redundantly Control *AGAMOUS* during Early Stages of Flower Development in Arabidopsis. Plant Cell *18*, 1373–1382. https://doi.org/10.1105/tpc.106.041798.

Gregis, V., Sessa, A., Dorca-Fornell, C., and Kater, M.M. (2009). The Arabidopsis floral meristem identity genes *AP1*, *AGL24* and *SVP* directly repress class B and C floral homeotic genes. Plant J. *60*, 626–637. https://doi.org/10.1111/j.1365-313X.2009.03985.x.

Hamès, C., Ptchelkine, D., Grimm, C., Thevenon, E., Moyroud, E., Gérard, F., Martiel, J.-L., Benlloch, R., Parcy, F., and Müller, C.W. (2008). Structural basis for LEAFY floral switch function and similarity with helix-turn-helix proteins. EMBO J. *27*, 2628–2637. https://doi.org/10.1038/emboj.2008.184.

Hill, T.A., Day, C.D., Zondlo, S.C., Thackeray, A.G., and Irish, V.F. (1998). Discrete spatial and temporal cis-acting elements regulate transcription of the Arabidopsis floral homeotic gene *APETALA3*. Development *125*, 1711–1721. https://doi.org/10.1242/dev.125.9.1711.

Honma, T., and Goto, K. (2000). The Arabidopsis floral homeotic gene *PISTILLATA* is regulated by discrete cis-elements responsive to induction and maintenance signals. Development *127*, 2021–2030. https://doi.org/10.1242/dev.127.10.2021.

van der Horst, A., de Vries-Smits, A.M.M., Brenkman, A.B., van Triest, M.H., van den Broek, N., Colland, F., Maurice, M.M., and Burgering, B.M.T. (2006). FOXO4 transcriptional activity is regulated by monoubiquitination and USP7/HAUSP. Nat. Cell Biol. *8*, 1064–1073. https://doi.org/10.1038/ncb1469.

Irish, V.F. (2010). The flowering of Arabidopsis flower development. Plant J. *61*, 1014–1028. https://doi.org/10.1111/j.1365-313X.2009.04065.x.

Iwata, Y., Lee, M.H., and Koizumi, N. (2011). Analysis of a transcription factor using transient assay in Arabidopsis protoplasts. Methods Mol. Biol. *754*, 107–117. https://doi.org/10.1007/978-1-61779-154-3_6.

Jack, T., Fox, G.L., and Meyerowitz, E.M. (1994). Arabidopsis homeotic gene *APETALA3* ectopic expression: Transcriptional and posttranscriptional regulation determine floral organ identity. Cell *76*, 703–716. https://doi.org/10.1016/0092-8674(94)90509-6.

Jain, M., Nijhawan, A., Arora, R., Agarwal, P., Ray, S., Sharma, P., Kapoor, S., Tyagi, A.K., and Khurana, J.P. (2007). F-box proteins in rice. Genome-wide analysis, classification, temporal and spatial gene expression during panicle and seed development, and regulation by light and abiotic stress. Plant Physiol. *143*, 1467–1483. https://doi.org/10.1104/PP.106.091900.

Jin, R., Klasfeld, S., Zhu, Y., Fernandez Garcia, M., Xiao, J., Han, S.K., Konkol, A., and Wagner, D. (2021). LEAFY is a pioneer transcription factor and licenses cell reprogramming to floral fate. Nat. Commun. 2021 121 *12*, 1–14. https://doi.org/10.1038/s41467-020-20883-w.

Jofuku, K.D., den Boer, B.G.W., Montagu, M. Van, and Okamuro, J.K. (1994). Control of Arabidopsis Flower and Seed Development by the Homeotic Gene *APETALA2*. Plant Cell *6*, 1211. https://doi.org/10.2307/3869820.

Kodadek, T., Sikder, D., and Nalley, K. (2006). Keeping Transcriptional Activators under Control. Cell *127*, 261–264. https://doi.org/10.1016/j.cell.2006.10.002.

Krizek, B.A., and Meyerowitz, E.M. (1996). The Arabidopsis homeotic genes *APETALA3* and *PISTILLATA* are sufficient to provide the B class organ identity function. Development *122*, 11–22. https://doi.org/10.1242/DEV.122.1.11.

Krizek, B.A., Lewis, M.W., and Fletcher, J.C. (2006). *RABBIT EARS* is a second-whorl repressor of *AGAMOUS* that maintains spatial boundaries in Arabidopsis flowers. Plant J. *45*, 369–383. https://doi.org/10.1111/j.1365-313X.2005.02633.x.

Lai, X., Blanc-Mathieu, R., GrandVuillemin, L., Huang, Y., Stigliani, A., Lucas, J., Thévenon, E., Loue-Manifel, J., Turchi, L., Daher, H., et al. (2021). The LEAFY floral regulator displays pioneer transcription factor properties. Mol. Plant *14*, 829–837. https://doi.org/10.1016/J.MOLP.2021.03.004.

Lamb, R.S., Hill, T. a, Tan, Q.K.-G., and Irish, V.F. (2002). Regulation of *APETALA3* floral homeotic gene expression by meristem identity genes. Development *129*, 2079–2086. https://doi.org/https://doi.org/10.1242/dev.129.9.2079.

Lang, P.L.M., Christie, M.D., Dogan, E.S., Schwab, R., Hagmann, J., van de Weyer, A.-L., Scacchi, E., and Weigel, D. (2018). A Role for the F-Box Protein HAWAIIAN SKIRT in Plant microRNA Function. Plant Physiol. *176*, 730–741. https://doi.org/10.1104/pp.17.01313.

Laufs, P., Coen, E., Kronenberger, J., Traas, J., and Doonan, J. (2003). Separable roles of *UFO* during floral development revealed by conditional restoration of gene function. Development *130*, 785–796. https://doi.org/10.1242/DEV.00295.

Lee, I., Wolfe, D.S., Nilsson, O., and Weigel, D. (1997). A *LEAFY* co-regulator encoded by *UNUSUAL FLORAL ORGANS*. Curr. Biol. *7*, 95–104. https://doi.org/10.1016/S0960-9822(06)00053-4.

Lee, J., Oh, M., Park, H., and Lee, I. (2008). SOC1 translocated to the nucleus by interaction with AGL24 directly regulates *LEAFY*. Plant J. *55*, 832–843. https://doi.org/10.1111/J.1365-313X.2008.03552.X.

Levin, J.Z., and Meyerowitz, E.M. (1995). *UFO*: an Arabidopsis gene involved in both floral meristem and floral organ development. Plant Cell *7*, 529–548. https://doi.org/10.1105/tpc.7.5.529.

Levin, J.Z., Fletcher, J.C., Chen, X., and Meyerowitz, E.M. (1998). A genetic screen for modifiers of *UFO* meristem activity identifies three novel *FUSED FLORAL ORGANS* genes required for early flower development in Arabidopsis. Genetics *149*, 579–595. https://doi.org/https://doi.org/10.1093/genetics/149.2.579.

Li, S. (2015). The Arabidopsis thaliana TCP transcription factors: A broadening horizon beyond development. Plant Signal. Behav. *10*, e1044192. https://doi.org/10.1080/15592324.2015.1044192.

Li, H., Yao, R., Ma, S., Hu, S., Li, S., Wang, Y., Yan, C., Xie, D., and Yan, J. (2017). Efficient ASK-

assisted system for expression and purification of plant F-box proteins. Plant J. *92*, 736–743. https://doi.org/10.1111/tpj.13708.

Li, X., Sun, L., Tan, L., Liu, F., Zhu, Z., Fu, Y., Sun, X., Sun, X., Xie, D., and Sun, C. (2012). *TH1*, a DUF640 domain-like gene controls lemma and palea development in rice. Plant Mol. Biol. *78*, 351–359. https://doi.org/10.1007/s11103-011-9868-8.

Liu, C., Xi, W., Shen, L., Tan, C., and Yu, H. (2009). Regulation of floral patterning by flowering time genes. Dev. Cell *16*, 711–722. https://doi.org/10.1016/j.devcel.2009.03.011.

Lohmann, J.U., Hong, R.L., Hobe, M., Busch, M.A., Parcy, F., Simon, R., and Weigel, D. (2001). A molecular link between stem cell regulation and floral patterning in Arabidopsis. Cell *105*, 793–803. https://doi.org/10.1016/S0092-8674(01)00384-1.

Long, J.A., and Barton, M.K. (1998). The development of apical embryonic pattern in Arabidopsis. *3035*, 3027–3035. .

MacAlister, C.A., Park, S.J., Jiang, K., Marcel, F., Bendahmane, A., Izkovich, Y., Eshed, Y., and Lippman, Z.B. (2012). Synchronization of the flowering transition by the tomato *TERMINATING FLOWER* gene. Nat. Genet. *44*, 1393–1398. https://doi.org/10.1038/NG.2465.

Mair, A., Xu, S.L., Branon, T.C., Ting, A.Y., and Bergmann, D.C. (2019). Proximity labeling of protein complexes and cell type specific organellar proteomes in Arabidopsis enabled by TurboID. Elife *8*. https://doi.org/10.7554/ELIFE.47864.

Maizel, A., Busch, M.A., Tanahashi, T., Perkovic, J., Kato, M., Hasebe, M., and Weigel, D. (2005). The Floral Regulator *LEAFY* Evolves by Substitutions in the DNA Binding Domain. Science *308*, 260–263. https://doi.org/10.1126/science.1108229.

McNabb, D.S., Reed, R., and Marciniak, R.A. (2005). Dual Luciferase Assay System for Rapid Assessment of Gene Expression in Saccharomyces cerevisiae. Eukaryot. Cell *4*, 1539–1549. https://doi.org/10.1128/EC.4.9.1539-1549.2005.

McShane, E., and Selbach, M. (2014). Gene expression: degrade to derepress. EMBO J. *33*, 407–408. https://doi.org/10.1002/embj.201387752.

Moyroud, E., Kusters, E., Monniaux, M., Koes, R., and Parcy, F. (2010). LEAFY blossoms. Trends Plant Sci. *15*, 346–352. https://doi.org/10.1016/j.tplants.2010.03.007.

Moyroud, E., Minguet, E.G., Ott, F., Yant, L., Posé, D., Monniaux, M., Blanchet, S., Bastien, O., Thévenon, E., Weigel, D., et al. (2011). Prediction of Regulatory Interactions from Genome Sequences Using a Biophysical Model for the *Arabidopsis* LEAFY Transcription Factor. Plant Cell *23*, 1293–1306. https://doi.org/10.1105/tpc.111.083329.

Nag, A., King, S., and Jack, T. (2009). miR319a targeting of *TCP4* is critical for petal growth and development in Arabidopsis.

Ng, M., and Yanofsky, M.F. (2001). Activation of the Arabidopsis B Class Homeotic Genes by *APETALA1*.

Parcy, F., Nilsson, O., Busch, M.A., Lee, I., and Weigel, D. (1998). A genetic framework for floral patterning. Nature *395*, 561–566. https://doi.org/10.1038/26903.

Risseeuw, E., Venglat, P., Xiang, D., Komendant, K., Daskalchuk, T., Babic, V., Crosby, W., and Datla, R. (2013). An activated form of UFO alters leaf development and produces ectopic floral and inflorescence meristems. PLoS One *8*. https://doi.org/10.1371/journal.pone.0083807.

Samach, A., Klenz, J.E., Kohalmi, S.E., Risseeuw, E., Haughn, G.W., and Crosby, W.L. (1999). The *UNUSUAL FLORAL ORGANS* gene of Arabidopsis thaliana is an F-box protein required for normal patterning and growth in the floral meristem. Plant J. *20*, 433–445. https://doi.org/10.1046/j.1365-313x.1999.00617.x.

Sánchez-Montesino, R., and Oñate-Sánchez, L. (2018). Screening arrayed libraries with DNA and protein baits to identify interacting proteins. Methods Mol. Biol. *1794*, 131–149.

https://doi.org/10.1007/978-1-4939-7871-7_9/COVER.

Sayou, C., Nanao, M.H., Jamin, M., Posé, D., Thévenon, E., Grégoire, L., Tichtinsky, G., Denay, G., Ott, F., Peirats Llobet, M., et al. (2016). A SAM oligomerization domain shapes the genomic binding landscape of the LEAFY transcription factor. Nat. Commun. *7*, 11222. https://doi.org/10.1038/ncomms11222.

Schumann, N., Navarro-Quezada, A., Ullrich, K., Kuhl, C., and Quint, M. (2011). Molecular Evolution and Selection Patterns of Plant F-Box Proteins with C-Terminal Kelch Repeats. Plant Physiol. *155*, 835–850. https://doi.org/10.1104/pp.110.166579.

Sheard, L.B., Tan, X., Mao, H., Withers, J., Ben-Nissan, G., Hinds, T.R., Kobayashi, Y., Hsu, F.F., Sharon, M., Browse, J., et al. (2010). Jasmonate perception by inositol-phosphate-potentiated COI1-JAZ co-receptor. Nature *468*, 400–407. https://doi.org/10.1038/nature09430.

Souer, E., Rebocho, A.B., Bliek, M., Kusters, E., de Bruin, R.A.M., and Koes, R. (2008). Patterning of Inflorescences and Flowers by the F-Box Protein DOUBLE TOP and the LEAFY Homolog ABERRANT LEAF AND FLOWER of Petunia. Plant Cell Online *20*, 2033–2048. https://doi.org/10.1105/tpc.108.060871.

Stefanowicz, K., Lannoo, N., and Van Damme, E.J.M. (2015). Plant F-box Proteins – Judges between Life and Death. CRC. Crit. Rev. Plant Sci. *34*, 523–552. https://doi.org/10.1080/07352689.2015.1024566.

Takeda, S., Hanano, K., Kariya, A., Shimizu, S., Zhao, L., Matsui, M., Tasaka, M., and Aida, M. (2011). CUP-SHAPED COTYLEDON1 transcription factor activates the expression of LSH4 and LSH3, two members of the ALOG gene family, in shoot organ boundary cells. Plant J. *66*, 1066–1077. https://doi.org/10.1111/j.1365-313X.2011.04571.x.

Thines, B., Katsir, L., Melotto, M., Niu, Y., Mandaokar, A., Liu, G., Nomura, K., He, S.Y., Howe, G.A., and Browse, J. (2007). JAZ repressor proteins are targets of the SCFCOI1 complex during jasmonate signalling. Nature *448*, 661–665. https://doi.org/10.1038/nature05960.

Tilly, J.J., Allen, D.W., and Jack, T. (1998). The CArG boxes in the promoter of the Arabidopsis floral organ identity gene *APETALA3* mediate diverse regulatory effects. Development *125*, 1647–1657. https://doi.org/10.1242/dev.125.9.1647.

Wagner, D., Sablowski, R.W.M., and Meyerowitz, E.M. (1999). Transcriptional activation of *APETALA1* by LEAFY. Science *285*, 582–584. https://doi.org/10.1126/science.285.5427.582.

Wasternack, C., and Hause, B. (2013). Jasmonates: biosynthesis, perception, signal transduction and action in plant stress response, growth and development. An update to the 2007 review in Annals of Botany. Ann. Bot. *111*, 1021–1058. https://doi.org/10.1093/aob/mct067.

Weigel, D., and Nilsson, O. (1995). A developmental switch sufficient for flower initiation in diverse plants. Nature *377*, 495–500. https://doi.org/10.1038/377495a0.

Weigel, D., Alvarez, J., Smyth, D.R., Yanofsky, M.F., and Meyerowitz, E.M. (1992). *LEAFY* controls floral meristem identity in *Arabidopsis*. Cell *69*, 843–859. https://doi.org/10.1016/0092-8674(92)90295-N.

Wilkinson, and Haughn (1995). *UNUSUAL FLORAL ORGANS* Controls Meristem Identity and Organ Primordia Fate in Arabidopsis. Plant Cell *7*, 1485–1499. https://doi.org/10.1105/tpc.7.9.1485.

Winter, C.M., Austin, R.S., Blanvillain-Baufumé, S., Reback, M.A., Monniaux, M., Wu, M.F., Sang, Y., Yamaguchi, A., Yamaguchi, N., Parker, J.E., et al. (2011). LEAFY Target Genes Reveal Floral Regulatory Logic, cis Motifs, and a Link to Biotic Stimulus Response. Dev. Cell *20*, 430–443. https://doi.org/10.1016/j.devcel.2011.03.019.

Wu, R.-C., Feng, Q., Lonard, D.M., and O'Malley, B.W. (2007). SRC-3 Coactivator Functional

Lifetime Is Regulated by a Phospho-Dependent Ubiquitin Time Clock. Cell *129*, 1125–1140. https://doi.org/10.1016/j.cell.2007.04.039.

Yamaguchi, N., Jeong, C.W., Nole-Wilson, S., Krizek, B.A., and Wagner, D. (2016). AINTEGUMENTA and AINTEGUMENTA-LIKE6/PLETHORA3 Induce *LEAFY* Expression in Response to Auxin to Promote the Onset of Flower Formation in Arabidopsis. Plant Physiol. *170*, 283–293. https://doi.org/10.1104/pp.15.00969.

Yoshida, A., Suzaki, T., Tanaka, W., and Hirano, H.Y. (2009). The homeotic gene long sterile lemma (*G1*) specifies sterile lemma identity in the rice spikelet. Proc. Natl. Acad. Sci. U. S. A. *106*, 20103–20108. https://doi.org/10.1073/pnas.0907896106.

Yoshida, A., Sasao, M., Yasuno, N., Takagi, K., Daimon, Y., Chen, R., Yamazaki, R., Tokunaga, H., Kitaguchi, Y., Sato, Y., et al. (2013). *TAWAWA1*, a regulator of rice inflorescence architecture, functions through the suppression of meristem phase transition. Proc. Natl. Acad. Sci. U. S. A. *110*, 767–772. https://doi.org/10.1073/pnas.1216151110.

Zhao, L., Nakazawa, M., Takase, T., Manabe, K., Kobayashi, M., Seki, M., Shinozaki, K., and Matsui, M. (2004). Overexpression of *LSH1*, a member of an uncharacterised gene family, causes enhanced light regulation of seedling development. Plant J. *37*, 694–706. https://doi.org/10.1111/J.1365-313X.2003.01993.X.

Résumé

Le développement des fleurs est crucial pour le succès reproductif des plantes. Cette étape du développement nécessite une reprogrammation génétique profonde, avec l'activation de gènes spécifiques à la fleur. Chez les angiospermes, le facteur de transcription (FT) LEAFY (LFY) est un régulateur clé de ce processus. Des études précédentes ont montré que LFY agit avec des cofacteurs qui spécifient spatialement son activité. Le cofacteur de LFY le mieux décrit est la protéine à F-box UNUSUAL FLORAL ORGANS (UFO). Cependant, comment UFO régule l'activité de LFY au niveau moléculaire restait incompris.

J'ai d'abord montré que le rôle d'UFO en tant que composant d'un complexe E3 ligase n'était pas essentiel à sa fonction *in planta*. Puis j'ai montré que LFY et UFO agissent en formant un complexe qui reconnaît des éléments *cis* spécifiques. La caractérisation structurale de ce complexe a révélé qu'UFO se lie à la fois à LFY et à une séquence précise d'ADN, expliquant son rôle de cofacteur transcriptionnel. Enfin, des données préliminaires suggèrent que la formation du complexe LFY-UFO est conservée au sein des angiospermes et des plantes sans fleurs. Ainsi, cette étude présente un cas original chez les plantes où une protéine à F-box agit principalement comme cofacteur de transcription par sa capacité à lier l'ADN.

Une deuxième partie de ma thèse a été consacrée à l'étude des gènes *Arabidopsis LSH Oryza G1* (*ALOG*), une classe de FTs spécifique aux plantes et régulée par LFY. Peu de données étaient disponibles dans la littérature sur leurs propriétés biochimiques, et je me suis concentré sur l'interaction du domaine ALOG avec l'ADN. J'ai montré que plusieurs protéines ALOG lient toutes le même motif d'ADN et j'ai caractérisé le mécanisme de liaison à l'ADN.

Abstract

Flower development is crucial for the reproductive success of plants. This developmental step requires a deep genetic reprogramming, with the activation of flower-specific genes. In angiosperms, the LEAFY (LFY) Transcription Factor (TF) is a key regulator of flower development. Previous studies showed that LFY acts with cofactors that spatially specify its activity. The best-described LFY cofactor is the F-box protein UNUSUAL FLORAL ORGANS (UFO). However, how UFO regulates LFY's activity at the molecular level remained unclear.

I first showed that the role of UFO as a component of an E3 ligase complex was not essential for its functions *in planta*. Then, I found that LFY and UFO act together by forming a complex that recognizes specific *cis*-elements. The structural characterization of this complex revealed that UFO binds both LFY and a precise DNA sequence, explaining its role as a transcriptional cofactor. Finally, preliminary data suggest that the formation of the LFY-UFO complex is conserved within angiosperms and non-flowering plants. Altogether, this study presents an original case in plant where an F-box protein acts mostly as a transcriptional cofactor through its ability to bind DNA.

A second part of my PhD was dedicated to the study of *Arabidopsis LSH Oryza G1* (*ALOG*) genes, a plant-specific class of TFs regulated by LFY. Few data were available in the literature about their biochemical properties, and I focused on the interaction of the ALOG domain with DNA. I found that several ALOG proteins bind the same DNA motif and I characterized the DNA-binding mechanism.